Chemical, Metabolic and Structure–Activity Relationships to Probe Abacavir Toxicity

Thesis submitted in the accordance with the requirements of the University of Liverpool for the degree of Doctor of Philosophy by

Emma Louise Yang

August 2014

DECLARATION

This thesis is the result of my own work. The material contained in the thesis has not been presented, nor is currently being presented, either wholly or in part for any other degree or other qualification.

Emma Louise Yang

This research was carried out in the Department of Chemistry and Department of Pharmacology at The University of Liverpool.

ACKNOWLEDGEMENTS

Firstly, I must thank my supervisors, Prof. B. Kevin Park and Prof. Paul O'Neill for giving me this fantastic opportunity, and for all their help and advice over the last 4 years. Certainly without that, this wouldn't have been possible. I would also like to thank the BBSRC and GSK for funding this study.

I don't know where I would be without the endless support and guidance from the PON group. To all past and present members (the list is far too long!), thank you. They have not only been there to assist with my work, but have been great friends. I wouldn't have survived the 4 years without you. In particular, I would like to thank Mike, Natalie, Alex and Raman: Their advice, support and knowledge has been exceptional and they have all played different friendship roles – something that has meant so much to me and I will treasure. Special thanks must go to Neil for reading my whole thesis and to Alex Lawrenson for performing all molecular docking studies.

I would like to express my gratitude to all those who have assisted me in pharmacology: To Catherine Bell, John Farrell and Mohammad Alhaidari for conducting all the immunology experiments and to Phil Martin for performing all cytotoxicity and efficacy experiments. I must particularly thank them for their patience and for taking the time to sit down with me and explain things so well. A special thank you to Anahi Santoyo-Castelazo for assisting with metabolism experiments and assisting with performing LC-MS/MS studies. Thank you for all your endless help, and I'm sorry for dragging you in on 'that Saturday' and ringing you on weekends when the LC-MS machine wasn't doing as it was told!

I must thank everyone else, whom I haven't mentioned, but have helped me along the way, in particular, all other academic and technical staff whom I haven't mentioned. They have seen countless smiles and tears but the support I have received from them has been invaluable. I must say a special thank you to Moya, whom not only ran my mass spec. samples (always on time!) but became a good friend of mine. I think she's seen it all from me over the last 4 years, and she has been the first 'in-house' port of call to comfort me when I thought it couldn't get any worse – thank you.

To my family: Mum, Dad, Nan, Phil & Emma, Sara & Phil and Lucinda & Courtney. Thank you Mum, Dad and Nan for your extra special support and for being there to encourage me. I think it's pertinent to say a special thank you to my sister Sara and her fiancée, Phil. You have not only been a much-needed distraction at times, but you've been great friends. Thank you for feeding and housing me when I had no money. I owe you both. To my late granddad, whom I know would have been so proud to see this completed.

To the person whom has supported me throughout this and has listened to me moan almost daily, cry and jump with excitement; whom has comforted and encouraged me when I thought I couldn't do any more – Dan, thank you so much. I am forever indebted to you. I love you.

Finally, something that was often said to me and helped me through the difficult days…"The true test of character comes, not when times are easy, but when they are hard." — Thanks Moy!

CONTENTS

ABSTRACT

Adverse drug reactions (ADRs) are responsible for an increasing number of hospitalised patients, with the large majority of these ADRs classed as either type A or type B. Drug hypersensitivity reactions fall within the type B category and one such drug responsible for this form of ADR is abacavir (ABC). ABC, a nucleoside reverse transcriptase inhibitor, is used to treat the HIV-1 virus. It is responsible for a potentially life-threatening type IV hypersensitivity reaction which occurs in patients bearing the HLA-B*57:01 allele. Although many mechanisms have been proposed, it was the objective of this research to examine all these previous proposals to further extend and develop the mechanism of ABC toxicity.

In Chapter 2, deuterated-ABC (D_2-ABC) was designed and synthesised where the two 5'-H atoms were replaced with two 5'-D atoms. The design of this analogue was intended to retard the oxidative metabolism of ABC to its aldehyde and carboxylic acid metabolites. The synthesis of this compound was paramount to investigating this metabolism and through a series of metabolic experiments, described in Chapter 3, a kinetic isotope effect between ABC and D_2-ABC was determined, ultimately showing an altered metabolism between the two compounds.

To investigate binding of ABC within the HLA-B*57:01 protein, analogues of ABC, with alterations at varying positions within the molecule, were required. Using a racemic method, ABC enantiomers were synthesised and ABC's enantiomer failed to stimulate T-cells *in vitro*. The creation of further analogues required the development of an asymmetric synthetic route. A total synthetic method was desired to synthesise intermediates to be used in future analogue synthesis.

Finally, as described in Chapter 5, a range of 6-position analogues were designed, using a structure-activity relationship method, and synthesised, to further investigate the altered repertoire mechanism. These analogues, consisting of primary and secondary amine and oxy moieties, were subjected to *in vitro* immunological assays to determine their stimulation of T-cells. Additionally, the synthesised analogues were modelled *in silico* using molecular docking within the HLA protein. The *in silico* results assisted in explaining the basis of such T-cell activation/inactivation and will direct future analogue design. IC_{50} and EC_{50} values were determined for analogues that presented a negative T-cell response and a compound showing positive values was subjected to further pharmacokinetic testing.

The oxidative metabolism of ABC was affected by isotopic substitution, but initial results have shown no altered T-cell stimulation of D_2-ABC compared to ABC. This mechanism cannot be discarded, with further investigational work required. However, the synthesised 6-position analogues have assisted in further examining the altered repertoire mechanism and initial findings have enabled further understanding of the binding of ABC within HLA-B*57:01. This mechanism of ABC toxicity appears paramount to others proposed and the results presented in this thesis support this. Additional analogue synthesis and *in vivo* experiments will assist in confirming this further.

PUBLICATIONS

Published Papers

Bell, C. C., Santoyo-Castelazo, A., Yang, E. L., Maggs, J. L., Jenkins, R. E., Tugwood, J., O'Neill, P. M., Naisbitt, D. J., Park, B. K.

Oxidative Bioactivation of Abacavir in Subcellular Fractions of Human Antigen Presenting Cells. *Chem. Res. Toxicol.*, **2013**, *26* (7), 1064

Manuscripts in Preparation

Yang, E. L., Santoyo-Castelazo, A., Bell, C. C., Martin, P., Owen, A., Naisbitt, D. J., O'Neill, P. M., Park, B. K.

Deuterium Isotope Effects on the Oxidation of Abacavir in Human Liver Cytosol: Inhibition of Metabolic Dehydrogenation as a Strategy for Enhancing Drug Safety and Efficacy

Naisbitt D. J., Yang E. L., Alhaidari M., Berry N., Lawrenson A. S., Farrell J., Martin P., Owen A., Pye M., Clarke S. E., O'Neill P. M., Park B. K.

Towards Depersonalised Abacavir-Containing Therapy: Chemical Modification of the 6-Amino Cyclopropyl Eliminates HLA-B*57:01-Restricted CD8^{+} T-Cell Activation without Loss of Antiviral Activity

ABBREVIATIONS, ACRONYMS & SYMBOLS

|	
λ	Wavelength
%	Percent
μCi	Microcurie
°C	degrees Celsius
$[α]_D$	Specific rotation (wavelength at 589 nm)
-ve	Negative
+ve	Positive
^{1}H	Proton-1
^{3}H	Proton-3 (Tritium)
^{13}C	Carbon-13
^{14}C	Carbon-14
4-MP	4-Methylpyrazole
ABC	Abacavir
ABC-CHO	Abacavir aldehyde (ABC-**14**)
ABC-COOH	Abacavir carboxylic acid (ABC-**15**)
ACN	Acetonitrile
ADH	Alcohol dehydrogenase
ADR	Adverse drug reaction
ABC-HSR	Abacavir hypersensitivity reaction
AIDS	Acquired immunodeficiency virus
ALDH	Aldehyde dehydrogenase
APC	Antigen presenting cell
ATP	Adenosine triphosphate
AUC	Area under the curve
BIAB	(Diacetoxyiodo)benzene
Boc	*tert*-Butyloxycarbonyl
BQL	Below quantifiable limit
br	Broad
BSA	Bovine serum albumin
c	Concentration
cat.	Catalytic
CBV	Carbovir
CBZ	Carbamazepine
$CDCl_3$	Deuterated chloroform
CI	Chemical ionisation
CL	Clearance
Cl-ABC	Chloro-abacavir
CNS	Central nervous system
COX-1 / COX-2	Prostaglandin-endoperoxide synthase-1 / -2
cpm	Counts per minute
cps	Counts per second
CRF_1	Corticotropin-releasing hormone receptor 1
CSI	Chlorosulfonyl isocyanate
CTL	Cytotoxic T-lymphocytes
CV	Cross-validation error

CYP P450	Cytochrome P450 enzymes
d	Doublet
Da	Daltons
D$_2$-ABC	Deuterated-abacavir
DADCP	2,5-Diamino-4,6-dichloropyrimidine
DBBT	Dibutylboryl triflate
DBU	1,8-Diazabicycloundec-7-ene
DCC	Dicyclohexylcarbodiimide
DCM	Dichloromethane
DDC	N,N-Diethyldithiocarbamate
DDI	Drug-drug interactions
DEAD	Diethyl azodicarboxylate
DH-ABC	Dihydro-abacavir
DHR	Drug hypersensitivity reaction
DHS	Drug hypersensitivity syndrome
DIAD	Diisopropylazodicarboxylate
DIEA	N,N-Diisopropylethylamine
DMAP	4-Dimethylaminopyridine
DME	Dimethoxyethane
DMF	Dimethylformamide
DMP	Dess-Martin periodinane
DMPU	1,3-Dimethyl-3,4,5,6-tetrahydro-2-pyrimidinone
DMSO	Dimethyl sulfoxide
DMSO-d$_6$	Deuterated DMSO
DNA	Deoxyribonucleic acid
DP	Diphosphate
DSF	Disulfiram
DTH	Delayed type hypersensitivity
EBV	Epstein-Barr virus
EDTA	Ethylenediaminetetraacetic acid
ee	Enantiomeric excess
ELISpot	Enzyme linked immunospot
EPI	Enhanced product ion
equiv	Equivalent
ER	Endoplasmic reticulum
ES(I)	Electrospray (ionisation)
F	Bioavailability
FA	Formic acid
FBS	Foetal bovine serum
FDA	Food and drug administration
FMO	Flavin monooxygenase
FMOC	Fluorenylmethyloxycarbonyl
g	Gram(s)
GABA	γ-aminobutyric acid
GSK	GlaxoSmithKline
GST(P)	Glutathione *S*-transferase (Pi)
h	Hour(s)
HAART	Highly active antiretroviral therapy
Hb	Haemoglobin
HBSS	Hanks balanced salt solution

HEPES	4-(2-Hydroxyethyl)-1-piperazineethanesulfonic acid
HIV	Human immunodeficiency virus
HLA	Human leukocyte antigen
HMPA	Hexamethylphosphoramide
HoBT	1-Hydroxybenzotriazole
HPLC	High-performance liquid chromatography
HSA	Human serum albumin
Hz	Hertz
IFN-γ	Interferon-γ
IgE / IgM / IgG	Immunoglobulin-E / -M / -G
IL-2 / IL-8	Interleukin-2 / -8
IPA	Isopropyl alcohol
IR	Infrared
IS	Internal standard
IV	Intravenous
K(D)IE	Kinetic (deuterium) isotope effect
k_D	Deuterium rate constant
k_H	Proton rate constant
KHMDS	Potassium bis(trimethylsilyl)amide
LC-MS/MS	Liquid chromatography-tandem mass spectrometry
LC-UV	Liquid chromatography-ultraviolet
LDA	Lithium diisopropylamide
LTT	Lymphocyte transformation test
m	Multiplet
M	Molar
MeDDC	S-Methyl-*N,N*-diethyldithiocarbamate
MeDTC	S-Methyl-*N,N*-diethylthiocarbamate
MeOD	Deuterated methanol
mesna	Sodium-2-mercaptoethane sulfonate
Methoxy	Methoxylamine
MHC	Major histocompatability complex
min	Minute(s)
mL	Millilitres
MMFF	Molecular mechanics force field
(m)mol(s)	(milli)mol(s)
MNL	Mononuclear leukocytes
MoOPD	Oxodiperoxymolybdenum (pyridine) (1,3-dimethyl-3,4,5,6-tetrahydro-2-pyrimidinone)
mp	Melting point
MP	Monophosphate
MPO	Myeloperoxidase
MPTP	1-Methyl-4-phenyl-l,2,3,6-tetrahydropyridine
MRM	Multiple reaction monitoring
MTT	Thiazolyl blue tetrazolium bromide
mtDNA	Mitochondrial DNA
MW	Microwave
m/z	Mass to charge ratio
n	Nano
NAD^+	Nicotinamide adenine dinucleotide
$NADP^+$	Nicotinamide adenine dinucleotide phosphate

NAPQI	N-Acetyl-*p*-benzoquinoneimine
NAT	N-Acetyltransferases
NDV	N-Desmethylvenlafaxine
NIBSC	National Institute for Biological Standards
NM	Nornitrogen mustard
NMP	N-Methyl-2-pyrrolidone
NMR	Nuclear magnetic resonance
NRTI	Nucleoside reverse transcriptase inhibitor
NSAID	Non-steroidal anti-inflammatory drug
ODV	O-Desmethylvenlafaxine
o/n	Overnight
PΩ	C-terminal residue
PA	Procainamide
PAHA	Procainamide hydroxylamine
PAPS	3'-phosphoadenosine 5'-phosphosulfate
PBMC	Peripheral blood mononucleated cell
PCC	Pyridinium chlorochromate
PD	Pharmacodynamic
Pd/C	10% Palladium on carbon
PDC	Pyridinium dichromate
pH	Power of hydrogen
p-i	Pharmacological interaction
PK	Pharmacokinetic
pK_a	Acid dissociation constant
PM	Phosphoramide mustard
PMA	Phorbol myristate acetate
PMN	Polymorphonuclear leukocytes
PO	*Per os* (oral administration)
ppm	Parts per million
quant.	Quantitative
RCM	Ring closing metathesis
RDS	Rate determining step
RNA	Ribonucleic acid
R$_t$	Retention time
r.t.	Room temperature
s	Singlet
SAR	Structure-activity relationship
SDS	Sodium dodecyl sulfate
SFC	Spot forming cells
SIE	Systemic lupus erythematosus syndrome
SJS	Stevens–Johnson syndrome
SM	Starting material
SMX	Sulfamethoxazole
ST	Sulfotransferases
t	Triplet
TAP	Transporter associated with antigen processing
TBAF	Tetra-*n*-butylammonium fluoride
TBDMS-Cl	*tert*-Butyldimethylsilyl chloride
***t*-BME**	*tert*-Butyl methyl ether
TCR	T-cell receptor

TEMPO	2,2,6,6-Tetramethylpiperidinyloxy
TEN	Toxic epidermal necrolysis
TEOF	Triethylorthoformate
TFA	Trifluoroacetic acid
TFDA	Trimethylsilyl fluorosulfonyldifluoroacetate
T$_h$1	Type 1 T-helper cell
T$_h$2	Type 2 T-helper cell
THAB	Tetrahexylammonium bromide
THF	Tetrohydrofuran
THP	Tris(hydroxymethyl)phosphine
TLC	Thin layer chromatography
TMS	Tetramethylsilane
TNF-α	Tumour necrosis factor-α
TP	Triphosphate
Ts	Tosylate
UDP	Uridine diphosphate
UGT	UDP-glucuronosyl transferase
UV	Ultraviolet
UV/Vis	Ultraviolet/Visible light
v	Rate of reaction
(e)V	(electro)Volts
v/v	Volume/volume
WHO	World Heath Organisation
w/v	Weight/volume
XPhos	2-Dicyclohexylphosphino-2',4',6'-triisopropylbiphenyl

Numbering of carbonucleosides used throughout this thesis
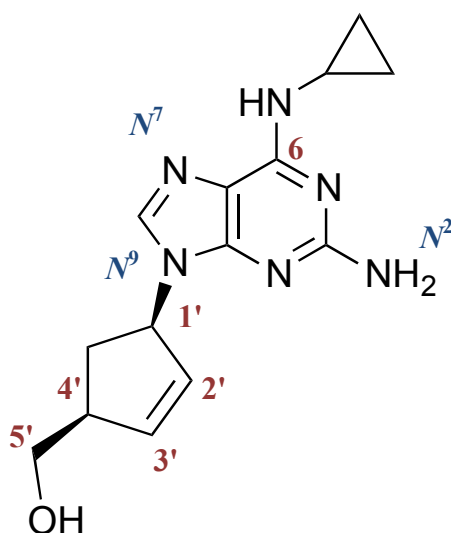
CHAPTER 1

General Introduction

CHAPTER 1

General Introduction

1.1 Introduction

1.2 Adverse Drug Reactions

Adverse drug reactions (ADRs) pose a major risk to patients and are a cause of increasing hospital admissions.[1] These adverse reactions are not limited to a certain class of drugs, although analgesics and cardiovascular drugs often contribute to a higher percentage of hospitalised patients.[2] Careful drug design and thorough explanations of mechanisms of current ADRs will help in the future design and release of drugs, thereby reducing the number of hospital admissions and lowering the mortality rate resulting from ADRs.

The widely accepted definition of an ADR is as follows:

"An appreciably harmful or unpleasant reaction, resulting from an intervention related to the use of a medicinal product, which predicts hazard from future administration and warrants prevention or specific treatment, or alteration of the dosage regimen, or withdrawal of the product."[3]

1.2.1 Classification of adverse drug reactions.

There are 5 classes of ADRs (Table **1.1**), with most of these categorised into either type A or type B. Other less common ADRs fall into types C–E. The current classification system of ADRs was established in 2000 and previously only type A and B categories existed.

Table 1.1: Classification of ADRs, types A–E. ADR, adverse drug reaction; HIV, human immunodeficiency virus. Adapted from Edwards *et al.*[3] and Park *et al.*[4]

Type of Reaction	Feature of ADR	Example Effect – Drug (Use)
A	• **Dose-related** • Common • Predictable • Usually resulting from pharmacological action of drug	Excess bleeding – Warfarin (anticoagulant)
B	• **Non-dose related** • Uncommon • Idiosyncratic • Not related to pharmacological action of drug	Hypersensitivity – Abacavir (antiviral, HIV)
C	• **Dose-related and time related (continuing)** • Uncommon • Resulting from cumulative dose	Hepatotoxicity – Acetaminophen (analgesic)
D	• **Time-related (delayed)** • Uncommon • Usually dose-related • Delayed onset time	Fetal hydantoin syndrome – Phenytoin (epilepsy)
E	• **Withdrawal (end-of-use)** • Uncommon • Symptoms appear quickly after withdrawal of drug	Benzodiazepine withdrawal syndrome – Diazepam (sedative benzodiazepines)

Type A ADRs are more common and are more likely to be dose-related than type B ADRs. They account for over 80% of ADRs.[5] Type A ADRs are predictable from the known pharmacology of the drug, whether these are primary or secondary pharmacological characteristics. These ADRs are quite often mild in nature in comparison to type B reactions; they have low mortality rates and are usually first detected in phase I–III clinical trials.[6] Factors that influence development of a type A ADR include genetic polymorphisms, pharmacokinetic (PK) and pharmacodynamic (PD) variations and drug–drug interactions (DDIs).[5,6] Frequently, these ADRs are seen in elderly patients[5] or those undertaking numerous drug therapies.[7] An example of a type A ADR can be seen in Table **1.1** where warfarin can cause excess bleeding – a toxicity that arises through genetic factors and DDIs, but can be reduced through a strict dosing regimen.

Type B ADRs are less common, liable to higher mortality rates and are idiosyncratic, leading to their highly unpredictable nature. Type B reactions account for approximately 16% of ADRs.[8] There is no dose-dependent relationship with this toxicity and they can often arise not only from the parent drug or metabolite, but from chemically reactive metabolites.[5] Although these reactions are relatively rare, they are often more serious in nature, affect multiple organ systems and can have a significant clinical and drug discovery impact. Understanding the mechanisms behind these type B adverse reactions is vital to drug discovery and development.

1.3 Immune Reactions

A common reaction seen within the type B ADR category is drug hypersensitivity syndrome (DHS). It results from an undesired stimulation of the immune system,

presenting serious effects and can often result in fatal consequences. DHS accounts for approximately 13% of ADRs.[9] During the 1960s, Coombs and Gell[10] divided hypersensitivity reactions into four classes: I, II, III and IV, the latter with its own set of subclasses (Table **1.2**).

Table 1.2: Classification of type I–IVd hypersensitivity reactions.

Hypersensitivity Class	Reaction Type (Mediators)	Mechanism
I	IgE-mediated reactions (IgE)	• Binding of IgE to IgE-specific Fc receptors • IgE antibodies trigger mast cells and basophils to release active agents stimulating a response • Reactions are quickly onset
II	Cytotoxic reactions (IgM or IgG)	• IgM or IgG antibodies bind to cell membrane or tissue and activate complement cascade, resulting in destruction of cell
III	Immune complex reactions (IgM or IgG)	• Complexes of antigen and IgM or IgG antibody accumulate in tissue and activate complement cascade
IV	Delayed-type reactions (T-cells)	• Antigen causes activation of T-cells which release cytokines, resulting in activation of macrophages. The types of T-cells involved define the subclass:
IVa		• Type 1 T-helper cells (T_h1 cells)
IVb		• Type 2 T-helper cells (T_h2 cells)
IVc		• Cytotoxic T-cells
IVd		• IL-8 secreting T-cells

1.3.1 Type IV hypersensitivity.

Of the four discrete classes, it is delayed-type hypersensitivity (DTH) class IV that is of most interest to this research, due to its relation with T-cell lymphocytes rather than antibodies (as seen with type I–III hypersensitivity reactions). The first encounter of the antigen with the patient will sensitise them, and upon re-exposure to the antigen, type 1 T-helper cells (T_h1) cells are activated and a hypersensitivity reaction will occur. It is known as DTH due to the time delay of onset of symptoms – usually 24–72 hours after exposure to the antigen.[11] Such a delay arises due to the migration of macrophages and T-cells to the site of exposure.[11] The appearance of skin rashes, raised thickening of skin and itching are all typical characteristics of this type of hypersensitivity reaction.

1.3.2 Mechanism of T-cell activation.

There are two forms of the major histocompatability complex (MHC), MHC class I and MHC class II, which facilitate the presentation of both endogenous and exogenous peptides to T-cells. Several differences occur between the two classes: MHC I molecules are found expressed within most cells and MHC II only within antigen presenting cells (APCs); MHC I molecules interact with $CD8^+$ T-cells, whereas MHC II molecules interact with $CD4^+$ T-cells and MHC I molecules are responsible for the presentation of smaller peptides (typically 9–11 amino acids in length) whilst MHC II present larger peptide chains.

Within this research, it has been vital to understand the mechanism of T-cell activation, facilitated by MHC class I molecules only. The MHC I molecules are coded for in humans by three major human leukocyte alleles (HLA): HLA-A, HLA-

B and HLA-C genes. Firstly, a peptide must be transported to the endoplasmic reticulum (ER) using the transporter associated with antigen processing (TAP) pathway and once in the ER, it is loaded onto the MHC molecule with the assistance of the chaperones, ERp57 and tapasin. The MHC-peptide molecule is then transported to the cell surface and is available for presentation to T-cells. MHC I self-peptide complexes will interact with CD8^{+} T-cells with insufficient strength to stimulate a T-cell response. However, should an exogenous peptide be bound within the MHC molecule, complementary T-cell receptors (TCRs) on T-cells will be activated, resulting in a cascade of mechanisms occurring due to this immune response.

1.4 Mechanisms of Drug Hypersensitivity Reactions

Three major concepts are well known that present possible mechanisms of immune-mediated drug-induced responses in an MHC class I manner: The hapten hypothesis, the pharmacological interaction (p-i) concept and the danger hypothesis.

1.4.1 Hapten hypothesis.

The hapten hypothesis is the most widely applied mechanism to idiosyncratic drug reactions.[12] A hapten is a small, chemically reactive compound that must bind covalently to self-proteins/peptides before antigen processing[4,13-16] (Figure **1.1**). A hapten molecule cannot initiate an immune response itself, but only when chemically bonded to a (endogenous) protein, forming a novel complex which is immunogenic.[4] Penicillins are example drugs that act in this manner.[17] Other further examples include halothane[18,19] and clozapine.[20]

A prohapten is a seemingly inert molecule but once metabolised, it forms a highly reactive species that is capable of covalently binding to proteins and subsequently activating an antigen-mediated T-cell response. The metabolism usually occurs with the aid of cytochrome (CYP) P450 enzymes during phase I metabolism. Once metabolised, molecules that are susceptible to becoming immunogenic will form electrophilic functional groups, such as quinone imines[21] and nitroso intermediates.[22]
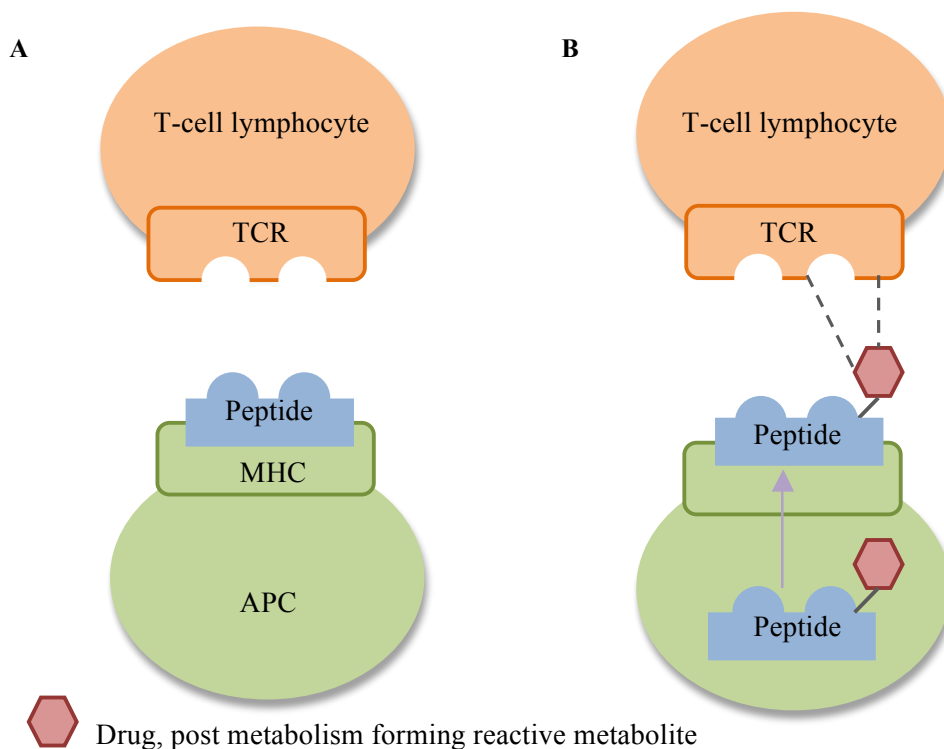

Figure 1.1: Presentation and recognition of a peptide within the MHC to the TCR (**A**). The hapten hypothesis: A drug is processed either within the APC, or previously, to form a reactive metabolite, which covalently (solid line) binds with endogenous proteins/peptides. This adduct is presented on the MHC to T-cell lymphocytes (*via* TCR) forming non-covalent bonds (dashed lines) and as it is immunogenic, stimulates an immune response (**B**). MHC, major histocompatability complex; TCR, T-cell receptor; APC, antigen-presenting cell.

1.4.2 Pharmacological interaction concept.

The p-i concept explains the mechanism behind T-cell activation with small drug molecules that are chemically inert, before or after metabolism.[16,23] There is an absence of covalent binding with the TCR or the MHC during antigen presentation and weaker, non-covalent binding occurs[8] (*e.g.* hydrogen, van der Waals bonding) (Figure **1.2**). It is the direct interaction of the molecule between the TCR and MHC that stimulates a response, with no previous metabolism or intracellular processing of the drug[24] or other chemical reactions with endogenous proteins. This mechanism has been applied to drugs such as sulfamethoxazole (SMX)[25] and lidocaine.[26]
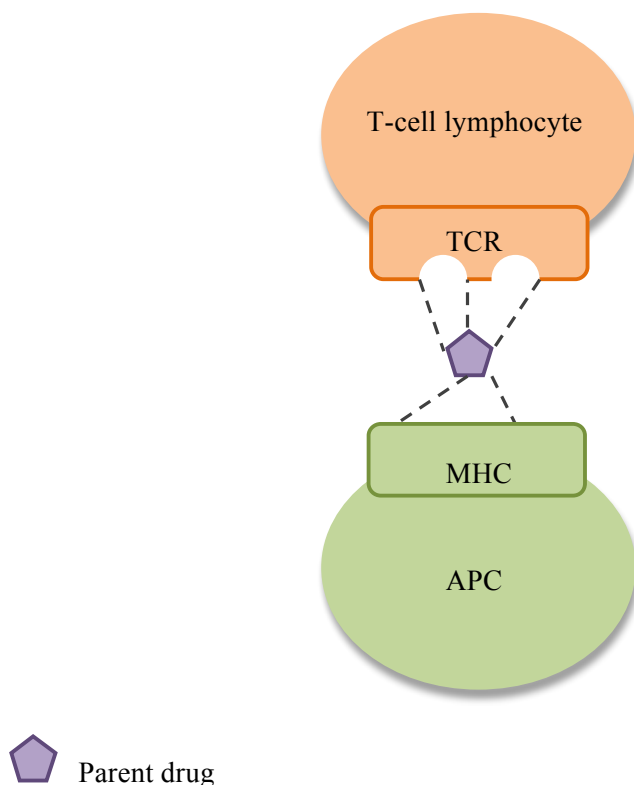

Figure 1.2: The pharmacological (p-i) concept. This concept explains the stimulation of an immune response directly from a chemically inert drug. There are no covalent bonds, but non-covalent bonds (dashed lines) are present between both the MHC and the TCR, resulting in a positive T-cell response.
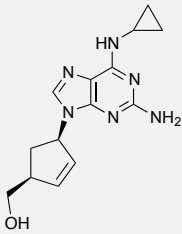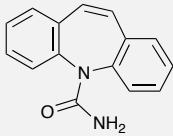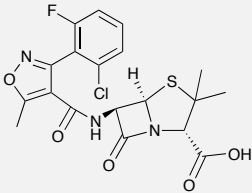
1.4.3 Danger hypothesis.

The danger hypothesis, proposed by Matzinger,[27] provides an alternative approach to induced DHS, the basis of which is developed from the difficulty for the immune system to differentiate between self and non-self molecules.[12] The hypothesis states that three signals must be present in order to induce an immune response.[28] Signal 1, antigen recognition by T-cells, is not sufficient to stimulate T-lymphocytes and without signal 2 (co-stimulatory signal), tolerance will occur. However, should signal 2, interaction of co-stimulatory molecules between the APC and T-cell, and signal 3, the presence of cytokines that act on T-cells, occur, T-lymphocytes will be activated.[14]

1.5 HLA Association with DHS

Although many factors, both genotypic and phenotypic, can affect a patient's likelihood of developing DHS, there is a strong connection of HLA association due to the nature of its function. The HLA, in particular types A, B and C, genes are some of the most variable genes within the human genome and are widely researched with respect to their connection with DHS.[29] Examples of drugs that cause ADRs within an HLA-restricted manner can be seen in Table **1.3**. Of these drug examples, abacavir (ABC) and carbamazepine (CBZ) are both immune-mediated (associated with a DHS or Stevens–Johnson syndrome/toxic epidermal necrolysis (SJS/TEN) respectively) and these toxicities have positive HLA association.[30-32] Flucloxacillin is responsible for a drug-induced liver injury, and this too has an HLA association.[33]

13

Table 1.3: Examples of drug treatments and their HLA (MHC class I) relations with their associated toxicity. HLA, human leukocyte antigen; ABC-HSR, abacavir hypersensitivity reaction; SJS/TEN, Stevens–Johnson syndrome/toxic epidermal necrolysis. Adapted from Bharadwaj *et al*.[29]

Drug	Treatment	Toxicity	HLA Association
Abacavir	HIV	ABC-HSR	B*57:01
Carbamazepine	Epilepsy	SJS/TEN	B*15:02
Flucloxacillin	Bacterial infections (antibiotic)	Hepatitis	B*57:01

1.6 Drug Metabolism

Once a non-polar drug enters the body, it is metabolised to more polar metabolites to increase water solubility for easier excretion. The majority of metabolism reactions occur in the liver, but some may occur in blood plasma or other tissues and such reactions are split into two categories: Phase I and phase II metabolism.

1.6.1 Phase I metabolism.

CYP P450 enzymes most commonly prefer phase I metabolism. These enzymes are haemoproteins and are divided into 4 classes: CYP1–CYP4. Most drugs are metabolised by a select number of these isozymes including CYP3A4, CYP3A5, CYP2D6 and CYP1A2. During this metabolism, polar groups are either added to the drug molecule, or are unmasked. Two or more metabolism reactions often occur per molecule or in some cases, no metabolism takes place. Oxidation is the major phase I metabolism pathway, but reduction and hydrolysis reactions will also take place. Examples of these reactions can be found in Table **1.4**.

Oxidation will occur on alkyl groups, alkenes and aromatic rings as well as dealkylation of amines and ethers and dehalogenation of alkyl halides. Heteroatoms (namely nitrogen, sulfur and phosphorus) will also undergo oxidation reactions. During these oxidation reactions, co-factor reduced nicotinamide adenine dinucleotide phosphate (NADPH) and molecular oxidation is required (Figure **1.3**).
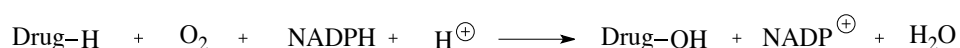
$$\text{Drug–H} \ + \ O_2 \ + \ \text{NADPH} + \ H^{\oplus} \longrightarrow \text{Drug–OH} \ + \ \text{NADP}^{\oplus} \ + \ H_2O$$
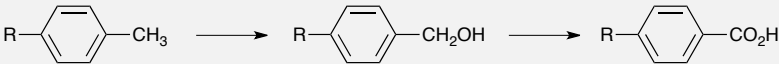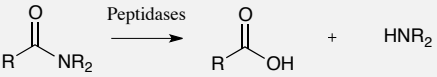
Figure 1.3: Oxidation of a drug by CYP P450 enzymes using molecular oxygen and reduced NADPH. CYP, cytochrome; NADPH, nicotinamide adenine dinucleotide phosphate.

Further to the CYP P450 enzymes, other enzymes such as monoamine oxidases (metabolism of primary amines to aldehydes), alcohol and aldehyde dehydrogenases (oxidation of primary alcohols to aldehydes and aldehydes to carboxylic acids

respectively) and reductases, esterases and peptidases also metabolise drugs during phase I metabolism.
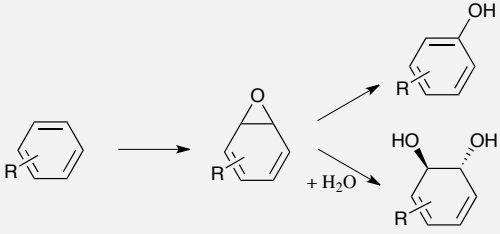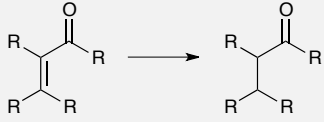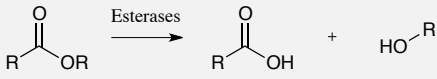
Table 1.4: Oxidation, reduction and hydrolysis phase I metabolism reactions. Adapted from Introduction to Medicinal Chemistry.[34]

Chemical Reaction	Example
Oxidation (alkyl)	$RCH_3 \longrightarrow RCH_2OH \longrightarrow RCHO \longrightarrow RCO_2H$
Oxidation (alkyl aromatic)	
Oxidation (aromatic)	
Oxidation (1° amine)	$ArNH_2 \longrightarrow ArNHOH \longrightarrow ArN{=}O \longrightarrow ArNO_2$
Reduction	$ArNO_2 \longrightarrow ArNH_2$
Hydrolysis	

1.6.2 Phase II metabolism.

Most conjugation reactions occur during phase II metabolism.   During this metabolism, a large polar group is reacted with phase I products to increase the molecular weight and polarity of the metabolite.   These changes are designed not only to increase the water-solubility of the metabolite to aid the rate of excretion, but also to detoxify these phase I metabolites which are quite often reactive species. Examples of these metabolic pathways can be seen in Table **1.5**. The enzymes often implicated in these metabolic pathways include glucuronyltransferases (UGT), sulfotransferases (ST), glutathione-*S*-transferases (GST) and *N*-acetyltransferases (NAT). These enzymes metabolise a wide range of substrates.

Glucuronic acid conjugation, catalysed by UGT enzymes, is the most common method of phase II metabolism. The formation of *O*-, *N*-, *S*- and C-glucuronides are possible, with phenols, alcohols and carboxylic acids common substrates for this metabolism.

Sulfoconjugation also occurs during this metabolism, through addition of a sulfate group onto a nucleophilic part of a drug. This process is mainly limited to secondary alcohols, phenols and aryl amines. These reactions are catalysed by ST enzymes requiring 3'-phosphoadenosine-5'-phosphosulfate as the co-factor. Primary alcohols are unsuitable substrates for this metabolic pathway due to the formation of reactive sulfate conjugates.

GST enzymes will catalyse the reactions of electrophilic moieties, such as epoxides, alkyl halides and free radicals to form glutathione conjugates, which will undergo

further metabolism to mercapturic acids. The electrophilic metabolites will react with the thiol of the glutathione tripeptide. This method of metabolism is particularly useful in the removal of toxins or highly reactive electrophilic species. Carboxylic acids are often conjugated to amino acids (often glycine) during phase II metabolism following activation to a co-enzyme A thioester.

Table 1.5: Glucuronidation, sulfoconjugation and glutathione conjugation phase II metabolism pathways. UDP, uridine diphosphate; PAPS, 3'-phosphoadenosine-5'-phosphosulfate. Adapted from Introduction to Medicinal Chemistry.[34]

Chemical Reaction	Example
Glucuoronidation (phenols, alcohols, carboxylic acids)	
Sulfoconjugation (phenols, 2° alcohols, 1° amines)	
Glutathione conjugation (epoxides, alkyl halides, free radicals)	

Other less frequently used phase II reactions include amino acid conjugation and methylation conjugation. Methylation and acetylation reactions form less polar metabolites. Methylation occurs on substrates such as phenols, amines and thiols, and such reactions are catalysed by catechol *O*-methyltransferase and co-factor *S*-

adenosyl methionine. Acetylation of primary amines will also occur through use of the acetyl-coA co-factor.

The phase II metabolites are actively transported across the cellular membrane for excretion during phase III metabolism. This is often achieved using the adenosine triphosphate (ATP)-binding cassette family of transporters (primary active transporters) where ATP hydrolysis is required.[35] These transporters are found in the liver, brain, intestine and kidney and will prevent accumulation of metabolised xenobiotics.

Together, phase I and phase II metabolism affects the overall change of a drug and its chemical properties through functionalisation. Phase I metabolism, through addition of polar groups, prepares the drug for phase II metabolism, where often the pharmacological activity is terminated through addition of a larger functional group *e.g.* sulfate group, and this enhances excretion of the drug. These processes in effect, prevent accumulation of a potentially toxic therapeutic agent.

1.6.3 Adverse metabolic reactions.

There is significant variability of metabolic reactions and metabolite formation from patient to patient. This is not only due to the formation of toxic or reactive metabolite intermediates but also to many other contributing factors. All drugs are metabolised: Pro-drugs or active drugs are/can be metabolised to their active metabolites and/or toxic metabolites, as well as possible metabolism to an inactive compound, resulting in loss of activity. The variability of CYP P450 enzymes is a key factor when analysing the metabolism of a drug. There is a 10-fold variability of

CYP3A4[34] in humans and this can have a huge impact on the metabolism of a drug. Additionally, some patients will lack the correct isozymes, increasing any risk further. Certain chemicals can affect CYP P450 enzyme activity such as grapefruit juice, which inhibits CYP3A4.[36] DDIs can also have a significant effect on metabolism. Warfarin and cimetidine cannot be taken simultaneously as the latter inhibits CYP P450 enzymes, slowing the metabolism of warfarin and significantly impacting on drug plasma concentration levels.[37]

1.6.4 Drug metabolite formation inducing drug toxicity.

Further to enzymatic variability from patient to patient and DDIs, toxic metabolite formation is inevitable with select drug therapies and this is often found with type B ADRs. The pro-drug or active drug is metabolised to a reactive metabolite through a process known as bioactivation. This toxic metabolite, often possessing electrophilic properties, must have a long enough lifetime to accumulate within cells and undergo attack with cellular components or proteins.[38] An example of this is terfenadine, which presents serious side effects, through enzyme inhibition, if ingested with grapefruit juice. This enzyme inhibition prevents metabolism of the parent drug and accumulation of this drug leads to toxicity.

The formation of reactive metabolites can be formed from a large proportion of enzymes involved in drug metabolism and unsurprisingly, this form of toxicity is species dependent; the inter species difference in PK and PD properties is usually responsible for this.[39,40] Further to this, toxicity can be enantiomerically dependent *e.g.* thalidomide. Such reactive metabolites can cause toxicity through two major mechanisms: i.) Covalent binding to macromolecules or ii.) Non-covalent binding

20

e.g. induction of oxidative stress or lipid peroxidation.[41,42] Rather than a certain class of drug therapeutics contributing to drug-induced toxicity, it is the chemical functional groups that lead to the formation of such toxic metabolites. A small number of these include acetanilides *e.g.* acetaminophen; hydrazines *e.g.* isoniazid; amines *e.g.* procainamide and heteroatoms *e.g.* furosemide. A number of drugs known to form toxic metabolites *in vivo* are discussed here within.

1.6.4.1 Acetaminophen.

Acetaminophen is an analgesic drug that although is safe in therapeutic doses, a larger dose can cause serious hepatotoxicity, and possible kidney and ocular damage.[43,44] It is a widely studied drug and a key example of the toxicity associated with drug metabolism. Acetaminophen undergoes dehydrogenation through metabolism by CYP P450 enzymes to form *N*-acetyl-*p*-benzoquinoneimine (NAPQI) (Figure **1.4**).[21,45] NAPQI, a highly electrophilic species, is the metabolite responsible for acetaminophen toxicity.[21,46] At lower levels of NAPQI, glutathione is able to detoxify this metabolite through glutathione conjugation. However, at excess levels of NAPQI, glutathione levels are depleted resulting in liver protein thiol covalent binding (Figure **1.4**). Although, through oxidative stress, non-covalent binding has also been shown to occur along with the covalent pathway.[47]
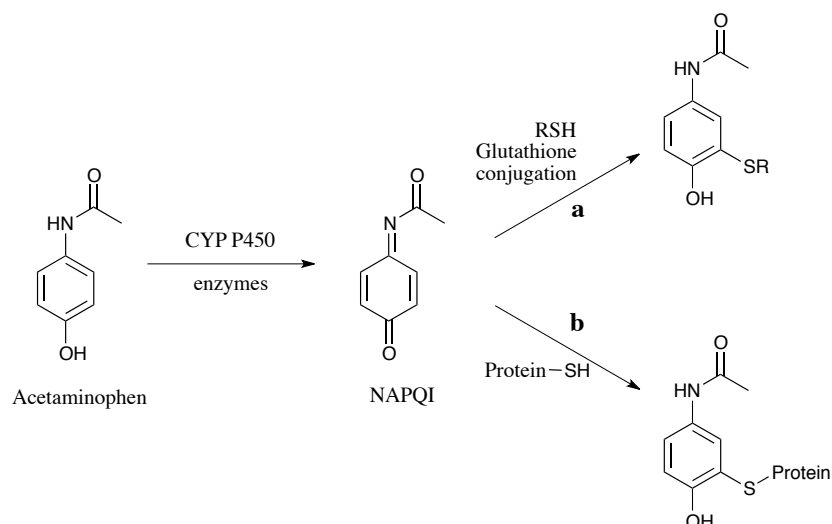
Figure 1.4: Metabolism of acetaminophen through a CYP P450-mediated dehydrogenation mechanism to the toxic metabolite, NAPQI, followed by detoxification through phase II glutathione metabolism (pathway **a**). Administration of a high dose of acetaminophen will result in high levels of NAPQI, leading to glutathione depletion. This depletion would result in NAPQI binding with liver proteins leading to hepatotoxicity (pathway **b**). NAPQI, *N*-acetyl-*p*-benzoquinoneimine.

1.6.4.2 Procainamide.

Procainamide (PA) is a class IA anti-arrythmic drug and through long-term use can cause hypersensitivity reactions, agranulocytosis and systemic lupus erythematosus syndrome (SIE). PA is metabolised to its equally active metabolite, *N*-acetylprocainamide. Alternatively, it can undergo metabolism to form a hydroxylamine intermediate (PAHA), which is in equilibrium with a highly reactive nitroso intermediate (Figure **1.5**). This intermediate is able to undergo covalent protein binding with hepatic proteins[48-50] and histone protein.[49] This has also shown to be the case with SMX, where SMX is also metabolised to a toxic nitroso metabolite, which has been shown to form protein adducts.[22] Outside of the liver, Uetrecht *et al.* had shown the binding of this reactive metabolite to activated

monocytes,[51] leading to the stimulation of T-cells and antibody synthesis,[52] resulting in immunological toxicity.
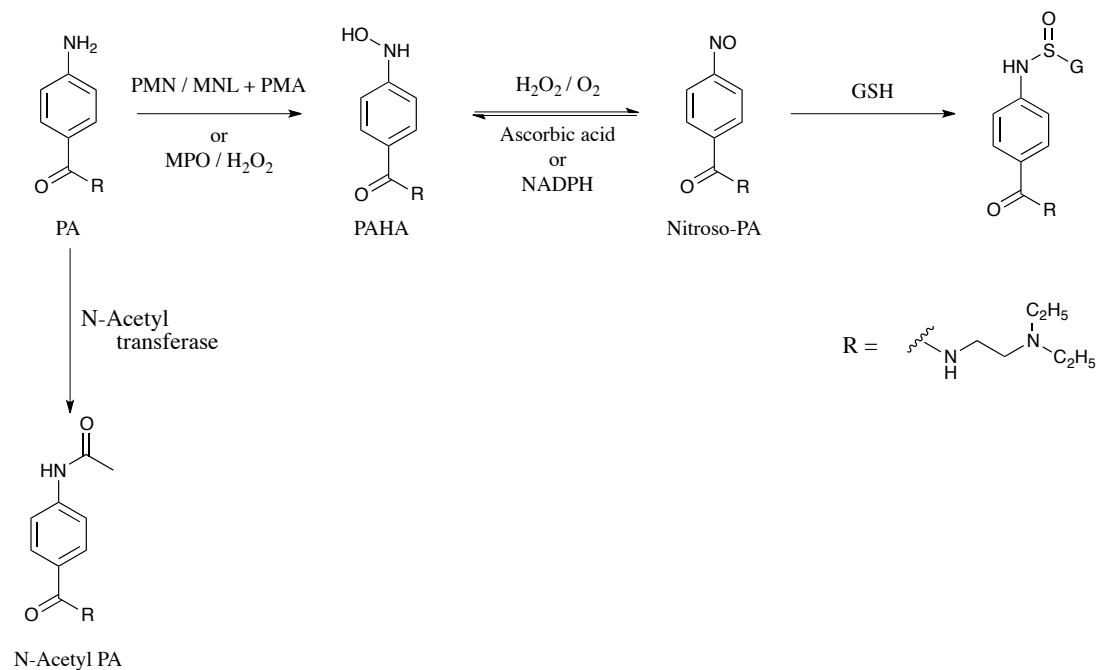

Figure 1.5: Metabolism of procainamide (PA) to its active metabolite *N*-acetyl PA. Alternatively, PA can be metabolised to a hydroxylamine intermediate (PAHA), which is in equilibrium with nitroso-PA. Nitroso-PA has been shown to undergo covalent protein binding with hepatic and histone proteins leading to its associated toxicity. PMN, polymorphonuclear leukocytes; MNL, mononuclear leukocytes; PMA, phorbol myristate acetate; MPO, myeloperoxidase. Adapted from Uetrecht *et al*.[49,53]

1.6.4.3 Cyclophosphamide.

An additional example of the formation of toxic metabolites can be shown with cyclophosphamide (Figure **1.6**), which is used as an alkylating or immunosuppressive agent. It is a pro-drug, which once administered is metabolised by CYP oxidases to 4-hydroxycyclophosphamide. This compound is in rapid equilibrium with its acyclic equivalent, aldophosphamide.[54] From here, oxidation of

4-hydroxycyclophosphamide to 4-ketocyclophosphamide or aldophosphamide to carboxyphosphamide can occur enzymatically.[54] This metabolic pathway is in competition with a non-enzymatic pathway through a β-elimination mechanism to form phosphoramide mustard (PM), which is the actively cytotoxic compound. However, this metabolic pathway also yields acrolein.[54] Acrolein is highly reactive and has shown to cause bladder toxicity.[55] This toxicity can be alleviated by increasing fluid intake and through administration of sulfhydroxyl donor compounds *e.g.* sodium-2-mercaptoethane sulfonate (mesna). Additionally, PM and acrolein are associated with teratogenicity[56] and nornitrogen mustard (NM), a metabolite of PM, has shown to contribute to the mutagenicity and carcinogenicity associated with this drug.[57]
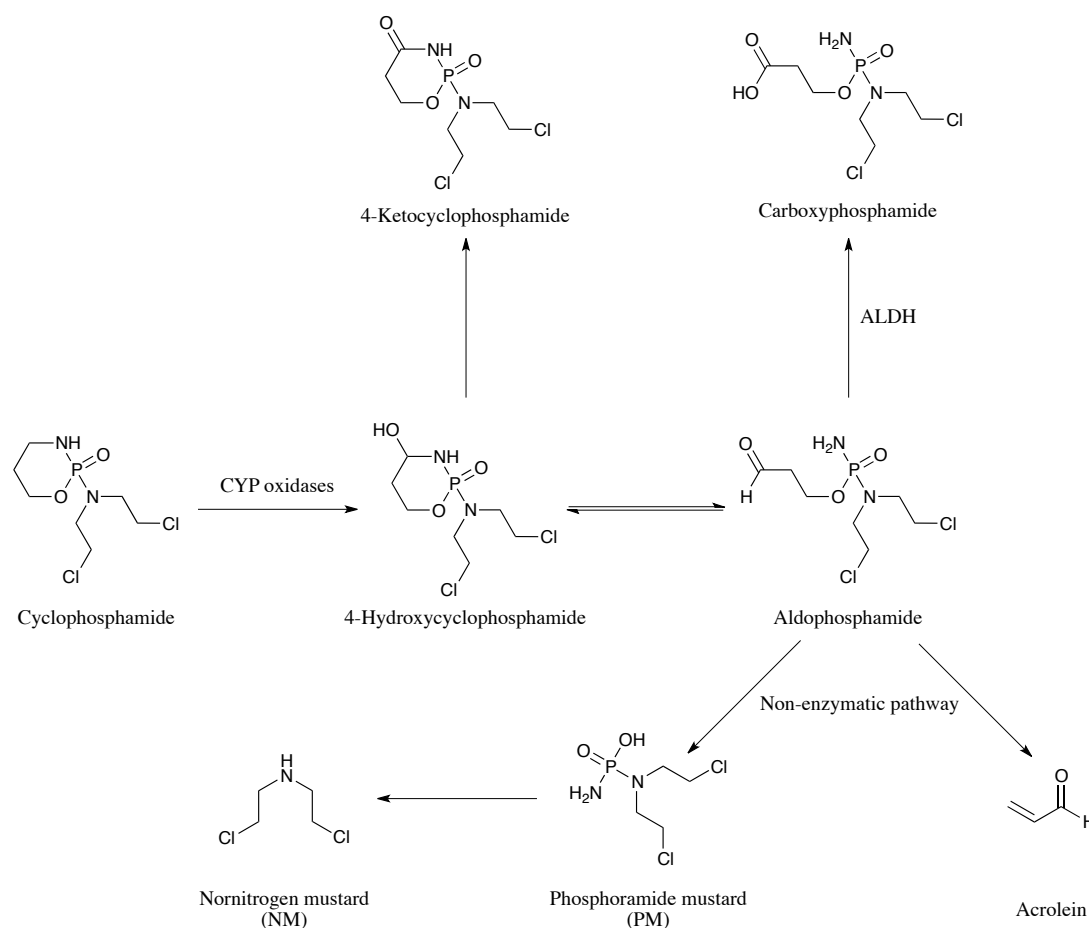
Figure 1.6: Metabolism of cyclophosphamide to a variety of metabolites, of which PM is the active metabolite. However, PM can contribute to its toxicity (teratogenicity), along with acrolein (bladder toxicity) – a highly reactive by-product of this metabolic pathway. Further to this, NM has also shown to contribute to mutagenic and carcinogen toxicity associated with this drug. PM, phosphoramide mustard; NM, nornitrogen mustard; ALDH, aldehyde dehydrogenase. Adapted from Foster *et al.*[54]

The examples in Figure **1.6** demonstrate key structural toxicophores present in three drugs that become evident post drug metabolism. Structure–activity relationship (SAR) studies are often required to abolish these drug metabolism related toxicities.

1.7 Structure–Activity Relationship

With a selection of marketed therapeutic reagents responsible for ADRs, there has been much research into the elimination of their associated toxicities and this is often achieved in a SAR fashion. SAR relates a 3D chemical structure of a drug to its properties or biological activity. It has often been utilised to improve a drugs therapeutic activity, reduce toxicological issues and to probe mechanisms of drug mechanisms; either to determine a drugs pharmacophore, binding interactions, drug optimisation or within a toxicological sense. In improving a drugs therapeutic value, it is essential that the drugs pharmacophore is not lost and its associated toxicological issues are ideally eliminated. SAR is employed not only as a useful tool for medicinal chemists, but also in a biological and toxicological sense.

Whilst improving a drugs therapeutic value from a medicinal chemistry viewpoint, strong consideration must be taken into the metabolism of the drug. Drugs that must undergo metabolism to produce their high toxic effects can be modified to prevent toxic metabolite formation, through the use of SAR and isosteres. Known functional groups that are avoided in drug design to avoid such metabolic liabilities include aromatic nitro and amine compounds and hydrazines.[34]

During SAR studies, it is standard practice to use (bio)isosteres for analogue synthesis. Isosteres are atoms or groups of molecules that have similar chemical or physical properties whilst maintaining the same valency. Bioisosteres are functional groups that are used to replace other groups of atoms whilst maintaining the drugs therapeutic value. Bioisosteres are often used when a functional group that is key to

the drugs activity also contributes to its toxicity. A selection of classical bioisosteres can be seen in Table **1.6**.

Table 1.6: Example classical bioisosteres used within drug discovery and drug optimisation as well as for probing mechanistic pathways. Adapted from Meanwell.[58]

Valency	Bioisosteres
Monovalent	D or F and H
	NH and OH
	F, OH, NH_2 and CH_3
Bivalent	C=C, C=N, C=O
	$-CH_2-$, $-NH-$, $-O-$
	$RCOR^1$, $RCONHR^1$, $RCOOR^1$
Trivalent	R_3CH, R_3N
	Alkene, Imine
	$-CH=CH-$ and $-S-$

1.7.1 Case study: Nimesulide.

There are many examples where an SAR approach has been used to improve a drug, such as modifications to achieve increased potency, improve PK parameters, or to reduce toxicity. An example of where an SAR approach has been key to identifying and eliminating reactive metabolites whilst improving potency is seen with nimesulide **1** (Figure **1.7**). Nimesulide is within the non-steroidal anti-inflammatory drug (NSAID) class of drug compounds and more specifically, it is a COX-2 inhibitor. This drug has a poor safety profile and as a consequence, it has either failed to reach the drug market in many countries, or where it has been marketed, it has subsequently been withdrawn.[59] Compound **1** is responsible for an idiosyncratic but rare hepatotoxicity.[59] Once the drug is metabolised by CYP P450 enzymes, an amino *des*-nitro compound **2** is formed and upon further oxidation by CYP2C19 and

27

CYP1A2, a diiminoquinone intermediate **3** is formed (Figure **1.7**). This is a highly reactive electrophilic species, which has shown to irreversibly alkylate human serum albumin (HSA) *in vitro* to form adducts **4**.[59] Such adducts can exhibit antigenic properties.[4,60] Further to this, it was found that this reactive metabolite also irreversibly inhibited CYP2C19, postulated to result from covalent bonding of the drug to amino acids in the enzymes active site.
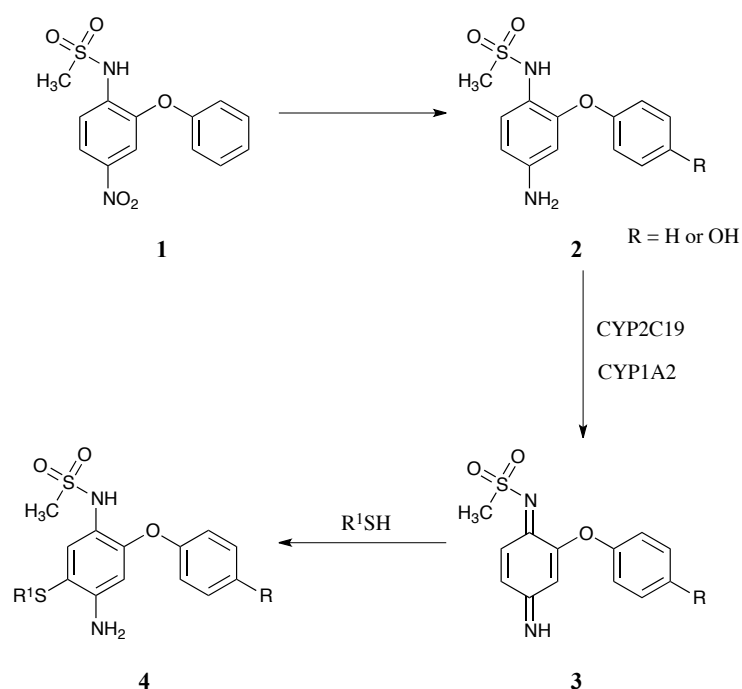

Figure 1.7: Reductive metabolism of nimesulide **1** to form an amino *des*-nitro intermediate **2**. Upon oxidation by CYP2C19 and CYP1A2, a diiminoquinone species **3** is formed. This species can undergo electrophilic reactions with thiol proteins forming potential antigenic adducts **4**.

To improve, not only the safety profiles of this drug, but also the potency, several SAR studies were conducted.[61,62] To overcome the formation of the diiminoquinone intermediate, the benzene ring was replaced with pyridine.[61] Further to this, the alkyl sulfonamide was replaced with a trifluoromethane sulfonamide and the bridge between the two aromatic moieties was also probed; with a secondary amine linkage

showing the most promising results (Figure **1.8**).[62] Compound **5** was shown to have increased potency and reduced toxicity than the parent drug but was less selective for COX-2.[62]

Increasing COX-2 potency

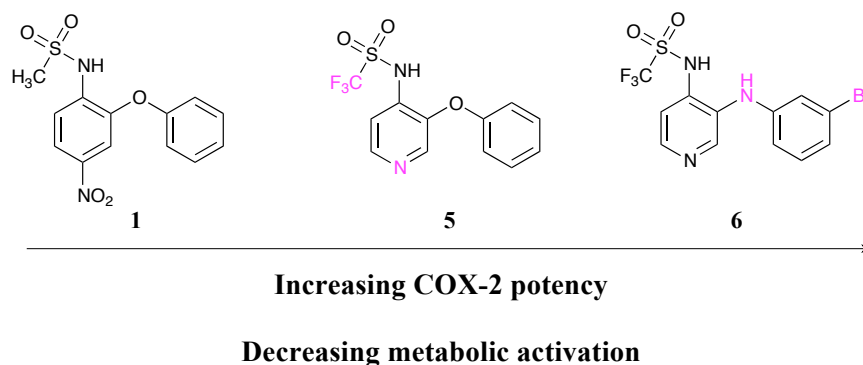**Decreasing metabolic activation**

Figure 1.8: To reduce toxic metabolite formation and improve potency, SAR studies for nimesulide **1** were completed. The most promising compounds **5** and **6** from the first and second studies respectively are shown. Compound **5** shows replacement of the benzene ring with pyridine and the alkyl sulfonamide moiety was replaced with a trifluoromethane sulfonamide. Compound **6** was developed from compound **5** through replacement of the oxygen linker with an amine linker and benzene substitution with bromine. SAR, structure–activity relationship.

To improve **5** further, the benzene ring was probed with a halogen, alkyl or alkoxy chain substitution and replacement with cycloalkyl rings (Figure **1.8**).[62] Thirty-six analogues were synthesised in this SAR study and **6** showed the most promising results, with the highest COX-1/COX-2 inhibitory properties and improved anti-inflammatory activity and safety profile compared to **1**.

This example has shown that (bio)isosteric substitution of functional groups can not only reduce the formation of toxic reactive metabolites, but also improve the potency of a drug.

1.7.2 2',3'-dideoxynucleoside compounds: Use of isosteres to reduce compound toxicity.

Deoxynucleosides have been shown to be extremely effective against viruses, in particular, human immunodeficiency virus (HIV) treatment. However, this class of compounds can cause a delayed clinical toxicity through inhibition of mitochondrial DNA (mtDNA) synthesis.[63] A range of 2'- and 5-fluorinated deoxynucleosides were synthesised (isosteric substitution of H with F) by Tsai and co-workers (Figure **1.9**),[63] and the 2'-β-fluorinated analogues were much less potent for inhibiting mtDNA with only slightly decreased activity against the HIV virus, compared to their non-fluorinated compounds. It was discovered that β-F-ddC was 5000 times less potent than its non-fluorinated equivalent, ddC (Figure **1.9**). The effect of 2'-β-hydrogen substitution for fluorine decreases the likelihood of reducing mtDNA synthesis.
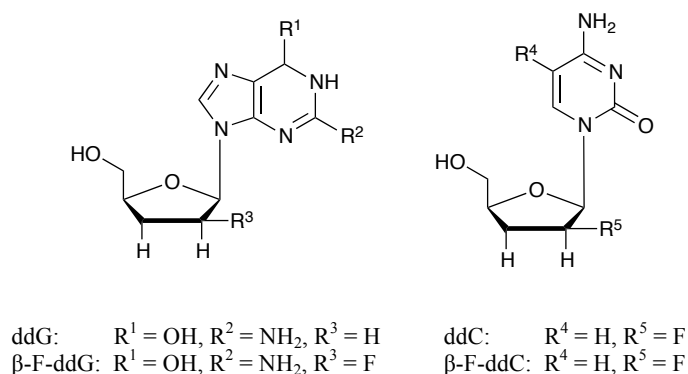

ddG: R^1 = OH, R^2 = NH$_2$, R^3 = H   ddC: R^4 = H, R^5 = F
β-F-ddG: R^1 = OH, R^2 = NH$_2$, R^3 = F   β-F-ddC: R^4 = H, R^5 = F

Figure 1.9: A selection of non-fluorinated and 2'- and 5-fluorinated deoxynucleosides synthesised by Tsai *et al.*[63] to reduce deoxynucleoside toxicity: Demonstrated through inhibition of mtDNA. It was shown that the 2'-β-fluorinated analogues were much less potent for inhibiting mtDNA compared with their deoxynucleoside equivalents.

1.8 Abacavir

A model compound that probes the HLA association with DTH is ABC. ABC **7**, Figure **1.10**, is a drug used within highly active antiretroviral therapy (HAART) in the treatment of the HIV-1 virus. It is less commonly used alone as Ziagen® and more commonly in combination therapy with lamivudine (Kivexa™) or lamivudine and zidovudine (Trizivir™). Patented in 1998 by GlaxoSmithKline (GSK), it has been a well-utilised drug in antiviral therapy.

The structural foundations of ABC were developed from carbovir (CBV) **8** (Figure **1.10**), an anti-HIV drug that was designed in the late 1980s. CBV showed high potency against the HIV-1 virus *in vitro*, however, it was also associated with toxicity resulting from its low aqueous solubility and this impacted on its oral absorption.[64,65] Further to this, CBV was shown to have difficulties in crossing the central nervous system (CNS)[64,66] and these problems led to CBV being ineffective as a marketable HIV drug. In order to resolve these problems, a library of novel carbocyclic analogues, based upon the CBV structure, were designed and ABC showed the most promising results.

ABC falls within the nucleoside reverse transcriptase inhibitor (NRTI) class of HIV therapy as it acts as a DNA chain terminator, due to the lack of a 3'-OH group (replaced with a 2',3'-unsaturated bond). ABC is an analogue of guanosine **9** (Figure **1.10**) and aside from the removal of the 3'-hydroxyl group, a carbocyclic ring replaces the sugar moiety, and a cyclopropylamino group is present at the 6-position.
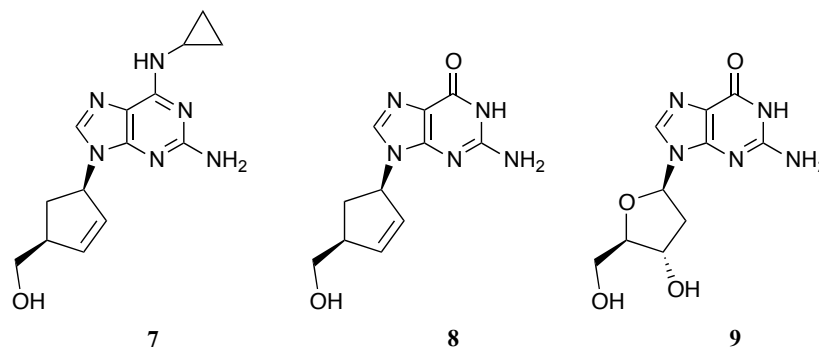
Figure 1.10: Abacavir, **7** (ABC), carbovir (CBV) **8** and guanosine **9**.

ABC is responsible for a potentially life-threatening type IV hypersensitivity reaction (ABC-HSR) in patients whom possess the HLA-B*57:01 allele.[30,67] Symptoms of ABC-HSR reaction include fever, nausea, headache, skin rash and respiratory and gastrointestinal problems.[68] These symptoms usually appear within 6 weeks of commencing treatment and stops within 72 hours of discontinuing the drug.[24] Any re-challenge with the drug can cause more serious and life-threatening conditions with quicker on-set of symptoms.

1.8.1 ABC-HSR and HLA association.

There is a strong association of ABC-HSR with the HLA-B*57:01 allele. Two independent studies conducted in 2001 connected the presence of the allele HLA-B*57:01 in those patients who displayed symptoms of ABC-HSR.[30,67] Both studies were performed on a cohort of 200 patients. Hetherington *et al.* found the association of this allele to patients with suspected ABC-HSR to be 55%, compared to 1% control population.[67] Mallal *et al.* reported this association in 78% of patients, compared to 2% in the control population, although this study was almost exclusively Caucasian origin.[30] In a further study, toxicity was found to be race dependent, reflecting occurrence of the HLA-B*57:01 allele, with a higher incidence

rate seen in Caucasians and Hispanics in comparison with other ethnic groups.[69,70] As a result of these findings, patients who wish to commence ABC treatment must undertake a patch test to determine the presence of the HLA-B*57:01 allele. This non-invasive procedure has a 99% success rate[71,72] and any patients who present a positive result are denied ABC therapy. This efficient test effectively eliminates toxicity from ABC in susceptible patients.

1.8.2 Metabolism and pharmacology of ABC.

The pharmacology of ABC has been extensively studied.[73-75] ABC itself is a prodrug. Following the major anabolic pathway (Figure **1.11**): It initially undergoes phosphorylation to form abacavir monophosphate (ABC-MP) **12**, and then undergoes a deamination reaction by a cytosolic deaminase[76] to form carbovir monophosphate (CBV-MP) **13**. Finally, following further phosphorylation *via* carbovir diphosphate (CBV-DP) **14** to its triphosphate form (CBV-TP) **15**, the active drug is produced. This pathway bypasses the direct formation of CBV and so the problems associated with CBV are eliminated.
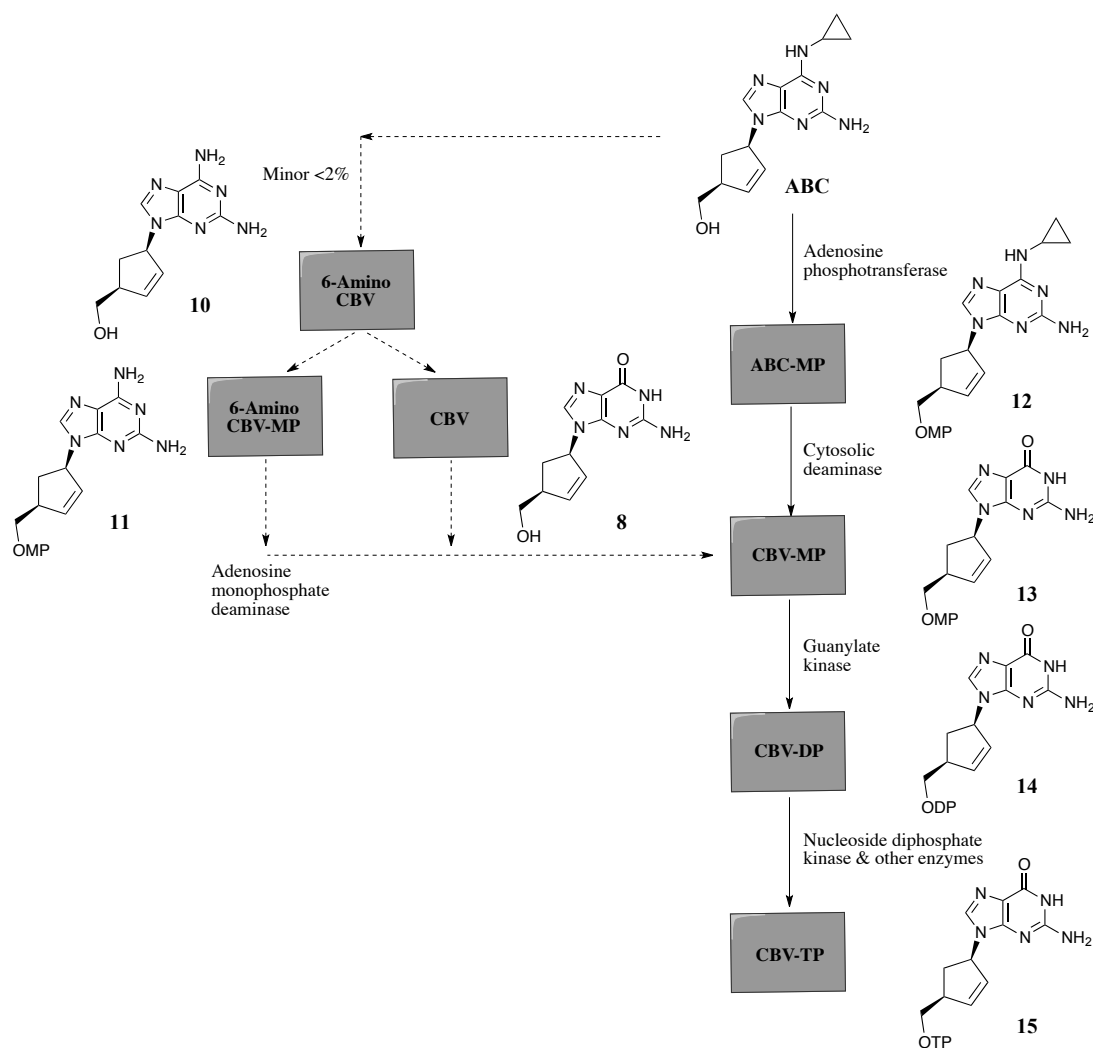
Figure 1.11: *In vivo* metabolism of ABC **7** to the active compound CBV-TP **15**. Following the major anabolic pathway: ABC undergoes phosphorylation to form ABC-MP **12** and this metabolite is oxidised by a cytosolic deaminase to form CBV-MP **13**. Further phosphorylation yields CBV-TP **15** as the active compound. Alternatively, less than 2% of ABC undertakes the minor pathway to form 6-amino CBV **10**, which is phosphorylated to form 6-amino CBV-MP **11**. Alternatively, **10** is oxidised to CBV **8**. The major pathway from **13**–**15** is then followed. ABC, abacavir; CBV, carbovir; CBV-MP, carbovir monophosphate; DP, diphosphate; TP, triphosphate. Adapted from Piliero *et al.*[75]

Two alternative metabolic pathways are shown in Figure **1.11**, but both ultimately form the active compound **15**.

1.8.3 Oxidative metabolism of ABC.

The final phase I and phase II metabolites of ABC, determined by MacDowell *et al.*[77] are a carboxylic acid **17a** and a glucuronide metabolite **18** (Figure **1.12**). Using ^{14}C-ABC to determine the presence of metabolites, in urine; 30% of the dose was **17a**; 36% as **18**; 1% as ABC itself and the final 16% as other metabolites, which have not all been characterised. For those that were determined, they were found to be isomers of the carboxylic acid metabolite. In faecal matter, the metabolites were mainly unmetabolised ABC and **17a**.
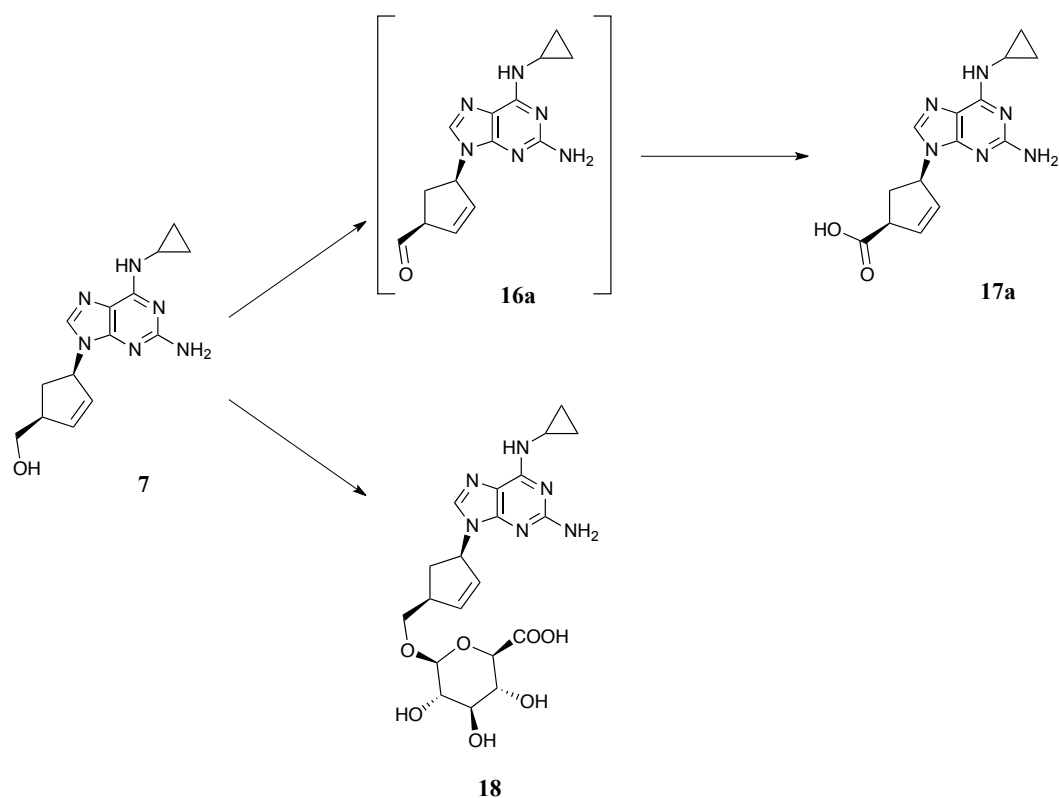

Figure 1.12: Basic phase I and phase II metabolic pathways of ABC **7**. ABC is metabolised during phase I metabolism to the carboxylic acid metabolite **17a** *via* an aldehyde intermediate **16a** or alternatively, it is metabolised during phase II metabolism to the glucuronide metabolite **18**. Adapted from Walsh *et al.*[78]

To probe this oxidation mechanism, it is important to understand the mechanisms of the enzymes involved in ABC metabolism: Liver alcohol dehydrogenase (ADH) and liver aldehyde dehydrogenase (ALDH).

1.8.3.1 Liver alcohol dehydrogenase.

ADH belongs to a class of oxidoreductase enzymes. There are 5 (I–V) classes of ADH and the genes that code for this class of enzymes are ADH1, ADH2 and ADH3. ADH class I is of the most abundance in the liver (85–90%)[79] and is most commonly associated with the oxidation of ethanol to acetaldehyde, although, the ADH enzymes are capable of oxidising a wide range of primary and secondary alcohols to their aldehydes and ketones[80] respectively. Three isoforms of ADH class I exist: ADH1A (α), ADH1B (β) and ADH1C (γ). In mammals, a molecule of nicotinamide adenine dinucleotide (NAD$^+$) is required for the reversible oxidation process[81-83] (Figure **1.13**) and an overall redox reaction occurs.
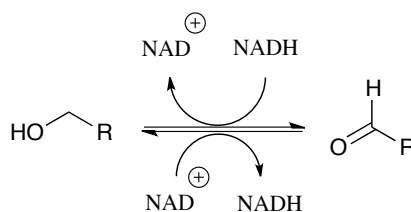

Figure 1.13: Oxidation of a primary alcohol to its aldehyde by ADH, using one molecule of NAD$^+$ as the co-factor. ADH, alcohol dehydrogenase; NAD$^+$, nicotinamide adenine dinucleotide.

1.8.3.1.1 Mechanism of ADH.

The mechanism of ADH is shown in Figure **1.14**. It is crucial for the oxidation that a zinc ion and an NAD$^+$ molecule are present.[84] Initially, Zn^{2+} co-ordinates with the primary alcohol and then hydride transfer occurs from His 51 through Ser 48, from the substrate alcohol onto the molecule of NAD$^+$.[85]
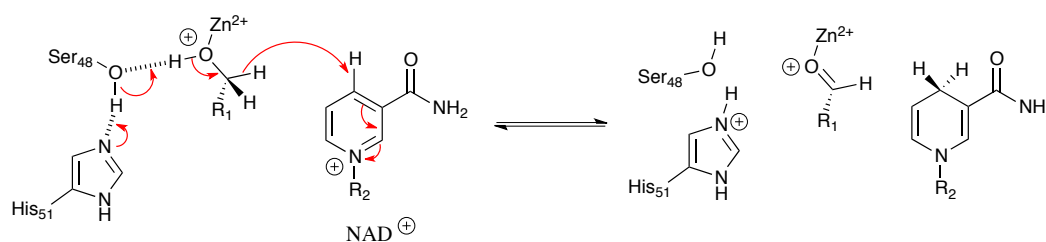

Figure 1.14: Mechanism of ADH, where a primary alcohol to oxidised to its aldehyde using a Zn^{2+} to co-ordinate and an NAD$^+$ molecule for hydride transfer. This occurs as a one-step process in which H is transferred through His 51 and Ser 48 from the alcohol substrate into a molecule of NAD$^+$. Adapted from Introduction to Enzyme and Co-Enzyme Chemistry.[85]

1.8.3.1.2 ADH and ABC oxidation.

As discussed in Section **1.8.3** and established by Walsh *et al.*,[78] ABC is oxidised to **17a** *via* an aldehyde intermediate **16a**. ADH completes the initial oxidation step with the second oxidation step potentially completed by ALDH (Figure **1.15**). ADH has been shown to also participate in this final oxidation step.[78] Two isoforms of ADH class I (ADH1A (αα) and ADH1C (γ2γ2)) have been found to oxidise ABC, as can be seen in Figure **1.15**.[78] Only the ADH1A isoform is involved in the oxidation to **16a** and formation of the different carboxylic acid isomers **17a**, **17b** and **17c**. ADH1C is also involved in the formation of **16a** but its products are isomers of ABC (**7b**, **7c**).
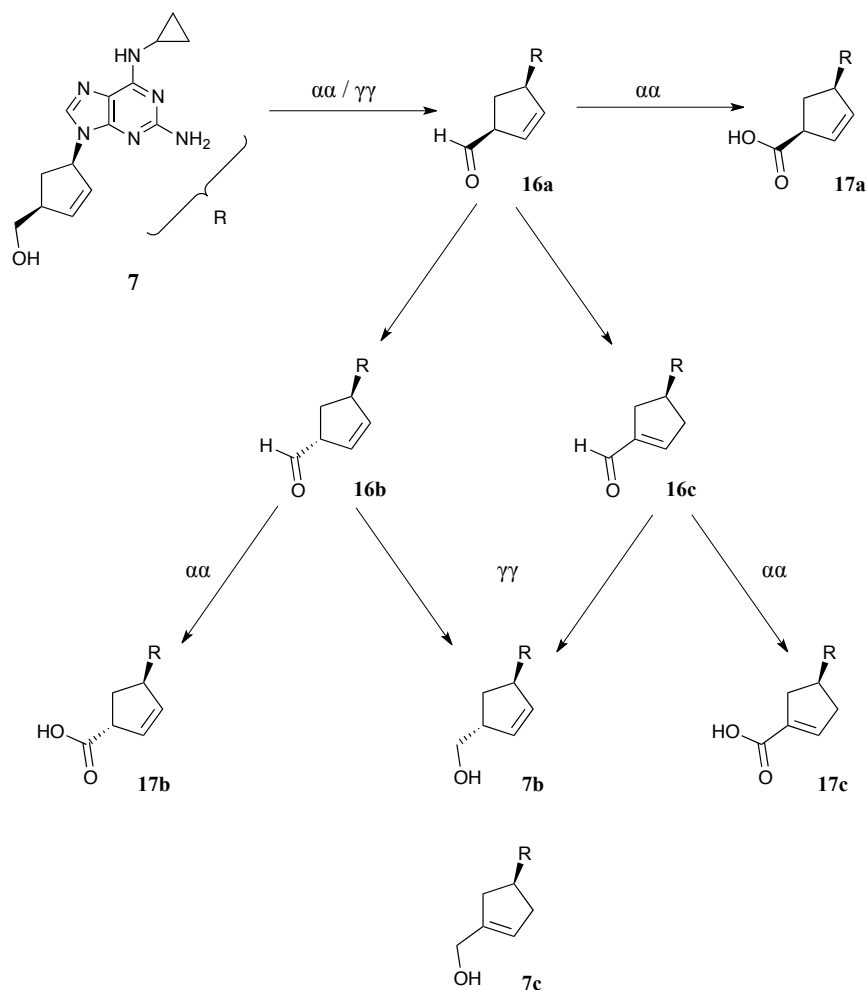
Figure 1.15: Oxidation of ABC **7** to the major carboxylic acid **17a** *via* an aldehyde intermediate **16a** through metabolism of ADH isozymes αα and γ2γ2. These ADH isoforms are also responsible for the formation of two alternative carboxylic acid metabolites (**17b** and **17c**) *via* their respective aldehyde intermediates **16b** and **16c**. Adapted from Walsh *et al.*[78]

1.8.3.2 Liver aldehyde dehydrogenase.

There are 3 different classes of ALDH (ALDH1, ALDH2, ALDH3) in humans, with classes I and II being most abundant in the liver.[86] ALDH enzymes are involved in the oxidation of aldehydes to their respective carboxylic acids. Aldehydes are highly reactive species that are formed in many endogenous metabolic pathways.[87] They react readily with a variety of nucleophiles *in vivo*, namely thiols, and so rapid

metabolism to their carboxylic acids is vital.[87] The oxidation process is $NAD(P)^+$ dependent and the enzymes act in an irreversible manner.[88] As determined through kinetic experiments with ADH, there is also ordered binding of co-factor and substrate with ALDH.[89,90] ALDH2 is the main contributing isozyme involved in acetaldehyde oxidation to ethanolic acid[88] and other substrates of ALDH include retinal, to form retinoic acid[91] and γ-aminobutyraldehyde, forming γ-aminobutyric acid (GABA).[87] Unlike the ADH enzymes, which have been extensively studied, significantly less literature can be found for the ALDH isozymes, with a proposed mechanism only suggested in 1999.[92]

1.8.3.2.1 Mechanism of ALDH.

Hempel *et al.*[92] determined the precise mechanism of ALDH (Figure **1.16**). The amino acids involved in hydride transfer are Cys 302, Glu 268 and Asn 169 with amino acids Glu 399 and Lys 192 used for $NAD(P)^+$ stability, *via* hydrogen bonding. Initially, Glu 268 extracts a proton from a molecule of water, which in turn extracts a proton from Cys 302. This activates the thiol group, which undergoes nucleophilic addition into the carbonyl group of the aldehyde. Through electronic arrangement, a hydride is transferred onto a molecule of $NAD(P)^+$, which is stabilised by Glu 300 and Lys 192. Another molecule of water undergoes nucleophilic addition into the thioester and the carboxylic acid product is released along with a molecule of NAD(P)H.
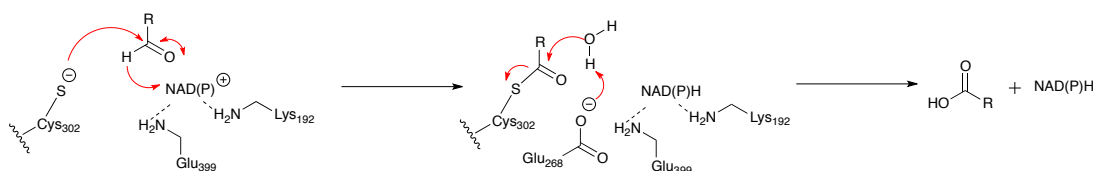
Figure 1.16: Mechanism of human liver ALDH. Amino acid residues Glu 399 and Lys 192 undergo hydrogen bonding with co-factor, NAD(P)$^+$. The thiol group of Cys 302 is activated and undergoes nucleophilic addition into the carbonyl group of the aldehyde substrate with hydride transfer onto NAD(P)$^+$. The thioester undergoes nucleophilic substitution with a molecule of water, through assistance with Glu 268, forming the carboxylic acid product. NAD(P)$^+$, nicotinamide adenine dinucleotide (phosphate).

1.8.3.2.2 ALDH and ABC oxidation.

To date, no research has been published which confirms that aldehyde **16a** is oxidised to carboxylic acid **17a** by ALDH, but as stated earlier, it is possible that this can occur by ADH1A.[78] However, it cannot be ruled out that ALDH may contribute to the ABC oxidation process.

1.8.4 ABC metabolism applied to ABC-HSR: Hapten hypothesis.

With the developing knowledge of drug metabolites associated with ADRs and in particular hypersensitivity reactions, it is formally recognised that aldehyde metabolites could act as haptens and have been connected with (idiosyncratic) adverse reactions.[93,94] With this knowledge, it was suggested that ABC toxicity arose from the formation of a reactive aldehyde metabolite.[78]

Within this research, Walsh *et al*. showed with pure isoforms of ADH (αα and γ2γ2), that ABC was metabolised to **17a** *via* **16a**. This aldehyde was trapped with methoxylamine forming compound **19** (Figure **1.17**), and this was the only method of

detection due to the short half-life of this intermediate. Metabolism was blocked using 4-methylpyrazole (4-MP), a known inhibitor of ADH, and furthermore, ABC-protein adducts were detected: The structures of these were unknown. Incubations with dihydro-abacavir (DH-ABC) **20** (Figure **1.17**) showed less ABC-protein adduct formation, suggesting involvement of the 2',3'-unsaturated bond in adduct formation.
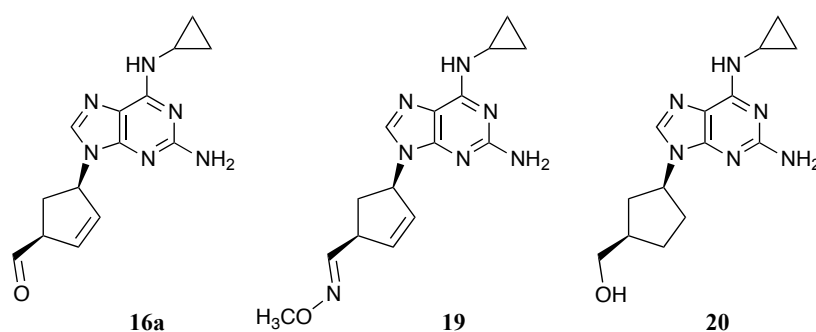

Figure 1.17: Compounds: Aldehyde **16a**; 'trapping' product of **16a** with methoxylamine to form compound **19** and DH-ABC **20**. DH-ABC, dihydro-ABC.

α,β-Unsaturated aldehydes can react *via* two mechanisms with proteins: Schiff base or 1,4-Michael addition. Both mechanisms would form a protein–drug metabolite conjugate leading to a possible T-cell mediated immune response.[4] The work presented by Walsh and co-workers supported a hapten hypothesis.

1.8.5 The hapten hypothesis *vs.* p-i mechanism for ABC toxicity.

Chessman *et al*. conducted a thorough immunological investigation into ABC-HSR. Chessman and co-workers found that CD8^{+} T-cells were activated by ABC, measured by an increase in cytokine release, interferon-γ (IFN-γ) and tumour necrosis factor-α (TNF-α). This study was conducted using CD8^{+} T-cells from both HLA-B*57:01 ABC naïve patients and those patients who had previously

experienced ABC-HSR.[95] Further to this, Chessman *et al*. were able to eliminate any involvement from the HIV-1 virus from use of T-cells obtained from healthy, normal individuals. It has been proposed that for an immune response, the MHC-I antigen presentation pathway is required[95] suggesting relation to the hapten hypothesis and as shown by Chessman *et al*., unmodified ABC was insufficient to stimulate the T-cells.

Chessman *et al*. found slight amino acid variations, namely 114 Asp-Asn and 116 Ser-Tyr (HLA-B*57:03) within the HLA-B*57:01 allele altered MHC presentation and affected the T-cell response. A >50% reduction in IFN-γ release was observed with 114 Asp-Asn, and a T-cell response from 116 Ser-Tyr was completely eliminated. Amino acid 116 was of particular interest as it has key involvement in the structure of the F-pocket and influences the peptides that bind within the HLA-B*57:01 protein. This residue will only accommodate peptides with a particular C-terminal amino acid, namely Trp or Phe. Further to this, HLA-B*57:01 has previously shown to allow the binding of peptides with Tyr at the C-terminus showing that polymorphism within the F-pocket can alter the peptide repertoire.[96] These amino acid alterations (residues 114 and 116) could affect both covalent and non-covalent binding leading to postulate that both the hapten and p-i hypotheses are applicable. At the onset of this work, no *in vivo* haptenated-ABC product had been isolated.

The p-i mechanism for ABC-HSR is also yet to be proven: The residues that differ HLA-B*57:01 from HLA-B*57:03 (an allele that does not induce ABC-HSR) do not interact with the TCR directly so the p-i mechanism may not be appropriate. Further

to this, McCluskey *et al*. have shown that ABC undergoes the antigen-processing pathway: It is TAP and tapasin protein dependent demonstrating that the p-i mechanism is not applicable.[97]

The work undertaken by Chessman and co-workers led them to postulate that 6-cyclopropylamine had involvement in ABC-HSR due to the lack of T-cell response against CBV, didanosine and guanosine. They concluded that ABC, or a derivative of ABC, conjugates with a self-peptide to form a haptenated immunogenic compound and either this immunogen, ABC itself or a metabolite of ABC is accommodated within the F-pocket of HLA-B*57:01.

1.8.6 Altered repertoire mechanism.

A mechanism, newly proposed while this study was in progress, has been applied to both ABC, and less so to CBZ, toxicity.[29] The proposal suggests that ABC binds directly within the HLA-B*57:01 allele and exhibits several stabilising interactions within a number of pockets of the protein.[98,99] These hydrogen bonding and van der Waals interactions allow ABC to bind well within the HLA protein and in doing so, the normal selection of peptides presented to the TCR cannot bind and an altered set of peptides are displayed, initiating an immune response.[100] This mechanism is discussed further in Chapter 5.

1.8.7 Synthesis of ABC analogues.

To probe the suggested mechanisms of ABC-HSR, it would be essential to synthesise a range of ABC analogues using a SAR approach. Research and reviews of all possible total synthetic routes used to synthesise carbocyclic nucleosides is therefore key for this approach.

1.9 Carbocyclic Nucleoside Analogues

There is much interest for the use of nucleoside analogues as drug therapy, especially as antiviral and anticancer drugs.[101] However, several issues can develop with the use of this class of drugs: Problems with triphosphorylation to the active drug (nucleoside analogues are invariably administered as pro-drugs) and instability of the *N*-glycosidic bond in the presence of phosphorylases.[101,102] The latter problem has been overcome with the design and synthesis of carbocyclic nucleosides; where the furanose oxygen is replaced with a methylene group. This replacement much improves the metabolic stability of carbocyclic nucleosides in comparison to their glycosidic equivalents.[102-105] However, carbocyclic nucleosides are less active than their furanose equivalents.[106,107]

1.9.1 Synthesis of cyclopentyl carbocyclic nucleosides.

There has been vast research into the synthetic production of carbocyclic nucleosides. The formation of these compounds is achieved using three main methods[108,109] (Figure **1.18**): Nucleophilic substitution of hydroxycyclopentane with a nucleoside base;[110-112] palladium-catalysed allylic reactions between a cyclopentene pseudosugar and nucleoside base[113-115] and addition of a heterocycle to an

44

aminocyclopentane followed by further construction of the heterocycle moiety, forming a nucleoside base.[116-118]
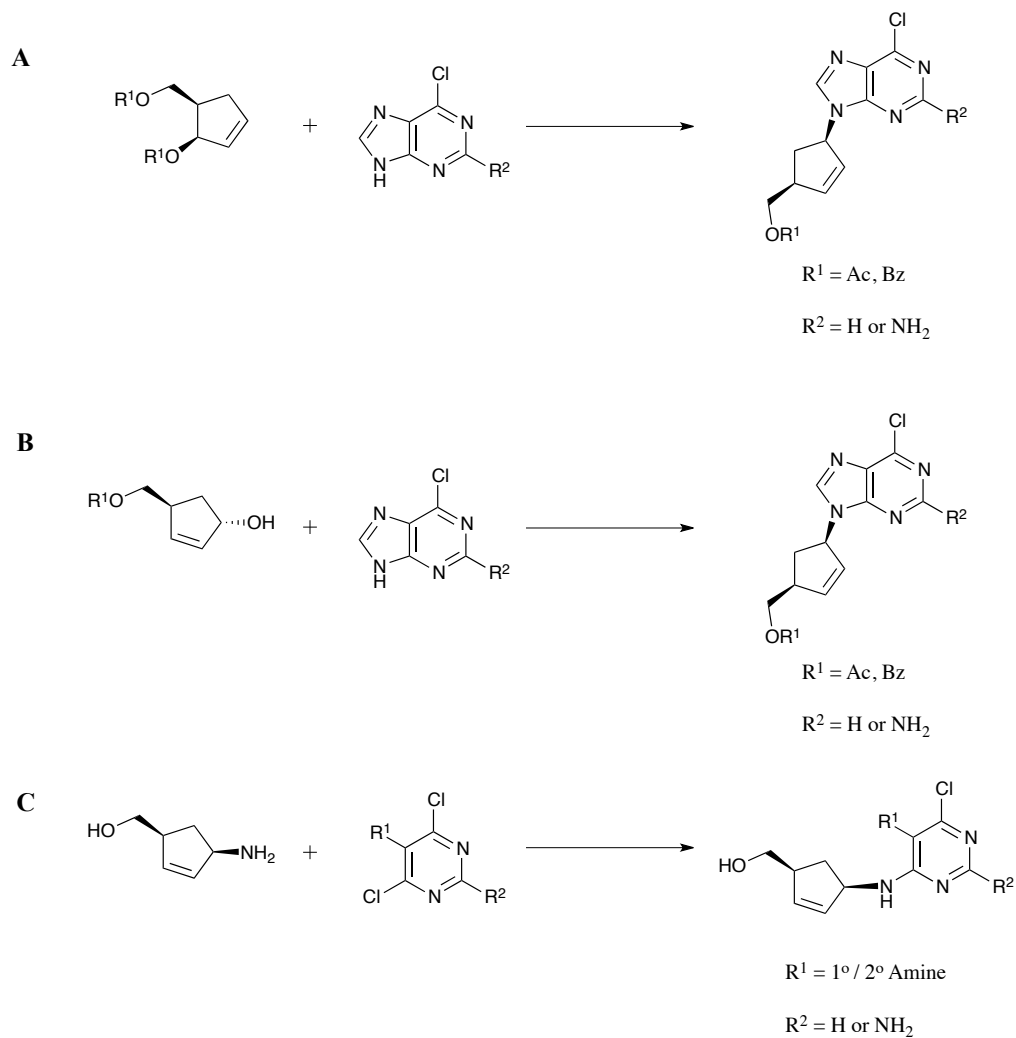

Figure 1.18: Three major methods used to synthesise nucleosides: Substitution of hydroxycyclopentane with a nucleoside base (**A**); palladium-catalysed allylic reactions between a pseudosugar and nucleobase (**B**) and addition of a heterocycle to an aminocyclopentane (**C**).

The synthesis of carbocyclic derivatives and analogues can be achieved using any of the aforementioned methods. The following discussion of these methods involves the synthesis of guanosine carbocyclic analogues only. The literature precedent for the synthesis of carbocyclic nucleoside analogues, in particular cyclopentyl analogues are vast and only a select number of examples are discussed here within. The synthesis of these compounds can be divided into two parts: Synthesis of carbocyclic pseudosugar and coupling/construction of the nucleoside base.

1.9.1.1 Construction of cyclopentene carbocycle.

The formation of the cyclopentene structure can be achieved *via* two methods: Ring closing of a linear structure using either the Wittig reaction or ring-closing metathesis (RCM) or alternatively using cyclopentadiene as the starting material.

Both Wittig and RCM conditions can be utilised to form the basic pseudosugar structure. The chiral starting materials are often carbohydrates[119-122] *e.g.* D-ribose, L-tartrate[123] or chiral auxiliaries.[124,125] RCM has become the most popular method for synthesising the pseudosugar compounds over using the Wittig reaction (Figure **1.19**).[102] This has been demonstrated by Choi *et al.*,[121] where D-isoascorbic acid was converted to lactol **21** over 4 steps. This compound was subjected to Wittig reaction conditions, using methyltriphenylphosphonium bromide and dimethylsulfoxide (DMSO) anion, to give exclusively stereoisomer **22**. Compound **22** underwent RCM, using Grubbs catalyst, to yield **23**, which was further oxidised using manganese oxide (MnO_2) forming cyclopentenone **24**. This target compound, compound **24**, can be used in carbocyclic nucleoside synthesis. In these RCM

reactions, it is often Grubbs catalyst (ruthenium-based) that is of choice, rather than Schrok catalyst (molybdenum) or Nugent & Jacobsen catalyst (tungsten).
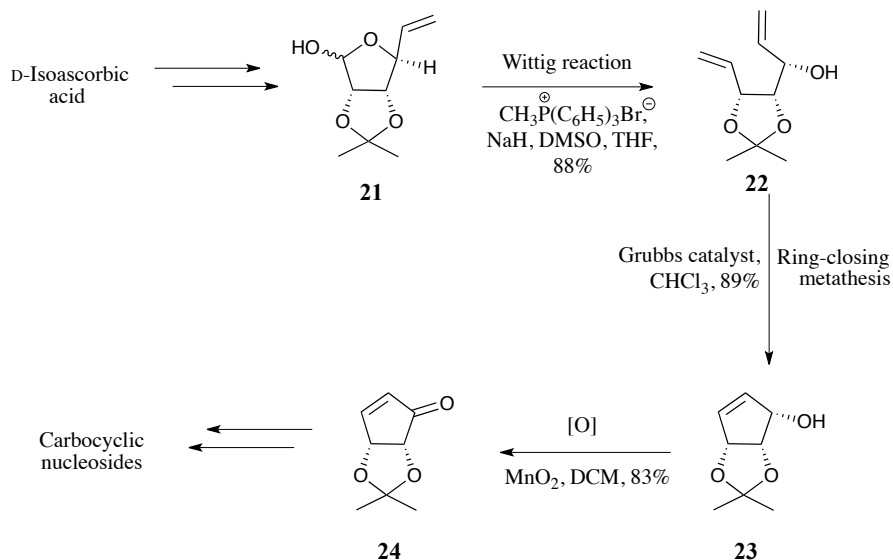

Figure 1.19: The synthesis of a pseudosugar intermediate can be achieved using a RCM approach from carbohydrate starting materials *e.g.* D-isoascorbic acid.[121] RCM is usually achieved using a ruthenium-based Grubbs catalyst. RCM, ring-closing metathesis.

Although scarcely used, other ring closing methods have been used to synthesise cyclopentene carbocycles. Such methods include aldol reactions,[126] radical cyclisation reactions[127] and transition metal-catalysed reactions using rhodium[128] or cobalt.[129]

Other than ring closing methods, cyclopentene carbocycles can be synthesised from cyclopentadiene. The most widely used methods are [4+2] Diels–Alder cycloaddition reactions, through use of molecular oxygen as the dienophile, to form cyclopent-4-ene-1,3-diol or formation of bicyclic lactams from addition of sulfonyl cyanides and isocyanate or nitrosocarbonyls.[102] The formation of cyclopent-4-ene-

1,3-diol from cycloaddition of O_2 is followed by reduction with thiourea and protection of the diol (acetate, benzoate or carbonate) to yield an intermediate **25** which is ideal for enzymatic catalysis.[130] This is followed by a Mitsunobu reaction with a nucleobase to yield compound **26**. Alternatively, the required product can be achieved using a palladium(0)- (Pd^0)-catalysed allylic substitution method utilising chiral ligands (Figure **1.20**). This has been shown to occur with retention of configuration [131,132] and has been applied in the synthesis of CBV **8**.[131]

25

26
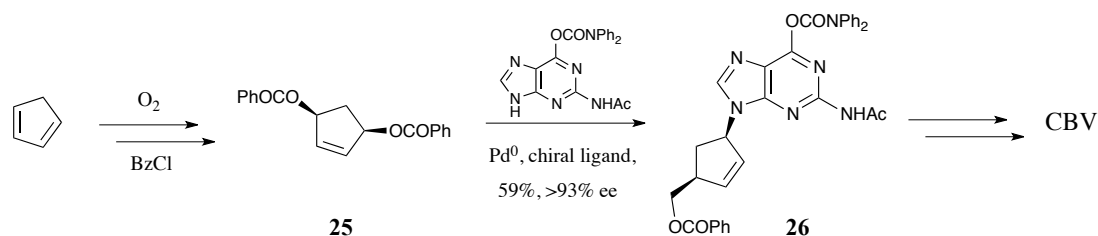
Figure 1.20: Cyclopentadiene will react with molecular oxygen to form cyclopent-4-ene-1,3-diol which can be di-protected, and this pseudosugar **25** can in turn undergo Pd^0-catalysed allylic substitution with a nucleobase to yield compound **26**. Relative stereochemistry is achieved with the use of chiral ligands. Application of this pathway has been shown by Trost *et al.* in the formation of CBV **8**.[132]

Although commercially available, Vince lactam (2-azabicyclo[2.2.1]hept-5-en-3-one) **28** (Figure **1.21**) can be synthesised from cyclopentadiene using toluene sulfonyl cyanide (TsCN) and chlorosulfonyl isocyanate *via* a thermodynamically controlled aza Diels–Alder cycloaddition to yield racemic compound **27**.[102] This is followed by enzymatic resolution using a γ-lactamase enzyme to yield Vince lactam **28**. Compound **28** has extended use in the synthesis of carbocyclic nucleosides. It is a particularly good intermediate for carbocyclic nucleosides where functionalisation

at the 2'- and 3'-positions of the pseudosugar is necessary. Hydrolysis of **28** would

yield amino-alcohol cyclopentene compound **29** (Figure **1.21**), which can undergo

further coupling with 2,5-diamino-4,6-dichloropyrimidine (DADCP) **30** to yield

compound **31**. A ring-closing reaction of **31** with triethylorthoformate (TEOF)

yields chloro-ABC (Cl-ABC) **32**.[133] This method is particularly useful for the

synthesis of purine carbocyclic nucleosides,[134] although through Pd[0]-catalysed allylic

substitution, pyrimidine carbocyclic nucleosides synthesis is also possible.[135] The use

of nitrosocarbonyl compounds in the hetero Diels–Alder cycloaddition reactions with

cyclopentadiene can also yield a bi-lactam intermediate that has valuable use,

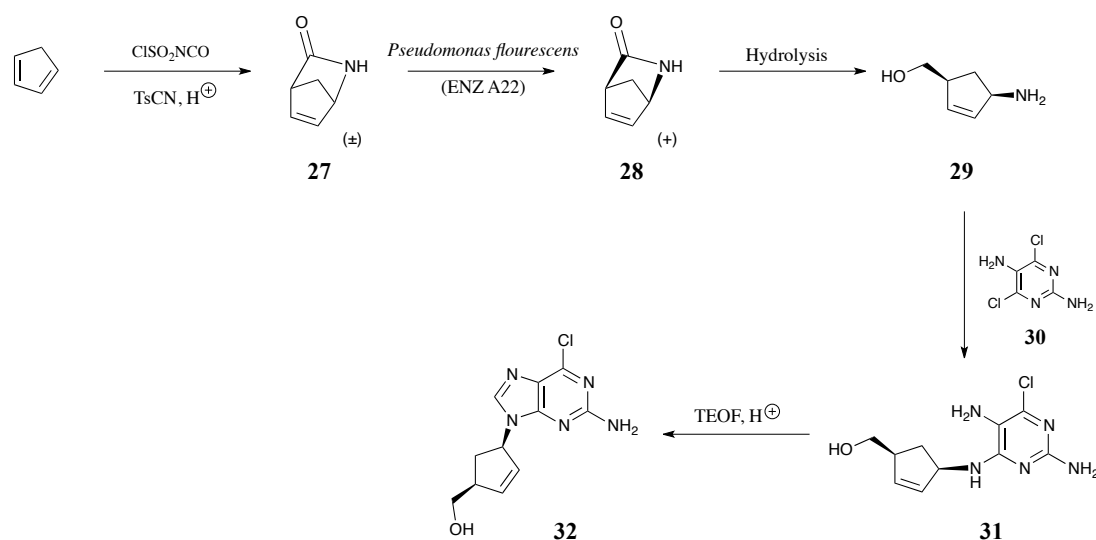especially in the synthesis of 5'-*nor* carbocyclic nucleosides.

Figure 1.21: Synthesis of Vince lactam **28** can be achieved from cyclopentadiene *via* racemic **27**.[102]

Hydrolysis of lactam **28** would yield amino-alcohol cyclopentene **29**. Following this, a heterocycle

coupling of **29** with **30** to yield intermediate **31** and ring-closing of **31** with TEOF can be utilised to

yield carbocyclic nucleoside **32**.[133] TEOF, triethylorthoformate.

Although less well utilised, [2+2] cycloaddition reactions also yield bi-lactam intermediates obtained through kinetic control of reactions of cyclopentadiene with chlorosulfonyl isocyanate.[136] The pseudosugar moieties can also be obtained from cyclopentadiene from an asymmetric hydroboration reaction[137] or through resolution of cyclopentene epoxides.[138]

1.9.1.2 Methods to couple cyclopentyl carbocycle and nucleobase moieties.

The addition of a nucleoside base to a carbocycle essentially occurs *via* an S_N2 mechanism. This process can be achieved *via* two major routes: A direct nucleophilic route, or construction of the nucleobase from a heterocycle base following addition into an aminocyclopentene intermediate.

Nucleophilic substitution of a hydroxy carbocycle with a nucleobase can be achieved using Mitsunobu reaction conditions or alternatively an alcohol-protected allylic carbocycle can be coupled with a nucleobase using a Pd^0 allylic substitution reaction (Figure **1.22**). Both methods are prevalent in nucleoside synthesis. The Mitsunobu method requires the presence of diethyl azodicarboxylate (DEAD) and triphenylphosphine (PPh$_3$) and substitution of a carbocyclic alcohol with either a pyrimidinic or purinic base occurs with inversion of configuration. Conversely, palladium-mediated coupling occurs with retention of configuration.
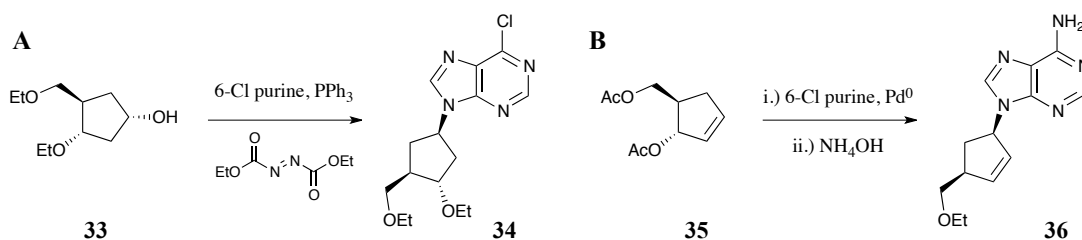
Figure 1.22: Example construction of carbocyclic nucleoside **34** from carbocycle **33** using the Mitsunobu reaction with inversion of configuration (**A**). Alternatively, this can be achieved using palladium(0)- (Pd⁰)-allylic substitution with retention of configuration, where di-protected alcohol **35** can be coupled with 6-Cl purine to form compound **36** (**B**).[102]

Construction of pyrimidinic and purinic bases can be achieved from addition of a heterocycle to an amino carbocycle (Figure **1.23**). The assembly of the nucleobase is dependent upon the carbocycle starting material. Using a carbocyclic amine, guanine bases can be constructed from coupling amine **37** to 5-amino-4,6-dichloropyrimidine to yield intermediate **38**. Following this, the addition of an amine group at the 2-position is achieved using benzene diazonium chloride (4-ClC$_6$H$_4$N$_2$$^+Cl^-$) and this is followed by reduction with Zn and acetic acid (AcOH) yielding compound **39**. The 6-Cl position can be modified as required to synthesise the required analogue. Alternatively, a ring-closing reaction of **39** creating the imidazole ring using TEOF in the presence of catalytic H$^+$, can yield product **40**.
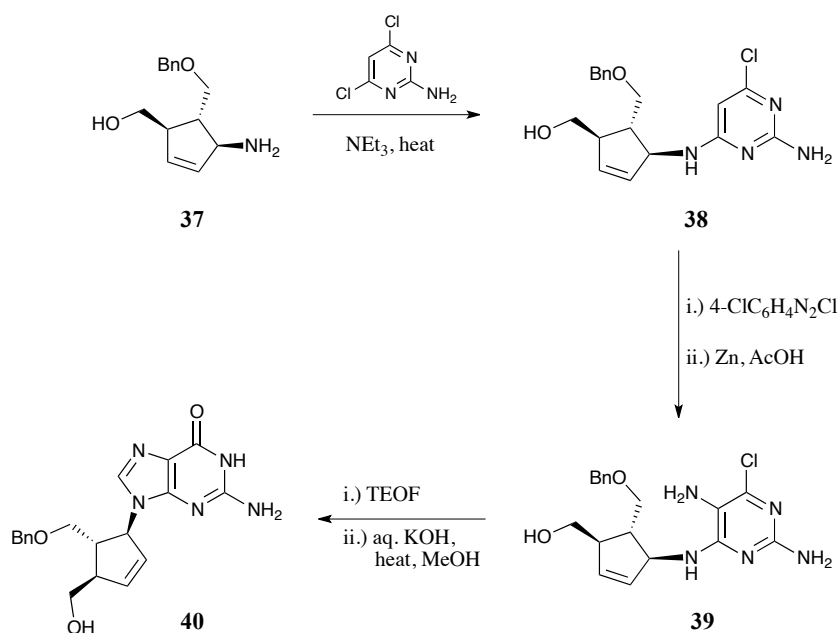
Figure 1.23: Linear construction of a purine carbocyclic nucleoside from an amino-alcohol pseudosugar **37** and a heterocycle, 5-amino-4,6-dichloropyrimidine. Following addition of the heterocycle to the carbocycle yielding **38**, NH_2 is placed at the 2-position using 4-$ClC_6H_4N_2^+Cl^-$ and Zn/AcOH to yield intermediate **39**. Ring-closing of compound **39** with TEOF followed by hydrolysis yields the guanine nucleobase **40**.[139]

Alternatively, the guanine-based moiety can be synthesised from coupling of DADCP **30** (Figure **1.21**) with a 1,4-disubstituted amino-alcohol carbocycle obtained from hydrolysis of Vince lactam. Formation of the imidazole ring is again achieved using TEOF and catalytic H^+. The applications of a variety of these synthetic routes to ABC are discussed in Chapter 4.

1.10 *In Vitro* Immunological Assays

Drugs or compounds that illicit, or are thought to induce, a $CD8^+$ mediated T-cell response can undergo a series of *in vitro* immunological assays to confirm or check induction of an immune response, as depicted and applied to ABC, in Figure **1.24**.

1.10.1 Lymphocyte transformation test.

One such assay that can utilised is the lymphocyte transformation test (LTT) which is used to check for DTH.[140] Cells, from a patient who has experienced a drug-induced idiosyncratic reaction, are incubated with this drug along with APCs and radiolabelled thymidine ($[^3H]$-thymidine). Should these T-cells be specific for this drug, proliferation will occur which can be monitored by uptake of $[^3H]$-thymidine into replicating lymphocyte DNA. These results can then be quantified, using a scintillation counter, to monitor the extent of proliferation, which is usually expressed as stimulation index (ratio of the proliferative response ± drug).
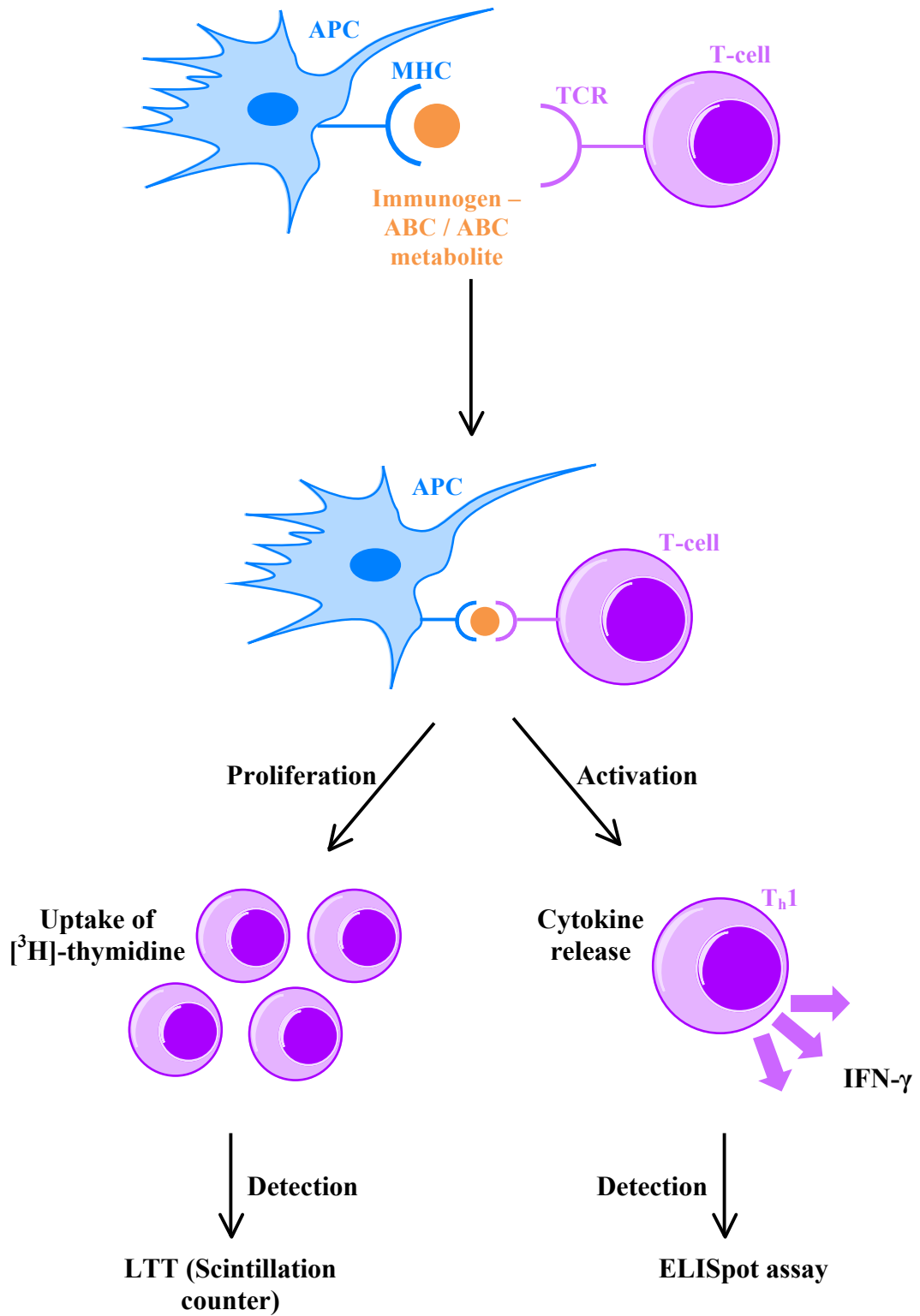
Figure 1.24: An APC displays an immunogenic molecule *via* the MHC to a T helper cell. The formation of such a complex causes the T-cell to become stimulated and such activation will result in cytokine release from T_h1 cells. One such cytokine, IFN-γ, can be detected using the ELISpot assay. The T helper cells will also proliferate once stimulated. The addition of radiolabelled thymidine to

proliferating T-cells will cause the uptake of [^{3}H]-thymidine into replicating DNA. The extent of proliferation can be quantified using a scintillation counter.

1.10.2 Enzyme-linked immunosorbent spot.

Alongside the LTT assay, a cytokine release assay (enzyme-linked immunosorbent spot (ELISpot)) can be used.[141] This assay allows the visualisation of cytokine release, where CD8$^+$ cytotoxic T-cells that have been stimulated will be shown as blue-black spots. The cells are incubated with the antigenic compound and should the T_h1 cells be stimulated, released cytokine (IFN-γ, TNF-α or IL-2) will be captured using a specific antibody.[142] Following this, a biotinylated monoclonal antibody and a chromogenic substrate are added.[142] The visualised spots can be counted, using an ELISpot reader, allowing the data to become quantitative with higher numbers of spot forming cells per well representing a larger cytokine release.

Both immunological assays will be used throughout this research to help probe the mechanism of ABC toxicity.

1.11 *In Vitro* Cytotoxicological and Pharmacological Assays

In addition to immunological assays pharmacological assays, in which the cytotoxicity and antiviral efficacy of the compounds will be measured. The assessment will involve the use of the spectrophotometric thiazolyl blue tetrazolium bromide (3-(4,5-dimethylthiazol-2-yl)-2,5-diphenyltetrazolium bromide, MTT) assay in MT4 cells. MT4 cells are a T-cell leukaemia cell line transformed by human T-cell lymphotropic virus-I (HTLV-I), is highly sensitive to infection by HIV-1 infection and routinely used to test efficacy of antiretroviral drugs.[143] MTT, a yellow colour, can be reduced to MTT formazan, a purple colour, in isolated cells and

tissues by mitochondrial enzymes and electron carriers[144,145] and this indicator of 'cell redox activity' can be used to determine cell viability (Figure **1.25**).[146]
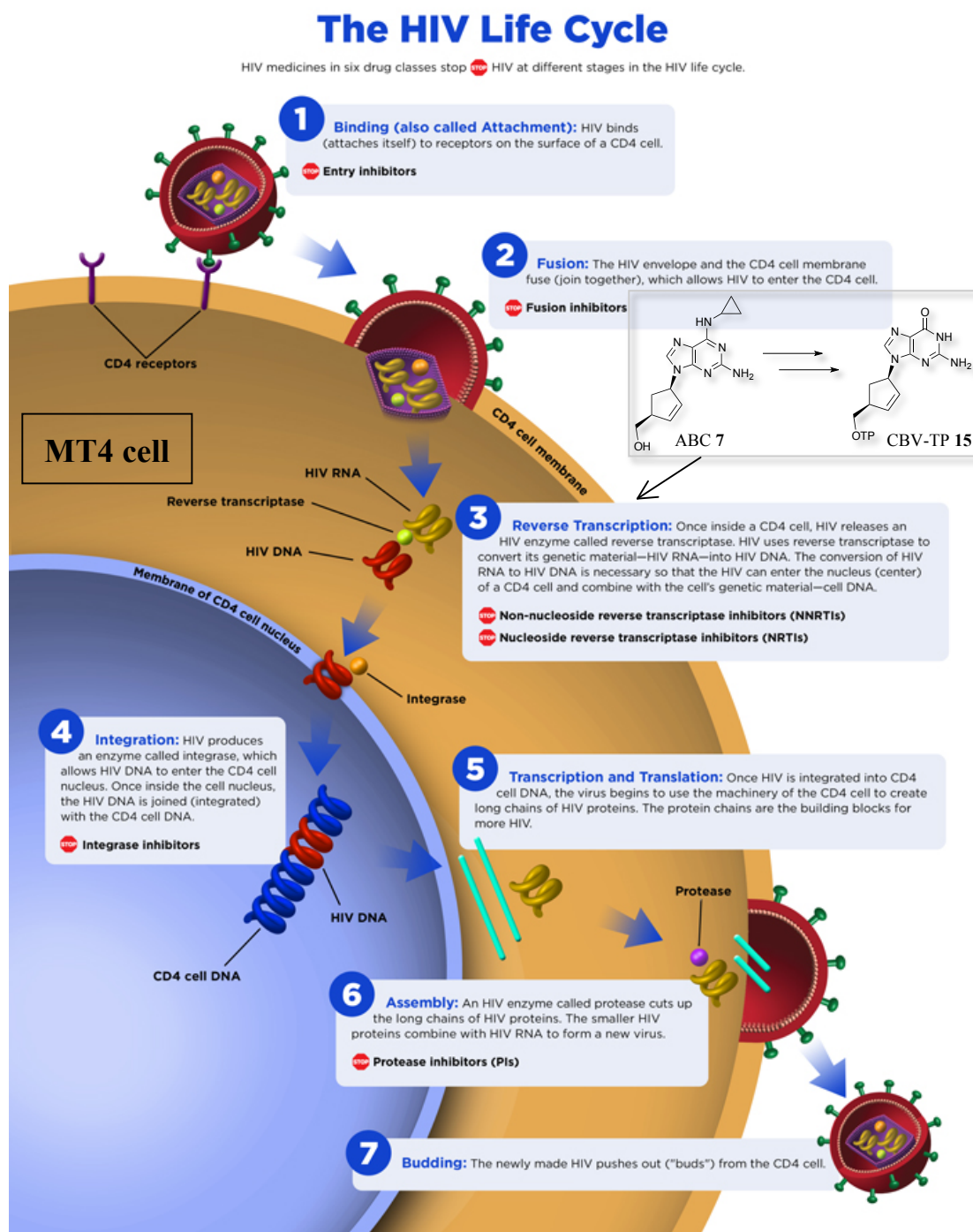

The HIV Life Cycle

HIV medicines in six drug classes stop 🛑 HIV at different stages in the HIV life cycle.

1 Binding (also called Attachment): HIV binds (attaches itself) to receptors on the surface of a CD4 cell.
🛑 **Entry inhibitors**

2 Fusion: The HIV envelope and the CD4 cell membrane fuse (join together), which allows HIV to enter the CD4 cell.
🛑 **Fusion inhibitors**

CD4 receptors

CD4 cell membrane

MT4 cell

HIV RNA

Reverse transcriptase

HIV DNA

Membrane of CD4 cell nucleus

ABC **7** → CBV-TP **15**

3 Reverse Transcription: Once inside a CD4 cell, HIV releases an HIV enzyme called reverse transcriptase. HIV uses reverse transcriptase to convert its genetic material—HIV RNA—into HIV DNA. The conversion of HIV RNA to HIV DNA is necessary so that the HIV can enter the nucleus (center) of a CD4 cell and combine with the cell's genetic material—cell DNA.
🛑 **Non-nucleoside reverse transcriptase inhibitors (NNRTIs)**
🛑 **Nucleoside reverse transcriptase inhibitors (NRTIs)**

Integrase

4 Integration: HIV produces an enzyme called integrase, which allows HIV DNA to enter the CD4 cell nucleus. Once inside the cell nucleus, the HIV DNA is joined (integrated) with the CD4 cell DNA.
🛑 **Integrase inhibitors**

5 Transcription and Translation: Once HIV is integrated into CD4 cell DNA, the virus begins to use the machinery of the CD4 cell to create long chains of HIV proteins. The protein chains are the building blocks for more HIV.

HIV DNA

CD4 cell DNA

Protease

6 Assembly: An HIV enzyme called protease cuts up the long chains of HIV proteins. The smaller HIV proteins combine with HIV RNA to form a new virus.
🛑 **Protease inhibitors (PIs)**

7 Budding: The newly made HIV pushes out ("buds") from the CD4 cell.

Figure 1.25: Diagram depicting the HIV life cycle in a monocyte (*e.g.* MT4 cell), through 7 main stages: Binding (1); fusion (2); reverse transcription (3); integration (4); transcription and translation (5); assembly (6) and budding (7). The 6 classes of anti-HIV drugs are also depicted, in particular, it

Figure 1.25 continued:

is at stage 3 (reverse transcription) that ABC **7** acts (as an NRTI), once it has been metabolised to the active compound, CBV-TP **15**. In the MTT assay, the compounds to be tested will act at this stage (3) and inhibit the replication of the virus. NRTI, nucleoside reverse transcriptase inhibitor. Adapted from National Institute of Allergy and Infectious Disease.[147]

Once MTT is metabolised to MTT formazan the colour change can be measured spectrophotometrically, as absorbance values or optical density detection, at a wavelength of 570 nm (Figure **1.26 A**). This is a direct measure of cell viability: A reduced number of MT4 cells results in less conversion of MTT to MTT formazan. This basic concept and methodology can be applied to assessing cell cytotoxicity and antiviral efficacy assays. For the latter, the MT4 cells are infected with the HIVIII$_B$ strain and incubated with the respective test compounds. Should the compounds possess efficacy against the virus, the MT4 cells will remain viable and turnover of MTT to MTT formazan should be higher than those compounds with poor potency (Figure **1.26 B**) where the virus replicates resulting in increased MT4 cell death.

A

B
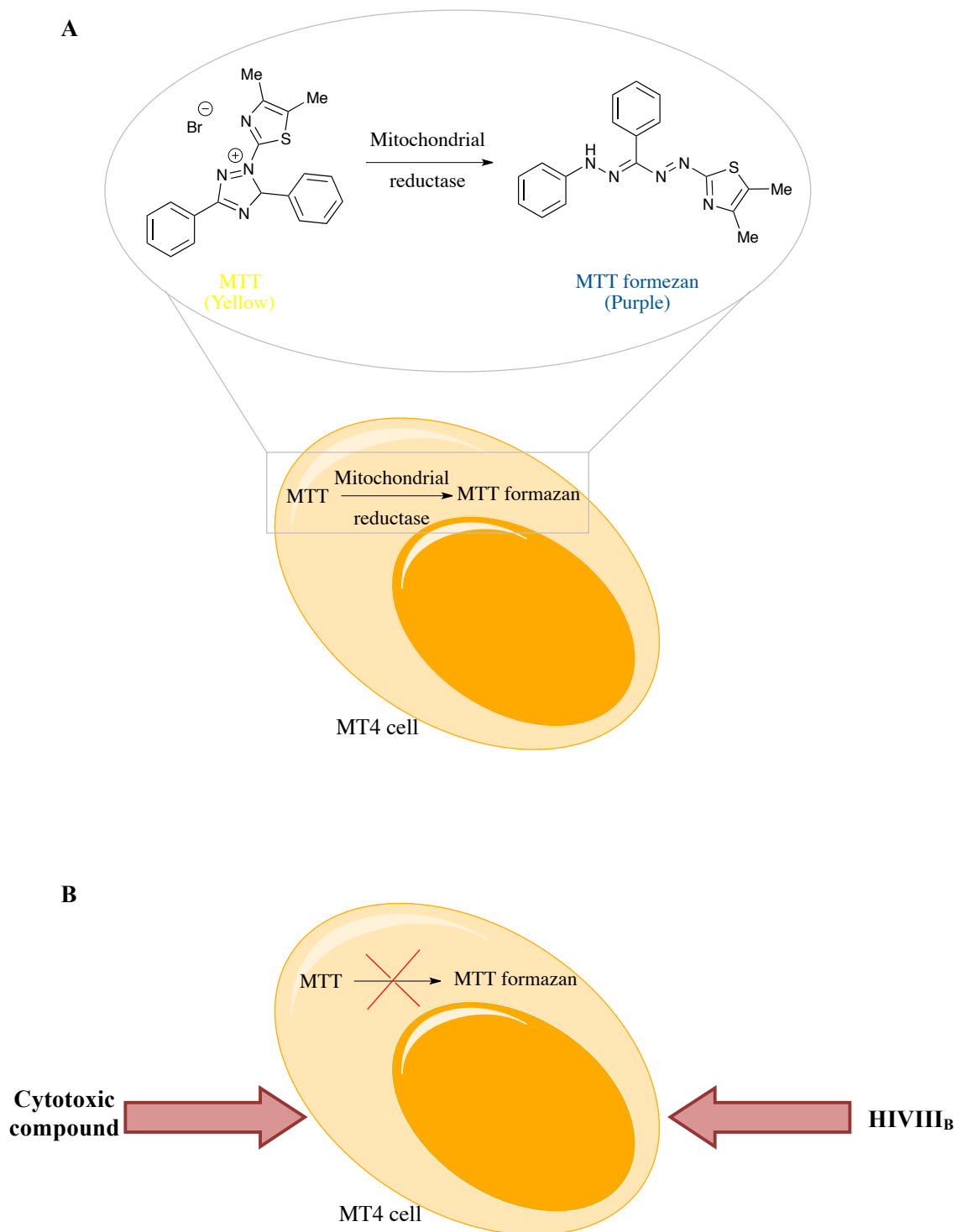
Figure 1.26: MTT (yellow) is metabolised to MTT formazan (purple) by mitochondrial reductases, and such metabolism can be used as a direct indicator of cell (MT4) viability. MT4 cells are a virally transformed human T-cell leukaemia line. The spectrophotometric MTT assay can be used to determine a compounds cytotoxicity and antiviral efficacy with a colour change of yellow to purple (**A**). Should the cell viability decrease, through presence of cytotoxic compounds or a virus, this

would be reflected in the spectrophotometric reading, with less MTT conversion to MTT formazan. The efficacy of compounds against the HIV virus will be determined using the HIVIII$_B$ strain (**B**). MTT, thiazolyl blue tetrazolium bromide.

1.12 Overall Aims

Although much research has been conducted, along with proposed mechanisms to probe ABC toxicity, a conclusive hypothesis to understand the chemical basis of ABC-HSR remains unidentified. It was therefore the overall aim of this study to design and synthesise analogues of ABC, which could not only be used to probe its oxidative metabolism, but to determine the immunogenic mechanism of ABC-HSR.

The overall aims are as follows:

- To develop a synthesis for a deuterated form of ABC to probe 5'-OH oxidative ABC metabolism

- To undertake a series of metabolism experiments to determine contribution of ABC metabolism to its associated toxicity

- To synthesise a range of ABC analogues using a SAR approach to block metabolism and/or binding within HLA-B*57:01

- To use synthesised analogues in a range of toxicological assays to further probe its toxicity

- To use all chemical, metabolic and toxicology results to deduce or validate a mechanism of ABC toxicity.

1.13 References

(1)   Wu, T.-Y.; Jen, M.-H.; Bottle, A.; Molokhia, M.; Aylin, P.; Bell, D.; Majeed, A. *J. R. Soc. Med.* **2010**, *103*, 239.

(2)   Pirmohamed, M.; James, S.; Meakin, S.; Green, C.; Scott, A. K.; Walley, T. J.; Farrar, K.; Park, B. K.; Breckenridge, A. M. *Br. Med. J.* **2004**, *329*, 15.

(3)   Edwards, R.; Aronson, J. K. *The Lancet* **2000**, *356*.

(4)   Park, B. E.; Pirmohamed, M.; Kitteringham, N. R. *Chem. Res. Toxicol.* **1998**, *11*, 969.

(5)   Pirmohamed, M.; Breckenridge, A. M.; Kitteringham, N. R.; Park, B. K. *Br. Med. J.* **1998**, *316*, 1295.

(6)   Mann, R. D.; Andrews, E. B. *Pharmacovigilance / editors, Ronald D. Mann, Elizabeth B. Andrews*; Chichester : John Wiley & Sons, 2007. 2nd ed., 2007; Vol. Chapter 8 - Mechanisms of Adverse Drug Reactions, Pirmohamed, M. & Park, B.K.

(7)   Atkin, P. A.; Shenfield, G. M. *Adverse Drug React. Toxicol. Rev.* **1995**, *14*, 175.

(8)   Pichler, W. J.; Beeler, A.; Keller, M.; Lerch, M.; Posadas, S.; Schmid, D.; Spanou, Z.; Zawodniak, A.; Gerber, B. *Allergology international : Official Journal of the Japanese Society of Allergology* **2006**, *55*, 17.

(9)   Hunziker, T.; Bruppacher, R.; Kuenzi, U. P.; Maibach, R.; Braunschweig, S.; Halter, F.; Hoigne, R. V. *Pharmacoepidemiol. Drug Saf.* **2002**, *11*, 159.

(10)   Gell, P. G. H. C., R.R.A. *The classification of allergic reactions underlying disease. In Clinical Aspects of Immunology*; Blackwell Science, 1963.

(11)   Benjamini, E.; Sunshine, G.; Leskowitz, S. *Immunology: a short course*; Wiley-Liss, New York, 3rd ed. 1996, 1996.

(12)   Uetrecht, J. P. *Chem. Res. Toxicol.* **1999**, *12*, 387.

(13)   Park, B. K.; Laverty, H.; Srivastava, A.; Antoine, D. J.; Naisbitt, D.; Williams, D. P. *Chem. Biol. Interact.* **2011**, *192*, 30.

(14)   Pirmohamed, M.; Naisbitt, D. J.; Gordon, F.; Park, B. K. *Toxicology* **2002**, *181*, 55.

(15)   Pichler, W. J. *Ann. Intern. Med.* **2003**, *139*, 683.

(16)   Pichler, W. J.; Naisbitt, D. J.; Park, B. K. *J. Allergy Clin. Immunol.* **2011**, *127*, S74.

(17)   Levine, B. B.; Ovary, Z. *The Journal of Experimental Medicine* **1961**, *114*, 875.

(18)   Satoh, H.; Martin, B. M.; Schulick, A. H.; Christ, D. D.; Kenna, J. G.; Pohl, L. R. *Proc. Natl. Acad. Sci. U. S. A.* **1989**, *86*, 322.

(19)   Vergani, D.; Mielivergani, G.; Alberti, A.; Neuberger, J.; Eddleston, A.; Davis, M.; Williams, R. *N. Engl. J. Med.* **1980**, *303*, 66.

(20)   Maggs, J. L.; Williams, D.; Pirmohamed, M.; Park, B. K. *J. Pharmacol. Exp. Ther.* **1995**, *275*, 1463.

(21)   Dahlin, D. C.; Miwa, G. T.; Lu, A. Y. H.; Nelson, S. D. *Proceedings of the National Academy of Sciences of the United States of America-Biological Sciences* **1984**, *81*, 1327.

(22)   Callan, H. E.; Jenkins, R. E.; Maggs, J. L.; Lavergne, S. N.; Clarke, S. E.; Naisbitt, D. J.; Park, B. K. *Chem. Res. Toxicol.* **2009**, *22*, 937.

(23) Pichler, W. J. *Current Opinion in Allergy and Clinical Immunology* **2002**, *2*, 301.

(24) Pichler, W. J. *Drug Hypersensitivity / editor, W. J. Pichler*; Basel; Karger, 2007, 2007.

(25) Schnyder, B.; Mauri Hellweg, D.; Zanni, M.; Bettens, F.; Pichler, W. J. *J. Clin. Invest.* **1997**, *100*, 136.

(26) Zanni, M. P.; von Greyerz, S.; Schnyder, B.; Brander, K. A.; Frutig, K.; Hari, Y.; Valitutti, S.; Pichler, W. J. *J. Clin. Invest.* **1998**, *102*, 1591.

(27) Matzinger, P. *Annu. Rev. Immunol.* **1994**, *12*, 991.

(28) Curtsinger, J. M.; Schmidt, C. S.; Mondino, A.; Lins, D. C.; Kedl, R. M.; Jenkins, M. K.; Mescher, M. F. *J. Immunol.* **1999**, *162*, 3256.

(29) Bharadwaj, M.; Illing, P.; Theodossis, A.; Purcell, A. W.; Rossjohn, J.; McCluskey, J. In *Annual Review of Pharmacology and Toxicology, Vol 52*; Insel, P. A., Amara, S. G., Blaschke, T. F., Eds. 2012; Vol. 52, p 401.

(30) Mallal, S., Nolan, D., Witt, C., Masel, G., Martin, A.M., Moore, C., Sayer, D., Castley, A., Mamotte, C., Maxwell, D., James, I. *The Lancet* **2002**, *359*.

(31) Chung, W. H.; Hung, S. I.; Hong, H. S.; Hsih, M. S.; Yang, L. C.; Ho, H. C.; Wu, J. Y.; Chen, Y. T. *Nature* **2004**, *428*, 486.

(32) Hung, S. L.; Chung, W. H.; Jee, S. H.; Chen, W. C.; Chang, Y. T.; Lee, W. R.; Hu, S. L.; Wu, M. T.; Chen, G. S.; Wong, T. W.; Hsiao, P. F.; Chen, W. H.; Shih, H. Y.; Fang, W. H.; Wei, C. Y.; Lou, Y. H.; Huang, Y. L.; Lin, J. J.; Chen, Y. T. *Pharmacogenetics and Genomics* **2006**, *16*, 297.

(33) Daly, A. K.; Donaldson, P. T.; Bhatnagar, P.; Shen, Y.; Pe'er, I.; Floratos, A.; Daly, M. J.; Goldstein, D. B.; John, S.; Nelson, M. R.; Graham, J.; Park, B. K.; Dillon, J. F.; Bernal, W.; Cordell, H. J.; Pirmohamed, M.; Aithal, G. P.; Day, C. P.; Study, D.; Int, S. A. E. C. *Nat. Genet.* **2009**, *41*, 816.

(34) Patrick, G. L. *An Introduction to Medicinal Chemistry / Graham L. Patrick*; Oxford : Oxford University Press, 2013. Fifth edition., 2013.

(35) Mizuno, N.; Niwa, T.; Yotsumoto, Y.; Sugiyama, Y. *Pharmacol. Rev.* **2003**, *55*, 425.

(36) Dresser, G. K.; Spence, J. D.; Bailey, D. G. *Clin. Pharmacokinet.* **2000**, *38*, 41.

(37) Silver, B. A.; Bell, W. R. *Ann. Intern. Med.* **1979**, *90*, 348.

(38) Macherey, A.-C.; Dansette, P. M. *Practice of Medicinal Chemistry, 3rd Edition* **2008**, *Chapter 3*, 674.

(39) Clark, B.; Smith, D. A. *CRC Crit. Rev. Toxicol.* **1984**, *12*, 343.

(40) Lin, J. H.; Lu, A. Y. H. *Pharmacol. Rev.* **1997**, *49*, 403.

(41) Nelson, S. D. *J. Med. Chem.* **1982**, *25*, 753.

(42) Holtzman, J. L. *Life Sci.* **1982**, *30*, 1.

(43) Prescott, L. F. *Br. J. Clin. Pharmacol.* **1979**, *7*, 453.

(44) Cobden, I.; Record, C. O.; Ward, M. K.; Kerr, D. N. S. *Br. Med. J.* **1982**, *284*, 21.

(45) Lohmann, W.; Karst, U. *Anal. Bioanal. Chem.* **2008**, *391*, 79.

(46) Hinson, J. A.; Pohl, L. R.; Monks, T. J.; Gillette, J. R. *Life Sci.* **1981**, *29*, 107.

(47) Nelson, S. D.; Pearson, P. G. *Annu. Rev. Pharmacol. Toxicol.* **1990**, *30*, 169.

(48) Freeman, R. W.; Uetrecht, J. P.; Woosley, R. L.; Oates, J. A.; Harbison, R. D. *Drug Metab. Disposition* **1981**, *9*, 188.

(49) Uetrecht, J. P. *J. Pharmacol. Exp. Ther.* **1985**, *232*, 420.

(50) Gardner, I.; Popovic, M.; Zahid, N.; Uetrecht, J. P. *Chem. Res. Toxicol.* **2005**, *18*, 1384.

(51)   Uetrecht, J.; Zahid, N.; Rubin, R. *Chem. Res. Toxicol.* **1988**, *1*, 74.

(52)   Ahlstedt, S.; Kristofferson, A. *Prog. Allergy* **1982**, *30*, 67.

(53)   Uetrecht, J. P.; Sweetman, B. J.; Woosley, R. L.; Oates, J. A. *Drug Metab. Disposition* **1984**, *12*, 77.

(54)   Foster, A. B.; Jarman, M.; Kinas, R. W.; Vanmaanen, J. M. S.; Taylor, G. N.; Gaston, J. L.; Parkin, A.; Richardson, A. C. *J. Med. Chem.* **1981**, *24*, 1399.

(55)   Cox, P. J. *Biochem. Pharmacol.* **1979**, *28*, 2045.

(56)   Mirkes, P. E.; Fantel, A. G.; Greenaway, J. C.; Shepard, T. H. *Toxicol. Appl. Pharmacol.* **1981**, *58*, 322.

(57)   Balbinder, E.; Reich, C. I.; Shugarts, D.; Keogh, J.; Fibiger, R.; Jones, T.; Banks, A. *Cancer Res.* **1981**, *41*, 2967.   (58)   Meanwell, N. A. *J. Med. Chem.* **2011**, *54*, 2529.

(59)   Li, F.; Chordia, M. D.; Huang, T.; Macdonald, T. L. *Chem. Res. Toxicol.* **2009**, *22*, 72.

(60)   Uetrecht, J. *Chem. Res. Toxicol.* **2008**, *21*, 84.

(61)   Julemont, F.; de Leval, X.; Michaux, C.; Damas, J.; Charlier, C.; Durant, F.; Pirotte, B.; Dogne, J. M. *J. Med. Chem.* **2002**, *45*, 5182.

(62)   Julemont, F.; de Leval, X.; Michaux, C.; Renard, J. F.; Winum, J. Y.; Montero, J. L.; Damas, J.; Dogne, J. M.; Pirotte, B. *J. Med. Chem.* **2004**, *47*, 6749.

(63)   Tsai, C. H.; Doong, S. L.; Johns, D. G.; Driscoll, J. S.; Cheng, Y. C. *Biochem. Pharmacol.* **1994**, *48*, 1477.

(64)   Daluge, S. M.; Good, S. S.; Faletto, M. B.; Miller, W. H.; StClair, M. H.; Boone, L. R.; Tisdale, M.; Parry, N. R.; Reardon, J. E.; Dornsife, R. E.; Averett, D. R.; Krenitsky, T. A. *Antimicrob. Agents Chemother.* **1997**, *41*, 1082.

(65)   Daluge, S. M.; Good, S. S.; Martin, M. T.; Tibbels, S. R.; Miller, W. H.; Averett, D. R.; St Clair, M. H.; Ayers, K. M. *Abstracts of the Interscience Conference on Antimicrobial Agents and Chemotherapy* **1994**, *34*, 7.

(66)   Daluge, S. M.; Martin, M. T.; Sickles, B. R.; Livingston, D. A. *Nucleosides Nucleotides & Nucleic Acids* **2000**, *19*, 297.

(67)   Hetherington, S.; Hughes, A. R.; Mosteller, M.; Shortino, D.; Baker, K. L.; Spreen, W.; Lai, E.; Davies, K.; Handley, A.; Dow, D. J.; Fling, M. E.; Stocum, M.; Bowman, C.; Thurmond, L. M.; Roses, A. D. *Lancet* **2002**, *359*, 1121.

(68)   Hewitt, R. G. *Clin. Infect. Dis.* **2002**, *34*, 1137.

(69)   Hughes, A. R.; Mosteller, M.; Bansal, A. T.; Davies, K.; Haneline, S. A.; Lai, E. H.; Nangle, K.; Scott, T.; Spreen, W. R.; Warren, L. L.; Roses, A. D.; Team, C. N. A. S. *Pharmacogenomics* **2004**, *5*, 203.

(70)   Hughes, A. R., Spreen, W.R., Mosteller, M., Warren, L.L., Lai, E.H., Brothers, C.H., Cox, C., Nelson, A.J., Hughes, S., Thorborn, D.E., Stancil, B., Hetherington, S.V., Burns, D.K., Roses, A.D. *The Pharmacogenomics Journal* **2008**, *8*, 365.

(71)   Mallal, S., Phillips, E., Carosi, G., Molina, J. M., Workman, C., Tomazic, J., Jagel-Guedes, E., Rugina, S., Kozyrev, O., Cid, J. F., Hay, P., Nolan, D., Hughes, S., Hughes, A., Ryan, S., Fitch, N., Thorborn, D., Benbow, A. and Team, P.-S. *The New England Journal of Medicine* **2008**, *358*, 568.

(72)   Giorgini, S.; Martinelli, C.; Tognetti, L.; Carocci, A.; Giuntini, R.; Mastronardi, V.; Torricellio, F.; Leoncini, F.; Lotti, T. *Dermatologic Therapy* **2011**, *24*, 591.

(73) Yuen, G. J.; Weller, S.; Pakes, G. E. *Clin. Pharmacokinet.* **2008**, *47*, 351.

(74) Faletto, M. B.; Miller, W. H.; Garvey, E. P.; Clair, M. H. S.; Daluge, S. M.; Good, S. S. *Antimicrob. Agents Chemother.* **1997**, *41*, 1099.

(75) Piliero, P. J. *JAIDS - Journal of Acquired Immune Deficiency Syndromes* **2004**, *37*, S2.

(76) Schinkmanova, M.; Votruba, I.; Shibata, R.; Han, B.; Liu, X.; Cihlar, T.; Holy, A. *Collect. Czech. Chem. Commun.* **2008**, *73*, 275.

(77) McDowell, J. A.; Chittick, G. E.; Ravitch, J. R.; Polk, R. E.; Kerkering, T. M.; Stein, D. S. *Antimicrob. Agents Chemother.* **1999**, *43*, 2855.

(78) Walsh, J. S.; Reese, M. J.; Thurmond, L. M. *Chem. Biol. Interact.* **2002**, *142*, 135.

(79) Kassam, J. P.; Tang, B. K.; Kadar, D.; Kalow, W. *Drug Metab. Disposition* **1989**, *17*, 567.

(80) Merritt, A. D.; Tomkins, G. M. *J. Biol. Chem.* **1959**, *234*, 2778.

(81) Theorell, H.; Bonnichsen, R. *Acta Chem. Scand.* **1951**, *5*, 1105.

(82) Bush, K.; Shiner, V. J.; Mahler, H. R. *Biochemistry (Mosc).* **1973**, *12*, 4802.

(83) Vonwartburg, J. P.; Vallee, B. L.; Bethune, J. L. *Biochemistry (Mosc).* **1964**, *3*, 1775.

(84) Vallee, B. L.; Hoch, F. L. *Proc. Natl. Acad. Sci. U. S. A.* **1955**, *41*, 327.

(85) Bugg, T. *Introduction to Enzyme and Coenzyme Chemistry / T. D. H. Bugg*; Chichester : Wiley, 2012. 3rd ed., 2012.

(86) O'Brien, P. J.; Siraki, A. G.; Shangari, N. *Crit. Rev. Toxicol.* **2005**, *35*, 609.

(87) Vasiliou, V.; Nebert, D. W. *Human Genomics* **2005**, *2*, 138.

(88) Koppaka, V.; Thompson, D. C.; Chen, Y.; Ellermann, M.; Nicolaou, K. C.; Juvonen, R. O.; Petersen, D.; Deitrich, R. A.; Hurley, T. D.; Vasiliou, V. *Pharmacol. Rev.* **2012**, *64*, 520.

(89) Sidhu, R. S.; Blair, A. H. *J. Biol. Chem.* **1975**, *250*, 7899.

(90) Feldman, R. I.; Weiner, H. *J. Biol. Chem.* **1972**, *247*, 260.

(91) Yoshida, A.; Hsu, L. C.; Dave, V. *Enzyme* **1992**, *46*, 239.

(92) Hempel, J.; Perozich, J.; Chapman, T.; Rose, J.; Boesch, J. S.; Liu, X.-J.; Lindahl, R.; Wang, B.-C. In *Advances in Experimental Medicine and Biology; Enzymology and Molecular Biology of Carbonyl Metabolism, 7*; Weiner, H., Maser, E., Crabb, D. W., Lindahl, R., Eds. 1999; Vol. 463, p 53.

(93) Lash, L. H.; Woods, E. B. *Arch. Biochem. Biophys.* **1991**, *286*, 46.

(94) Laurent, A.; Perdu-Durand, E.; Alary, J.; Debrauwer, L.; Cravedi, J. P. *Toxicol. Lett.* **2000**, *114*, 203.

(95) Chessman, D.; Kostenko, L.; Lethborg, T.; Purcell, A. W.; Williamson, N. A.; Chen, Z.; Kjer-Nielsen, L.; Mifsud, N. A.; Tait, B. D.; Holdsworth, R.; Almeida, C. A.; Nolan, D.; Macdonald, W. A.; Archbold, J. K.; Kellerher, A. D.; Marriott, D.; Mallal, S.; Bharadwaj, M.; Rossjohn, J.; McCluskey, J. *Immunity* **2008**, *28*, 822.

(96) Barber, L. D.; Percival, L.; Arnett, K. L.; Gumperz, J. E.; Chen, L.; Parham, P. *J. Immunol.* **1997**, *158*, 1660.

(97) McCluskey, J.; Peh, C. A. *Reviews in Immunogenetics* **1999**, *1*, 3.

(98) Ostrov, D. A.; Grant, B. J.; Pompeu, Y. A.; Sidney, J.; Harndahl, M.; Southwood, S.; Oseroff, C.; Lu, S.; Jakoncic, J.; de Oliveira, C. A. F.; Yang, L.; Mei, H.; Shi, L.; Shabanowitz, J.; English, A. M.; Wriston, A.; Lucas, A.; Phillips, E.; Mallal, S.; Grey, H. M.; Sette, A.; Hunt, D. F.; Buus, S.; Peters, B. *Proc. Natl. Acad. Sci. U. S. A.* **2012**, *109*, 9959.

(99)   Illing, P. T.; Vivian, J. P.; Dudek, N. L.; Kostenko, L.; Chen, Z.; Bharadwaj, M.; Miles, J. J.; Kjer-Nielsen, L.; Gras, S.; Williamson, N. A.; Burrows, S. R.; Purcell, A. W.; Rossjohn, J.; McCluskey, J. *Nature* **2012**, *486*, 554.

(100) Norcross, M. A.; Luo, S.; Lu, L.; Boyne, M. T.; Gomarteli, M.; Rennels, A. D.; Woodcock, J.; Margulies, D. H.; McMurtrey, C.; Vernon, S.; Hildebrand, W. H.; Buchli, R. *AIDS* **2012**, *26*, F21.

(101) McGuigan, C.; Hassan-Abdallah, A.; Srinivasan, S.; Wang, Y.; Siddiqui, A.; Daluge, S. M.; Gudmundsson, K. S.; Zhou, H.; McLean, E. W.; Peckham, J. P.; Burnette, T. C.; Marr, H.; Hazen, R.; Condreay, L. D.; Johnson, L.; Balzarini, J. *J. Med. Chem.* **2006**, *49*, 7215.

(102) Boutureira, O.; Isabel Matheu, M.; Diaz, Y.; Castillon, S. *Chem. Soc. Rev.* **2013**, *42*, 5056.

(103) Rodriguez, J. B.; Comin, M. J. *Mini-Rev. Med. Chem.* **2003**, *3*, 95.

(104) Borthwick, A. D.; Biggadike, K.; Paternoster, I. L.; Coates, J. A. V.; Knight, D. J. *Bioorg. Med. Chem. Lett.* **1993**, *3*, 2577.

(105) Marquez, V. E.; Lim, M. I. *Med. Res. Rev.* **1986**, *6*, 1.

(106) Shealy, Y. F.; Odell, C. A.; Shannon, W. M.; Arnett, G. *J. Med. Chem.* **1983**, *26*, 156.

(107) Herdewijn, P.; Declercq, E.; Balzarini, J.; Vanderhaeghe, H. *J. Med. Chem.* **1985**, *28*, 550.

(108) Lin, W.; Virga, K. G.; Kim, K.-H.; Zajicek, J.; Mendel, D.; Miller, M. J. *J. Org. Chem.* **2009**, *74*, 5941.

(109) Crimmins, M. T. *Tetrahedron* **1998**, *54*, 9229.

(110) Slusarchyk, W. A.; Young, M. G.; Bisacchi, G. S.; Hockstein, D. R.; Zahler, R. *Tetrahedron Lett.* **1989**, *30*, 6453.

(111) Mulvihill, M. J.; Miller, M. J. *Tetrahedron* **1998**, *54*, 6605.

(112) Bremond, P.; Audran, G.; Aubin, Y.; Monti, H. *Synlett* **2007**, 1124.

(113) Kitade, Y.; Ando, T.; Yamaguchi, T.; Hori, A.; Nakanishi, M.; Ueno, Y. *Biorg. Med. Chem.* **2006**, *14*, 5578.

(114) Jung, M. E.; Rhee, H. *J. Org. Chem.* **1994**, *59*, 4719.

(115) Trost, B. M.; Kuo, G. H.; Benneche, T. *J. Am. Chem. Soc.* **1988**, *110*, 621.

(116) Patil, S. D.; Schneller, S. W. *J. Heterocycl. Chem.* **1991**, *28*, 823.

(117) Bergmeier, S. C.; Cobas, A. A.; Rapoport, H. *J. Org. Chem.* **1993**, *58*, 2369.

(118) Saito, Y.; Nakamura, M.; Ohno, T.; Chaicharoenpong, C.; Ichikawa, E.; Yamamura, S.; Kato, K.; Umezawa, K. *Journal of the Chemical Society-Perkin Transactions 1* **2001**, 298.

(119) Song, G. Y.; Paul, V.; Choo, H.; Morrey, J.; Sidwell, R. W.; Schinazi, R. F.; Chu, C. K. *J. Med. Chem.* **2001**, *44*, 3985.

(120) Ali, S. M.; Ramesh, K.; Borchardt, R. T. *Tetrahedron Lett.* **1990**, *31*, 1509.

(121) Choi, W. J.; Park, J. G.; Yoo, S. J.; Kim, H. O.; Moon, H. R.; Chun, M. W.; Jung, Y. H.; Jeong, L. S. *J. Org. Chem.* **2001**, *66*, 6490.

(122) Ovaa, H.; Lastdrager, B.; Codee, J. D. C.; van der Marel, G. A.; Overkleeft, H. S.; van Boom, J. H. *Journal of the Chemical Society-Perkin Transactions 1* **2002**, 2370.

(123) Callam, C. S.; Lowary, T. L. *Organic Letters* **2000**, *2*, 167.

(124) Crimmins, M. T.; King, B. W.; Zuercher, W. J.; Choy, A. L. *J. Org. Chem.* **2000**, *65*, 8499.

(125) Zhou, J.; Yang, M.; Akdag, A.; Wang, H.; Schneller, S. W. *Tetrahedron* **2008**, *64*, 433.

(126) Ono, M.; Nishimura, K.; Tsubouchi, H.; Nagaoka, Y.; Tomioka, K. *J. Org. Chem.* **2001**, *66*, 8199.

(127) Takagi, C.; Sukeda, M.; Kim, H. S.; Wataya, Y.; Yabe, S.; Kitade, Y.; Matsuda, A.; Shuto, S. *Organic & Biomolecular Chemistry* **2005**, *3*, 1245.

(128) Marce, P.; Diaz, Y.; Matheu, M. I.; Castillon, S. *Org. Lett.* **2008**, *10*, 4735.

(129) Lanver, A.; Schmalz, H. G. *Eur. J. Org. Chem.* **2005**, 1444.

(130) Tietze, L. F.; Stadler, C.; Boehnke, N.; Brasche, G.; Grube, A. *Synlett* **2007**, 485.

(131) Trost, B. M. *J. Org. Chem.* **2004**, *69*, 5813.

(132) Trost, B. M.; Machacek, M. R.; Aponick, A. *Acc. Chem. Res.* **2006**, *39*, 747.

(133) Lawrence, R. M.; Process for the preparation of (1S,4R)-cis-4-[2-amino-6-chloro-9H-purin-9-yl]-2-cyclopentene-1-methanol. Glaxo Group Limited. Patent Number: EP1660498 B1: 2009.

(134) Vince, R.; Hua, M. *Current Protocols in Nucleic Acid Chemistry / edited by Serge L. Beaucage et al.* **2006**, *Chapter 14*, Unit 14.4.

(135) Shi, J. X.; Ray, A. S.; Mathew, J. S.; Anderson, K. S.; Chu, C. K.; Schinazi, R. F. *Bioorg. Med. Chem. Lett.* **2004**, *14*, 2159.

(136) Boyle, G. A.; Edlin, C. D.; Li, Y.; Liotta, D. C.; Morgans, G. L.; Musonda, C. C. *Organic & Biomolecular Chemistry* **2012**, *10*, 1870.

(137) Jessel, S.; Meier, C. *Eur. J. Org. Chem.* **2011**, 1702.

(138) Hodgson, D. M.; Witherington, J.; Moloney, B. A. *Journal of the Chemical Society-Perkin Transactions 1* **1994**, 3373.

(139) Katagiri, N.; Nomura, M.; Sato, H.; Kaneko, C.; Yusa, K.; Tsuruo, T. *J. Med. Chem.* **1992**, *35*, 1882.

(140) Pichler, W. J.; Tilch, J. *Allergy* **2004**, *59*, 809.

(141) Czerkinsky, C. C.; Nilsson, L. A.; Nygren, H.; Ouchterlony, O.; Tarkowski, A. *J. Immunol. Methods* **1983**, *65*, 109.

(142) Miyahira, Y.; Murata, K.; Rodriguez, D.; Rodriguez, J. R.; Esteban, M.; Rodrigues, M. M.; Zavala, F. *J. Immunol. Methods* **1995**, *181*, 45.

(143) Orenstein, J. M. *AIDS Res. Hum. Retroviruses* **2008**, *24*, 947.

(144) Marshall, N. J.; Goodwin, C. J.; Holt, S. J. *Growth Regul.* **1995**, *5*, 69.

(145) Pereira, C.; Santos, M. S.; Oliveira, C. *J. Neurosci. Res.* **1998**, *51*, 360.

(146) Mosmann, T. *J. Immunol. Methods* **1983**, *65*, 55.

(147)
http://www.niaid.nih.gov/topics/HIVAIDS/Understanding/Treatment/Pages/arvDrugClasses.aspx.

CHAPTER 2

Synthetic Chemistry to Probe
Abacavir's Oxidative Pathway

CHAPTER 2

Synthetic Chemistry to Probe Abacavir's Oxidative Pathway

2.1 Introduction

As discussed in Chapter 1, oxidative metabolism of ABC **7** may contribute to its toxicity.[1] This major oxidative pathway occurs on the 5'-C to yield ABC-aldehyde (ABC-CHO) isomers **16a–16c** and ABC-carboxylic acid (ABC-COOH) isomers **17a–17c**. It was of great interest to have synthetic standards of compounds that would assist in probing this pathway further.

2.1.1 Chemical oxidation methods applied to purine nucleosides.

There are a wide variety of methods to oxidise primary alcohols to their respective aldehydes and carboxylic acids. Many of the methods available use strong oxidising conditions, often resulting from metal-based reagents. Milder oxidation conditions are always highly sought after as they often ease work-up procedures and enable easy removal of excess oxidant. There is much published literature for the oxidation at 5'-C of purine based nucleoside 5'-primary alcohols to their carboxylate compounds.[2-6] Comparatively, less literature can be found for aldehyde products.[7-9] It is necessary to find an oxidation procedure that will oxidise the 5'-C atom in ABC to its corresponding aldehyde and carboxylic acid, using an oxidising reagent, which will not react with the other functional groups present within the molecule.

2.1.1.1 Oxidation of 5'-primary alcohols to 5'-carboxylate products.

The most common method for oxidising 5'-primary alcohols to their COOH products is *via* a 2,2,6,6-tetramethylpiperidinyloxy/[bis(acetoxy)iodo]benzene (TEMPO/BIAB) route. This mild oxidation method has been employed for a variety of purine nucleoside substrates.[2,3,10-12] An example of such an oxidation is shown in

Scheme **2.1**. In the presence of 1:1 H$_2$O–acetonitrile (ACN), the COOH product will be formed. In anhydrous conditions, the aldehyde would be formed. This method often achieves very good yields, and with precipitation of the final product, purification is often not required.[2] Another well-utilised method uses potassium permanganate (KMnO$_4$) and potassium hydroxide (KOH) as reagents.[5,13,14]

Other less utilised methods include sodium periodate/ruthenium (IV) oxide (NaIO$_4$/RuO$_2$) oxidations[6,15] (Scheme **2.1**) and enzymatic oxidations using nucleoside oxidase isolated from *S. maltophilia*.[4] This enzyme has a wide substrate range, within which it can accommodate non-biological nucleosides.
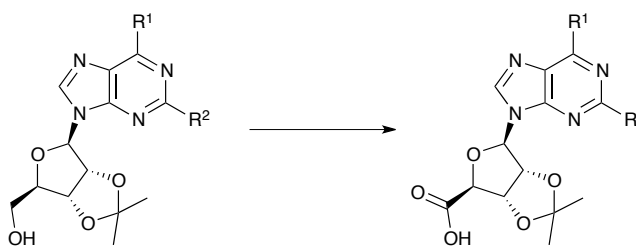
TEMPO / BIAB: R^1 = Cl, R^2 = H

KMnO$_4$ / KOH: R^1 = Cl, R^2 = NH$_2$

RuO$_2$ / NaIO$_4$: R^1 = NH$_2$, R^2 = I

Scheme 2.1: Examples of nucleoside substrates and the conditions used for primary alcohol oxidation to carboxylic acid products. Reagents and conditions used: TEMPO, BIAB, 1:1 H$_2$O−ACN, r.t.;[3] KMnO$_4$, KOH, H$_2$O, r.t.[13] and Ru (IV) oxide, NaIO$_4$, K$_2$CO$_3$, 1:1:2 ACN−CHCl$_3$−H$_2$O.[6] TEMPO, 2,6,6-tetramethylpiperidinyloxy; BIAB, [bis(acetoxy)iodo]benzene; ACN, acetonitrile.

2.1.1.2 Oxidation of 5'-primary alcohols to 5'-aldehyde products.

Due to the highly reactive nature of aldehydes, there is little literature precedent for oxidation methods of purine nucleoside alcohols to aldehyde products. The two major methods use a Dess–Martin periodinane procedure[7,9] or the Moffatt oxidation.[8]

2.1.2 Introduction to deuterium and its use in drug therapeutics.

Deuterium is a naturally occurring non-radioactive isotope of hydrogen to which it has very similar properties, notably its size and shape. Of recent interest for a hydrogen (protium) substitute, it is known to reduce toxicological and PK issues in certain approved drugs as well as being used as a probe to determine mechanisms of drug bioactivation.[16] Most importantly, it has no intrinsic toxicological problems and has equivalent efficacy to hydrogen.

2.1.2.1 Deuterated drugs in clinical trials.

There are several deuterated forms of existing drugs currently or recently in clinical trials, four of which include: CTP-347 (deuterated paroxetine),[17] CTP-518 (deuterated atazanavir),[18] SD-254 (deuterated venlafaxine)[19] and BDD-10103 (deuterated tolperisone)[20] (Figure **2.1**). These drugs have been designed to eliminate and/or address toxicity and PK issues and are discussed within.

A

B

C

D
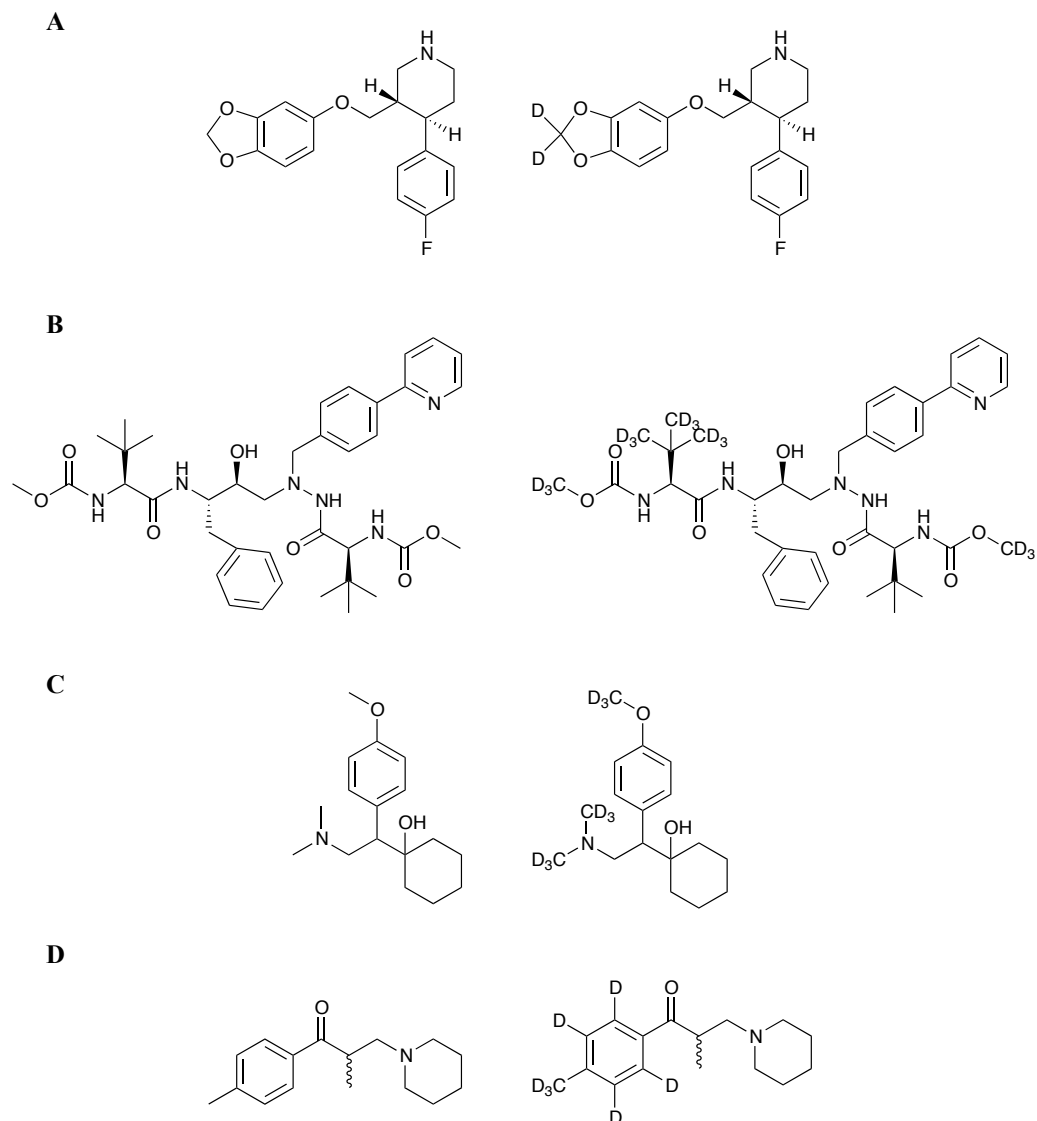
Figure 2.1: Proposed structures of existing drugs and their deuterated equivalents, which have been designed in order to combat toxicity or PK issues: Paroxetine and CTP-347 (deuterated paroxetine) (**A**);[17] atazanavir and CTP-518 (deuterated atazanavir) (**B**);[18] venlafaxine and SD-254 (deuterated venlafaxine) (**C**)[19] and tolperisone and BDD-10103 (deuterated tolperisone) (**D**).[20] PK, pharmacokinetic.

2.1.2.1.1 CTP-347 (deuterated paroxetine).

CTP-347, a deuterated form of paroxetine (Figures **2.1** and **2.2**), is a Concert Pharmaceuticals compound. Paroxetine, a serotonin re-uptake inhibitor, can cause serious DDIs, which are thought to arise from reactive metabolite formation,

followed by deactivation of a cytochrome P450, CYP2D6 (Figure **2.2**).[19] Deuteration of paroxetine has been shown to reduce irreversible CYP2D6 inactivation in pre-clinical trials.[21] By reducing the rate of reactive metabolite formation, CTP-347 can preclude the DDIs normally found with paroxetine.[21] It is currently in clinical trials.
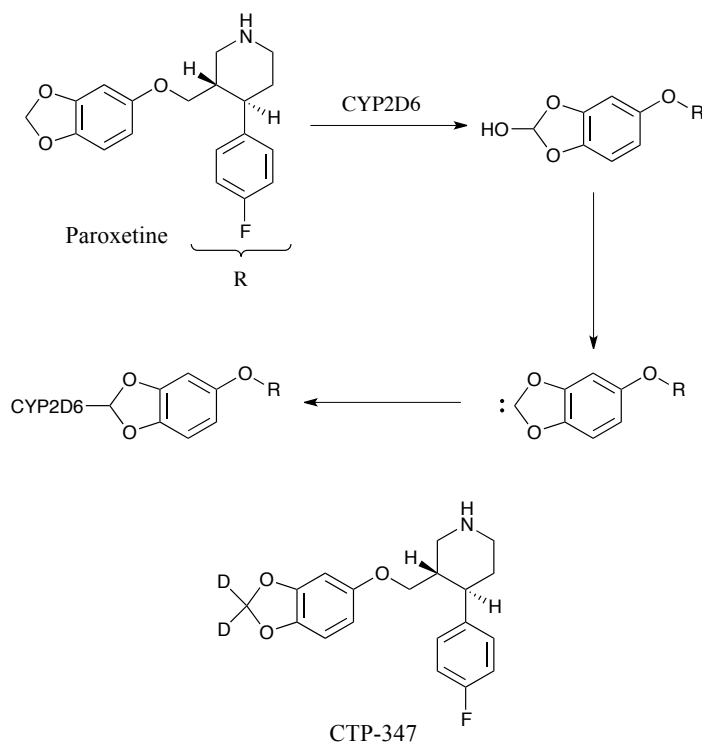
Figure 2.2: Proposed mechanism of paroxetine's DDIs *via* selective P450 inhibition, with carbene formation and irreversible reactivity with CYP2D6. The structure of CTP-347 is undisclosed but a proposed structure of CTP-347 is shown. DDI, drug–drug interaction. Adapted from Concert Pharmaceuticals IPT32.[17]

2.1.2.1.2 CTP-518 (deuterated atazanavir).

CTP-518, a GSK and Concert Pharmaceuticals compound, was designed as a deuterated form of atazanavir (an HIV protease inhibitor), which is administered with ritonavir to boost its PK properties. The compound, whose official structure has

not yet been released (but the structure of D_{15}-atazanavir has been released in a patent, Figure **2.1**)[18] entered phase I clinical trials in 2010.[22] In pre-clinical trials it was found that due to the presence of the deuterium atoms, the drugs metabolism was greatly reduced, with increased liver microsomal stability[18] and half-life.[23] Consequently, combination therapy with ritonavir would not be required.

2.1.2.1.3 SD-254 (deuterated venlafaxine).

Venlafaxine is a selective serotonin re-uptake inhibitor that is used for the treatment of a variety of anxiety disorders. It is metabolised largely by CYP2D6 enzymes to its active major metabolite, *O*-desmethylvenlafaxine (ODV) (Figure **2.3**).[24-26] Further to this, it is also metabolised, mainly by CYP3A4 enzymes, to an inactive metabolite *N*-desmethylvenlafaxine (NDV) (Figure **2.3**).[25] Due to the genetic variability with CYP2D6 enzymes, and as ODV is equally as active as the parent compound,[27] the consequence for both poor and extensive metabolisers can be high plasma concentration levels of an active compound.[26] SD-254, designed by Auspex Pharmaceuticals and having completed phase I clinical trials, is such as to retard the metabolism to ODV, preventing high plasma concentrations of the active compound. The structure has also not been revealed, and limited clinical data is available, however a proposed structure is shown in Figures **2.1** and **2.3**.[19]
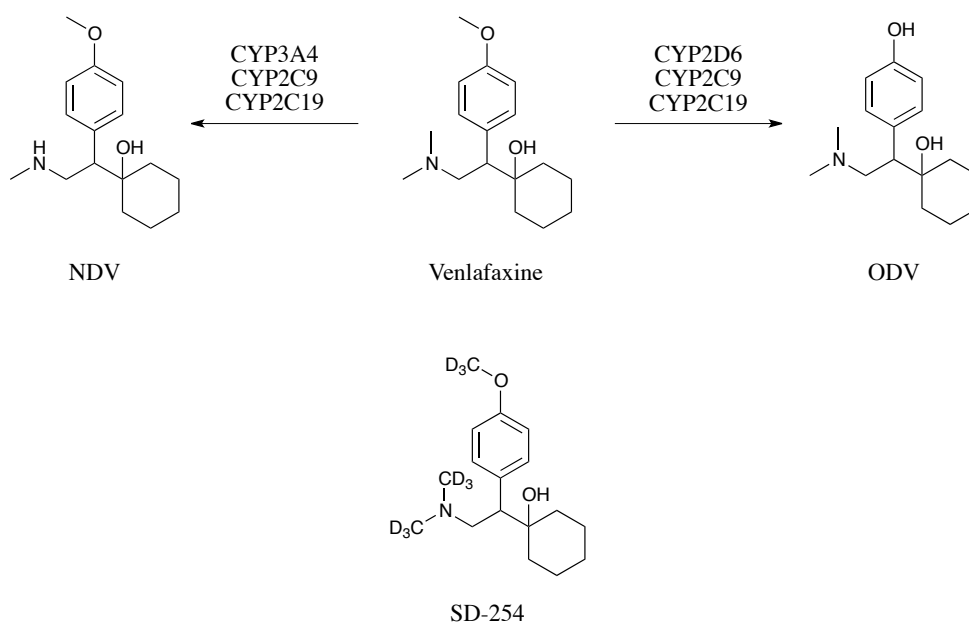
Figure 2.3: Venlafaxine, a selective serotonin re-uptake inhibitor, is used in the treatment of a variety of anxiety disorders. Venlafaxine is principally metabolised to an equally active metabolite ODV[27] by CYP2D6 enzymes and to an inactive metabolite NDV by CYP3A4 enzymes.[24-26] The inter-patient variability associated with CYP2D6 enzymes has resulted in high plasma concentrations levels in both poor and extensive metabolisers of either the parent compound venlafaxine or ODV. SD-254 (deuterated venlafaxine) has completed phase I clinical trials and was been designed to slow the metabolism to ODV, reducing plasma concentration levels. ODV, *O*-desmethylvenlafaxine; NDV, *N*-desmethylvenlafaxine.

2.1.2.1.4 BDD-10103 (deuterated tolperisone).

Tolperisone is an orally administered drug used as a centrally acting muscle relaxant.[28] There is low toxicity associated with the drug and it is largely metabolised by CYP2D6 (with minor CYP2C19 and CYP1A2 contribution) to an inactive aryl methyl hydroxylated metabolite (Figure **2.4**).[29] As previously mentioned, there is high genetic variability associated in particular with CYP2D6 enzymes, and as a consequence, tolperisone is associated with low bioavailability in extensive metabolisers resulting in the requirement of high daily doses.[28] Although the

structure of its deuterated equivalent, BDD-10103 is undisclosed, the structure of D_7-tolperisone (Figures **2.1** and **2.4**) has been revealed in a patent.[20] Little clinical data has been revealed for BDD-10103, but this deuterated compound has shown to exhibit a 10-fold decrease (in pre-clinical trials) in the hydroxylated metabolite compared to its non-deuterated equivalent.[19] Should BDD-10103 be successful in further clinical trials, it has the potential to reduce the first-pass metabolism effect and the inter-patient variability linked with tolperisone would be reduced.
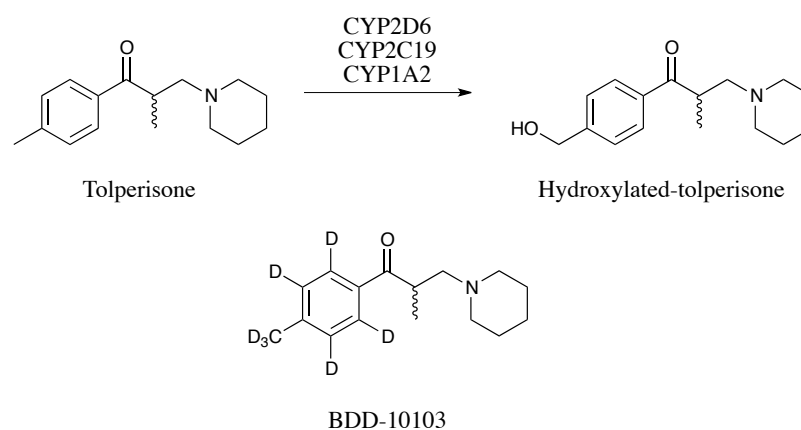
Figure 2.4: Tolperisone, a centrally acting muscle relaxant, is associated with low bioavailability and as a result, in certain patients, high daily doses are required. Tolperisone is extensively metabolised, largely by CYP2D6 enzymes, to a pharmacologically inactive aryl methyl hydroxylated product.[29] The structure of BDD-10103 has not been disclosed, but D_7-tolperisone has been released.[20] Although limited clinical data is available, it has been shown that there is a 10-fold decrease in plasma concentration of the hydroxylated metabolite from BDD-10103 compared to tolperisone.[19] The deuterated equivalent has the potential of reducing the first-pass metabolism effect and the inter-patient PK variation can be reduced.

2.1.3 Investigation into ABC metabolism.

With the suggestion that the aldehyde metabolite could contribute to ABC's toxicity,[30] it would be advantageous if the production and fate of this metabolite were characterised thoroughly. However, **16**, a short-lived, highly reactive intermediate, is notoriously difficult to isolate.[1] There is little documented data for the oxidation chemistry of ABC, however, in 2011, Charneira *et al.* published the chemical synthesis of **16c** (and its β,γ-unsaturated isomer **16a/16b**), using Swern oxidation conditions (Scheme **2.2**).[31] The base used in the reaction determined which isomer was formed: Triethylamine (NEt₃) formed the isomer **16c** and *N,N*-diisopropylethylamine (DIEA) formed predominantly the β,γ-unsaturated isomers **16a** and **16b**. The stereochemistry of the isomers formed from using DIEA as the base could not be determined and with **16a** able to undergo epimerisation to **16b**, they used this pathway solely to form the β,γ-unsaturated collectively. They did however discover that **16a/16b** were able to isomerise to **16c** and these samples were often contaminated with these isomers. With isomerisation to the more thermodynamically stable product, NEt₃ is known to assist in the formation of α,β-unsaturated aldehyde.[31]
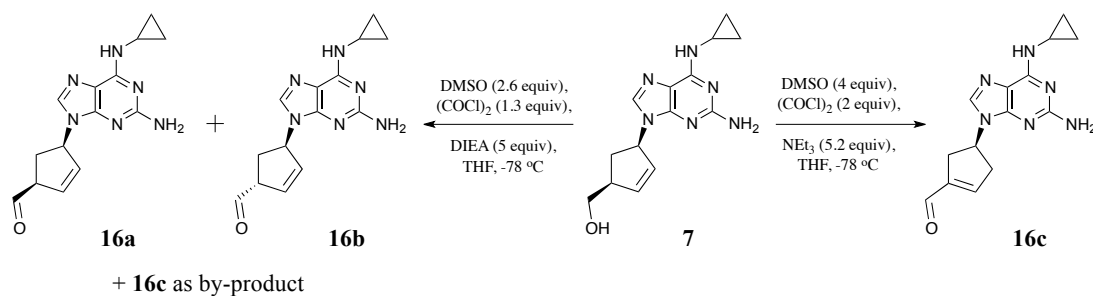
Scheme 2.2: The aldehyde products (**16a–16c**) that Charneira *et al.* had previously synthesised from ABC using standard and modified Swern conditions.[31] The formation of two β,γ-unsaturated products (**16a** and **16b**) is hypothetical; the stereochemistry of the β,γ-unsaturated aldehyde at 4'-C was not determined. The synthesis of **16a/16b**, always a low yielding reaction, also formed compound **16c** as a by-product through isomerisation.[31] DMSO, dimethylsulfoxide; DIEA, *N,N*-diisopropylethylamine, THF, tetrahydrofuran.

Further studies with the synthetic aldehyde isomers **16a/16b** and **16c** have shown that covalent protein binding can occur *in vitro* to haemoglobin (Hb),[31] HSA[32] and glutathione *S*-transferase Pi (GSTP).[32] *In vivo*, the aldehyde metabolites bind covalently and form protein adducts with Hb in rats[33] and human,[34] and with HSA in humans.[32] Through use of the *N*-alkyl Edman procedure (Figure **2.5**), it was found that **16c** can bind to the *N*-terminal valine residue of Hb using a Schiff base mechanism,[31-33] through detection of product **41** *in vitro* and *in vivo*, although further *in vivo* studies are required on a larger cohort of patients to determine the frequency of adduction accurately. Further to this reactivity, **16c** reacts with cysteine, *via* a 1,4-Michael addition mechanism. The *in vitro* studies on reactions of **16c** with HSA and GSTP found that the aldehyde covalently bonded through Michael addition or *via* cross-linking mechanisms with Cys, His, and Lys in HSA and Cys 47 in GSTP.[32] *In vitro* reactions with **16a/16b** found no adduct formation with this isomer, confirming the isomerisation of **16a** to **16c**.[31] Furthermore, research conducted within the

Liverpool group has shown that ABC can undergo oxidative metabolism in the cytosolic fraction of human APCs.[35]
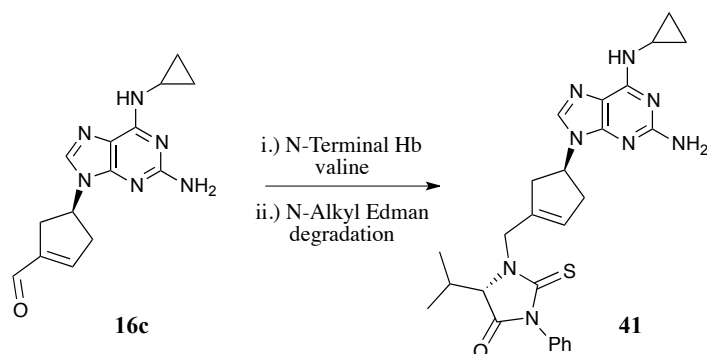
Figure 2.5: N-Alkyl Edman degradation product **41** can be synthesised and detected both *in vitro* and *in vivo* from covalent binding of **16c** with Hb.[31,33] Hb, haemoglobin.

The mechanisms of ABC's enzymic oxidations are not fully understood and the synthesis of di-deuterated ABC **42** (D$_2$-ABC, Figure **2.6**), initially designed as an improved drug to ABC, could be used as an investigational reagent in the discussed oxidation pathway. Two deuterium atoms will replace the 5'-methylene protons, and in doing this it will be possible to determine whether isotopic substitution at this carbon can alter metabolic turnover, effectively comparing oxidative metabolism between the non-deuterated and deuterated form. Deuteration of ABC should slow the rate of oxidative metabolism due to the slower abstraction of 5'-D atoms when the drug is metabolised to the carboxylic acid *via* the aldehyde. Further to this, the toxicity and antiviral activity of D$_2$-ABC can be determined with comparison to ABC. In principle, the metabolic data will allow research of the hapten mechanism and its involvement with ABC-associated hypersensitivity and whether isotopic substitution at 5'-C can eliminate or reduce ABC's toxicity.
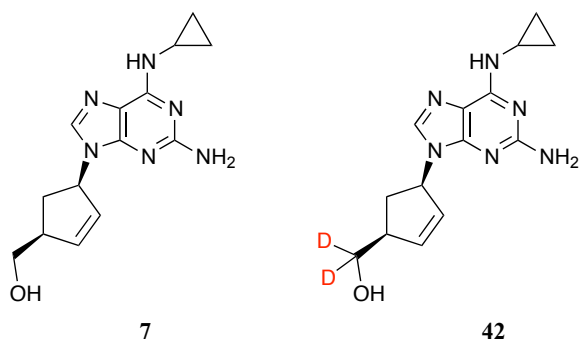
Figure 2.6: ABC **7** shown with its designed di-deuterated analogue, D_2-ABC **42**; where two 5'-H (ABC) atoms have been replaced with 2 5'-D atoms (D_2-ABC). D_2-ABC, deuterated-ABC.

2.2 Aims

- To develop a synthetic route to D_2-ABC **42**

- To synthesise and isolate ABC-CHO (**16a/16b** and **16c**)

- To synthesise and isolate ABC-COOH (**17a**) using a variety of synthetic methods and/or routes.

2.3 Results & Discussion

2.3.1 Synthesis of ABC-aldehyde 16.

The initial focus of the chemical research was to synthesise ABC aldehyde **16**. The isolation of this intermediate would be very useful in further immunology and proteomic experiments to determine any T-cell stimulation and protein binding.

Previous research has highlighted the difficulty in obtaining the aldehyde due to its reactive nature with either a molecule of itself or other reagents present.[1,31] Also, **16a**, the primary product of the chemical and enzymic oxidation of ABC, rearranges to **16c** spontaneously. Consideration had to be made that the alkene must be unaffected by the oxidant.

Before the Charneira paper was published in 2011,[31] several oxidation reactions were attempted. The first attempt used pyridinium chlorochromate (PCC) in dichloromethane (DCM) (Figure **2.7**). PCC is a stable, well-utilised chromium (VI) oxidising agent, used for selectively oxidising primary alcohols to aldehydes.[36-38]
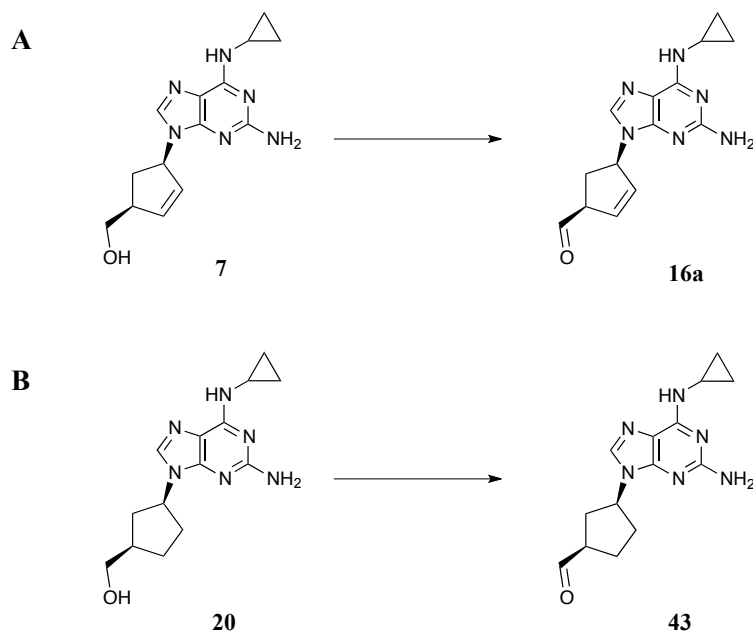
Figure 2.7: Attempted oxidation of ABC **7** using the following oxidising reagents: PCC or TEMPO/BIAB or BaMnO$_4$ to synthesise aldehyde **16a** (**A**) and oxidation of DH-ABC **20** using PCC as the oxidising agent to theoretically yield **43** (**B**). PCC, pyridinium chlorochromate.

The reaction was attempted several times with varying reaction times (2–24 h), and equivalents of PCC (1.5–3.0 equiv). Analysis of the crude reactions using ^{1}H NMR showed the presence of an aldehyde product (9.96 ppm), but due to the crude nature of the mixture, confirmation of aldehyde stereochemistry and formation was difficult. It was evident that side reactions were occurring, shown by thin layer chromatography (TLC) and ^{1}H NMR. These reactions were either pre- or post-aldehyde formation, and following simple work-up and purification by column chromatography, no aldehyde product could be obtained *via* this method. The formation of the aldehyde appeared to be short-lived and even liquid chromatography-tandem mass spectrometry (LC-MS/MS) also failed to detect product formation, with significant side-product formation being detected instead. The crude nature of the mixture hindered analysis and confirmation of side-

products/products. It was likely, from the presence of several nucleophilic groups on ABC and the likelihood of double bond migration and further reactivity through a 1,4 mechanism, that the formation of side products was certain to occur (Figure **2.8**).
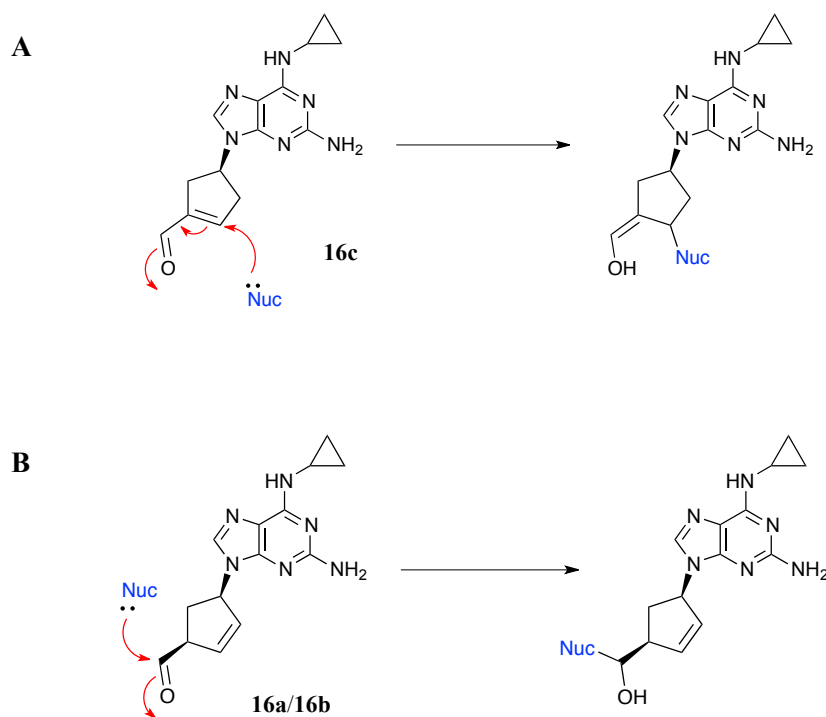
Figure 2.8: During the oxidation process, the α,β-unsaturated aldehyde **16c** becomes susceptible to 1,4 nucleophilic attack (**A**). The β,γ-unsaturated aldehyde **16a/16b** is also able to react *via* a 1,2 nucleophilic addition (**B**).

With this consequence in mind, the oxidation of DH-ABC **20** (see Chapter 4 for synthesis of **20**) to its aldehyde **43** was attempted under the same conditions (Figure **2.7**). Due to lack of a carbocyclic alkene, no double bond migration and/or 1,4 nucleophilic addition could occur. Unfortunately, analysis of the crude reaction detected no aldehyde formation and no product was isolated by silica gel column chromatography. Nucleophilic attack of the aldehyde could occur immediately after

it had been formed (Figure **2.8**). Side reactions of this nature are applicable to both **7** and **42**.

Following this attempt, further research was carried out into milder oxidising methods and so barium manganate $(BaMnO_4)$[39] was employed. This agent is capable of selectively oxidising primary alcohols to their respective aldehydes without oxidising alkenes. The $BaMnO_4$ reaction was heated to reflux (in DCM) for 48 h, and although only very few side reactions occurred, starting material (80%) was recovered.

Although often used for complete oxidation of primary alcohols to their respective carboxylic acids, TEMPO/BIAB reagent was used in an attempt to synthesise **16** (Figure **2.7**). The oxidation was attempted with one equivalent of TEMPO in anhydrous ACN. The desired aldehyde was not isolated and starting material was observed.

After the failure to obtain **16** *via* the traditional Swern oxidation method, a paper published in 2011 reported an application of modified Swern oxidation reagents, for the synthesis of **16a**/**16b** and its isomer **16c** (Scheme **2.2**) as previously discussed.[31]

By following this procedure, isomer **16c** (Scheme **2.3**) was synthesised and successfully isolated *via* silica gel column chromatography. The instability of **16c** was noticeable after purification, with apparent degradation products observed by ^{1}H NMR. This was likely to occur due to the instability of compound **16c**. Further work conducted within the Liverpool group has shown that this impurity yielded

[M+H]$^+$ at *m/z* 271 and the generic purine fragment at *m/z* 191, deducing the impurity to be ABC cyclopentenone. Minimal contact of **16c** with solvents and storing the aldehyde at –20 °C reduced the rate of product degradation. This compound could be used to further investigate covalent protein binding.[31]
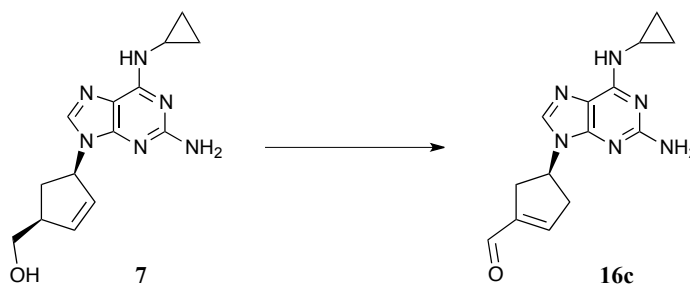
Scheme 2.3: Reagents and conditions: DMSO (2.5 equiv), C$_2$O$_2$Cl$_2$ (1 equiv), ABC **7** (1 equiv), NEt$_3$ (4.5 equiv), THF, –78 °C → r.t., N$_2$, 2 h, 18%.

Future work will involve the synthesis of aldehyde **16a/16b** under the conditions stated by Charneira *et al.*[31] although, Charneira and co-workers found the isolation of this aldehyde difficult with **16c** often contaminating the samples. With successful purification, both compound **16a/16b** and its isomer **16c** could be used in further studies.

2.3.2 Synthesis of ABC-carboxylic acid 17a.

ABC-COOH (**17a**) was required as a standard metabolite in future metabolic studies. GSK initially supplied this compound, namely standard compound 2269W93,[1] but due to limited supply additional material was required and attempts to synthesise it chemically from ABC itself are detailed below.

An oxidation method using $KMnO_4$ was discarded due to non-selective oxidation, as the alkene is also susceptible to oxidation. Other possible oxidation methods considered were ruthenium tetraoxide (RuO_4), pyridinium dichromate (PDC), Jones reagent, and TEMPO/BIAB oxidation. The first oxidation procedure attempted utilised freshly prepared Jones reagent (Figure **2.9**). Although ABC has limited solubility in organic solvents, the Jones oxidation was performed conventionally in acetone, in which ABC is moderately soluble. However, upon cooling to 0 °C in preparation for addition of Jones reagent, some precipitation was evident. After addition of the oxidising agent, rapid salt formation was observed. The equivalents of the reagent were reduced but the precipitate formation still occurred and through analysis *via* TLC, there was no conversion of starting material. The salt formation was likely due to the formation of ABC sulfate (sulfate originating from sulfuric acid in Jones reagent). In an attempt to overcome this problem, the succinate salt of ABC was used. However, using ABC succinate completely prevented any material dissolving in acetone, and although the reaction was attempted with solubility issues, no product was formed.
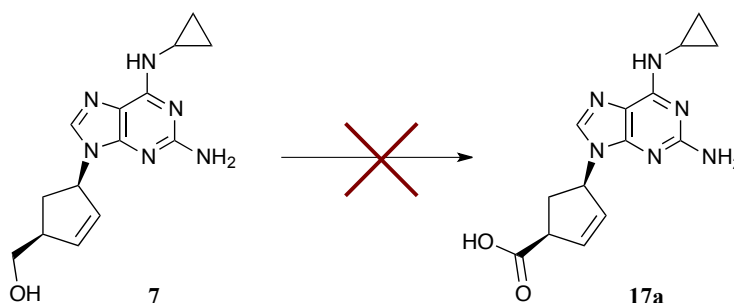
Figure 2.9: Direct formation of ABC-COOH **17a** from ABC **7** using three oxidising agents: Jones reagent, TEMPO/BIAB and molecular O_2 with Pd/C. ABC-COOH, abacavir carboxylic acid.

87

TEMPO oxidation was also attempted. Rather than anhydrous conditions, as seen with TEMPO oxidation to afford the corresponding aldehyde, a 1:1 mixture of ACN and H_2O was used. This procedure has been the method of choice for many oxidations of nucleoside 5'-primary alcohols to carboxylic acids.[2,3,10-12] The formation of these carboxylic acids is typically high yielding, using mild reaction conditions with no lengthy purification procedures: Products frequently precipitate and are obtained *via* filtration.[2] However, even with varying TEMPO equivalents (1–2 equiv), reaction times (4–24 h) and solvent volumes, no carboxylic acid product was obtained or detected. Although the reagents are relatively mild, in comparison to metallic oxidising agents, side reactions were still evident and seen within ^{1}H NMR analysis. The low solubility of ABC in most organic solvents was overcome in this reaction by using water, which readily solubilises ABC. Therefore, it is concluded that the solubility of ABC is not an issue in these reaction conditions, rather the problem lies with the reactivity of ABC itself.

The final direct oxidation method attempted utilised oxygen, palladium on carbon (Pd/C), sodium borohydride ($NaBH_4$) and KOH. This method, although relatively unemployed as a common oxidation procedure, has been applied to a variety of substrates.[40] ABC succinate was used rather than ABC itself due to solubility issues, but unfortunately no reaction occurred and only starting material was recovered.

Due to the problems of forming **17a** from ABC, an alternative route was designed. The procedure was adapted from a patent, published by GSK, for the efficient large-scale synthesis of ABC. The original route, a three-step method, used a chiral amino-alcohol and DADCP **30**.[41] The adapted route (Scheme **2.4**) consisted of five

steps and began with ring-opening chiral lactam **28**, followed by coupling with pyrimidine **30**.
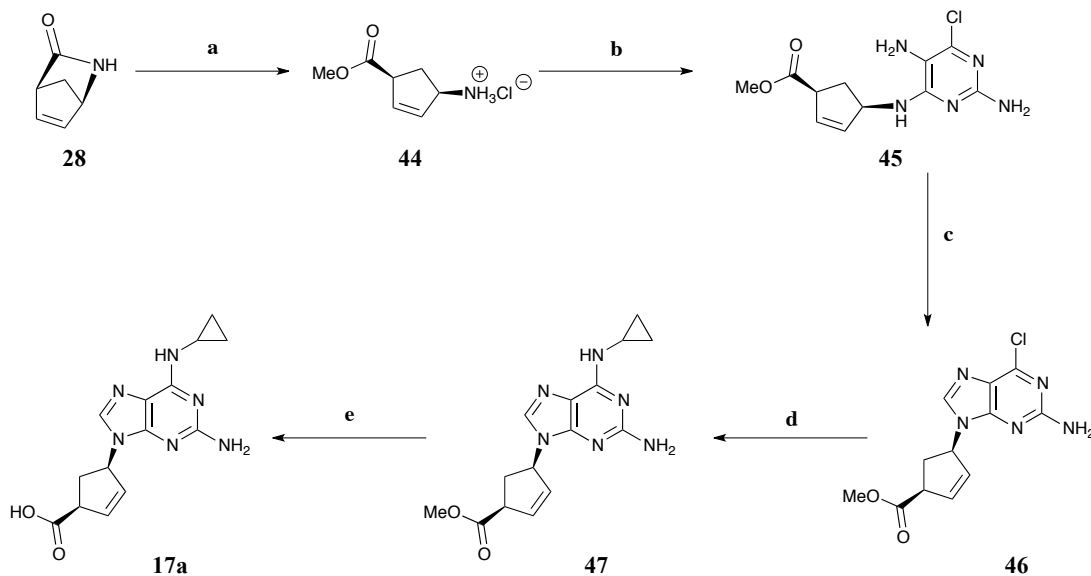
Scheme 2.4: Proposed route to synthesise **17a**. Reagents and conditions: a) $SOCl_2$ (2.2 equiv), MeOH, 0 °C, 1 h, 95%; b) DADCP **30** (2.0 equiv), $NaHCO_3$ (3.5 equiv), *t*-BuOH, 95 °C, 14 h, 42%; c) TEOF (1.2 equiv), H_2SO_4 (0.05 equiv), *n*-BuOH, 65 °C; d) Cyclopropylamine (1.2 equiv), MeOH, 60 °C; e) 2 M LiOH, MeOH, r.t. (Steps **c–e** were not fully completed). DADCP, 2,5-diamino-4,6-dichloropyrimidine.

At the initial step, ring opening of bi-cyclic lactam **28** using thionyl chloride ($SOCl_2$) and methanol (MeOH), formed the cyclopentyl portion of ABC with appropriate functionality and stereochemistry in excellent yields. By using MeOH in this step, the methyl ester at 5'-C was obtained. The ester, replacing the 5'-OH group in ABC, could be hydrolysed to the desired carboxylic acid at the end of the synthesis.

Compound **44** was coupled with DADCP **30** under conditions similar to those patented.[41] This step proved problematic, and in the first instance it was thought that

reduced electrophilicity and steric clashes with pyrimidine **30** were responsible for lack of product formation; nucleophilic substitution occurs more easily at positions 2, 4 and 6. To circumvent this problem, it was proposed that mono/di-protecting the amino groups on **30** would allow for easier nucleophilic substitution of either chlorine atom.
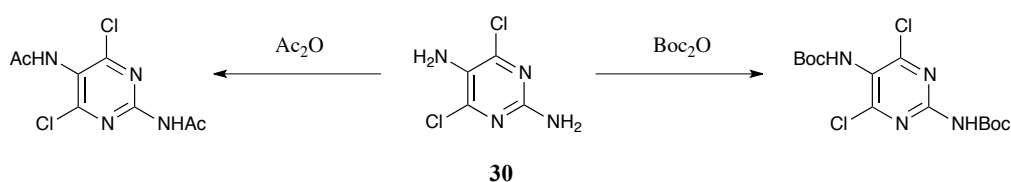
Figure 2.10: Attempts to di-protect compound **30** using Boc$_2$O and Ac$_2$O.

Di-amino protection of pyrimidines is notoriously difficult, with mono protection only likely at position 5.[42] Amine moieties at position 2 have the greatest electron density in comparison to the other positions and therefore protection of this position is much lower. Two reactions were attempted: Protection with a *t*-butyloxycarbonyl (Boc) and an acetyl group using di-*tert*-butyl dicarbonate (Boc$_2$O) and acetic anhydride (Ac$_2$O), respectively (Figure **2.10**). However, even with a large excess of reagents in both experiments, no reactions occurred, and the initial method using non-protected DADCP was revisited. Therefore, the focus of this step was the need to optimise the original reaction conditions (Table **2.1**).

Table 2.1: Table representing the set of reactions completed (A–G) to optimise conditions for the coupling reaction (step 2, Scheme **2.4**) of compound **44** with **30**. DBU, 1,8-diazabicyclo[5.4.0]undec-7-ene.

Reaction	Reagents and Reaction Conditions*			Yield (%)
	Solvent	Base (equiv)	Temperature (°C)	
A	n-BuOH	NaHCO$_3$ (3.5)	70	36 (crude)
B	MeOH (sealed tube or reflux)	K$_2$CO$_3$ (2.5)	80 (sealed tube / reflux)	Not obtained
C	t-BuOH (sealed tube)	NaHCO$_3$ (2.5)	85	42
D	EtOH	NEt$_3$ (2.5)	Reflux	Not obtained
E	t-BuOH	NEt$_3$ (2.5)	80 then 95	Not obtained
F	t-BuOH	DIEA & DBU (2.5)	85	15
G	EtOH	NaHCO$_3$ (2.5)	Microwave at 100 °C	Not isolated

*All reactions were completed on a 200 mg scale (of compound **44**).

The choice of base and solvent appeared critical to affording the desired product. Less hindered polar aliphatic solvents such as MeOH and ethanol (EtOH) proved problematic due to their aromatic nucleophilic tendencies to substitute chlorine at the 6-position. *t*-Butanol (*t*-BuOH), a more hindered protic solvent, was therefore

chosen. The base required for the reaction was also altered, so as to use an organic or inorganic base. Under organic base conditions, (reactions D, E and F) fewer side reactions were evident but product formation was slower. In reaction E, where NEt$_3$ was used, nucleophilic addition at the 6-position yielded the undesired product **48** (Figure **2.11 A**). To prevent this from occurring, a more hindered organic base, in this case DIEA followed by 1,8-diazabicyclo[5.4.0]undec-7-ene (DBU), was used. Although fewer side reactions occurred, the yield achieved was lower than that in reaction C. Under microwave (MW) conditions, reaction E, the greatest amount of side products was observed and no desired product was obtained.

A

48

B

28   **44**
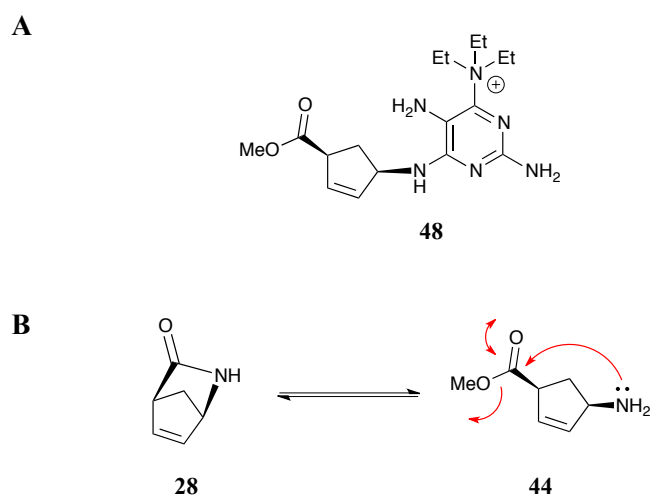
Figure 2.11: Diethylamine product **48** formed during reaction E (Table **2.1**), using NEt$_3$ as the base (**A**). The equilibrium between compounds **28** and **44** at step 2 may have contributed to low reaction yields (**B**).

The original conditions that have been adapted to this synthesis were taken from a patent for the synthesis of ABC.[41] The initial step in this patent, was coupling of a cyclopentyl amino-alcohol with DADCP **30**, rather than with the amino-ester **44** as used within this synthesis. The problems experienced in this coupling step are therefore thought to arise from a reversible reaction between lactam **28** and amino-

ester **44** (Figure **2.11 B**). Increased temperatures would favour this equilibrium: A condition that is essential in this step. Therefore it is postulated that the low yields experienced are as a result of this equilibrium. Nevertheless, reaction C conditions were chosen, and by using a sealed tube the temperature of the reaction could be increased, if necessary beyond the boiling point of the solvent.

The third step, ring closing to form purine **46**, also proved problematic. Purification of the step 2 product was extremely difficult and often resulted in low yields. To eliminate this problem, crude mixtures were used without purification in step 3. The number of side reactions also increased in step 3, and consequently compound **46** could not be isolated. Due to time constraints, these conditions were not optimised and the final two steps are yet to be completed. These steps would be a focus for future work.

2.3.3 Synthesis of D$_2$-ABC 42.

An efficient, high yielding total synthesis of D$_2$-ABC **42** was essential for this research. There are a variety of methods that can be adapted to incorporate D atoms. A synthetic route using chiral auxiliaries, as developed by Crimmins and co-workers,[43] was chosen as the optimal route. The two D atoms are introduced at step 4 and are placed on the 4'-C. The synthetic route is shown in Scheme **2.5**.
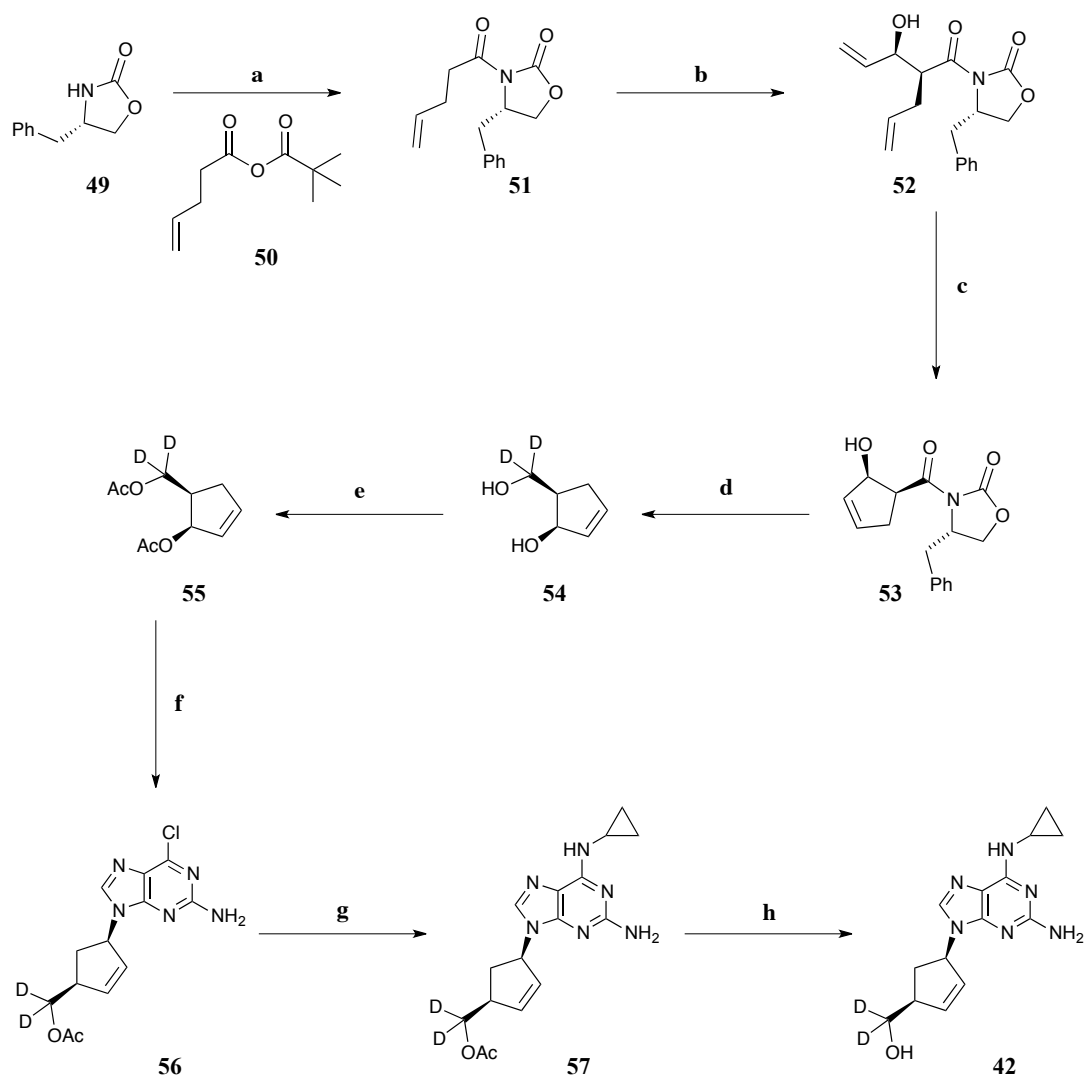
Scheme 2.5: Total synthetic route for synthesising D₂-ABC. Reagents and conditions: a) *n*-BuLi (1 equiv), pivaloyl chloride (1 equiv), NEt₃ (1 equiv), 4-pentenoic acid (1 equiv), *t*-BME, THF, −78 °C → r.t., N₂, 2 h, 85%; b) DIEA (2.2 equiv), DBBT (2.2 equiv), acrolein (2.1 equiv), DCM, −78 °C → r.t., N₂, 16 h, 87%; c) Grubbs catalyst 1st generation (5 mol %), DCM, r.t., Ar, 15 h, 70%; d) LiAlD₄ (2.2 equiv), THF, 0 °C, 2 h; e) Ac₂O (3 equiv), NEt₃ (3 equiv), DMAP (cat.), DCM, r.t., N₂, 16 h; f) 2-amino-6-chloro purine (1.5 equiv), NaH (1.5 equiv), Pd(PPh₃)₄ (10 mol %), THF, 50 °C, Ar, 16 h, 32%; g) Cyclopropylamine (1.2 equiv), MeOH, 60 °C, 16 h, 77%; h) 1 M NaOH (excess), EtOH, r.t., 48 h, 64%. *t*-BME, *t*-butylmethyl ether; DBBT, dibutylboryl triflate; DCM, dichloromethane; DMAP, 4-dimethylaminopyridine; cat., catalytic.

The initial step synthesised compound **51** from an enantiomerically pure benzyl oxazolidinone auxiliary **49**. Intermediate **50** was prepared from 4-pentenoic acid and pivaloyl chloride. It was used without purification, and upon reaction with the oxazolidinone auxiliary, compound **51** was obtained in high yields (78–85%). A terminal alkenyl side chain obtained from acrolein was added to **51** using dibutylboryl triflate (DBBT) to form the appropriate syn aldol geometry, yielding compound **52**.

The two terminal alkenes were now positioned ideally for RCM to form the cyclopentyl ring, compound **53**. Relatively near the start of the complete synthesis, it was paramount that this step achieved a good yield. Olefin metathesis was achieved using the ruthenium-based Grubbs catalyst. Four commonly used catalysts are Grubbs catalysts 1st and 2nd generation and Hoveyda-Grubbs catalysts 1st and 2nd generation. The catalyst chosen initially was Grubbs catalyst 1st generation.

The initial difficulties encountered with this reaction were low yield and removal of the catalyst. The conditions required optimisation; the results of which can be seen in Table **2.2**. Increasing the mol % of the catalyst from 0.5 (reaction A) to 2 mol % (reaction B) resulted in an increased yield of 35%. Increasing the mol % further to 5 or 7 mol % (reaction C) increased the yield further to 50%. Under an atmosphere of nitrogen, Hoveyda-Grubbs 2nd generation catalyst (reaction D) gave the best yields (62%) but this relatively new catalyst is expensive to use on a larger scale. Yields were improved further when the reaction was carried out under an argon atmosphere as opposed to nitrogen (reactions E and F).

Ruthenium-based catalysts have been shown to act as a catalyst in the reduction of alkene functional groups in the presence of $NaBH_4$.[44] It was therefore vital that all the Ru catalyst was removed prior to the following reduction step using lithium borodeuteride ($LiBD_4$). Tris(hydroxymethyl)phosphine (THP) (1 M) has proved an efficient Ru scavenger.[45,46] THP readily complexes with Ru, and in doing so, the metallic complex becomes water-soluble. The catalyst was then removed in a simple organic–water work-up. The optimised yield (70%), forming compound **53**, was achieved using conditions shown in reaction F.

Table 2.2: Table representing the set of reactions completed (A–F) in order to optimise conditions for the RCM of compound **53**. THP, tris(hydroxymethyl)phosphine.

Reaction	Reagents and Reaction Conditions[*]		Yield (%)
	Grubbs Catalyst	**Atmosphere**	
A	1st generation (0.5 mol %)	Nitrogen	10
B	1st generation (2 mol %)	Nitrogen	45
C	1st generation (5 / 7 mol %)	Constant flow of nitrogen	50 / 51
D	Hoveyda-Grubbs 2nd generation (5 mol %)	Nitrogen	55
E	1st generation (5 mol %)	Argon	62
F	1st generation (5 mol %)	Argon (with THP to remove catalyst)	58–70

[*] All reactions were left for 16 h at r.t. and trial experiments were completed on 50–100 mg scales.

Commercially available LiBD$_4$ was used to reduce **53** and in doing so, two D atoms were placed at the 5'-C position. ^{1}H NMR analysis showed a mixture of three products (Figure **2.12**): Non-deuterated, mono-deuterated and di-deuterated products.
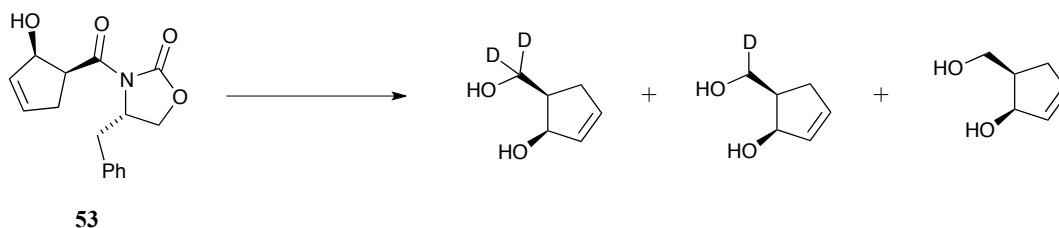
Figure 2.12: Mixture of three products formed (2.5:1:0.5 di-deuterated−mono-deuterated−non-deuterated) when using LiBD$_4$ as the reducing agent to reduce intermediate **53**.

To dispel the uncertainty as to why three products were formed, a test reaction using 3,5-dibromomethylbenzoate was attempted (Figure **2.13**). It was found that again, a mixture of three products were formed. From this finding, it was concluded that the reagent, LiBD$_4$, was contaminated with lithium borohydride (LiBH$_4$). The reducing agent was changed and commercially available lithium aluminum deuteride (LiAlD$_4$) was used. Although the yields using this reagent were low, a compromise was accepted as the reagent eliminated the mixture of products and only the required di-deuterated product **54** was formed. Due to the high water solubility and relative volatility of **54**, it was often taken on crude to the next step, after removal of inorganic salts. The following step was a simple diacetylation of the alcohol groups with Ac$_2$O to yield compound **55** in moderate yields (50–60%).
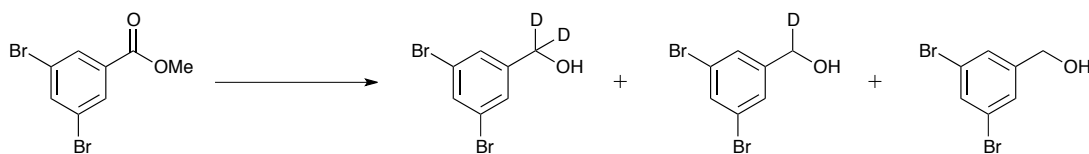
Figure 2.13: 3,5-Dibromomethylbenzoate was the compound used to test the purity of the reducing agent, $LiBD_4$. The reaction was conducted using $LiBD_4$ (2.2 equiv) with the formation of three products (di-deuterated, mono-deuterated and non-deuterated compound) showing some contamination of the deuterated reducing agent with $LiBH_4$.

The optimised conditions for step 6 were previously established for the non-deuterated route (see Chapter 4) and compound **56** was achieved with a 38% yield. The N^9 isomer was almost exclusively synthesised with very little N^7 isomer formation observed. Using NMR and reference standards, it was clear that the isomer N^9 was obtained. In ^{1}H NMR the C-8 proton of this isomer is usually upfield (approx. 7.9 ppm) compared to the C-8 proton of the N^7 isomer (approx. 8.1 ppm).[47] Subsequent nucleophilic aromatic substitution under standard conditions with cyclopropylamine, displacing chlorine at the 6-position, yielded compound **57** with good yields. The final step, deprotection of 5'-OH using 1 M sodium hydroxide (NaOH), yielded the desired compound, D_2-ABC **42**, in 63% yield. This material was used in metabolism studies (Chapter 3).

2.4 Conclusions & Future Work

Uncertainties remain in determining the contribution of the oxidative metabolites of ABC to its toxicity, although this pathway has been greatly researched.[1,23] To probe the oxidative pathway further, synthetic standards of both metabolites under investigation, ABC-CHO **16** and ABC-COOH **17** were required.

A variety of methods used in the attempted synthesis of either ABC-**16** or ABC-**17** have proven difficult to apply using a variety of oxidising agents. A modified Swern method used to synthesise two isomers of ABC-**16** was published recently[31] and this method has been utilised successfully to form an ABC-**16** isomer (isomer **16c**). The difficulties in forming ABC-**17** remain, however a 5-step synthetic route to the product has been started, with steps 1 and 2 successfully completed. Further work is needed to improve this route and to complete the final three steps. The α,β-unsaturated aldehyde and its isomers will be useful for testing possible haptenation reactions and for other research into protein modification.[34] The carboxylic acid, an *in vivo* metabolite, will be valuable as an assay standard, as seen in Chapter 3, for further metabolic studies on ABC.

D$_2$-ABC **42** was successfully synthesised using an 8-step synthesis. It was synthesised not only as an internal standard (IS) for quantitative metabolic studies on ABC (Chapter 3), but principally to probe the metabolic activation of ABC as a means of assessing the potential of the isotopically substituted compound to deliver enhanced drug safety. In respect of the initial hypothesis of ABC toxicity, namely

the hapten hypothesis, **42** was the ideal compound to probe this phenomenon, provided the rate of the major metabolic activation route was slowed (Chapter 3).

To further probe the oxidative metabolic pathway of ABC, the secondary isotope effect could be investigated. This would require synthesis of the 4'-D analogue of ABC (Figure **2.14 A**). Investigation of the secondary isotope effect will also probe the reaction mechanism and in particular, the rate determining step (RDS) of this oxidative pathway.
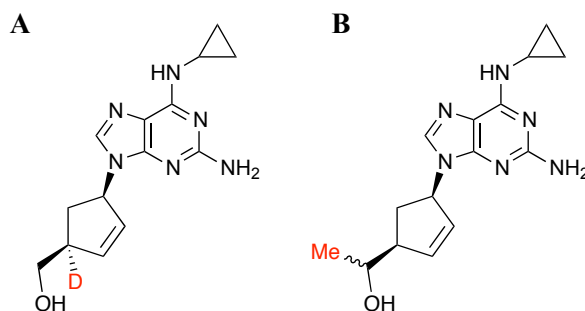
Figure 2.14: Structure of an alternative deuterated form of ABC, where the 4'-H is replaced with a D atom, rather than at the 5'-H position, as synthesised within this research (**A**). An alternative 5'-C analogue: An analogue that bears a methyl group at the 5'-C position. This analogue would prevent the oxidative pathway allowing for further probing of the mechanistic pathway (**B**).

Further to this, analogues at the 5'-C position could also be synthesised, such as the substitution of a 5'-H for a methyl group (Figure **2.14 B**). This would prevent the formation of both the aldehyde and carboxylic acid compounds. This analogue, under subjection to the same metabolic experiments as described in Chapter 3, would allow the oxidative mechanistic pathway to be explored further.

2.5 Experimental

2.5.1 General chemical methods.

All reagents were purchased from Sigma Aldrich (Poole, Dorset), Alfa Aesar (Heysham, Lancashire) or Apollo Scientific (Bredbury, Stockport, Cheshire) unless otherwise stated. Air and moisture sensitive reactions were carried out using oven-dried glassware and rubber septa. Such reactions were carried out under a positive pressure of a nitrogen or argon atmosphere and air or moisture sensitive liquids were transferred *via* syringe. All reactions were stirred using Teflon-coated magnetic stirrer bars and all organic solvents were removed using a Buchi rotary evaporator, unless otherwise stated. Anhydrous solvents were either obtained from commercial sources (Sigma Aldrich or Alfa Aesar) or distilled under an inert atmosphere prior to immediate use. Tetrahydrofuran (THF) was distilled from Na and DCM from calcium hydride (CaH_2). All other reagents were used without further purification unless stated otherwise.

All ^1H and ^{13}C NMR analyses were run on a Bruker ARX 400 (400 MHz) NMR spectrometer and all deuterated solvents were as stated within the text for each compound. Chemical shifts (δ) are in parts per million (ppm). Tetramethylsilane (TMS) was used as the internal reference. Multiplicities are recorded as singlet (s), doublet (d), triplet (t), multiplet (m) and broad (br). All *J* couplings are recorded in Hertz (Hz). Mass spectra were recorded on a Micromass LCT mass spectrometer using electron spray ionisation (ESI), a Fisons TRIO spectrometer or Agilent QTOF 700 spectrometer, using chemical ionisation (CI). Accurate mass values are stated

within ± 5 ppm. Infrared spectra (IR) were recorded using a Jasco FT/IR-4200 spectrometer and samples were run neat. Elemental analyses (C, H and N) were completed within the University of Liverpool Microanalysis Laboratory and values are stated within a ± 0.5% error. Melting points were determined on a Gallenkamp melting point apparatus. TLC was performed on silica gel 60-F_{254} (Merck) and visualised *via* ultraviolet (UV) light or by staining with *p*-anisaldehyde stain (*p*-anisaldehyde (3.7 mL), AcOH (1.5 mL), conc. H_2SO_4 (5 mL) in EtOH (135 mL)) or $KMnO_4$ stain ($KMnO_4$ (1.5 g), K_2CO_3 (10 g) and 10% NaOH (1.25 mL) dissolved in H_2O (200 mL)) followed by gentle heating. Silica gel 60 (Merck, 63–200 m) was used for flash column chromatography.

2.5.2 Synthesis.

49   **51**
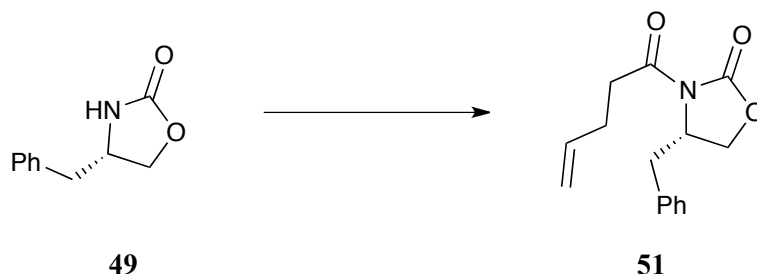
(*S*)-4-Benzyl-3-(pent-4-enoyl)oxazolidin-2-one 51:[47] To a solution of 4-pentenoic acid (7.7 mL, 0.08 mol) in *t*-butylmethyl ether (*t*-BME) (220 mL) cooled to –78 °C was added NEt_3 (10.5 mL, 0.08 mol) and the solution was allowed to stir for 5 min. Pivaloyl chloride (9.4 mL, 0.08 mol) was added, and after a further 15 min, the solution was allowed to warm to 0 °C and stirred for 1 h. In a separate flask, (*S*)-4-benzyl-2-oxazolidinone **49** (6.36 g, 0.04 mol) in THF (100 mL) was allowed to cool to –78 °C and *n*-butyl lithium (*n*-BuLi) (15.0 mL, 2.5 M in hexane) was added dropwise. The solution was allowed to stir for 20 min. The anhydride flask was

cooled back to –78 °C and the white auxiliary solution added. The resulting mixture was allowed to stir for 15 min at –78 °C and for 30 min at 0 °C, whereupon the reaction was quenched with saturated aqueous ammonium chloride (NH₄Cl). The mixture was extracted with DCM (4 × 500 mL) and the resulting organic extracts were washed with brine and dried over magnesium sulfate (MgSO₄). The solvent was removed *in vacuo*. The crude product was purified by column chromatography (1:4 ethyl acetate−*n*-hexane (EtOAc−*n*-hex)) to yield **51** (7.90 g, 85%) as a clear and colourless oil.[47] ^{1}H NMR (CDCl$_3$): δ 7.36–7.20 (m, 5H), 5.90–5.87 (m, 1H), 5.19–4.97 (m, 2H), 4.71–4.65 (m, 1H), 4.27–4.11 (m, 2H), 3.30 (dd, J = 13.3, 3.3 Hz, 1H), 3.08–3.04 (m, 2H), 2.76 (dd, J = 13.4, 9.7 Hz, 1H), 2.54–2.39 (m, 2H). ^{13}C NMR (CDCl$_3$): δ 173.0, 153.9, 137.1, 135.7, 129.8 (2C), 129.4 (2C), 127.8, 116.2, 66.6, 55.6, 38.3, 35.2, 28.6. *m/z* (ES+) 282.1110 calculated for C$_{15}$H$_{17}$NO$_3$Na: [M+Na]$^+$ 282.1106. Anal. calc. for C$_{15}$H$_{17}$NO$_3$: C, 69.48; H, 6.61; N, 5.40. Found: C, 69.34; H, 6.70; N, 5.49. IR (cm^{-1}): 2978 (C−H), 1778 (C=O), 1581 (C=C aromatic), 1203 (C−O).

51   **52**
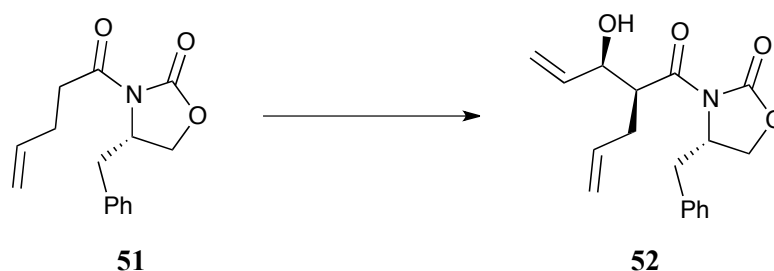
(*S*)-3-((2*S*,3*R*)-2-Allyl-3-hydroxypent-4-enoyl)-4-benzyloxazolidin-2-one 52:[47] To a solution of compound **51** (5.52 g, 0.02 mol) in DCM (20 mL) at –78 °C was added DIEA (8.2 mL, 0.05 mol) followed by DBBT (42.6 mL, 1 M solution in DCM). The mixture was allowed to stir at room temperature for 1 h. After re-cooling to –78 °C, a solution of acrolein (3.2 mL, 0.05 mol) in DCM (5 mL) was added dropwise. The

resulting mixture was allowed to stir at –78 °C for 2 h and then allowed to warm to room temperature overnight. The solution was quenched with saturated aqueous sodium hydrogen carbonate (NaHCO$_3$) and extracted into DCM (4 × 100 mL). The combined organic extracts were washed with brine and dried over MgSO$_4$. The solvent was removed *in vacuo*. The resulting crude product was purified by column chromatography (1:4 to 2:5 EtOAc–*n*-hex) to yield **52** (5.82 g, 87%) as a pale yellow oil.[47] ^{1}H NMR (CDCl$_3$): δ 7.33–7.19 (m, 5H), 5.91–5.87 (m, 2H), 5.36–5.04 (m, 4H), 4.72–4.61 (m, 1H), 4.47–4.45 (m, 1H), 4.37–4.25 (m, 1H), 4.18–4.11 (m, 2H), 3.30–3.24 (m, 1H), 2.76–2.64 (m, 1H), 2.63–2.52 (m, 1H), 2.51–2.35 (m, 1H). ^{13}C NMR (CDCl$_3$): δ 174.9, 153.8, 137.4, 135.6, 129.8, 129.3, 127.8, 117.8, 116.7, 73.7, 66.4, 56.0, 47.6, 38.4, 32.4. *m/z* (ES+) 338.1379 calculated for C$_{18}$H$_{21}$NO$_4$Na: [M+Na]$^+$ 338.1368. IR (cm^{-1}): 2970 (C−H), 1774 (C=O), 1697 (C=C), 1207 (C−O).

52   **53**
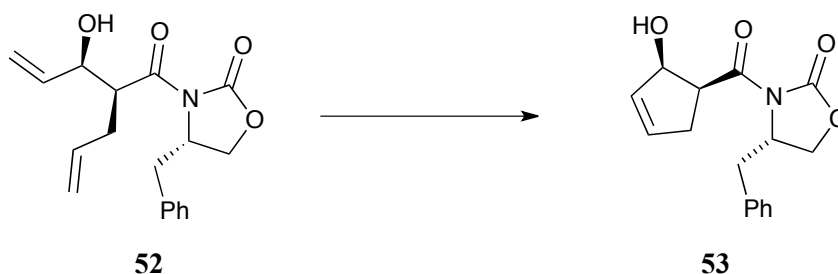
(*S*)-4-Benzyl-3-((1*S*,2*R*)-2-hydroxycyclopent-3-enecarbonyl)oxazolidin-2-one 53:[47] To a solution of **52** (2.75 g, 9.0 mmol) in anhydrous DCM (15 mL), in a degassed flask under argon, was added 1st generation Grubbs catalyst (0.26 g, 5 mol %) at room temperature. The reaction was allowed to stir overnight. Freshly prepared THP (8.0 mL, 1 M in isopropyl alcohol (IPA)) was added and the mixture was extracted into DCM (3 × 30 mL). The combined organic extracts were washed with brine and dried over MgSO$_4$. The solvent was removed *in vacuo*. The crude product was purified by column chromatography (1:1 EtOAc–*n*-hex) to yield **53**

(1.74 g, 70%) as a colourless crystalline solid.[47] mp: 81–83 °C. ^{1}H NMR (CDCl$_3$): δ 7.40–7.16 (m, 5H), 6.11–6.00 (m, 1H), 5.85–5.73 (m, 1H), 5.19–5.05 (m, 1H), 4.78–4.72 (m, 1H), 4.52–4.47 (m, 1H), 4.19–4.15 (m, 2H), 3.35 (dd, J = 13.3, 3.3 Hz, 1H), 3.22–3.08 (m, 1H), 2.79 (dd, J = 13.4, 9.8 Hz, 1H), 2.54–2.50 (m, 1H). ^{13}C NMR (CDCl$_3$): δ 172.6, 154.0, 135.8, 135.3, 131.5, 129.9 (2C), 129.4 (2C), 127.8, 66.6, 60.8, 56.0, 47.5, 38.5, 33.7. m/z (ES+) 310.1057 calculated for C$_{16}$H$_{17}$NO$_4$Na: [M+Na]$^{+}$ 310.1055. Anal. calc. for C$_{16}$H$_{17}$NO$_4$: C, 66.89; H, 5.96; N, 4.88. Found: C, 66.59; H, 5.99; N, 4.76. IR (cm^{-1}): 3471 (br, O−H), 2966 (C−H), 1781 (C=O), 1693 (C=C), 1207 (C−O).

53   **54**
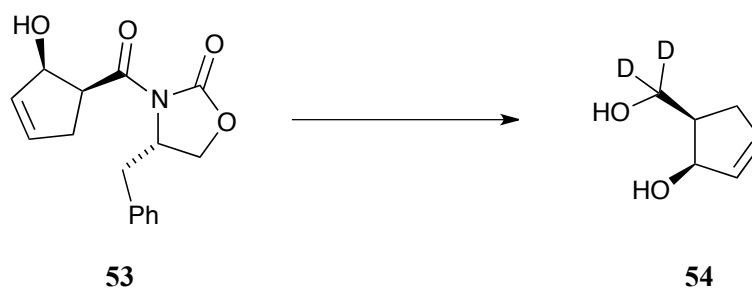
d$_2$-(1R,5R)-5-(Hydroxymethyl)cyclopent-2-enol 54: To a solution of **53** (1.16 g, 4.0 mmol) in THF (30 mL) at 0 °C was added LiAlD$_4$ (0.27 g, 7.0 mmol) slowly. The resulting suspension was stirred at 0 °C for 2 h and at 0 °C, H$_2$O (0.27 mL) was added dropwise. After stirring for 5 min, 15% aqueous NaOH (0.27 mL) was added and the solution was stirred for a further 5 min and finally water (0.81 mL) was added and the solution stirred for 15 min. MgSO$_4$ was added, and the suspension was stirred for 15 min before filtering the solution and removing the solvent *in vacuo*. The crude product (yellow liquid) was used without purification. ^{1}H NMR (CDCl$_3$): δ 6.03–6.01 (m, 1H), 5.85–5.82 (m, 1H), 4.95–4.93 (m, 1H), 2.52–2.48 (m, 1H), 2.42–2.35 (m, 1H), 2.27–2.20 (m, 1H), 2.04 (br s, 1H), 1.64 (br s, 1H). ^{13}C

NMR (CDCl$_3$): δ 135.9, 132.7, 78.5, 42.7, 34.0. *m/z* (CI) 116.08 calculated for

C$_6$H$_8$D$_2$O$_2$: [M+[NH$_4$]$^+$–H$_2$O]$^+$ 116.1.

54   **55**
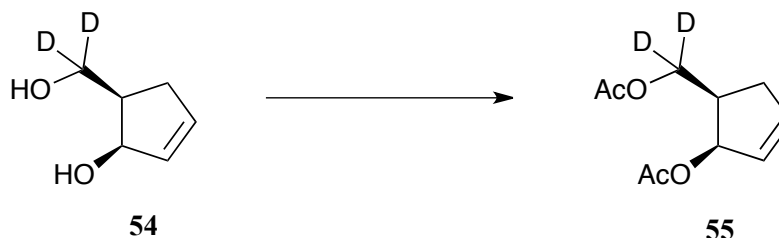
d$_2$-((1*R*,2*R*)-2-Acetoxycyclopent-3-en-1-yl)methyl acetate 55: To a stirred

solution of crude **54** (0.93 g) and 4-dimethylaminopyridine (DMAP, 0.08 g, 0.7

mmol) in DCM (10 mL) at 0 °C was added NEt$_3$ (1.6 mL, 11.0 mmol) and Ac$_2$O (1.1

mL, 12.0 mmol) dropwise. The resulting mixture was allowed to warm to room

temperature overnight whereupon it was quenched with water. The solution was

extracted into DCM (3 × 20 mL) and the combined organic extracts were dried over

MgSO$_4$ and the solvent removed *in vacuo*. The crude product was purified by

column chromatography (2:3 EtOAc–*n*-hex) to yield **55** (0.27 g) as a pale yellow oil.

^{1}H NMR (CDCl$_3$): δ 6.11–6.08 (m, 1H), 5.88–5.83 (m, 1H), 5.76–5.72 (m, 1H),

2.72–2.66 (m, 1H), 2.52–2.45 (m, 1H), 2.29–2.21 (m, 1H), 2.04 (s, 3H), 2.02 (s, 3H).

^{13}C NMR (CDCl$_3$): δ 171.4, 171.0, 137.1, 129.8, 78.5, 63.8–63.2 (q), 39.8, 35.0,

21.4, 21.3. *m/z* (CI) 200.10 calculated for C$_{10}$H$_{12}$D$_2$O$_4$: [M+H]$^+$ 200.1. IR (cm^{-1}):

2924 (C−H), 1734 (C=O), 1236 (C−O).
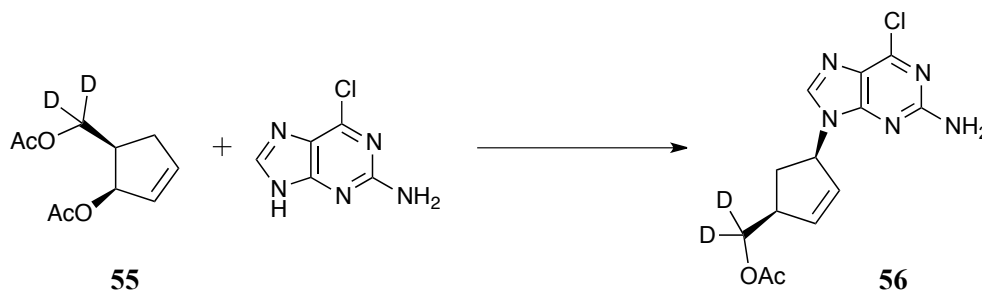
d$_2$-((1S,4R)-4-(2-Amino-6-chloro-9H-purin-9-yl)cyclopent-2-en-1-yl)methyl

acetate 56: Sodium hydride (NaH, 60% dispersed in mineral oil, 0.11 g, 2.9 mmol)

and 2-amino-6-chloro-purine (0.49 g , 2.5 mmol) in THF (10 mL) were stirred for 30

min at room temperature in the dark. The pale yellow solution was added to a flask,

equipped with reflux apparatus, containing tetrakis(triphenylphosphine)palladium(0)

(Pd(PPh$_3$)$_4$) (0.22 g, 10 mol %) and **55** (0.38 g, 1.9 mmol) in THF (10 mL), and the

resulting solution was degassed and heated under argon at 60 °C overnight in the

dark. The solution was cooled to room temperature whereupon H$_2$O (5 mL) was

added, the mixture was extracted with DCM (2 × 30 mL) and the combined organic

extracts were dried over MgSO$_4$. The solvent was removed *in vacuo*. The crude

material was purified by column chromatography (1:4 to 3:2 EtOAc–n-hex) to yield

56 (0.19 g, 32%) as an off-white solid. mp: 120–123 °C. ^{1}H NMR (CDCl$_3$): δ 7.83

(s, 1H), 6.15 (ddd, J = 5.6, 2.1, 2.0 Hz, 1H), 5.91 (ddd, J = 5.6, 2.2, 2.1 Hz, 1H),

5.58–5.56 (br m, 1H), 3.19–3.15 (m, 1H), 2.85 (ddd, J = 14.2, 8.9, 8.5 Hz, 1H), 2.06

(s, 3H), 1.70 (ddd, J = 14.2, 5.7, 5.5 Hz, 1H). ^{13}C NMR (CDCl$_3$): δ 171.4, 159.5,

153.8, 151.6, 140.9, 138.3, 130.2, 125.9, 59.9, 44.7, 34.9, 21.3. *m/z* (ES+) 332.09

calculated for C$_{13}$H$_{12}$D$_2$^{35}ClN$_5$O$_2$Na: [M+Na]$^+$ 332.1. IR (cm^{-1}): 3428 (N−H), 3301

(N−H), 1716 (C=N), 1612 (C=O), 1558 (C=C aromatic), 1257 (C−O).

56   **57**
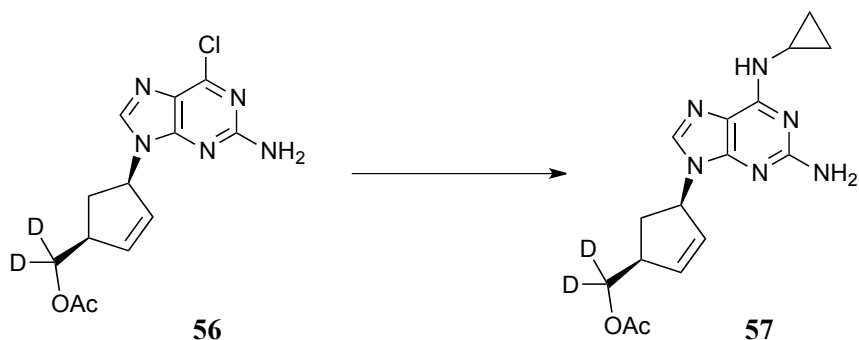
d$_2$-((1S,4R)-4-(2-Amino-6-(cyclopropylamino)-9H-purin-9-yl)cyclopent-2-en-1-yl)methyl acetate 57: To a solution of **56** (0.12 g, 0.4 mmol) in MeOH (10 mL) was added cyclopropylamine (0.07 mL, 1.0 mmol) at 0 °C and the solution was heated to 55 °C overnight. The reaction was allowed to cool and the solvent removed *in vacuo* to obtain **57** (0.10 g, 77%) as an off-white solid. ^{1}H NMR (CDCl$_3$): δ 7.52 (s, 1H), 6.10 (ddd, J = 5.6, 2.1, 2.1 Hz, 1H), 5.92–5.88 (m, 2H), 5.57–5.53 (br m, 1H), 4.83 (br s, 2H), 3.16–3.11 (m, 1H), 3.03–2.97 (m, 1H), 2.84 (ddd, J = 14.0, 8.8, 8.7 Hz, 1H), 2.07 (s, 3H), 1.64 (ddd, J = 14.0, 6.0, 5.8 Hz, 1H), 0.88–0.83 (m, 2H), 0.64–0.60 (m, 2H). ^{13}C NMR (CDCl$_3$): δ 171.4, 160.4, 156.7, 137.3, 135.7, 131.2, 115.3, 59.1, 44.6, 35.5, 24.1, 21.3, 7.8 (2C). *m/z* (ES+) 331.1854 calculated for C$_{16}$H$_{19}$D$_2$N$_6$O$_2$: [M+H]$^+$ 331.1852. IR (cm^{-1}): 3301 (N−H), 3201 (N−H), 2927 (C−H), 1731 (C=N), 1597 (C=C aromatic), 1477 (CH$_2$), 1257 (C−N).
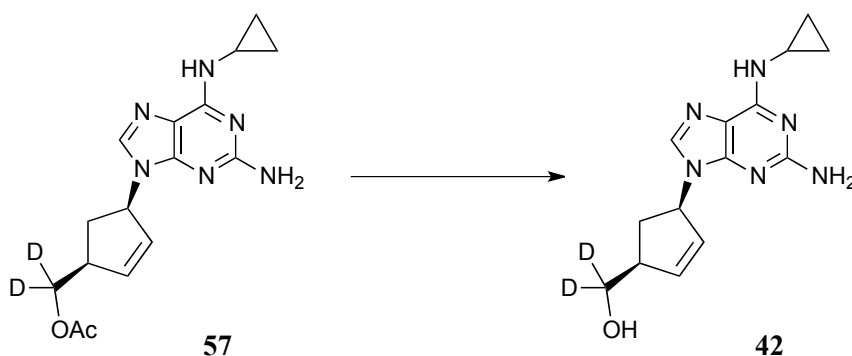
d$_2$-((1*S*,4*R*)-4-(2-Amino-6-(cyclopropylamino)-9*H*-purin-9-yl)cyclopent-2-en-1-yl)methanol 42: To a solution of **57** (0.09 g, 0.3 mmol) in EtOH (10 mL) was added 1 M NaOH (1.0 mL, 1.0 mmol) dropwise and the solution was allowed to stir at room temperature for 6 h. The solvent was removed *in vacuo* and the crude product was purified by column chromatography (1:19 MeOH–DCM) to yield **42** (0.05 g, 64%) as a colourless solid. mp: 136–140 °C. ^{1}H NMR (CDCl$_3$): δ 7.70 (s, 1H), 6.13 (ddd, *J* = 5.6, 2.1, 2.0 Hz, 1H), 5.86 (ddd, *J* = 5.6, 2.1, 2.0 Hz, 1H), 5.52–5.44 (br m, 1H), 3.29–3.25 (m, 2H), 3.01–2.93 (m, 1H), 2.73 (ddd, *J* = 13.9, 8.8, 8.5 Hz, 1H), 1.65 (ddd, *J* = 13.9, 5.8, 5.6 Hz, 1H), 0.87–0.74 (m, 2H), 0.61–0.51 (m, 2H). ^{13}C NMR (CDCl$_3$): δ 160.4, 156.2, 138.2, 136.0, 129.5, 113.4, 59.3, 48.3, 34.2, 23.0, 6.3 (2C). *m/z* (ES+) 289.1738 calculated for C$_{14}$H$_{17}$D$_2$N$_6$O: [M+H]$^+$ 289.1746. IR (cm^{-1}): 3332 (N−H), 1592 (C=C aromatic), 1481 (CH$_2$), 1392 (CH$_3$), 1261 (C−N), 1103 (C−O). The LC-MS/MS chromatogram for compound purity can be found in Supplementary Information Figure **S1**.
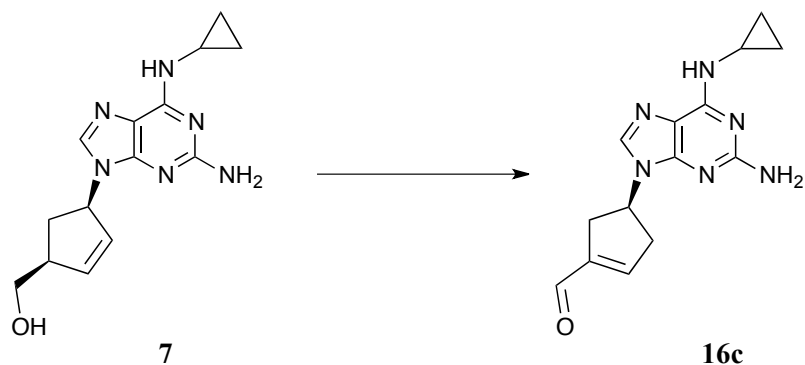
(*S*)-4-(2-Amino-6-(cyclopropylamino)-9*H*-purin-9-yl)cyclopent-1-enecarbaldehyde 16c:[32] To anhydrous DMSO (33 μL, 0.5 mmol) was added oxalyl chloride (20 μL, 0.2 mmol) in anhydrous THF (3 mL) under nitrogen at –78 °C. The mixture was stirred for 5 min and ABC **7** (0.05 g, 0.2 mmol) in anhydrous THF (5 mL) was added and stirring continued at –78 °C for 1 h. NEt₃ (127 μL, 0.9 mmol) was then added and the temperature allowed to rise to 0 °C over 1 h. Water (5 mL) was added to quench the reaction and the mixture extracted into diethyl ether (3 × 20 mL). The organic extracts were dried over MgSO₄ and the solvent removed *in vacuo*. The crude mixture was purified by column chromatography (1:99 to 1:24 MeOH–DCM) to yield **16c** (8 mg, 16%) as an off-white cloudy oil.[31] ¹H NMR (CDCl₃): δ 9.84 (s, 1H), 7.49 (s, 1H), 6.11–6.09 (m, 1H), 5.92–5.85 (m, 1H), 5.52–5.48 (m, 1H), 3.19–3.12 (m, 1H), 2.89–2.72 (m, 3H), 0.79–0.71 (m, 2H), 0.59–0.51 (m, 2H). *m/z* (ES+) 285.1475 calculated for $C_{14}H_{17}N_6O$: $[M+H]^+$ 285.1464.

28 **44**
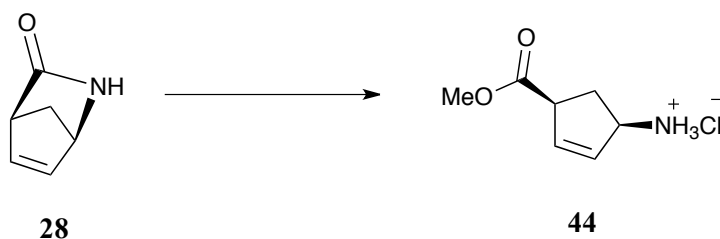
(1R,4S)-4-(Methoxycarbonyl)cyclopent-2-enaminium chloride 44:[48] SOCl$_2$ (1.5

mL, 0.02 mol) was added to MeOH (15 mL) dropwise at 0 °C. The solution was

allowed to stir for 5 min and (1R,4S)-2-azabicyclo[2.2.1]hept-5-en-3-one **28** (1.14 g,

0.01 mol) was added. The resulting mixture was allowed to stir at 0 °C under

nitrogen for 1 h. SOCl$_2$ and MeOH were removed *in vacuo* to yield **44** (1.73 g, 95%)

as a colourless crystalline solid. mp: 94–98 °C (lit.[48] mp: 91.1–94.2 °C). ^{1}H NMR

(DMSO-d$_6$): δ 8.40 (s, 3H), 6.08 (ddd, J = 5.5, 2.0, 1.9 Hz, 1H), 5.96–5.83 (m, 1H),

4.25–4.09 (m, 1H), 3.70 (ddd, J = 7.2, 5.9, 2.3 Hz, 1H), 3.65 (s, 3H), 2.58–2.51 (m,

1H), 2.04–1.83 (m, 1H). ^{13}C NMR (DMSO-d$_6$): δ 173.2, 134.7, 130.9, 55.7, 52.4,

49.4, 31.7. *m/z* (CI) 141.08 calculated for C$_7$H$_{11}$NO$_2$: [M+H]$^+$ 142. IR (cm^{-1}): 3102

(N−H), 3066 (N−H), 1700 (C=O), 1203 (C−O).

44 **45**
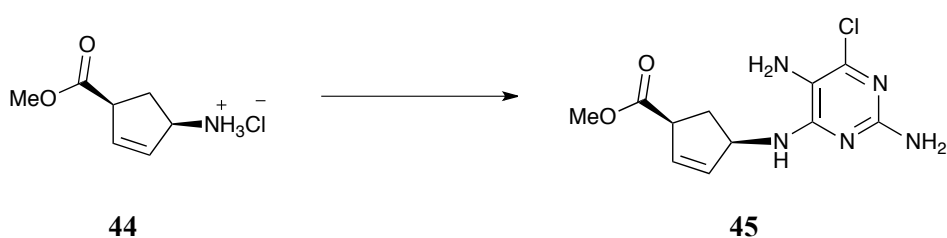
(1S,4R)-Methyl-4-((2,5-diamino-6-chloropyrimidin-4-yl)amino)cyclopent-2-

enecarboxylate 45: To DADCP **30** (0.70 g, 4.0 mmol) and **44** (0.70 g, 4.0 mmol) in

t-BuOH (10 mL) was added NaHCO$_3$ (1.20 g, 14.0 mmol) and the dark red solution

was stirred in a sealed tube at 90 °C for 14 h. The mixture was allowed to cool and

was filtered under suction. The solvents were removed *in vacuo* and the crude

product was purified by column chromatography (1:49 to 1:19 MeOH−DCM) to yield **45** (0.71 g, 42%) as a dark brown solid. ^{1}H NMR (CDCl$_3$): δ 6.00–5.95 (m, 1H), 5.94–5.92 (m, 1H), 5.28–5.26 (m, 1H), 3.74 (s, 3H), 3.58–3.53 (m, 1H), 2.74–2.67 (m, 1H), 2.57–2.50 (m, 1H). *m/z* (ES+) 284.0911 calculated for C$_{11}$H$_{15}$N$_5$O$_2$^{35}Cl: [M+H]$^+$ 284.0914 and 286.0888 calculated for C$_{11}$H$_{15}$N$_5$O$_2$^{37}Cl: [M+H]$^+$ 286.0885.

2.6 Supplementary Information
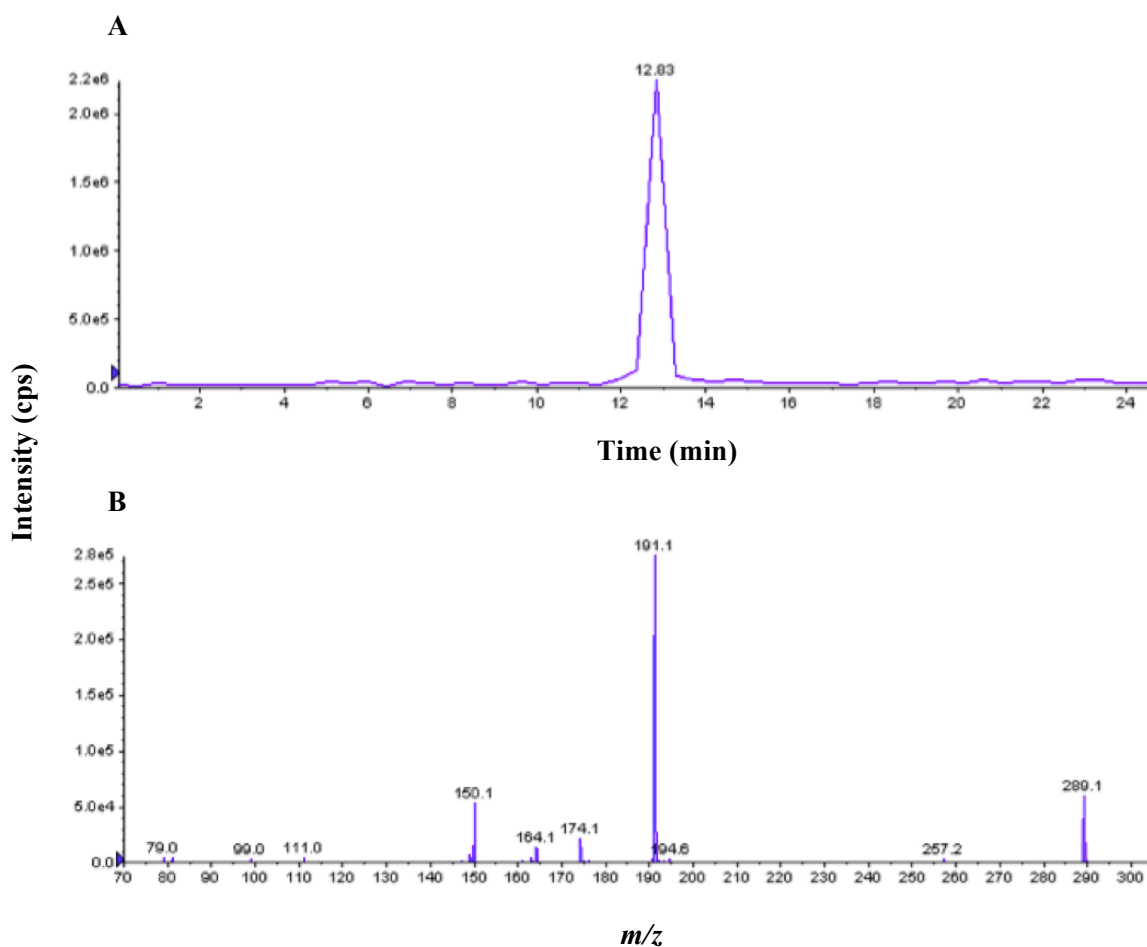
Figure S1: LC-MS/MS chromatogram (elution time 12.8 min) (**A**) and an EPI spectrum (precursor ion of m/z 289 and product ion of m/z 191) (**B**) for D_2-ABC. LC-MS/MS, liquid chromatography-tandem mass spectrometry; EPI, enhanced product ion.

2.7 References

(1)   Walsh, J. S.; Reese, M. J.; Thurmond, L. M. *Chem. Biol. Interact.* **2002**, *142*, 135.

(2)   Epp, J. B.; Widlanski, T. S. *J. Org. Chem.* **1999**, *64*, 293.

(3)   Zhu, R.; Frazier, C. R.; Linden, J.; Macdonald, T. L. *Bioorg. Med. Chem. Lett.* **2006**, *16*, 2416.

(4)   Mahmoudian, M.; Rudd, B. A. M.; Cox, B.; Drake, C. S.; Hall, R. M.; Stead, P.; Dawson, M. J.; Chandler, M.; Livermore, D. G.; Turner, N. J.; Jenkins, G. *Tetrahedron* **1998**, *54*, 8171.

(5)   Keeling, S. E.; Albinson, F. D.; Ayres, B. E.; Butchers, P. R.; Chambers, C. L.; Cherry, P. C.; Ellis, F.; Ewan, G. B.; Gregson, M.; Knight, J.; Mills, K.; Ravenscroft, P.; Reynolds, L. H.; Sanjar, S.; Sheehan, M. J. *Bioorg. Med. Chem. Lett.* **2000**, *10*, 403.

(6)   Homma, H.; Watanabe, Y.; Abiru, T.; Murayama, T.; Nomura, Y.; Matsuda, A. *J. Med. Chem.* **1992**, *35*, 2881.

(7)   Pradere, U.; Amblard, F.; Coats, S. J.; Schinazi, R. F. *Org. Lett.* **2012**, *14*, 4426.

(8)   Kohgo, S.; Yamada, K.; Kitano, K.; Iwai, Y.; Sakata, S.; Ashida, N.; Hayakawa, H.; Nameki, D.; Kodama, E.; Matsuoka, M.; Mitsuya, H.; Ohrui, H. *Nucleosides Nucleotides & Nucleic Acids* **2004**, *23*, 671.

(9)   Verma, V. A., Ashok; Njoroge, F. George; Chen, Kevin X.; 5'-substituted nucleoside analogs and methods of use thereof for the treatment of viral diseases. Merck Sharp & Dohme Corp. Patent Number WO2013009737: 2013.

(10)   Elzein, E.; Kalla, R.; Li, X.; Perry, T.; Marquart, T.; Micklatcher, M.; Li, Y.; Wu, Y.; Zeng, D.; Zablocki, J. *Bioorg. Med. Chem. Lett.* **2007**, *17*, 161.

(11)   Cappellacci, L.; Franchetti, P.; Pasqualini, M.; Petrelli, R.; Vita, P.; Lavecchia, A.; Novellino, E.; Costa, B.; Martini, C.; Klotz, K. N.; Grifantini, M. *J. Med. Chem.* **2005**, *48*, 1550.

(12)   Boojamra, C. G.; Mackman, R. L.; Markevitch, D. Y.; Prasad, V.; Ray, A. S.; Douglas, J.; Grant, D.; Kim, C. U.; Cihlar, T. *Bioorg. Med. Chem. Lett.* **2008**, *18*, 1120.

(13)   Cristalli, G.; Eleuteri, A.; Vittori, S.; Volpini, R.; Lohse, M. J.; Klotz, K. N. *J. Med. Chem.* **1992**, *35*, 2363.

(14)   Adachi, H.; Palaniappan, K. K.; Ivanov, A. A.; Bergman, N.; Gao, Z.-G.; Jacobson, K. A. *J. Med. Chem.* **2007**, *50*, 1810.

(15)   Ravi, G.; Lee, K.; Ji, X. D.; Kim, H. S.; Soltysiak, K. A.; Marquez, V. E.; Jacobson, K. A. *Bioorg. Med. Chem. Lett.* **2001**, *11*, 2295.

(16)   Kushner, D. J.; Baker, A.; Dunstall, T. G. *Can. J. Physiol. Pharmacol.* **1999**, *77*, 79.

(17)   Tung, R. D. In *Innovations in Pharmaceuticals Technology*; Pharmaceuticals, C., Ed. 2010.

(18)   Harbeson, S. L., Tung, R. D.; Concert Pharmaceuticals Inc.: 2009.

(19)   Barratt, M. J.; Frail, D. *Drug repositioning [electronic book]: Bringing New Life to Shelved Assets and Existing Drugs / edited by Michael J. Barratt, Donald E. Frail*; Hoboken : John Wiley & Sons, c.2012, 2012.

(20)   Alken, R.-G., Stabingis, T.; Alken, R-G., Stabingis, T.: 2004.

(21)   Gallegos, R. *Drug Metab. Rev.* **2009**, *41*, 92.

(22)   Shao, L.; Hewitt, M. C. *Drug News & Perspectives* **2010**, *23*, 398.

(23)   Pizzocolo, C.; Castagna, A.; Lazzarin, A. *Future Virology* **2011**, *6*, 571.

(24)   Fukuda, T.; Yamamoto, I.; Nishida, Y.; Zhou, Q.; Ohno, M.; Takada, K.; Azuma, J. *Br. J. Clin. Pharmacol.* **1999**, *47*, 450.

(25)   Fogelman, S. M.; Schmider, J.; Venkatakrishnan, K.; von Moltke, L. L.; Harmatz, J. S.; Shader, R. I.; Greenblatt, D. J. *Neuropsychopharmacology* **1999**, *20*, 480.

(26)   Otton, S. V.; Ball, S. E.; Cheung, S. W.; Inaba, T.; Rudolph, R. L.; Sellers, E. M. *Br. J. Clin. Pharmacol.* **1996**, *41*, 149.

(27)   Muth, E. A.; Moyer, J. A.; Haskins, J. T.; Andree, T. H.; Husbands, G. E. M. *Drug Dev. Res.* **1991**, *23*, 191.

(28)   Quasthoff, S.; Moeckel, C.; Zieglgaensberger, W.; Schreibmayer, W. *Cns Neuroscience & Therapeutics* **2008**, *14*, 107.

(29)   Dalmadi, B.; Leibinger, J.; Szeberenyi, S.; Borbas, T.; Farkas, S.; Szombathelyi, Z.; Tihanyi, K. *Drug Metab. Disposition* **2003**, *31*, 631.

(30)   Grilo, N. M.; Charneira, C.; Pereira, S. A.; Monteiro, E. C.; Matilde Marques, M.; Antunes, A. M. M. *Toxicol. Lett.* **2014**, *224*, 416.

(31)   Charneira, C.; Godinho, A. L. A.; Conceicao Oliveira, M.; Pereira, S. A.; Monteiro, E. C.; Matilde Marques, M.; Antunes, A. M. M. *Chem. Res. Toxicol.* **2011**, *24*, 2129.

(32)   Charneira, C.; Grilo, N. M.; Pereira, S. A.; Godinho, A. L. A.; Monteiro, E. C.; Marques, M. M.; Antunes, A. M. M. *Br. J. Pharmacol.* **2012**, *167*, 1353.

(33)   Grilo, N. M.; Antunes, A. M. M.; Caixas, U.; Marinho, A. T.; Charneira, C.; Conceicao Oliveira, M.; Monteiro, E. C.; Matilde Marques, M.; Pereira, S. A. *Toxicol. Lett.* **2013**, *219*, 59.

(34)   Meng, X.; Lawrenson, A. S.; Berry, N. G.; Maggs, J. L.; French, N. S.; Back, D. J.; Khoo, S. H.; Naisbitt, D. J.; Park, B. K. *Chem. Res. Toxicol.* **2014**.

(35)   Bell, C. C.; Castelazo, A. S.; Yang, E. L.; Maggs, J. L.; Jeankins, R. E.; Tugwood, J.; O'Neill, P. M.; Naisbitt, D. J.; Park, B. K. *Chem. Res. Toxicol.* **2013**, *26*, 1064.

(36)   Corey, E. J.; Suggs, J. W. *Tetrahedron Lett.* **1975**, 2647.

(37)   Piancatelli, G.; Scettri, A.; Dauria, M. *Synthesis-Stuttgart* **1982**, 245.

(38)   Muzart, J. *Chem. Rev.* **1992**, *92*, 113.

(39)   Firouzabadi, H.; Mostafavipoor, Z. *Bull. Chem. Soc. Jpn.* **1983**, *56*, 914.

(40)   An, G.; Minkyung, L.; Chun, K.-S.; Rhee, H. *Synlett* **2007**, 95.

(41)   Lawrence, R. M.; Process for the preparation of (1S,4R)-cis-4-[2-amino-6-chloro-9H-purin-9-yl]-2-cyclopentene-1-methanol. Glaxo Group Limited. Patent Number: EP1660498 B1: 2009.

(42)   Brown, D. J.; Mason, S. F.; Evans, R. F.; Batterham, T. J. *The Pyrimidines by D. J. Brown. The Chemistry of Heterocyclic Compounds, Vol. 16*; New York: Interscience, 1962., 1962.

(43)   Crimmins, M. T.; King, B. W. *J. Org. Chem.* **1996**, *61*, 4192.

(44)   Adair, G. R. A.; Kapoor, K. K.; Scolan, A. L. B.; Williams, J. M. *J. Tetrahedron Lett.* **2006**, *47*, 8943.

(45)   Pederson, R. L.; Fellows, I. M.; Ung, T. A.; Ishihara, H.; Hajela, S. P. *Adv. Synth. Catal.* **2002**, *344*, 728.

(46)   Maynard, H. D.; Grubbs, R. H. *Tetrahedron Lett.* **1999**, *40*, 4137.

(47)   Crimmins, M. T.; King, B. W.; Zuercher, W. J.; Choy, A. L. *J. Org. Chem.* **2000**, *65*, 8499.

(48)   Jia, F.; Hong, J.; Sun, P.-H.; Chen, J.-X.; Chen, W.-M. *Synth. Commun.* **2013**, *43*, 2641.

CHAPTER 3

Probing the Oxidative Metabolism of

Abacavir

CHAPTER 3

Probing the Oxidative Metabolism of Abacavir

3.1 Introduction

Many marketed drugs undergo an oxidative bioactivation;[1] a process that can be associated with adverse reactions in a small minority of patients.[2,3] Through theoretical study and applied research, the mechanisms leading to the bioactivation of drugs can be determined, and this knowledge can in turn serve to deliver a better design of drugs that might produce a lower or no incidence of ADRs.[4]

Oxidation of ABC in humans occurs on the 5'-C primary alcohol function, where it is metabolised *inter alia* by ADH isozymes ADH1A ($\alpha\alpha$) and ADH2C2 ($\gamma\gamma$) to the major carboxylic acid isomer **17a** *via* a highly reactive aldehyde intermediate **16a**.[5] Alternatively, ABC can undergo phase II metabolism by UGT, to its pharmacologically inactive glucuronide metabolite **18** (Figure **3.1**).[6] This is the major clearance route, as discussed in Chapter 1. Aldehyde **16a** is able to undergo epimerisation to aldehyde **16b** or isomerisation to aldehyde **16c** and these compounds can undergo further oxidation by ADH1A to their respective carboxylic acid metabolites **17b** and **17c**. Further to this, **16b** and **16c** can undergo reduction reactions by ADH2C2 to form isomeric parent compounds **7b** and **7c** respectively.

Although this oxidative metabolic route is known, it is not fully understood, with a lack of knowledge of the enzymology and stereochemistry of the products and the contribution of **16** to ABC's toxicity is unknown. Deuterated analogues of drugs or deuterated substrates are well known to probe metabolic activities, pharmacokinetics or bioactivation. Examples of these include, 1-methyl-4-phenyl-1,2,3,6-

tetrahydropyridine (MPTP), a neurotoxin,[7] domiodol, a mucolytic drug[8] and semi-synthetic artemisinin-based drugs.[9]
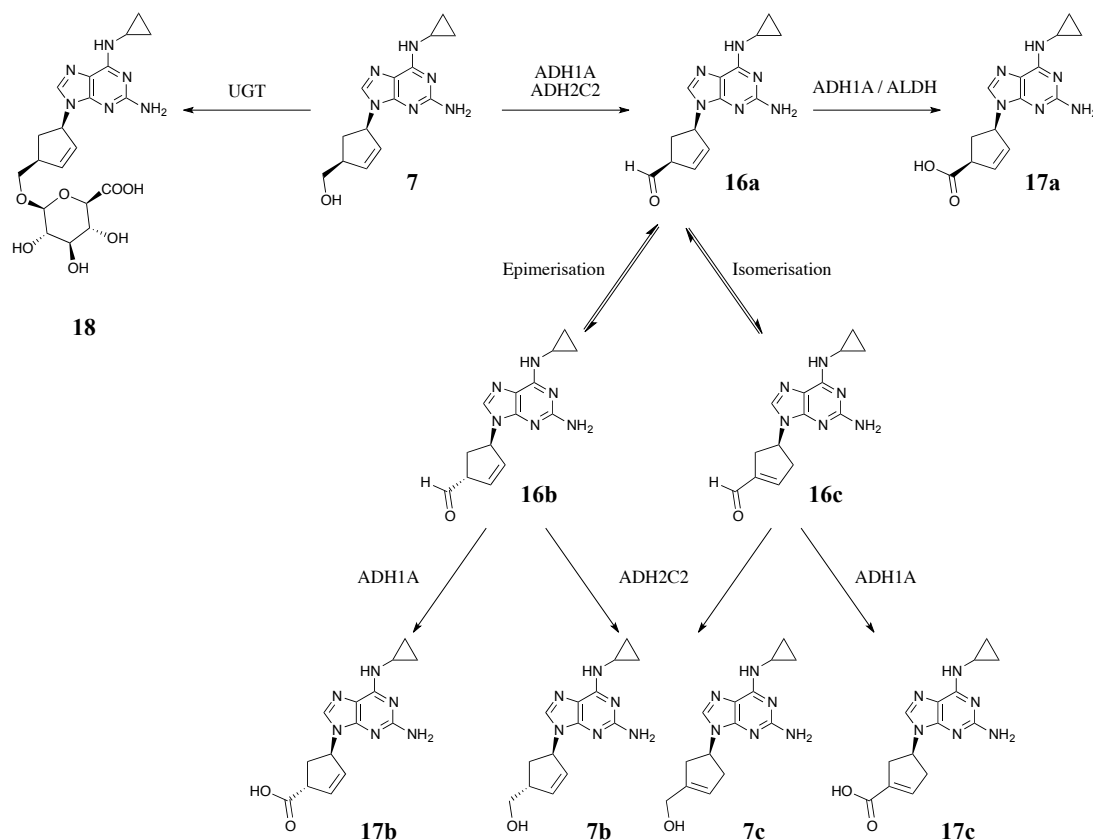
Figure 3.1: Biochemical oxidation of ABC **7** to its stereo-equivalent aldehyde intermediate **16a** by ADH and further metabolism of **16a** to the major carboxylic acid isomer **17a** *in vitro* by ADH1A (αα)/ALDH. At the beginning of this work, the involvement of ALDH in this oxidation pathway was unknown and ADH1A was shown to oxidise ABC to **17a**.[5] Aldehyde **16a** can undergo epimerisation to **16b**, which in turn is oxidised by ADH1A to carboxylic acid **17b** or reduced to an isomer of ABC, **7b**. Alternatively, **16a** can undergo isomerisation to aldehyde **16c**, which has shown to undergo *in vitro* and *in vivo* protein adduct formation. Isomer **16c** can also undergo further oxidation to carboxylic acid **17c** or reduction to an isomeric parent compound **7c**. Through a phase II pathway, ABC can be metabolised to its pharmacologically inactive glucuronide metabolite **18** by UGT. This is the major phase II clearance route, as discussed in Chapter 1. UDP, uridine diphosphate; UGT, UDP-glucuronosyl transferase. Adapted from Walsh *et al*.[5] and Charneira *et al*.[10]

3.1.1 ADH and ALDH inhibitors.

To probe the oxidative metabolism of ABC, the ADH inhibitor, 4-MP (Figure **3.2**) would be required. This would allow investigation into this pathway and has been shown to be effective in blocking this oxidative metabolism.[5,11] With no research available for the involvement of ALDH and its isozymes in ABC's metabolism, an effective ALDH inhibitor is unknown. The inhibitors cyanamide and disulfiram (DSF) were trialled.
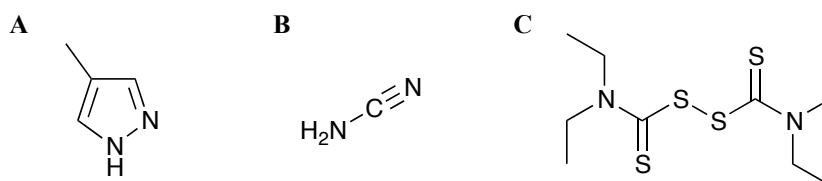
Figure 3.2: Inhibitor of ADH, 4-MP (**A**) and inhibitors of ALDH, cyanamide (**B**) and DSF (**C**) will be required to probe ABC's oxidative metabolism pathway. 4-MP has shown to be an effective ADH inhibitor in blocking ABC-**17** formation[5,11] but the involvement of ALDH in the metabolism pathway is unknown, resulting in the trialling of ALDH inhibitors cyanamide and DSF. 4-MP, 4-methylpyrazole; DSF, disulfiram.

3.1.1.1 ADH inhibitor: 4-MP.

4-MP (fomepizole) (Figure **3.2 A**) is a competitive inhibitor, with respect to EtOH, of ADH isozymes ADH1A, ADH1B1, ADH1B2, ADH1C1 and ADH1C2 and a non-competitive inhibitor of ADH1B3, ADH2 and ADH4.[12] It is known that ADH1A and ADH2C2 are involved in ABC metabolism however, whether 4-MP would act as a competitive or non-competitive inhibitor with respect to ABC is unknown. It is clear however, that 4-MP would inhibit the desired isozymes. 4-MP, acting as an enzyme

inhibitor, is often used as an antidote in the treatment of ethylene glycol and methanol poisoning.[12,13]

3.1.1.2 ALDH inhibitors: Cyanamide and DSF.

3.1.1.2.1 Cyanamide.

Cyanamide (Figure **3.2 B**), a pro-drug that once metabolised to a nitroxyl intermediate (Figure **3.3**) is an irreversible inhibitor of ALDH isozyme ALDH2,[14] and it is often used as a second-line treatment to treat alcoholism.[15] Furthermore, it is a catalase inhibitor.[16] Cyanamide is activated by catalase and hydrogen peroxide (H_2O_2) to a *N*-hydroxycyanamide intermediate,[16] which readily decomposes to cyanide and the active nitroxyl metabolite (Figure **3.3**).[17] This metabolite can act as both a reversible (*via* disulfide formation) and non-reversible inhibitor (*via* sulfinamide formation) (Figure **3.3**), depending on the environmental pH.[18]
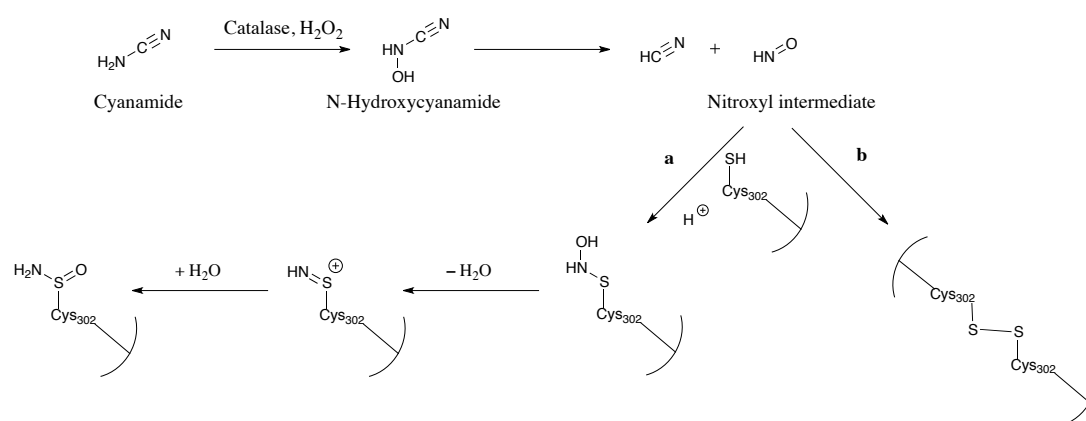
Figure 3.3: Cyanamide is metabolised by catalase and H_2O_2 to form an *N*-hydroxycyanamide intermediate,[16] which decomposes to cyanide and the active nitroxyl metabolite.[17] This intermediate will act as a non-reversible inhibitor through sulfinamide formation (pathway **a**) or as a reversible inhibitor through disulfide formation (pathway **b**). Adapted from Koppaka *et al*.[14]

3.1.1.2.2 DSF.

DSF (tetraethylthioperoxydicarbonic diamide) (Figure **3.2 C**) is an irreversible inhibitor of ALDH isozymes ALDH1A1 and ALDH2 although, it is a more efficient ALDH1A1 inhibitor.[19] DSF, marketed as Antabuse, is used to treat alcoholism. It is metabolised to a variety of substrates (Figure **3.4**), all of which are capable of inhibiting the ALDH enzyme[20-23] *via* the Cys 302 residue.[20] The first metabolism step, reduction of DSF, yields *N,N*-diethyldithiocarbamate (DDC). Further metabolism, by hepatic thiol methyltransferases, produces *S*-methyl-DDC (MeDDC). This intermediate can be metabolised by CYP P450 and flavin monooxygenase (FMO) enzymes[23] to a MeDDC sulfine and a MeDDC sulfoxide metabolite. MeDDC sulfine can be further oxidised to *S*-methyl-*N,N*-diethylthiocarbamate (MeDTC) followed by oxidation to MeDTC sulfoxide and then MeDTC sulfone (Figure **3.4**).
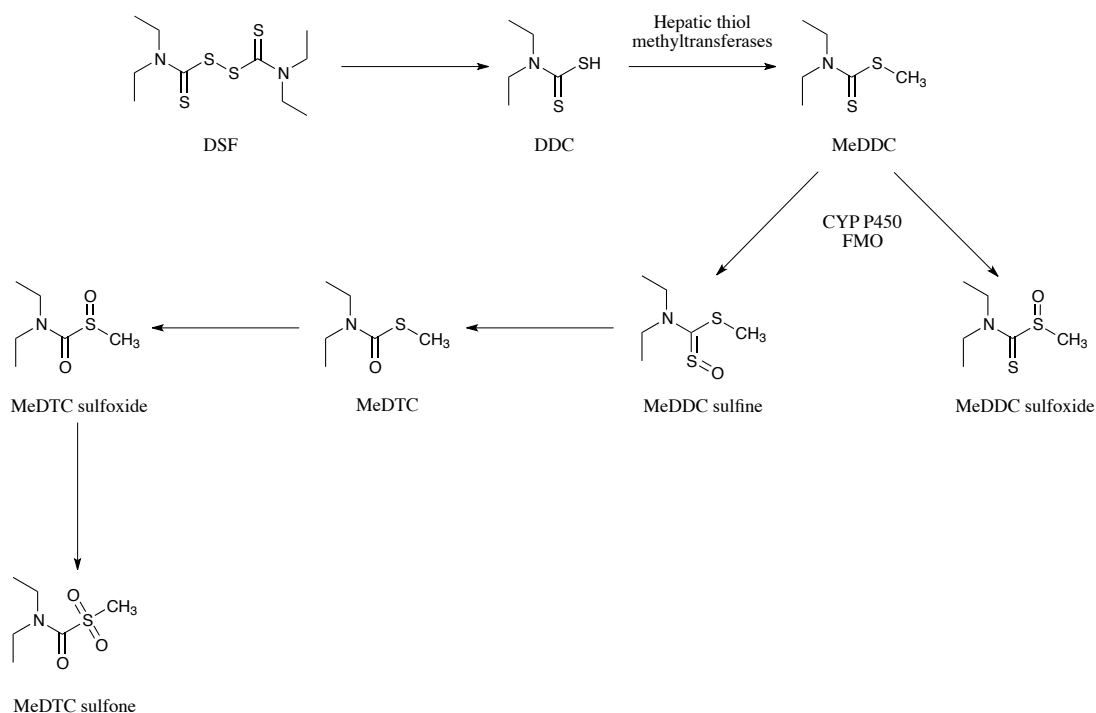
Figure 3.4: DSF is an irreversible ALDH (isozymes ALDH1A1 and ALDH2) inhibitor acting at the Cys 302 residue. It is metabolised, by a variety of, namely CYP P450, enzymes, to a number of substrates, all of which have been shown to possess ALDH inhibitory properties.[20,22] DDC, *N,N*-diethyldithiocarbamate; MeDDC, *S*-methyl-DDC; MeDTC, *S*-methyl-*N,N*-diethylthiocarbamate; FMO, flavin monooxygenase. Adapted from Koppaka *et al*.,[14] Pike *et al*.[23] and Mays *et al*.[22]

3.1.2 Kinetic isotope effect.

When comparing deuterated substances to their protium equivalents, the kinetic isotope effect (KIE) can explain altered rates of reactions/metabolism pathways. Where an atom, involved in the RDS step of a molecule, is replaced by an isotope, a primary KIE is seen. Thus, the KIE is defined as the observed rate change within a reaction where one of the atoms contributing to the rate mechanism is isotopically substituted.[24] The KIE can be expressed as a ratio of its rates:

$$KIE = \frac{k_H}{k_D}$$

The KIEs for hydrogen are larger than those for other elements due to the high mass ratios: H:D:T ≈ 1:2:3. For a KIE to be present, the ratio of the rate constants must be greater than one: The larger the ratio, the greater the KIE. In terms of H and D, the KIE can be explained by the difference between the energies of the reactant and transition states (Figure **3.5**). The C−D bond is of a lower zero point energy than the C−H bond, therefore more energy is required to break the C−D bond and form the transition state. The zero point energy difference between the transition states for both H and D reduces so overall more energy is required to break the C−D bond. The resulting effect is slower bond cleavage, and therefore the KIE can also be defined as the ratio of the rate constants of bond cleavage.

The KIE exists in two major forms: The primary and secondary KIE. The primary KIE, of most interest in this research, is such that the isotopically substituted atom is involved in the breaking or making of a covalent bond during the reaction.[24] When an isotopic effect is still observed, even though the isotopic atom is not involved in the bond breaking/making, it is termed the secondary kinetic isotope effect.[25] KIEs have been shown in several studies to develop and explain mechanisms of drug metabolism.[26-28]
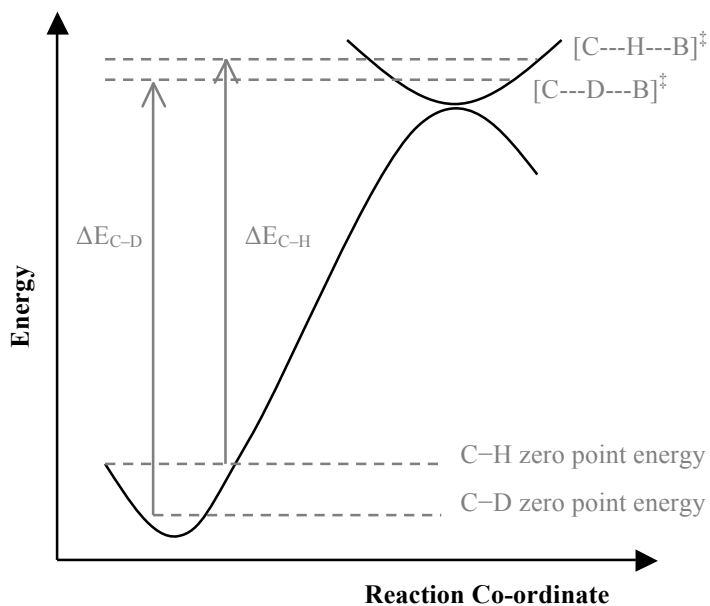
Figure 3.5: The zero point energy difference for C−D is less than that for C−H due to the heavier mass of deuterium. The zero point energy differences at the transition state levels for both [C---D---B]‡ and [C---H---B]‡ reduces so the energy values become comparable. Therefore overall, more energy is required to break the C−D bond compared to the C−H bond.

3.1.3 Michaelis–Menten parameters.

In order to determine any KIE for an enzymic reaction and to compare rates of metabolism between isotopically substituted compounds and their parent isotopologues, the Michaelis–Menten parameters, V_{max} and K_m, should be determined. They are defined as follows: V_{max} is the maximum rate at the saturating substrate concentration and K_m is the substrate concentration at the rate, which is half of V_{max}. They can both be determined by conducting rate experiments: The rate is calculated over increasing substrate concentrations. From this calculation, *via* graphical methods (plotting $1/v$ *vs.* $1/[S]$) as depicted in Figure **3.6**, the parameters can be determined.
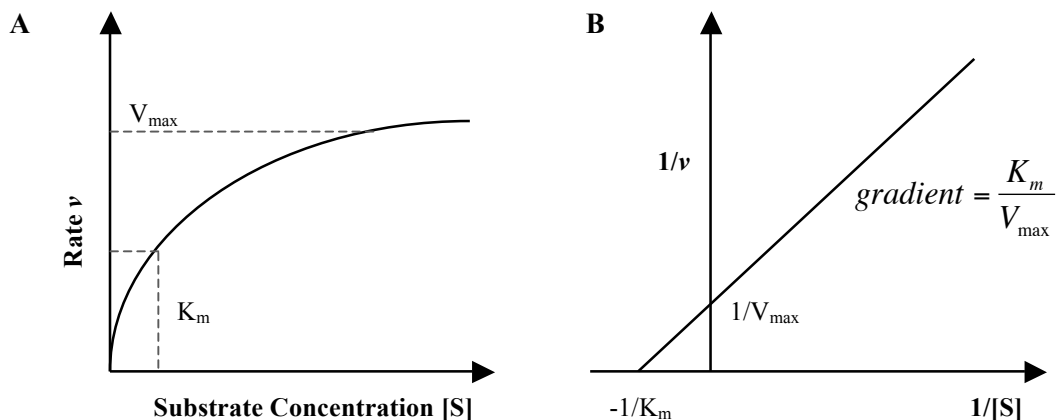
Figure 3.6: Graph showing enzymic reaction rate *vs.* [substrate], with the Michaelis–Menten parameters, V_{max} and K_m shown (**A**). Graph showing $1/v$ *vs.* $1/[S]$: The Michaelis–Menten parameters can be calculated from the gradient and the *y*- or *x*-axis intercepts (**B**).

In this research, the V_{max} parameters were used to determine any KIE according to the following equation:

$$KIE = \frac{V_{max}H}{V_{max}D}$$

Two aspects of ABC's oxidation in biological systems are unresolved: The isomerisation of **16a** (invoked to explain the formation of multiple carboxylate isomers but never characterised definitively) and the contribution of ALDH to the oxidation of ABC aldehyde. The following research conducted aims to further investigate these uncertainties. The Michaelis–Menten values will be calculated measuring product formation (ABC-**17**) as demonstrated by Patanella *et al.*[29]

3.2 Aims

- To determine the metabolic fate of D_2-ABC in human liver cytosol

- To determine the Michaelis–Menten parameters, K_m and V_{max}, and use their values to calculate whether a KIE is present with D_2-ABC in comparison with ABC

- To determine if oxidative metabolism of D_2-ABC can be retarded compared to ABC and investigate how deuteration of ABC at the 5'-position affects ABC toxicity.

3.3 Results & Discussion

3.3.1 Comparative metabolism of ABC and D$_2$-ABC in human liver cytosol.

3.3.1.1 Quantification of the formation of carboxylic acid.

For all experiments, the formation of ABC-**17** (Figure **3.7 A**) was used as the end-point. Although substrate or NAD(P)$^+$ has been shown to be a well utilised method for enzymatic metabolism experiments, product formation has also been shown to be effective as used by Patanella *et al.* when applied to CBV.[29] As three carboxylic acid isomers were formed (**17a**–**17c**), (Figure **3.7 B**) the peak areas of the isomers were combined and the analyte:IS ratio was then calculated. Results are therefore reported as the formation of collective carboxylic acid products.

A
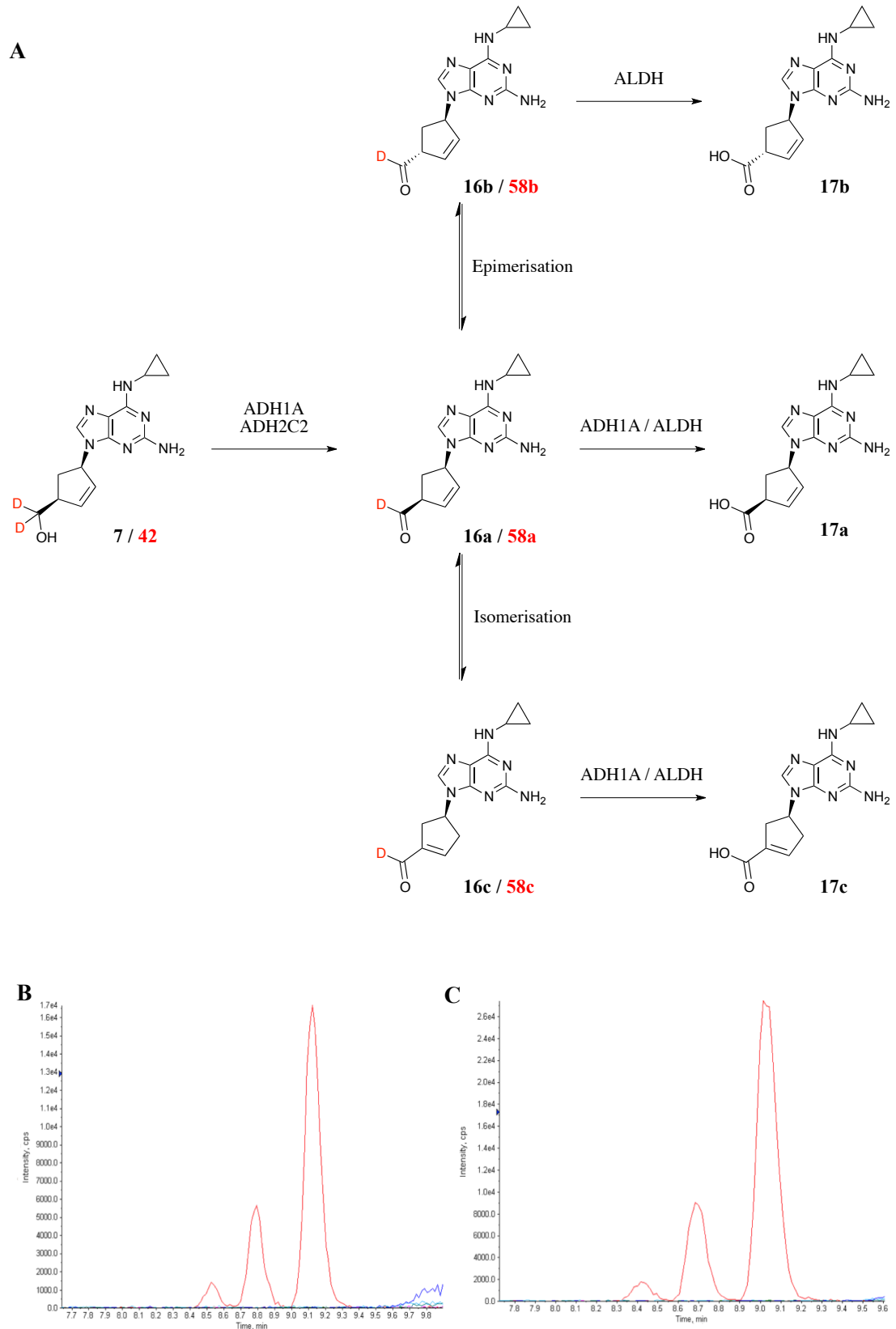
Figure 3.7: ABC **7** and D$_2$-ABC **42** are metabolised *via* aldehyde intermediates to their respective carboxylic acid metabolites with the formation of ABC-COOH **17a–17c** as the end-point for both **7**

Figure 3.7 continued:

and **42** (**A**). The formation of three carboxylic acid metabolites was evident from the LC-MS/MS chromatograms for both ABC (**B**) and D_2-ABC (**C**). The three COOH isomers eluted at 8.5, 8.8, and 9.2 min and 8.4, 8.7 and 9.0 min for ABC and D_2-ABC respectively. Carboxylic acid **17a** was the 3rd eluted isomer for both compounds and this was determined through comparison with the authentic standard 2269W93, supplied by GSK. Both chromatograms are taken from the inhibitor experiments, experiment 7 (Table **3.1**). GSK, GlaxoSmithKline.

Linear calibration curves, with concentration ranges determined previously,[11] were used to estimate analyte concentrations from LC-MS/MS data. A curve was generated by plotting the ratio of the peak areas of analyte:IS against concentration of analyte (nM). For experiments where ABC was the compound assayed, D_2-ABC (200 nM) was used as the IS. And conversely, ABC (200 nM) was used as the IS when D_2-ABC was the compound assayed. Representative calibration curves for ABC, D_2-ABC and ABC-**17** are shown in Figure **3.8**.

A   **ABC**

B   **D$_2$-ABC**

$y = 0.0064x - 0.0327$
$R^2 = 0.99985$

$y = 0.0034x - 0.0046$
$R^2 = 0.99915$

C   **ABC-COOH (ABC as IS)**

D   **ABC-COOH (D$_2$-ABC as IS)**

$y = 0.0005x - 0.001$
$R^2 = 0.99998$

$y = 0.0005x + 0.0015$
$R^2 = 0.99921$
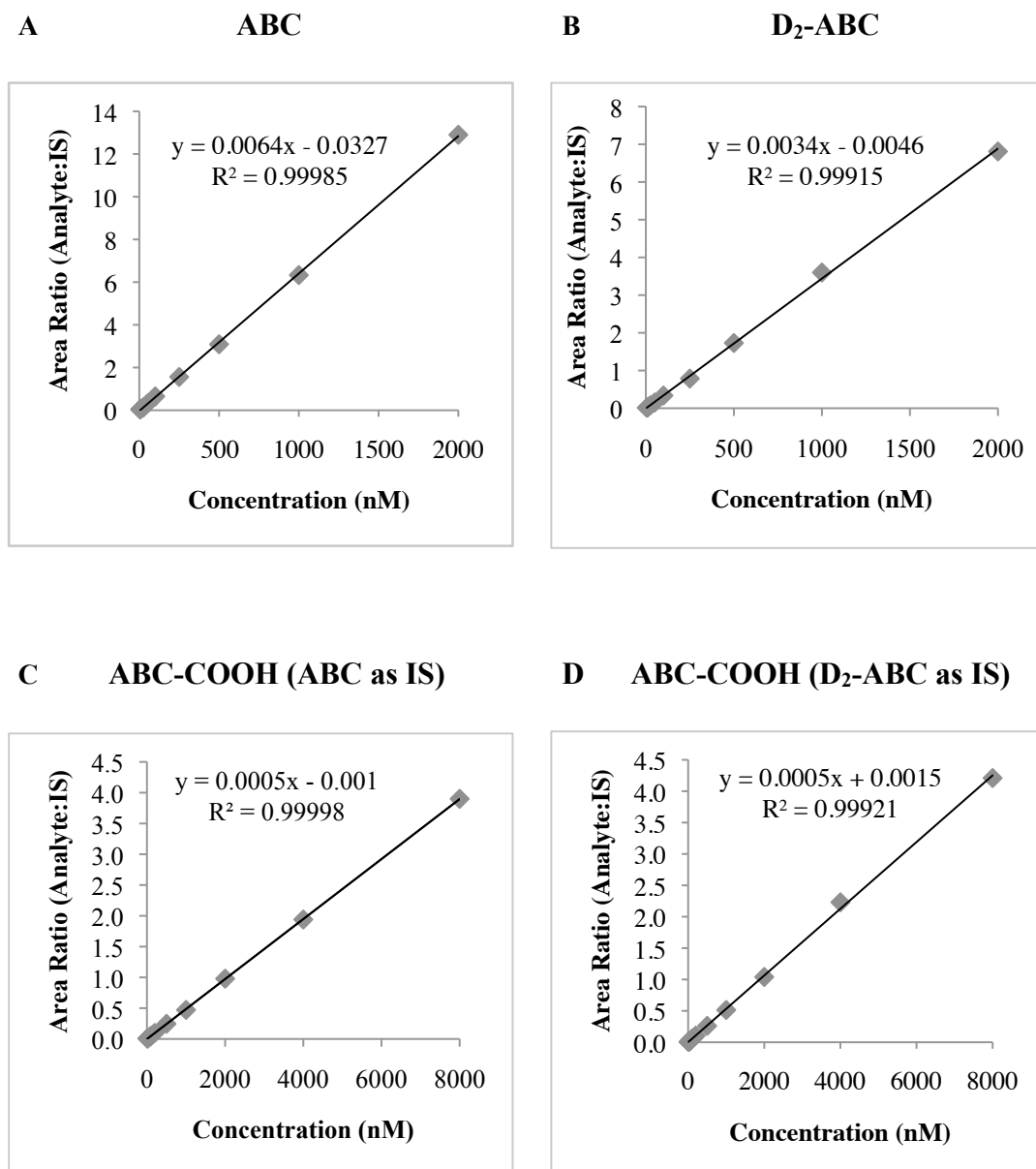
Figure 3.8: Representative calibration curves for ABC ($R^2 = 0.9999$) (**A**), D$_2$-ABC ($R^2 = 0.9992$) (**B**), ABC-COOH ($R^2 = 1.0000$) with ABC as the IS (**C**) and ABC-COOH ($R^2 = 0.9992$) with D$_2$-ABC as the IS (**D**). The range of analyte concentrations for ABC and D$_2$-ABC was 5–2000 nM and 10–4000 nM for ABC-COOH. Each graph represents data with the line of best fit not forced through the origin.

3.3.1.2 Linearity of the oxidation of ABC and D$_2$-ABC with respect to cytosolic protein concentration.

To determine the appropriate protein concentration for incubations of ABC and D$_2$-ABC with liver cytosol, and to ensure linearity of ABC-**17** formation with respect to protein concentration, the substrates (10 mM) were incubated with the following concentrations of cytosolic protein: 0.1, 0.25, 0.5, 0.75, 1.0, 1.25 and 1.5 mg/mL. The duration of each incubation was 2 h: After this length of time, the concentrations of carboxylic acid were sufficient for quantification by LC-MS/MS. Representative multiple reaction monitoring (MRM) chromatograms for ABC and D$_2$-ABC incubations at a protein concentration of 0.75 mg/mL are shown in Figure **3.9**. For both compounds, the COOH formation was linear at protein concentrations from 0.1–1.5 mg/mL and these results can be seen in Figure **3.10**.
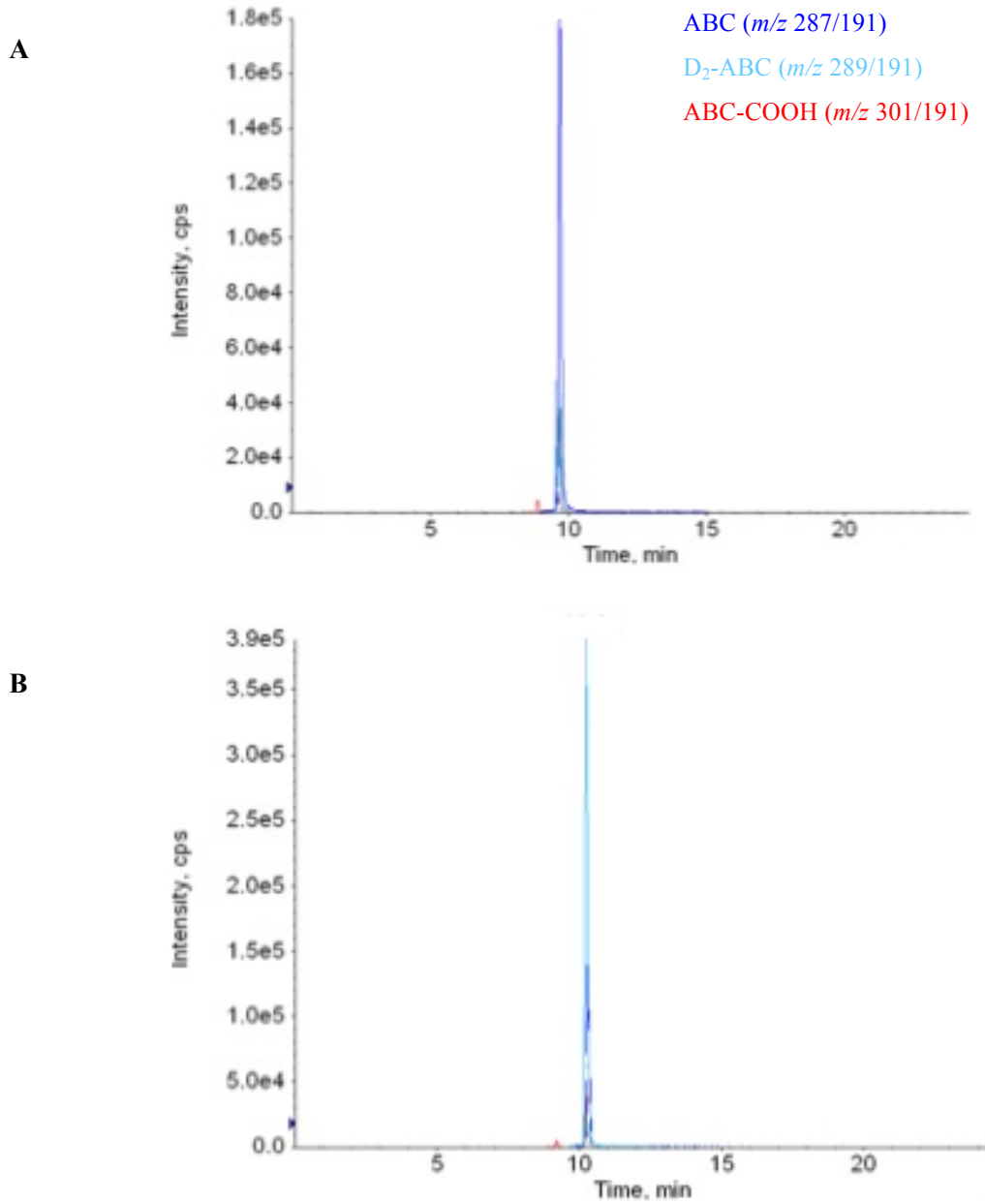
Figure 3.9: MRM chromatograms obtained after 2 h incubations of ABC (10 mM) at 0.75 mg/mL cytosolic protein (**A**) and D$_2$-ABC (10 mM) at 0.75 mg/mL cytosolic protein (**B**).

The mid-point concentration of liver cytosol protein, 0.75 mg/mL, was chosen as the concentration for all subsequent incubations.
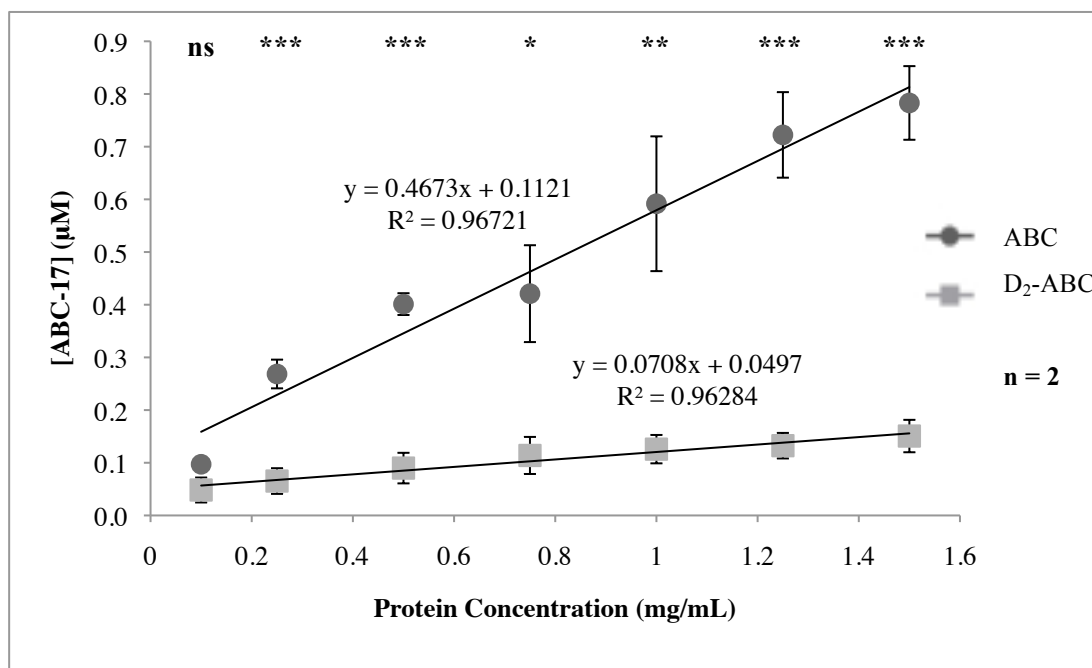
Figure 3.10: Graph representing the formation of ABC-COOH **17** (μM) from ABC ($R^2 = 0.967$) and D$_2$-ABC ($R^2 = 0.963$) against liver cytosolic protein concentrations (0.1–1.5 mg/mL) after 2 h incubations. The substrate concentration was 10 mM. The NAD$^+$ concentration was 7.5 mM. Data were obtained from two separate experiments over two days and are shown as the mean value (n = 2) ± standard deviation (ns = not significant, * $p < 0.05$, ** $p < 0.01$, *** $p < 0.0001$; ABC *vs.* D$_2$-ABC; unpaired t-test).

3.3.1.3 Formation of 17a from ABC and D$_2$-ABC with respect to time.

Preliminary work within the Liverpool group had shown that there was a statistically significant difference between the rate of formation of ABC-**17** from ABC and D$_2$-ABC by human liver cytosol over time. This observation was further investigated within this research. Using a fixed protein concentration of 0.75 mg/mL and ABC/D$_2$-ABC at 10 μM, the COOH formation was measured over 1, 4, 8, 16, 20 and 24 h. An early study of ABC's oxidation in human liver cytosol noted that a long incubation time (20 h) was required to yield detectable quantities of the carboxylic acids.[5] MRM chromatograms for both substrates over the individual times can be

seen in Supplementary Information **S1A** and **S1B**. The chromatograms obtained at 24 h can be seen in Figure **3.11**.
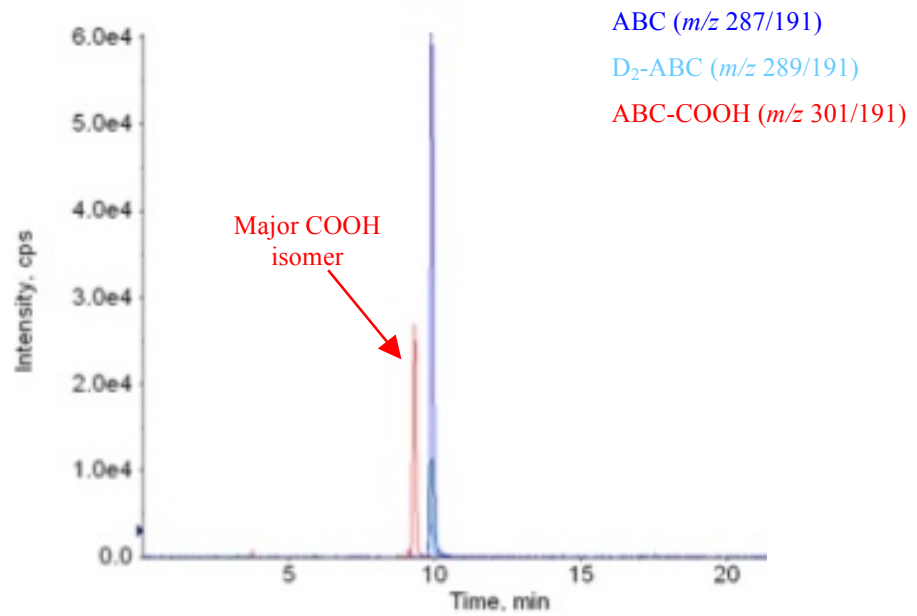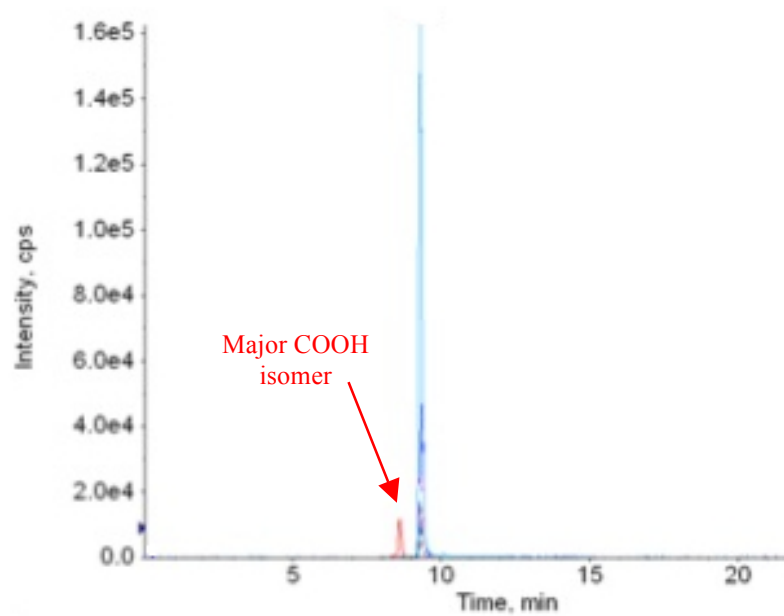
Figure 3.11: MRM chromatograms showing ABC-**17** formation after a 24 h incubation of ABC (10 μM) (**A**) or D$_2$-ABC (10 μM) (**B**) with human liver cytosol (protein concentration, 0.75 mg/mL).
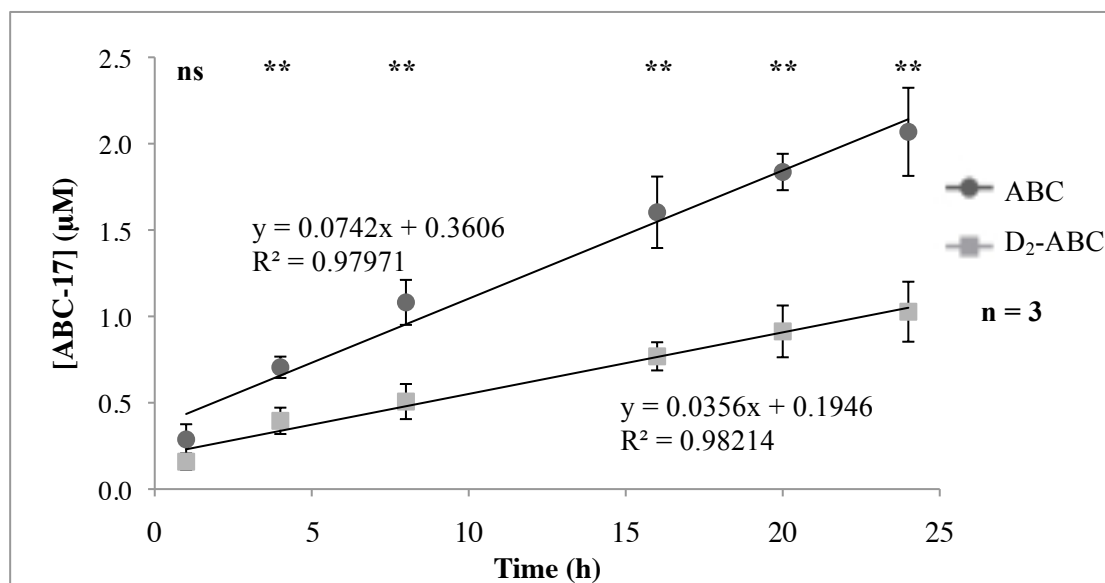
Figure 3.12: Formation of ABC-COOH **17** (μM) by human liver cytosol, with samples taken at 1, 4, 8, 16, 20 and 24 h for both ABC (R^2 = 0.9797) and D_2-ABC (R^2 = 0.9821). The substrate concentration was 10 mM. The protein concentration was 0.75 mg/mL. The NAD^+ concentration was 7.5 mM. Data were obtained from three separate experiments on different days. Data represent mean (n = 3) ± standard deviation (ns = not significant, ** p < 0.01; ABC *vs.* D_2-ABC; unpaired t-test).

Three COOH isomers are formed (Figure **3.7 B**), although there is one major isomer (Figure **3.11**): Compound **17a**, identified by chromatographic comparison with an authentic standard (compound 2269W93 supplied by GSK). This compound remains the major isomer over time. It can also be seen that the concentration of ABC-**17** formed is lower for D_2-ABC compared to ABC: At 24 h, 1.03 μM and 2.07 μM, respectively. This difference can be consistently seen throughout the experiments when comparing COOH formation over time (Figure **3.12** and Supplementary Information **S1A** and **S1B**). Both ABC and D_2-ABC oxidation follows the same pattern, albeit ABC-**17** is formed from D_2-ABC at a lower concentration. The slower COOH formation from D_2-ABC compared to ABC is due to the rate of abstraction of D compared to H. Due to the 100% mass difference between H and D atoms, the

bond cleavage of both D atoms would be slower, leading to a slower COOH formation. This overall comparable relationship (linear increase of COOH formation over time) was essential to obtain accurate data for comparison of the rate of COOH formation from ABC-**17** *vs.* D_2-ABC-**17**.

3.3.1.4 Determination of the oxidative metabolic fate of D_2-ABC compared to ABC.

To conduct enzymatic rate experiments, it was vital that ABC and D_2-ABC had the same oxidative metabolic fate in human liver cytosol. This was determined using two enzyme inhibitors, namely 4-MP[5,30] and DSF[31] for ADH and ALDH, respectively, and an aldehyde trapping agent, methoxylamine.[5] The two selective dehydrogenase inhibitors would enable confirmation of a two-step metabolic pathway for both compounds and the trapping agent would confirm that the aldehyde intermediate was formed during the oxidation process.

The initial metabolism of ABC by ADH has been documented[5] but the oxidation from aldehyde to carboxylic acid has received little research attention. Previous work completed within the Liverpool group has shown, using 4-MP (600 μM), that approximately 90% inhibition of ABC-**17** formation from ABC can be achieved in human liver cytosol, but no such experiments have been conducted with DSF, or any other ALDH inhibitor, in human liver cytosol.[11]

3.3.1.4.1 Identification of a suitable ALDH inhibitor.

Without knowing whether ALDH contributes to the oxidation of ABC-**16** in human liver cytosol,[5] it was decided that cyanamide, an irreversible inhibitor of human

139

ALDH2, would be used.[14] Cyanamide is known to inhibit the oxidation of carbovir to its carboxylic acid in rat liver cytosol.[32] However, ALDH2, which is highly expressed in human liver,[32] is a mitochondrial enzyme.[33] ALDH1 is expressed in human liver cytosol.[33] Therefore it seemed unlikely cyanamide would inhibit ABC's oxidation in human liver cytosol. Initial experiments were conducted with 10 mM ABC and cyanamide concentrations between 0.05–10 mM, cyanamide concentrations based upon those used by Patanella *et al.,*[29] but reproducible inhibition could not be obtained. Following this result, DSF, an irreversible inhibitor of isoforms ALDH1A1 and ALDH2, was the ALDH inhibitor of choice. Methoxylamine (10 mM) was used to trap the aldehyde intermediate,[5] and thereby inhibit the oxidation of ABC to the carboxylic acid. This agent provided confirmation that oxidation of ABC was occurring *via* the aldehyde.

3.3.1.5 Investigation into the oxidative metabolic fate of ABC and D_2-ABC.

The final experiments were completed as shown in Table **3.1**, with results shown in Figure **3.13**. Mass chromatograms obtained for ABC and D_2-ABC for all the incubations are shown in Supplementary Information **S2A** and **S2B**.

Table 3.1: Experiments using an ADH inhibitor (4-MP), an ALDH inhibitor (DSF) and an aldehyde trapping agent (methoxylamine) to confirm that the oxidative metabolic pathways of both ABC and D_2-ABC in human liver cytosol include an aldehyde intermediate.[*]

Experiment	Inhibitor/Trapping Agent (Final Concentration)	+/− NAD (7.5 mM)
1	-	-
2	4-Methylpyrazole (600 µM) Disulfiram (500 µM)	+
3	-	+
4	Methoxylamine (10 mM)	+
5	4-Methylpyrazole (600 µM)	+
6	Disulfiram (500 µM)	+
7	Methoxylamine (10 mM) Disulfiram (500 µM)	+

[*] Each experiment consisted of two incubations of substrate (10 µM) with human liver cytosol (protein concentration, 0.75 mg/mL): One containing D_2-ABC and the other containing ABC.

For experiment 1 (Table **3.1**), a negative control, it was predicted that no COOH formation would occur due to the absence of co-factor NAD^+, which is required for ADH to oxidise its substrates. The activities of most ALDH enzymes are optimal with NAD^+ as co-factor, and both human cytosolic ALDH1 and human mitochondrial ALDH2 use NAD^+.[34] It can be seen from mass chromatogram **A** in Figures **S2A** and **S2B** (Supplementary Information), and from Figure **3.13**, that a small amount of COOH formation occurred: ABC-**17** formation from ABC, 0.11

µM (8% formation), and ABC-**17** formation from D$_2$-ABC, 0.06 µM (7% formation), compared to 1.44 µM and 0.88 µM in the positive control, respectively (Figure **3.12**). All three isomers were formed. This unexpected COOH formation might have been due to minute amounts of NAD$^+$ present in the liver cytosol supplied (Sigma Aldrich, UK).

In experiment 2 (Table **3.1**), both ADH (4-MP, 600 µM) and ALDH (DSF, 500 µM) inhibitors were used to block COOH formation. This combination of inhibitors blocked the COOH formation by a 97% decrease for ABC (0.04 µM) and D$_2$-ABC (0.02 µM) compared to the positive control (Figure **3.13**). Although complete inhibition was not achieved, turnover of the compounds was inhibited to the same extent.

Experiment 3 (Table **3.1**), a positive control, was used to compare the formation of COOH from both ABC and D$_2$-ABC and to ensure that this product was being formed. The COOH formation from ABC and D$_2$-ABC was 1.44 µM and 0.88 µM, respectively (Figure **3.13**).
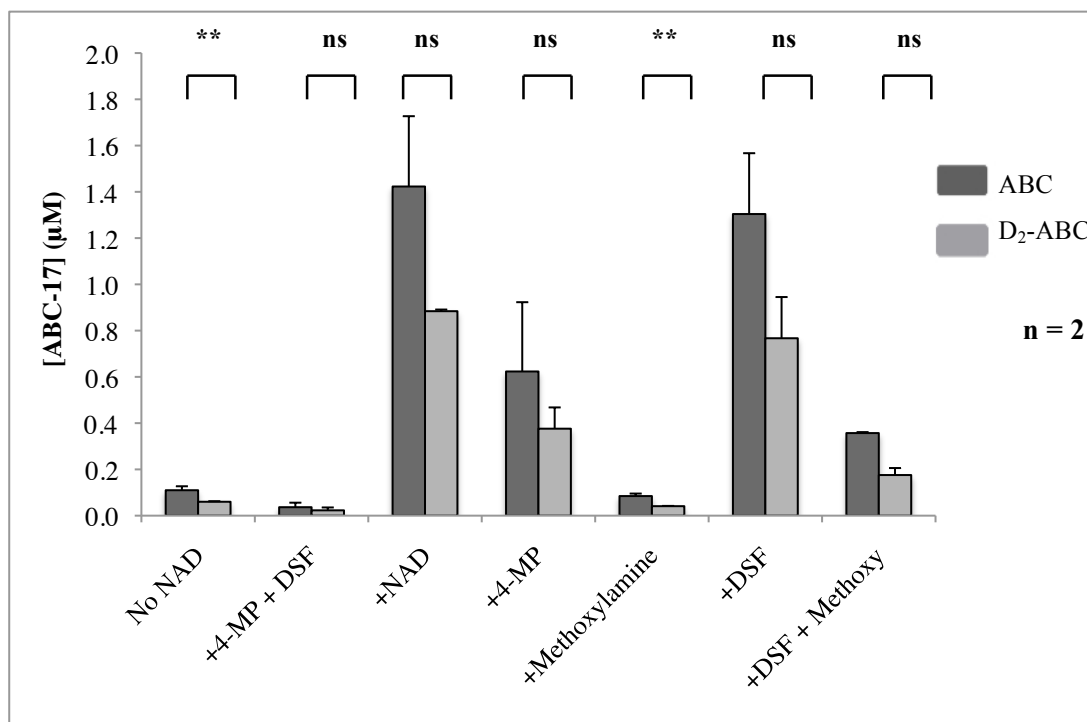
Figure 3.13: Metabolic experiments conducted with ABC and D_2-ABC to confirm the compounds undertook the same oxidative metabolic pathway in human liver cytosol. Values shown are the combined formation (µM) of three isomeric carboxylic acids. Incubations were conducted over 20 h in the presence of ABC (10 µM) or D_2-ABC (10 µM). The protein concentration was 0.75 mg/mL. The NAD^+ concentration was 7.5 mM. Data derived from two separate experiments conducted over two days. Data represent mean values (n = 2) ± standard deviation (ns = not significant, ** $p < 0.01$; ABC *vs.* D_2-ABC; unpaired t-test). Methoxy, methoxylamine.

Methoxylamine (10 mM) was used to trap the aldehyde through imine (oxime) formation (Figure **3.14**). Only the imine product for ABC was detected, but a reduction in ABC-**17** formation from D_2-ABC provides evidence that aldehyde formation is occurring. Methoxylamine was used at saturating concentrations but COOH formation was still observed (Figures **3.13**, **S2A** and **S2B**) with 0.09 µM (94% decrease) being detected for ABC and 0.04 µM (95% decrease) for D_2-ABC compared to the positive control. The nucleophilic tendencies of methoxylamine

allow it to react with a variety of compounds, and due to the crude nature of the pooled human liver cytosol used, it could have reacted with numerous compounds within the cytosol, resulting in by-product formation.

Evidently only small amounts of compounds **19a** and **19b** were produced, so it was not possible to detect either compound by conventional LC-MS/MS. An EPI LC-MS/MS scan was used to search selectively for the products of m/z 314 ([M+H]$^+$) (compound **19a**) and the products of m/z 315 ([M+H]$^+$) (compound **19b**). A peak at m/z 191 is the characteristic fragment of both molecules (Figure **3.14**). As can be seen from the mass spectra in Figure **3.15**, the detection of predicted parent and fragment masses led to the conclusion that formation of ABC aldehyde was occurring. For D_2-ABC, a parent ion of m/z 314 was detected, with no m/z 315 found. The reason for this unexpected molecular ion peak could be due to contamination from ABC. The slower rate of D_2-ABC dehydrogenation may have resulted in the preparation of D_2-ABC yielding more **19a** than **19b**, hence the dominant detection of the parent ion m/z 314. The mass spectra from the EPI scan for this experiment can be found in Supplementary Information **S2C**.

Nevertheless, from these experiments, it was clear that ADH and ALDH were key enzymes in this oxidation process for both ABC and D_2-ABC. Methoxylamine's inhibition of ABC-**17** from D_2-ABC provided enough evidence that D_2-ABC also yielded a discrete aldehyde species and therefore the oxidation pathway to the aldehyde is similar and the final product formation is the same.

m/z [M+H]$^+$ 314   *m/z* 191   *m/z* [M+H]$^+$ 315
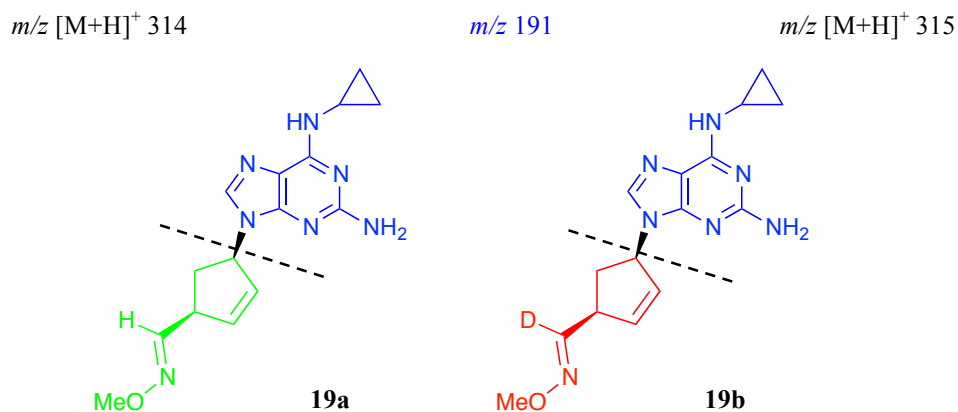
Figure 3.14: Structures of imine (oxime) products: **19a**, formed from trapping the aldehyde of ABC **7** with methoxylamine**,** and **19b**, formed from trapping the aldehyde of D$_2$-ABC **42** with methoxylamine. The key diagnostic ions were *m/z* 314 ([M+H]$^+$) and 191 (purine residue of molecule, as indicated in blue) for **19a** and *m/z* 315 ([M+H]$^+$) and 191 for **19b**.

In experiment 5, 4-MP (600 μM) was used to inhibit ADH enzymes. 4-MP is a selective inhibitor of class I ADH isoforms,[12,35] and previous research has shown that up to 90% of ABC-**17** formation from ABC can be prevented using this inhibitor in human liver cytosol at a concentration of 600 μM.[11] Carboxylic acid formation was reduced but 0.62 μM and 0.38 μM ABC-**17** were produced from ABC and D$_2$-ABC, respectively, representing a 56% and 57% decrease of ABC-**17** formation, respectively, compared to the positive control (Figure **3.13**). It was expected that a greater percentage decrease would be seen, so repeats of the experiments would seek to confirm this expectation with increased concentration of 4-MP. Chromatograms for these experiments can be seen in Supplementary Information Figures **S2A** and **S2B**.

DSF (500 μM) was used as the ALDH inhibitor, as previously discussed. It had not been used before to inhibit the oxidation of ABC. For experiment 6 (Table **3.1**), DSF

was co-incubated in human liver cytosol. Chromatograms for this experiment can be seen in Supplementary Information Figures **S2A** and **S2B**. From these assays, 1.3 µM ABC-**17** was formed from ABC and 0.77 µM from D_2-ABC, which represented an 8% and 13% decrease in the formation of ABC-**17**, respectively, compared to the positive control (1.44 µM and 0.88 µM for ABC and D_2-ABC, respectively) (Figure **3.13**). The COOH formation was not completely suppressed. However, solubility issues did occur with DSF and these may have contributed to inconsistent results. Nevertheless, these results are not surprising: As discussed previously, and as demonstrated by Walsh *et al.*,[5] human ADH1A is able to oxidise ABC to the COOH product without the involvement of ALDH. Due to this activity, COOH formation would not be stopped without the additional presence of an ADH inhibitor. However, the formation of COOH from both compounds was affected and so ALDH appeared to contribute approximately equally to the metabolic fate of these compounds.

Finally, in experiment 7 (Table **3.1**), both DSF (500 µM) and methoxylamine (10 mM) were used. This experiment was conducted to ensure that both substrates were largely oxidised *via* the ADH and ALDH pathways. The formation of COOH in these incubations was found to be 0.36 µM (75% decrease) and 1.77 µM (80% decrease) for ABC and D_2-ABC, respectively, compared to the positive control (1.44 µM and 0.88 µM for ABC and D_2-ABC respectively) (Figure **3.13**). The formation of carboxylic acids was greatly reduced in comparison with incubations containing exclusively DSF (experiment 5), but greater than that seen in experiment 3, where methoxylamine was used. It might be expected that COOH formation would be

reduced even further, but a possible reason for this not occurring could be reactivity between DSF and methoxylamine.

From the results of the seven experiments, it was concluded that ABC and D_2-ABC underwent the same oxidative metabolic fate in human liver cytosol, and so the final set of experiments, to determine the rates of metabolism, could be conducted.

ABC (*m/z* 287/191)
D₂-ABC (*m/z* 289/191)
ABC-COOH (*m/z* 301/191)
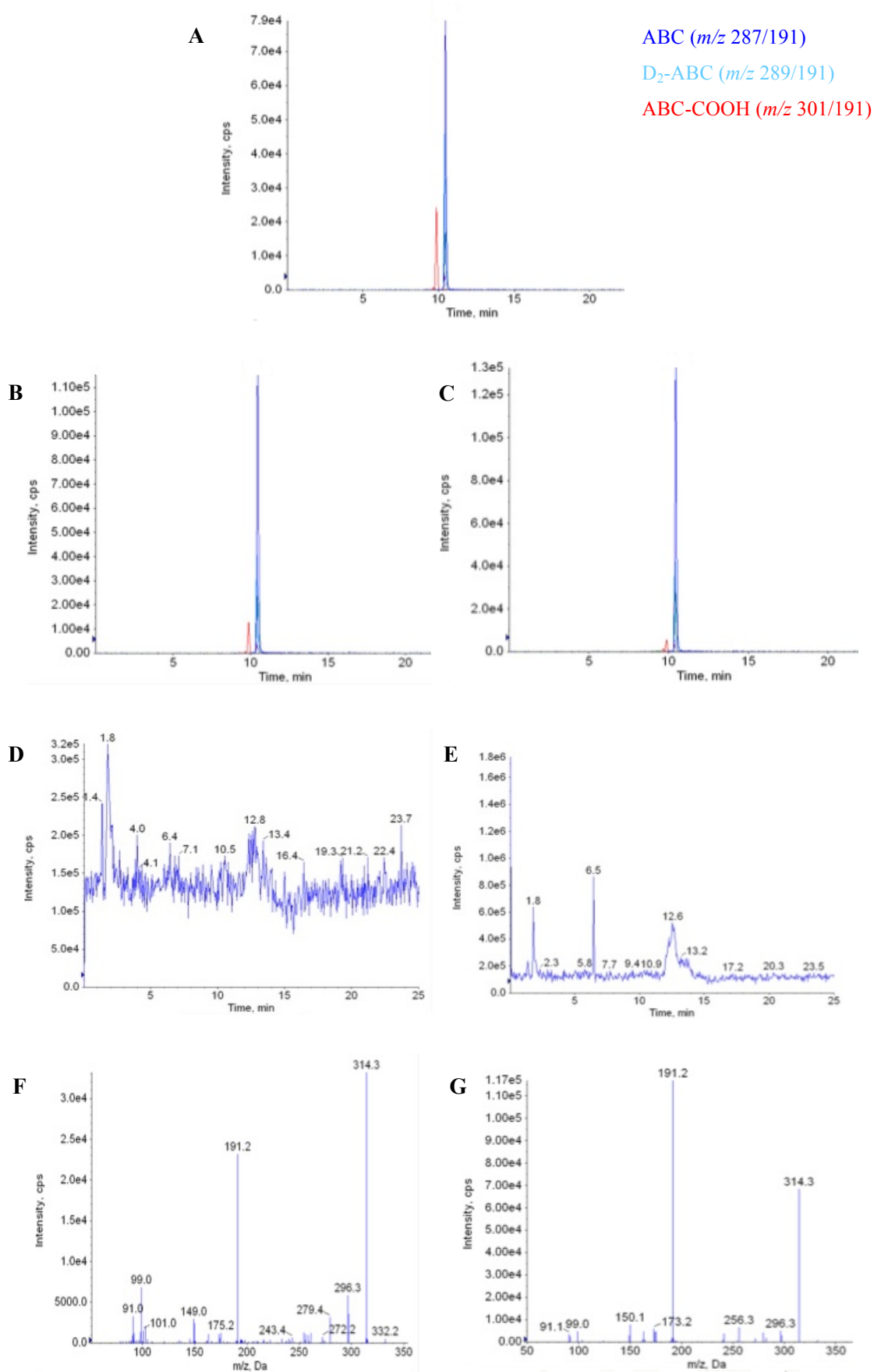
Figure 3.15 continued:

Figure 3.15: MRM chromatograms obtained from experiments 3 (positive control, + NAD) (**A**), 4 (co-incubation with methoxylamine) (**B**) and 7 (co-incubation with methoxylamine and DSF) (**C**) for the characterisation of the pathway of ABC oxidation by human liver cytosol (Table **3.1**). EPI scan for fragments of *m/z* 314 ([M+H]$^+$ for the oxime derivative of the ABC aldehyde intermediate) can be seen in diagrams **D** and **E** for experiments 4 and 7, respectively. The corresponding spectra are presented in diagrams **F** and **G**, with the predominant fragment of *m/z* 314 at *m/z* 191. MRM, multiple reaction monitoring.
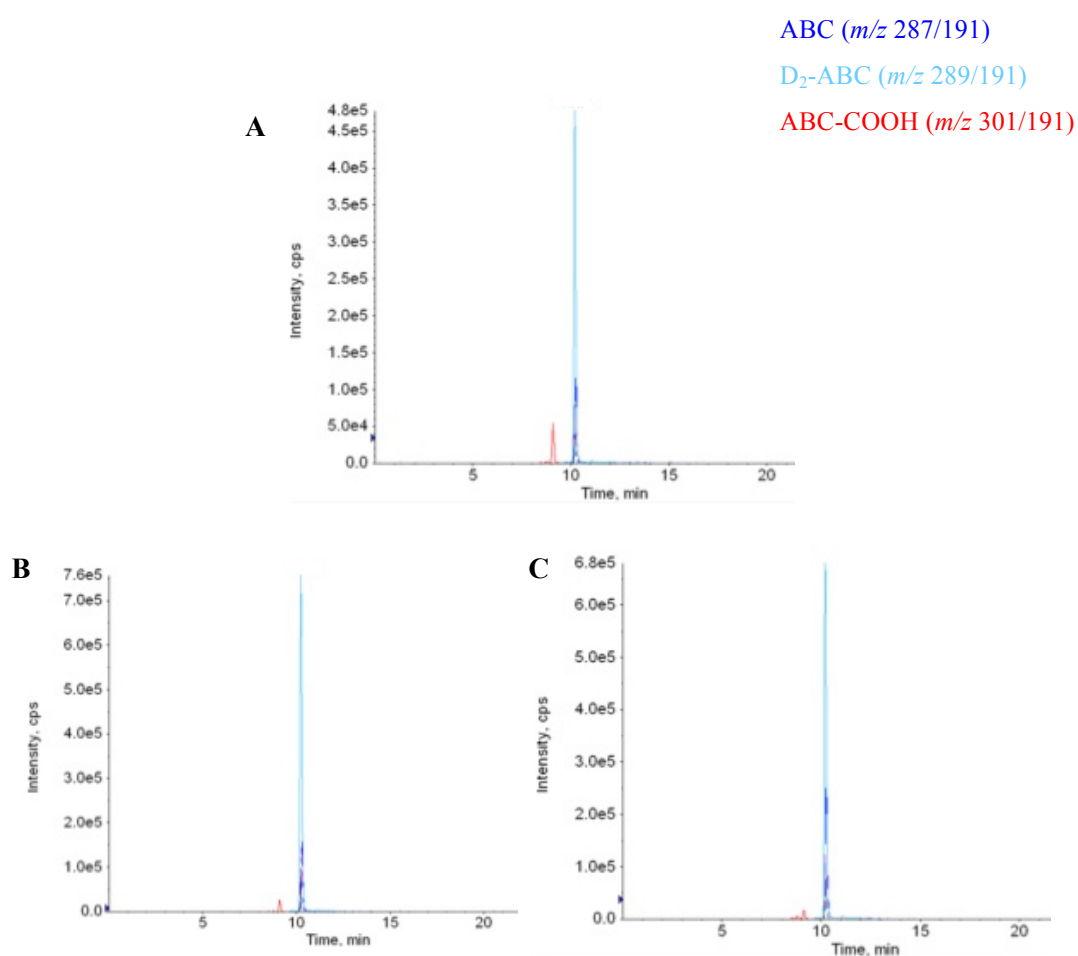
Figure 3.16: MRM chromatograms obtained from experiments 3 (positive control, + NAD) (**A**), 4 (co-incubation with methoxylamine) (**B**) and 7 (co-incubation with methoxylamine and DSF) (**C**) for the characterisation of the pathway of D$_2$-ABC oxidation by human liver cytosol (Table **3.1**).

3.3.1.6 Experimental determination of Michaelis–Menten parameters.

Once it was ensured that both ABC and D_2-ABC were metabolised in the same manner with respect to protein concentration, time and metabolic pathway, it was possible to conduct rate *vs.* substrate concentration experiments with human liver cytosol. By completing these experiments, the Michaelis–Menten parameters, K_m and V_{max}, were determined, and the difference of rate of D_2-ABC oxidation compared with ABC oxidation was calculated.

Following on from work published by Walsh *et al.*[5] and previous work within the Liverpool group,[11] a final concentration of 10 μM was used for ABC and D_2-ABC. To determine the saturating substrate concentration, it was decided to conduct experiments as described in Section **3.5.1.4**, where samples were taken every 10 min up to and including 60 min and every 30 min thereafter up to 120 min over a range of concentrations. Initially, the substrate concentrations attempted were ranging from 10 nM to 10 μM. Due to relatively slow turnover of substrate to COOH product, it was extremely difficult to detect product formation at the lowest concentrations (10–250 nM). However, at 500 nM to 10 μM, COOH product, isomer **17a**, was detected. Using these results to plot rate *vs.* substrate concentration, it was found that the saturating substrate concentration was not reached. This was determined due to the linearity of the Michaelis–Menten graph. At saturating substrate concentrations, the reaction rate should remain constant at increasing substrate concentration. Substrate concentrations greater than 10 μM were therefore required.

The second set of experiments completed were over the higher substrate concentrations, 50 μM to 1 mM. Product formation was easier to quantify with these

concentrations, but again, rate *vs.* substrate concentration showed linearity. In order to determine the required concentrations, the experiments were repeated with substrate concentrations ranging from 2.5–10 mM but similar results were obtained. Experiments conducted at two concentrations, 20 and 50 mM, gave positive results, with the graph showing saturating substrate concentration levels at 20 mM (Figure **3.17**). Representative mass chromatograms for concentrations 500 μM and 20 mM at 0 and 120 min can be seen in Supplementary Information Figures **S3A** and **S3B**.
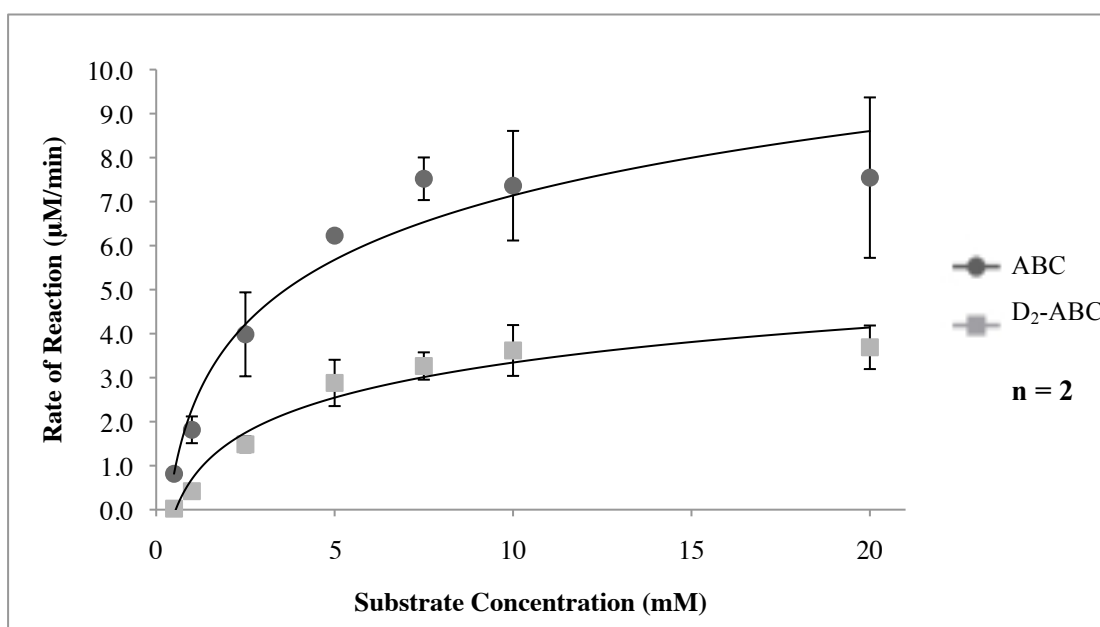
Figure 3.17: Michaelis–Menten graphs representing incubations of 500 μM to 20 mM substrate (ABC or D_2-ABC) in human liver cytosol *vs.* rate of reaction (μM/min). The protein concentration was 0.75 mg/mL. The concentration of NAD^+ was 7.5 mM. Data were derived from two separate experiments over two days. Data represent the mean values obtained (n = 2) ± standard deviation.

Due to solubility difficulties of ABC/D_2-ABC in the incubation buffer, it was decided that the most reliable results could only be obtained at the maximum substrate concentration of 20 mM. The results obtained at 50 mM were discarded. The experiments were completed for concentrations of 0.5, 1, 2.5, 5, 7.5, 10 and 20

mM for both ABC and D$_2$-ABC with the total formation of COOH as the analytical

end-point. The rate data were obtained initially from plotting product formation

[ABC-**17**] (μM) *vs.* time (min). Representative graphs at the 0.5 mM concentrations

for both compounds can be seen in Figure **3.18**.

A

B
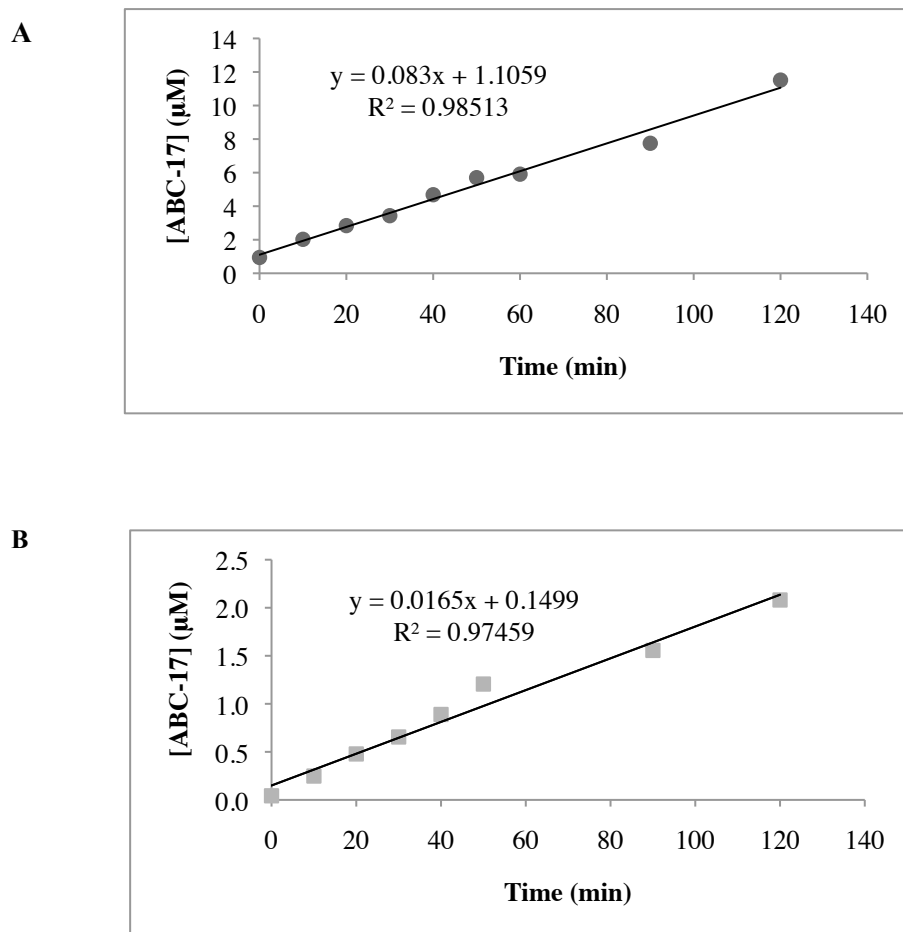
Figure 3.18: Representative graphs of ABC-**17** production for ABC (**A**) and D$_2$-ABC (**B**) obtained

for the 0.5 mM substrate concentration from 0 to 120 min. The gradient of the graph (ABC: 0.083,

R^2 = 0.985 and D$_2$-ABC: 0.0165, R^2 = 0.975) was the rate value for that specific concentration. The

protein concentration in the human liver cytosol was 0.75 mg/mL. The concentration of NAD$^+$ was

7.5 mM.

After confirming these individual graphs were linear, the gradient of each graph was calculated. This value represented the reaction rate (*v*). Finally, these *v* (μM min^{-1}) values were plotted against substrate concentration (mM) (Table **3.2**) and the Michaelis–Menten parameters were calculated using GraphPad Prism$^{®}$ Version 6 software (GraphPad Inc, La Jolla, CA, USA) (Table **3.3**).

Table 3.2: The final rate values for the oxidation of ABC and D$_2$-ABC in human liver cytosol over the range of 0.5–20 mM substrate concentrations. The rate values were obtained from the gradients of plots of [ABC-**17** formation] (μM) *vs.* time (min). Experiments were completed on two days and data are presented as the mean (n = 2) ± standard deviation.[*]

Substrate Concentration (mM)	Mean Rate for ABC (μM/min) ± SD	Mean Rate for D$_2$-ABC (μM/min) ± SD
0.5	0.815 ± 0.020	0.023 ± 0.000
1	1.815 ± 0.304	0.42 ± 0.028
2.5	3.985 ± 0.954	1.485 ± 0.181
5	6.227 ± 0.078	2.88 ± 0.526
7.5	7.52 ± 0.484	3.265 ± 0.310
10	7.362 ± 1.245	3.618 ± 0.578
20	7.545 ± 1.823	3.69 ± 0.495

[*] The protein concentration in the human liver cytosol was 0.75 mg/mL. The concentration of NAD$^+$ was 7.5 mM.

Table 3.3: Michaelis–Menten parameters (V_{max} and K_m) for the oxidation of ABC and D_2-ABC to ABC-**17** in human liver cytosol. The data represent values obtained from two separate experiments, completed on two days. Mean values (n = 2) are stated ± standard deviation. The values were calculated using GraphPad Prism® Version 6 software.

Substrate	V_{max} Value ± SD	K_m Value ± SD
ABC	9.56 ± 0.88	3.19 ± 0.90
D_2-ABC	5.09 ± 0.62	5.08 ± 1.60

It can be seen from Table **3.3** that the V_{max} and K_m values differ appreciably between ABC and D_2-ABC. Using the equation as stated below to determine the KIE,[25] the kinetic effect can be calculated and the KIE for ABC:D_2-ABC was found to be 1.88.

$$KIE = \frac{V_{max}H}{V_{max}D} = 1.88$$

For a KIE to be present, it must be that the isotopically substituted atom is directly involved in determining the rate of the overall reaction. This would be the abstraction of both D atoms from D_2-ABC over both oxidation steps (Figure **3.19**).
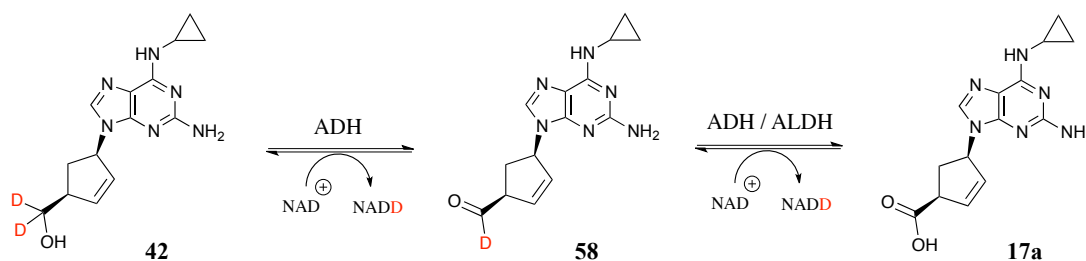
Figure 3.19: Abstraction of two D atoms from D_2-ABC **42** over both major oxidation steps to form intermediate **58** followed by carboxylic acid **17a**. ADH and/or ALDH would complete this oxidation pathway, with the use of the co-factor, NAD^+.

Practically, it is essential that the KIE value is greater than 1, with a larger value representing a larger effect. Therefore it can be concluded that as the ratio calculated for ABC:D_2-ABC is 1.88, there is a deuterium isotopic effect on the oxidative metabolism of ABC to its carboxylic acid metabolites. Whether both of the metabolic oxidation steps are subject to a KIE is yet to be determined.

3.3.2 Cross-reactivity of ABC-specific human T-cell clones with D_2-ABC.

ABC is known to stimulate $CD8^+$ T-cells from HLA-B*57:01 positive individuals,[11,36,37] therefore in addition to the metabolism studies, the ability of D_2-ABC to stimulate T-cells was also probed. The chemical cross-reactivity experiments were conducted within the University of Liverpool, with full details of all methodological protocols available.[11] In order to determine whether a D_2-ABC-stimulated T-cell response occurred, cytokine release (IFN-γ, ELISpot assay, Chapter 1, Section **1.10.2**) was examined.

T-cells isolated from HLA-B*57:01-positive individuals were cloned and used within all assays. These T-cells were incubated over 48 h with irradiated autologous Epstein–Barr Virus (EBV)-transformed B-cells in the presence of either ABC or D_2-ABC at concentrations of 10, 50 and 100 µM, and it was found that these concentrations of D_2-ABC stimulated T-cells to the same extent as ABC itself (Figure **3.20**).

As previously discussed in this chapter, D_2-ABC is metabolised oxidatively by human liver cytosol at a slower rate in comparison to ABC over 24 h. Whether this

difference continues to be statistically significant over 48 h is unknown. Due to the long incubation times (48 h) of both compounds in the ELISpot assay, it is also unknown whether a slower rate of drug metabolism would affect T-cell stimulation. The mechanism of T-cell stimulation by ABC remains uncertain, as it is still unclear whether the parent drug or a metabolite is responsible for the activation. However, it is known that cytosol from EBV-transformed B-cells can metabolise ABC to its carboxylic acids during a 16 h incubation.[30]
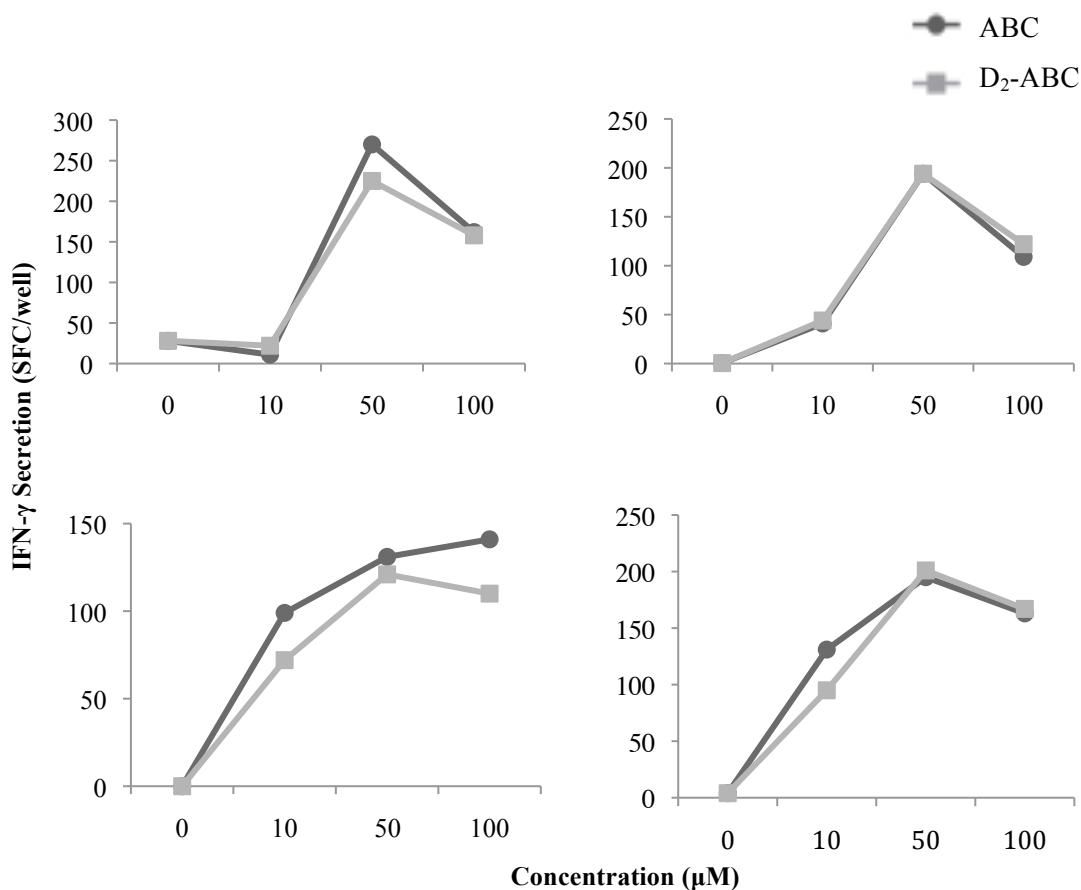
Figure 3.20:   Cross-reactivity results for ABC and D_2-ABC after a 48 h incubation with four individual ABC-specific T-cell clones isolated from HLA-B*57:01-positive individuals and autologous EBV-transformed B-cells. Data shown are results obtained from an ELISpot assay. IFN-γ was measured as spot-forming cells (SFC)/well. EBV, Epstein–Barr virus; IFN-γ, interferon-γ; ELISpot, enzyme-linked immunospot; SFC, spot-forming cells.

3.3.3 Cytotoxicological and pharmacological studies with D_2-ABC.

The cytotoxicity of ABC and D_2-ABC was determined in MT4 cells, using the MTT viability assay at 24 h and 5-day intervals. The theory and discussion of these assays are discussed in Chapter 1, Section **1.11**. Viable cells, with active redox metabolism,[38] reduce MTT to a purple formazan product that can be measured spectrophotometrically.[39] The MTT assay has been used previously with MT4 cells.[40] For both ABC and D_2-ABC, statistically significant cytotoxicity was seen in MT4 cells at 200 μM ($p = 0.0013$ and $p = 0.0021$, respectively), 1 mM and 5 mM concentrations (Figure **3.21**). In addition to this result, comparable IC_{50} values were obtained for ABC and D_2-ABC (370.4 μM and 397.2 μM, respectively). As at 24 h, significant cytotoxicity was also observed after 5 days for both compounds at 200 μM ($p < 0.0001$ for ABC and D_2-ABC), 1 mM and 5 mM concentrations (Figure **3.21**). Additionally, the IC_{50} values generated at this time point were 240.2 μM (ABC) and 255.7 μM (D_2-ABC). The cytotoxicity of ABC has been assessed in other cell types.[41]

In addition to cytotoxicity assays, the antiretroviral activities of both compounds were determined using HIVIII$_B$ virus replicating in MT4 cells (Figure **3.21**). ABC exhibits potent *in vitro* antiviral activity against wild-type HIV-1 in MT4 cells.[42,43] The EC_{50} values for ABC and D_2-ABC were 7.5 μM and 13.4 μM, respectively. Comparing these values, it can be seen that D_2-ABC maintains potency with comparison to ABC. It should be noted that the drugs countered the cytotoxicity caused by viral infection notwithstanding they were themselves somewhat toxic to MT4 cells.

The evaluations of both IC_{50} and EC_{50} values for D_2-ABC against ABC indicated D_2-ABC retained pharmacological potency without any change of toxicity in the same cell type. It can be concluded from these data that the placement of two deuterium atoms at the 5'-C position does not affect the antiretroviral activity compared to ABC.   Specifically, it appears deuteration does not significantly affect the metabolism of ABC in T-cells to its pharmacologically active derivative, namely (–)-CBV-TP; the first step of the pathway being formation of ABC 5'-MP.[44]
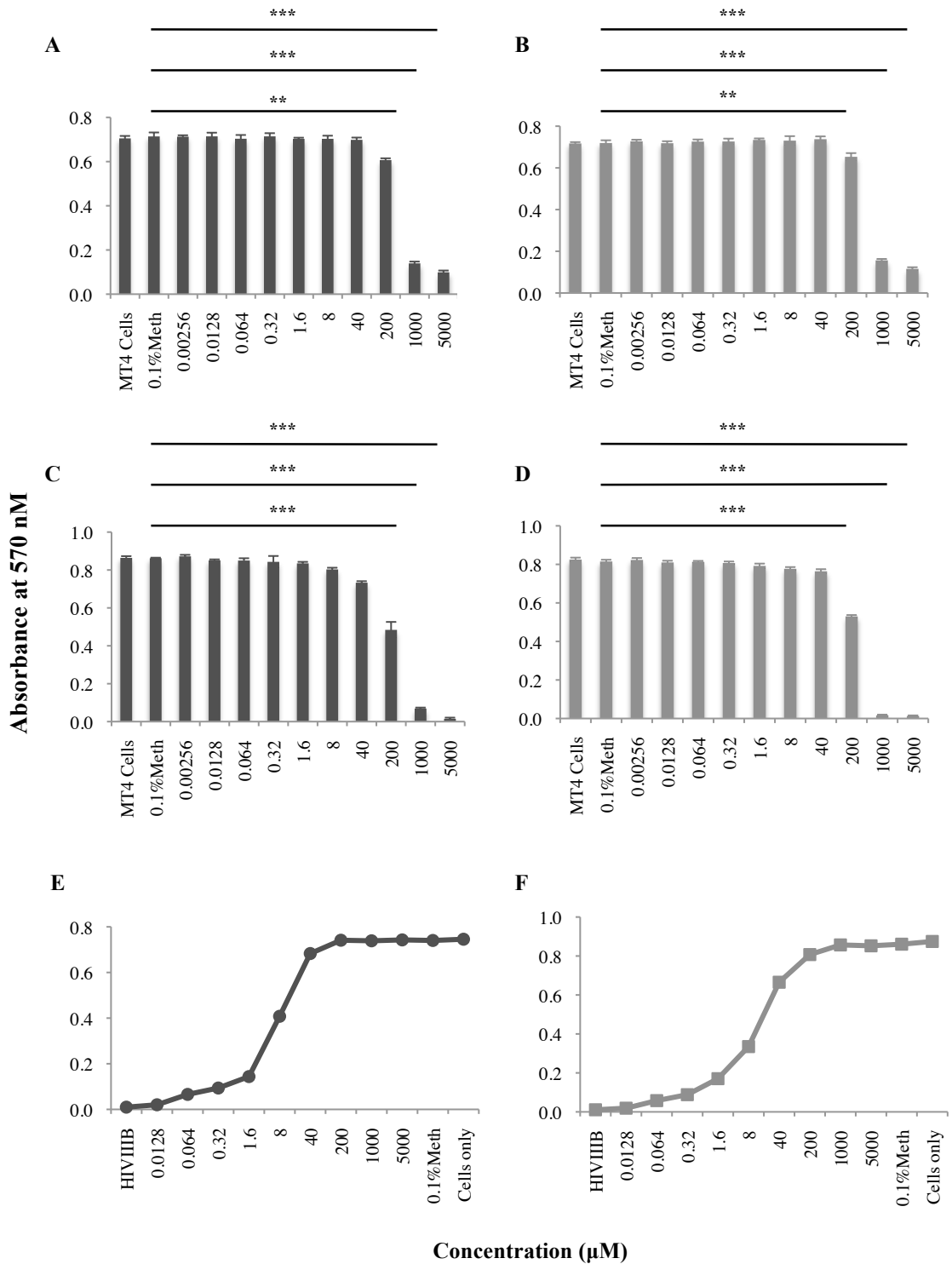
Figure 3.21: Determination of cytotoxicity after 24 h exposure to ABC (**A**) and D_2-ABC (**B**) and after 5-day exposure to ABC (**C**) and D_2-ABC (**D**) in MT4 cells. Cell viability was assessed using the spectrophotometric MTT assay. Antiretroviral activity of ABC (**E)** and D_2-ABC (**F**) against HIVIII$_B$ in MT4 cells was assessed indirectly using the spectrophotometric MTT assay, which visualises the viral cytotoxicity. All data are given as the mean ± standard deviation of four experiments conducted

on different days. All data were normally distributed. Statistical analysis was conducted using an unpaired t-test and two-tailed p values are given (* $p < 0.05$; ** $p < 0.01$; *** $p < 0.001$). IC$_{50}$ (μM) data were generated using GraphPad Prism 3.0 statistical analysis software. 0.1% Meth, 0.1% methanol.

3.4 Conclusions & Future Work

Although the biochemical oxidation of ABC has been widely studied,[5,45-47] the contribution of the intermediate/metabolite products of this pathway to ABC's toxicity is still unknown. The possibility ABC-**16** mediates the cytotoxicity of ABC in MT4 cells cannot be assessed because neither ADH expression by these cells nor the effect of ADH inhibitors has been investigated. ABC-**16**, an α,β-unsaturated aldehyde, has been shown to covalently bind to proteins both *in vitro* and *in vivo*, although a method for direct detection of this aldehyde intermediate in *in vivo* samples has yet to be discovered. Within this research, the oxidative metabolism was probed further.

To investigate the metabolism of D_2-ABC further, sets of experiments were designed to confirm that D_2-ABC undertook the same metabolic pathway as ABC. Related experiments proved linearity of ABC oxidation with respect to cytosolic protein concentration and time. By inhibiting the two enzymes involved in hepatic oxidation of ABC, ADH and ALDH, and trapping the aldehyde intermediate, it was possible to confirm that the compounds undertook the same metabolic pathway in human liver cytosol.

Finally, the Michaelis–Menten parameters (V_{max} and K_m) were obtained from a set of rate experiments, where the measure of product generation was cumulative COOH formation. Both values were calculated for ABC and D_2-ABC, and the V_{max} values have been used to determine whether an isotopic effect is present in the oxidative metabolism of ABC *vs.* D_2-ABC. This value was calculated at 1.88, illustrating that

the oxidative metabolism of the 5'-C OH group in human liver is significantly affected by isotopic substitution at this position. However, it should be noted that there might not be a KIE on ABC oxidation in all human cell types: The NAD-dependent oxidation of ABC to carboxylic acids in cytosol from EBV-transformed B-cells does not involve a 4-MP-sensitive enzyme, *i.e.* a class I ADH.[30]

There are limits within the work presented in this thesis and further metabolic studies are required in order to determine whether a KIE is present between ABC and D_2-ABC with respect to the rate constants k. For this analysis, crude liver cytosol cannot be used; purified forms of liver ADH and ALDH are required. Before this work can be undertaken, further research into the involvement of individual isoforms of both ADH and ALDH is also required and the exact ALDH isoform involved in the oxidation would need to be determined. This identification would also assist in choosing a more suitable inhibitor for these experiments.

Also, it will be important to extend the metabolic investigations with D_2-ABC to non-hepatic cell types, and especially skin cells because the major adverse reactions associated with ABC in HIV patients are cutaneous hypersensitivity reactions.[48]

It was clear from the T-cell cross-reactivity, cytotoxicity and pharmacological assays that deuteration of ABC had no ameliorating effect on T-cell activation or MT4 cell cytotoxicity but neither did it reduce antiviral activity in MT4 cells. The mechanism of ABC's toxicity in MT4 cells is unknown; in particular, whether it is an action of the parent drug or a metabolite. Notably, the possibility that the cytotoxicity of D_2-ABC is caused by (−)-D_2-CBV-TP or an intermediate of its biosynthesis cannot be

excluded because D_2-ABC retains the potent antiretroviral activity that is mediated exclusively by the anabolic triphosphate.[44] Due to the long incubations times of these assays, it is difficult to determine whether the slower metabolism of D_2-ABC would have a significant effect on the pharmacological activity or T-cell activation over a shorter period of time. The likely effect of D_2-ABC *in vivo* is also unclear, and the *in vivo* effects of deuterium substitution of drugs are much less documented. Although, initial studies on a corticotropin-releasing hormone receptor 1 **(CRF₁)** antagonist have shown that H replacement with D can slow its oxidative pathway, resulting in altered PK parameters.[49] By blocking one metabolic pathway *in vivo*, the metabolism of this drug was diverted to other metabolic routes. In the case of ABC, this switching effect would divert drug to the other major, but reversible, deactivating pathway, namely *O*-glucuronidation.[6]

Further work should include a repeat of the experiments with substrate disappearance measured, rather than product formation. Further to the primary isotope effect, it would be interesting to use another deuterated form of ABC, such as the product of mono-deuteration of the 4'-C position (Chapter 2, Figure **2.14**), which would allow for investigation into any possible secondary KIEs.

3.5 Experimental

Immunology (cross-reactivity) experiments were conducted and obtained at the University of Liverpool by Dr. Catherine Bell and John Farrell (Dr. Dean Naisbitt's research group). Cytotoxicity/efficacy experiments were also conducted and obtained at the University of Liverpool by Dr. Philip Martin (Prof. Andrew Owen's research group).

3.5.1 ABC and D_2-ABC metabolism in human liver cytosol.

All reagents were purchased from Sigma Aldrich, Fisher Scientific (Loughborough, UK) and Romil Ltd (Cambridge, UK) unless otherwise stated. ABC succinate, ABC sulfate and ABC carboxylic acid **17a** were kind gifts from GSK.

3.5.1.1 Determination of linearity of ABC/D_2-ABC oxidation in human liver cytosol with respect to protein concentration.

Reactions were conducted in sodium pyrophosphate buffer (50 mM, pH 8.8, 500 μL). ABC (10 μM) or D_2-ABC (10 μM) was incubated with human liver cytosol (pooled cytosol from human liver, Sigma Aldrich, UK) (protein concentration, 0.1, 0.25, 0.5, 0.75, 1.0, 1.25 and 1.5 mg/mL) and NAD (7.5 mM) at 37 °C in a shaking water bath for 2 h, whereupon the incubation vials were placed on ice for 5 min. An aliquot (10 μL) of the reaction mixture was taken, and to this, ACN (100 μL) was added. The samples were vortexed and the IS (ABC or D_2-ABC, 100 μL, 200 nM) was added. The precipitated protein was sedimented by centrifugation (14,000 × *g*, 20 min, 4 °C), and the supernatant was removed and evaporated to dry residue at 30 °C. The residues were re-dissolved in the mobile phase (100 μL, 10 mM ammonium

acetate (NH$_4$OAc, pH 3.8)) containing 5% ACN, filtered through 0.45 μM filter pore plates and transferred to high-performance liquid chromatography (HPLC) vials for LC-MS/MS analysis.

3.5.1.2 Comparative oxidation of ABC and D$_2$-ABC in human liver cytosol with respect to time.

Reactions were conducted in sodium pyrophosphate buffer (50 mM, pH 8.8, 500 μL). ABC (10 μM) or D$_2$-ABC (10 μM) was incubated with human liver cytosol (protein concentration, 0.75 mg/mL) and NAD (7.5 mM) at 37 °C in a shaking water bath for 1, 4, 8, 16, 20, and 24 h, whereupon the incubation vials were placed on ice for 5 min. An aliquot (10 μL) was taken, and to this ACN (100 μL) was added. The samples were vortexed and the IS (ABC or D$_2$-ABC, 100 μL, 200 nM) was added. The precipitated protein was sedimented by centrifugation (14,000 × g, 20 min, 4 °C), and the supernatant was removed and evaporated to dry residue at 30 °C. The residues were re-dissolved in the mobile phase (100 μL, 10 mM NH$_4$OAc, pH 3.8) containing 5% ACN, filtered through 0.45 μM filter pore plates and transferred to HPLC vials for LC-MS/MS analysis.

3.5.1.3 Enzyme inhibition and aldehyde trapping experiments for comparison of ABC and D$_2$-ABC oxidation in human liver cytosol.

Reactions were conducted in sodium pyrophosphate buffer (50 mM, pH 8.8, 500 μL). ABC (10 μM) or D$_2$-ABC (10 μM) was incubated with human liver cytosol (protein concentration, 0.75 mg/mL), +/– NAD (7.5 mM) (Table **3.1**, Section **3.3.1.5**) and where used, the following compounds (Table **3.1**, Section **3.3.1.5**) at 37 °C in a shaking water bath for 20 h. Following the incubation, the vials were placed on ice

for 5 min. An aliquot (10 μL) was taken, and to this ACN (100 μL) was added. The samples were vortexed and the IS (ABC or D_2-ABC, 100 μL, 200 nM) was added. The precipitated protein was sedimented by centrifugation (14,000 × g, 20 min, 4 °C), and the supernatant was removed and evaporated to dry residue at 30 °C. The residues were re-dissolved in the mobile phase (100 μL, 10 mM NH_4OAc, pH 3.8) containing 5% ACN, filtered through 0.45 μM filter pore plates and transferred to HPLC vials for LC-MS/MS analysis.

3.5.1.4 Determination of COOH formation with respect to substrate concentration and determination of deuterium isotope effects for D_2-ABC vs. ABC.

Reactions were conducted in sodium pyrophosphate buffer (50 mM, pH 8.8, 500 μL). ABC (500 μM, 1, 2.5, 5, 7.5, 10 and 20 mM) or D_2-ABC (500 μM, 1, 2.5, 5, 7.5, 10 and 20 mM) was incubated with human liver cytosol (protein concentration, 0.75 mg/mL) and NAD (7.5 mM) at 37 °C in a shaking water bath, and aliquots (10 μL) were taken at 0, 10, 20, 30, 40, 50, 60, 90 and 120 min from each incubation. The samples were placed on ice for 5 min and ACN (100 μL) was added. The samples were vortexed and the IS (ABC or D_2-ABC, 100 μL, 200 nM) was added. The precipitated protein was sedimented by centrifugation (14,000 × g, 20 min, 4 °C), and the supernatant was removed and evaporated to dry residue at 30 °C. The residues were re-dissolved in the mobile phase (100 μL, 10 mM NH_4OAc, pH 3.8) containing 5% ACN, filtered through 0.45 μM filter pore plates and transferred to HPLC vials for LC-MS/MS analysis.

3.5.1.5 LC-MS/MS conditions.

All samples were analysed on a 4000 QTRAP system (AB Sciex, Foster City, CA, USA). An Eclipse XBD C18 column (2.1 × 150 mm, 5 μm) (Agilent, Cheshire, UK) was used for chromatographic separation at 30 °C. An Ultimate 3000 liquid chromatography system (Dionex, CA, USA) was interfaced to the mass spectrometer. The sample injection volume was 5 μL. The mobile phases were as follows: Mobile phase A – NH_4OAc (10 mM, pH 3.8), mobile phase B – ACN. The compounds, including all metabolites, were eluted from the chromatographic column using a linear gradient (5–20% 'B') over 15 min and 20% 'B' for the remaining 5 min (20 min total) using a flow rate of 0.3 mL/min. The mass spectrometer was operated in positive-ion mode. Nitrogen was used as both the nebulising and drying gas. The source was operated at 500 °C. The electrospray voltage was set to 5 kV and analyses were performed in MRM mode. Compound-dependent parameters are shown in Table **3.4**.

Table 3.4: Compound dependent parameters for ABC **7**, D_2-ABC **42** and ABC-COOH **17**.

Compound	Precursor Ion (*m/z*)	Product Ion (*m/z*)	Declustering Potential (V)	Entrance Potential (V)	Collision Energy (eV)	Exit Potential (V)
ABC **7**	287	191	66	10	27	10
D_2-ABC **42**	289	191	66	10	27	10
COOH **17**	301	191	63	10	29	10

Where EPI scans were used, the mass spectrometer was targeted to scan for product ions of *m/z* 314 for ABC and *m/z* 315 for D$_2$-ABC. Data were analysed using Analyst software (AB Sciex).

3.5.1.6 Quantification of parent drug and carboxylic acid metabolite.

Standard samples (S1–S10) were prepared from stock solutions of ABC, D$_2$-ABC and ABC-**17**. The stock solutions were as follows: ABC and D$_2$-ABC: 0.1, 1, 10 and 100 μM, and ABC-**17**: 1 and 10 μM. They were prepared in distilled water, and stored at –20 °C. The solutions were used to generate the required concentrations for LC-MS/MS calibration as stated in Table **3.7**. Stock solutions were diluted with sodium pyrophosphate buffer (50 mM, pH 8.8). ABC and ABC-**17** were standard compounds obtained from GSK and D$_2$-ABC was synthetically produced (see Chapter 2).

Where ABC was analyte or substrate, D$_2$-ABC was the IS, and when D$_2$-ABC was the analyte or substrate, ABC was the IS. Once the standard samples (S1–S10) (90 μL) were generated, bovine serum albumin (BSA) (0.75 mg/mL, 10 μL), used as a substitute for blank human liver cytosol, dissolved in sodium pyrophosphate buffer (50 mM, pH 8.8)) was added to each sample and vortexed. The protein was precipitated with ACN (100 μL) and sedimented by centrifugation (14,000 × *g*, 20 min, 4 °C). The supernatant was removed and evaporated to dry residue at 30 °C. The residues were re-dissolved in the mobile phase (100 μL, 10 mM NH$_4$OAc, pH 3.8) containing 5% ACN, filtered through 0.45 μM filter pore plates and transferred to HPLC vials for LC-MS/MS analysis. The lower limits of detection (signal-to-noise ratio ≥3) and quantification (cross-validation (CV) error ≤20%) of ABC-**17**

under these conditions were 2.5 nM and 10 nM, respectively as determined previously.[11] Blank human liver cytosol processed in the same way did not yield MRM signals that interfered with those of ABC, D_2-ABC and ABC-**17**.

Table 3.5: Final concentrations of the calibration standards (ABC, D_2-ABC and ABC-**17**) and the IS (ABC or D_2-ABC) used to create a calibration curve.

Standard	ABC or D_2-ABC [nM]	ABC-17 [nM]	Internal Standard (ABC/D_2-ABC) [nM]
S10	5	10	200
S9	10	20	200
S8	25	50	200
S7	50	100	200
S6	100	200	200
S5	250	500	200
S4	500	1000	200
S3	1000	2000	200
S2	2000	4000	200
S1	4000	8000	200

3.5.1.7 Carboxylic acid formation, statistical analysis and kinetic parameters

The values of ABC-**17** production shown in figures and graphs present the total COOH formation as its concentration (μM), with values calculated as the sum of all three COOH isomers. Where percentage decrease/increase of COOH formation values are stated, this was calculated such that:

$$\% \text{ COOH change} = \frac{\text{difference between positive control and expt. sample (μM)}}{\text{positive control (μM)}} * 100$$

Statistical tests were conducted and Michaelis–Menten kinetic parameters were calculated using GraphPad Prism® Version 6 software. The statistical significance of a difference, where appropriate, was determined using an unpaired t-test.

3.5.2 Immunology studies.

Cells from three HLA-B*57:01-positive individuals were selected from our cell bank containing peripheral blood mononuclear cells ($70–150 \times 10^6$; stored in vials of 10×10^6 cells) from 1000 HLA-typed donors. The demographics of the first 400 study subjects and HLA allele frequencies have been reported previously.[50] Ethical approval for the study was obtained from the local research ethics committee and all volunteers were consented prior to blood donation. Confidentiality was maintained throughout the study.

All reagents were supplied by Sigma Aldrich (UK) unless otherwise stated. ABC-specific human T-cell clones were generated as described previously:[11,30] 1×10^6

peripheral blood mononucleated cells (PBMCs) from a HLA-B*57:01-positive volunteer were incubated with 50 μM ABC in RPMI medium supplemented with 10% human AB serum (Innovative Research, Novi, MI, USA), 1000 U/mL penicillin, 0.1 mg/mL streptomycin, HEPES and transferrin. On days 6 and 9, IL-2 (Peprotech, London) was added to the cultures. $CD8^+$ T-cells were isolated by magnetic separation (Multisort kit, Milteny Biotec, Surrey) and serially diluted according to established protocols.[51] Autologous EBV-transformed human B-cell lines were also generated from PBMCs, by transformation with supernatant from the virus-producing cell line B9.58. ABC-specificity of T-cell clones (5×10^4 cells/well) was determined by addition of 50 μM ABC and 1×10^4 irradiated autologous EBV-transformed B-cells to serve as APCs.

Cross-reactivity of ABC-specific T-cell clones was assessed by IFN-γ ELISpot assay (Mabtech, Stockholm, Sweden). T-cell clones (5×10^4 cells/well) were incubated with 10, 50 or 100 μM ABC or D_2-ABC in the presence of 1×10^4 irradiated autologous EBV-transformed B-cells. The ELISpot was developed after 48 h. SFCs were quantified using an AID ELISpot microplate reader (Cadama Medical, Stourbridge, UK).

3.5.3 Pharmacological studies.

3.5.3.1 Routine cell culture/cell maintenance.

MT4 cells were supplied by the EU programme's EVA Centre for AIDS Reagents, NIBSC (South Mimms, Hertfordshire, UK), and routinely maintained in RPMI-1640 supplemented with 10% sterile filtered foetal bovine serum (FBS; BioWhittaker, Berkshire, UK). They were incubated at 37 °C and 5% CO_2, and subcultured every

four days prior to use. Cell viability was determined by Trypan Blue exclusion assay and was typically <97%.

3.5.3.2 Determination of ABC and D₂-ABC cytotoxicity in MT4 cells by MTT assay.

MT4 cells were seeded at a density of 2.5×10^4 cells / 100 µL of RPMI-1640 and 10% sterile filtered FBS into each well of a 96-well plate (Nunclon^{TM}, Denmark), and incubated for 24 h at 37 °C and 5% CO_2. The medium was then aspirated and replaced with medium containing a range of concentrations (0.0026, 0.0128, 0.064, 0.32, 1.6, 8, 40, 200, 1000 or 5000 µM) of ABC or D_2-ABC dissolved in 0.1% MeOH (final concentration) and routine culture medium. The plates were then incubated for 24 h or 5 days at 37 °C and 5% CO_2. Plates were removed from the incubator and 20 µL of a 5 mg/mL solution of MTT (Sigma, UK) in Hanks balanced salt solution (HBSS; Sigma, UK) was added to each well. The plates were further incubated for 2 h at 37 °C and 5% CO_2. Finally, lysis buffer (100 µL) containing 50% v/v dimethylformamide (DMF, Sigma, UK) and 20% v/v sodium dodecyl sulfate (SDS; Sigma, UK) was added to each well and incubated for 24 h at 37 °C and 5% CO_2. Absorbance readings were taken at 570 nm using a Tecan Genesis plate reader (Tecan Magellan, Austria).

3.5.3.3 Inhibition of HIVIII$_B$ replication in MT4 cells.

The HIVIII$_B$ strain of virus was provided by the EU programmes EVA Centre for AIDS Reagents, National Institute for Biological Standards and Control (NIBSC, South Mimms, Hertfordshire, UK). MT4 cells and viral isolates (multiplicity of infection, 0.01) were dispensed into a 50 mL Falcon tube and centrifuged ($2000 \times g$,

15 min, 25 °C) in a Galaxy 170R incubator (Sanyo, Japan). The Falcon tube containing the MT4/HIVIII$_B$ pellet was then incubated at 37 °C and 5% CO_2. After 2 h, the supernatant was aspirated and the pellet resuspended in RPMI-1640 supplemented with 10% sterile filtered FBS. MT4 cells containing virus particles were then seeded at a density of 1×10^4 cells / 80 µL into each well of a 96-well plate also containing 20 µL of a range of concentrations ($5 \times$ concentrate) of ABC or D$_2$-ABC dissolved in 0.5% MeOH and RPMI-1640 supplemented with 10% sterile filtered FBS resulting in final concentrations 0.0128, 0.064, 0.32, 1.6, 8, 40, 200, 1000 or 5000 µM. The plates were then incubated for 5 days at 37 °C and 5% CO_2 prior to the MTT assay as described above. Inhibitory effects of drugs on HIV replication can be assessed indirectly through the inhibition of virus-induced cytotoxicity to the MT4 cells, estimated using an MTT assay.[39,52]

3.6 Supplementary Information

ABC (*m/z* 287/191)

D$_2$-ABC (*m/z* 289/191)

ABC-COOH (*m/z* 301/191)
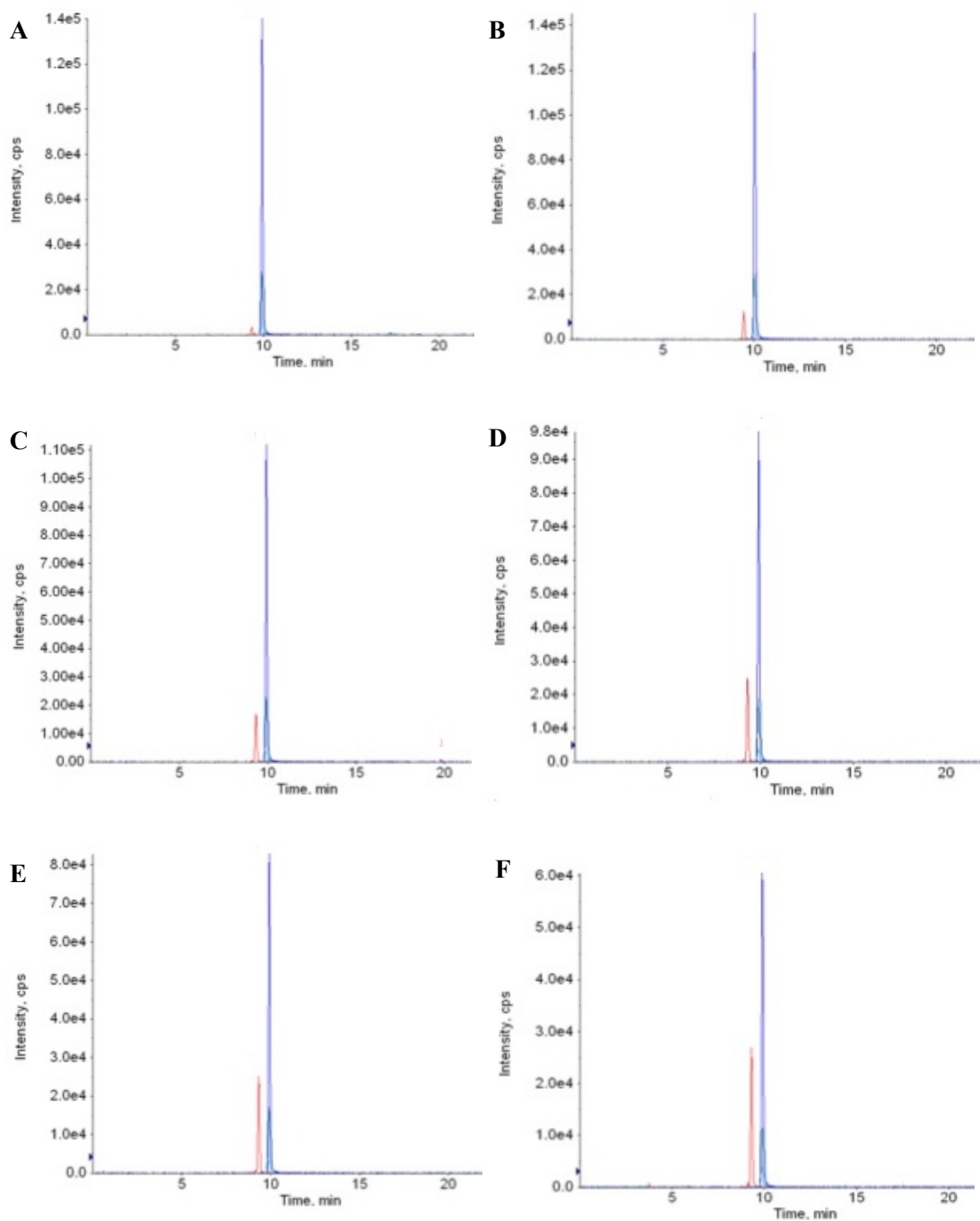
Figure S1A: MRM chromatograms for the formation of ABC-COOH **17** from ABC (10 µM) in human liver cytosol at the following hours: 1 h (**A**); 4 h (**B**); 8 h (**C**); 16 h (**D**); 20 h (**E**) and 24 h (**F**). Protein and NAD$^+$ concentrations were 0.75 mg/mL and 7.5 mM, respectively.

ABC (*m/z* 287/191)

D$_2$-ABC (*m/z* 289/191)

ABC-COOH (*m/z* 301/191)
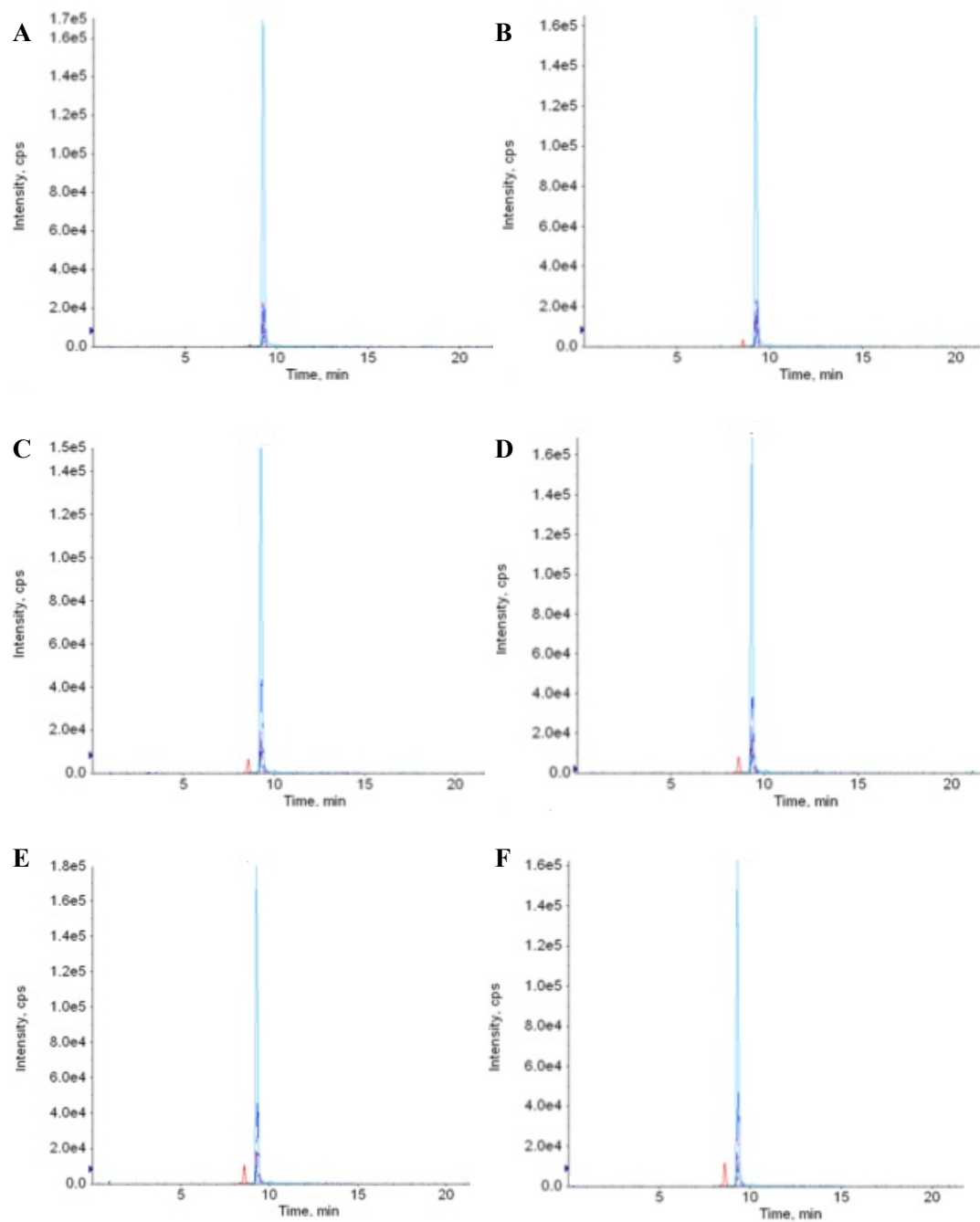
Figure S1B: MRM chromatograms for the formation of ABC-COOH **17** from D$_2$-ABC (10 μM) in human liver cytosol at the following hours: 1 h (**A**); 4 h (**B**); 8 h (**C**); 16 h (**D**); 20 h (**E**) and 24 h (**F**). Protein and NAD$^+$ concentrations were 0.75 mg/mL and 7.5 mM, respectively.
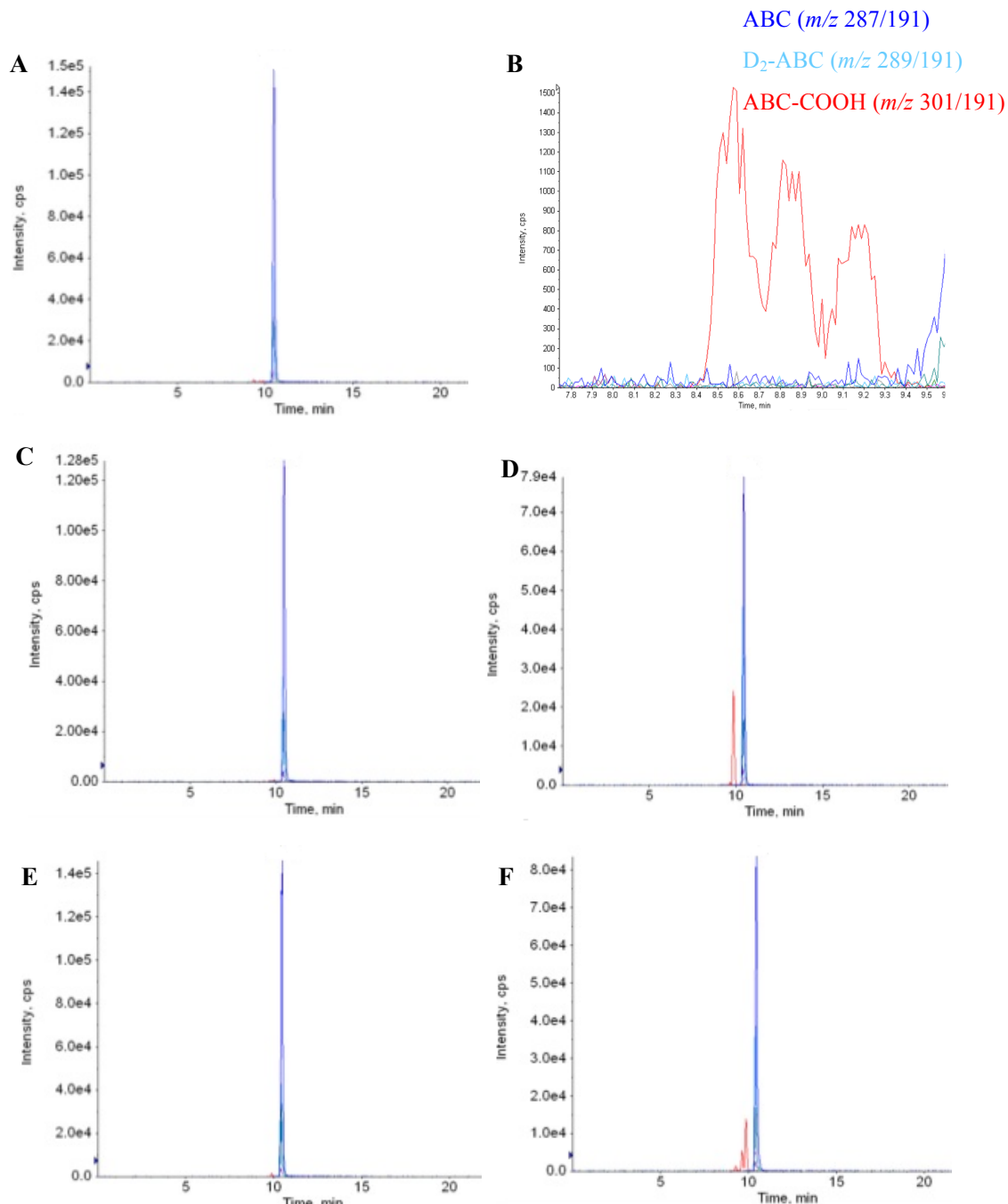
Figure S2A: MRM chromatograms representing experiments measuring COOH formation from ABC (10 μM) in human liver cytosol under a variety of compromised metabolic conditions: Without NAD (Experiment 1) (**A**); magnified image of the formation of 3 COOH isomers (Experiment 1) (**B**); with 4-MP (600 μM) and DSF (500 μM) (Experiment 2) (**C**); with NAD (Experiment 3) (**D**); with 4-MP (600 μM) (Experiment 5) (**E**); with DSF (500 μM) (Experiment 6) (**F**). Protein and NAD$^+$ concentrations were 0.75 mg/mL and 7.5 mM, respectively. Comparing experiments 3 (**D**) and 6 (**F**) there is a marked increase in the proportions of the lesser carboxylic acids **17b** and **17c**. Under the circumstances of ALDH inhibition, by DSF, when aldehyde oxidation might be catalysed principally by ADH1A, the selectivity of oxidation of the isomeric aldehydes is altered.

176

ABC (*m/z* 287/191)

D$_2$-ABC (*m/z* 289/191)

ABC-COOH (*m/z* 301/191)
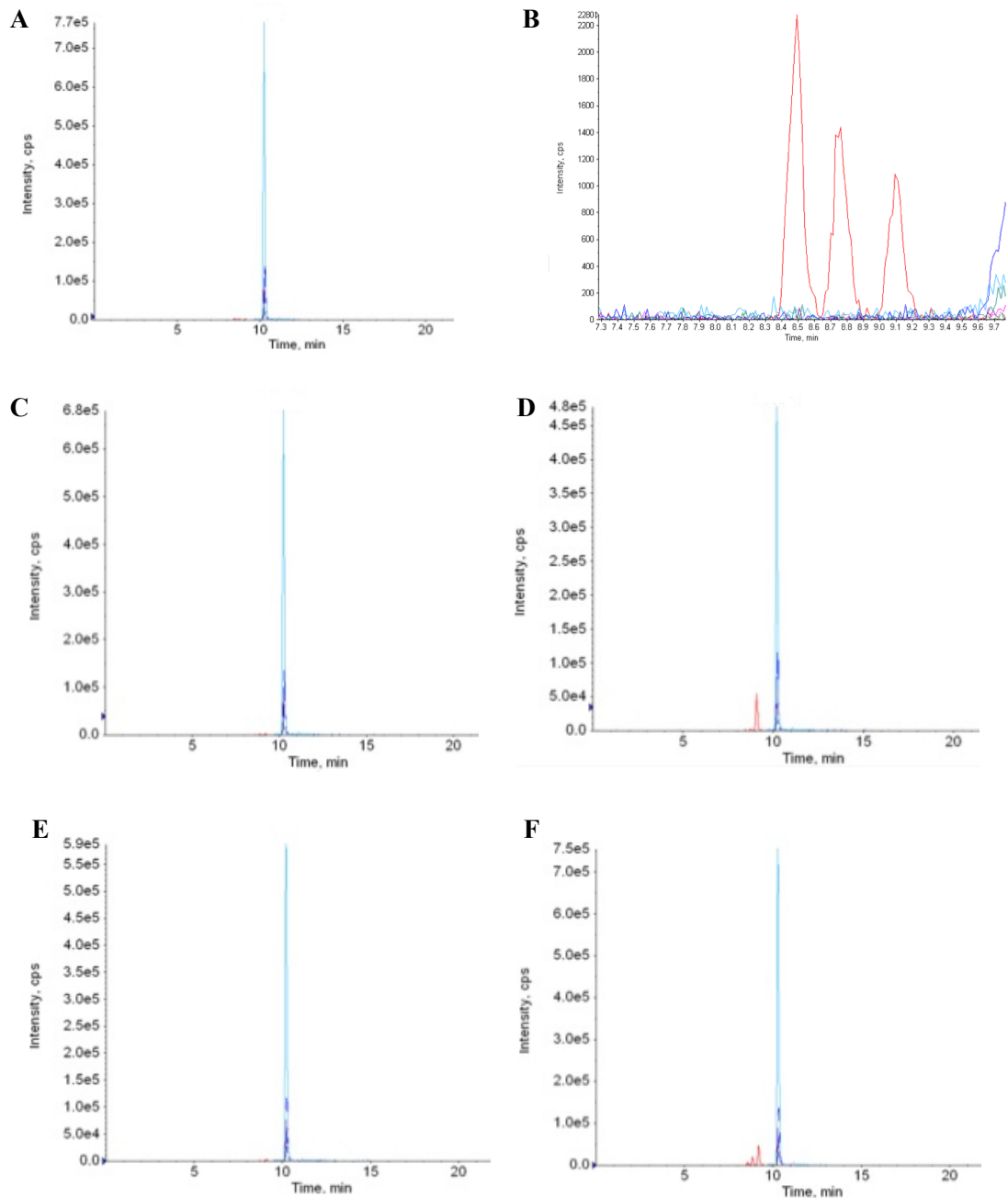
Figure S2B: MRM chromatograms representing experiments measuring COOH formation from D$_2$-ABC (10 μM) in human liver cytosol under a variety of compromised metabolic conditions: Without NAD (Experiment 1) (**A**); magnified image of the formation of 3 COOH isomers (Experiment 1) (**B**); with 4-MP (600 μM) and DSF (500 μM) (Experiment 2) (**C**); with NAD (Experiment 3) (**D**); with 4-MP (600 μM) (Experiment 5) (**E**); with DSF (500 μM) (Experiment 6) (**F**). Protein and NAD$^+$ concentrations were 0.75 mg/mL and 7.5 mM, respectively. Comparing experiments 3 (**D**) and 6 (**F**)

Figure S2B continued:

there is a marked increase in the proportions of the lesser carboxylic acids **17b** and **17c**. Under the circumstances of ALDH inhibition, by DSF, when aldehyde oxidation might be catalysed principally by ADH1A, the selectivity of oxidation of the isomeric aldehydes is altered.
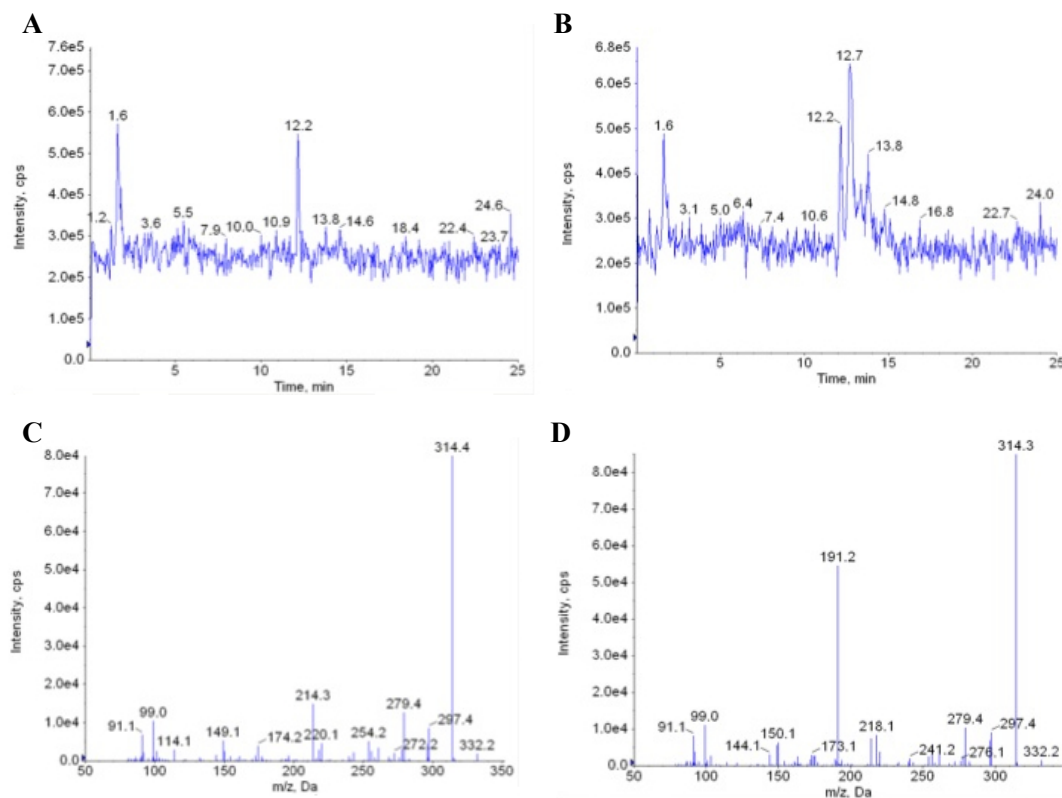
Figure S2C: EPI scans for fragments *m/z* 315 ([M+H]$^+$ for the oxime derivative of the D$_2$-ABC aldehyde intermediate) from experiments 4 (co-incubation with methoxylamine) and 7 (co-incubation with methoxylamine and DSF) for D$_2$-ABC (**A** and **B** respectively). The corresponding spectra are presented for experiments 4 and 7 (**C** and **D** respectively). The imine product **19b** (*m/z* 315) was not detected and the sample may have been contaminated with ABC, hence the detection of the precursor ion for **19a**. The slow dehydrogenation of D$_2$-ABC might have precluded production of detectable amounts of oxime **58**.

ABC (*m/z* 287/191)

D$_2$-ABC (*m/z* 289/191)

ABC-COOH (*m/z* 301/191)

A

B

C

D
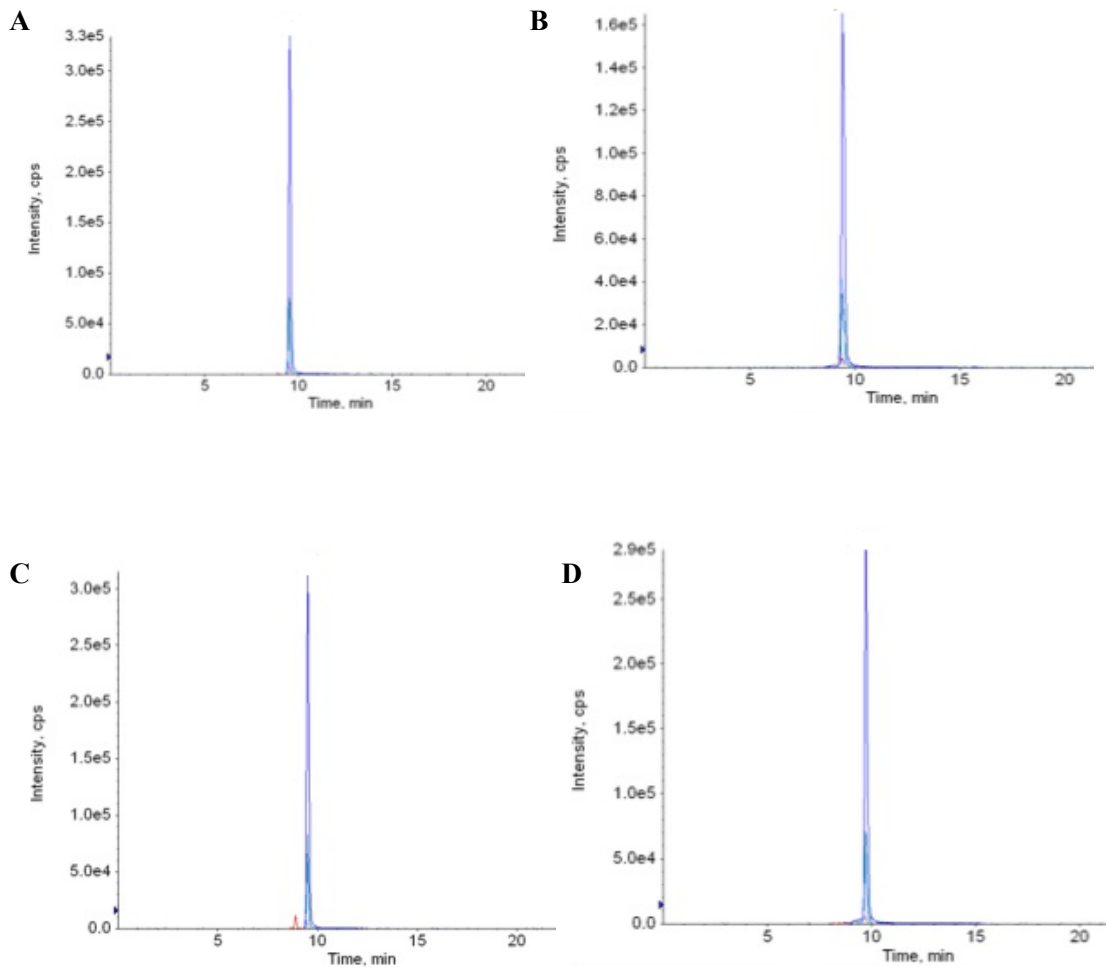
Figure S3A: MRM chromatograms obtained from the rate-substrate concentration experiments when ABC (10 μM) was incubated with human liver cytosol. Diagrams show representative chromatograms at the following concentrations and times: 500 μM at 0 min (**A**), 500 μM at 120 min (**B**), 20 mM at 0 min (**C**) and 20 mM at 120 min (**D**). Protein and NAD$^+$ concentrations were 0.75 mg/mL and 7.5 mM, respectively.

ABC (*m/z* 287/191)
D$_2$-ABC (*m/z* 289/191)
ABC-COOH (*m/z* 301/191)
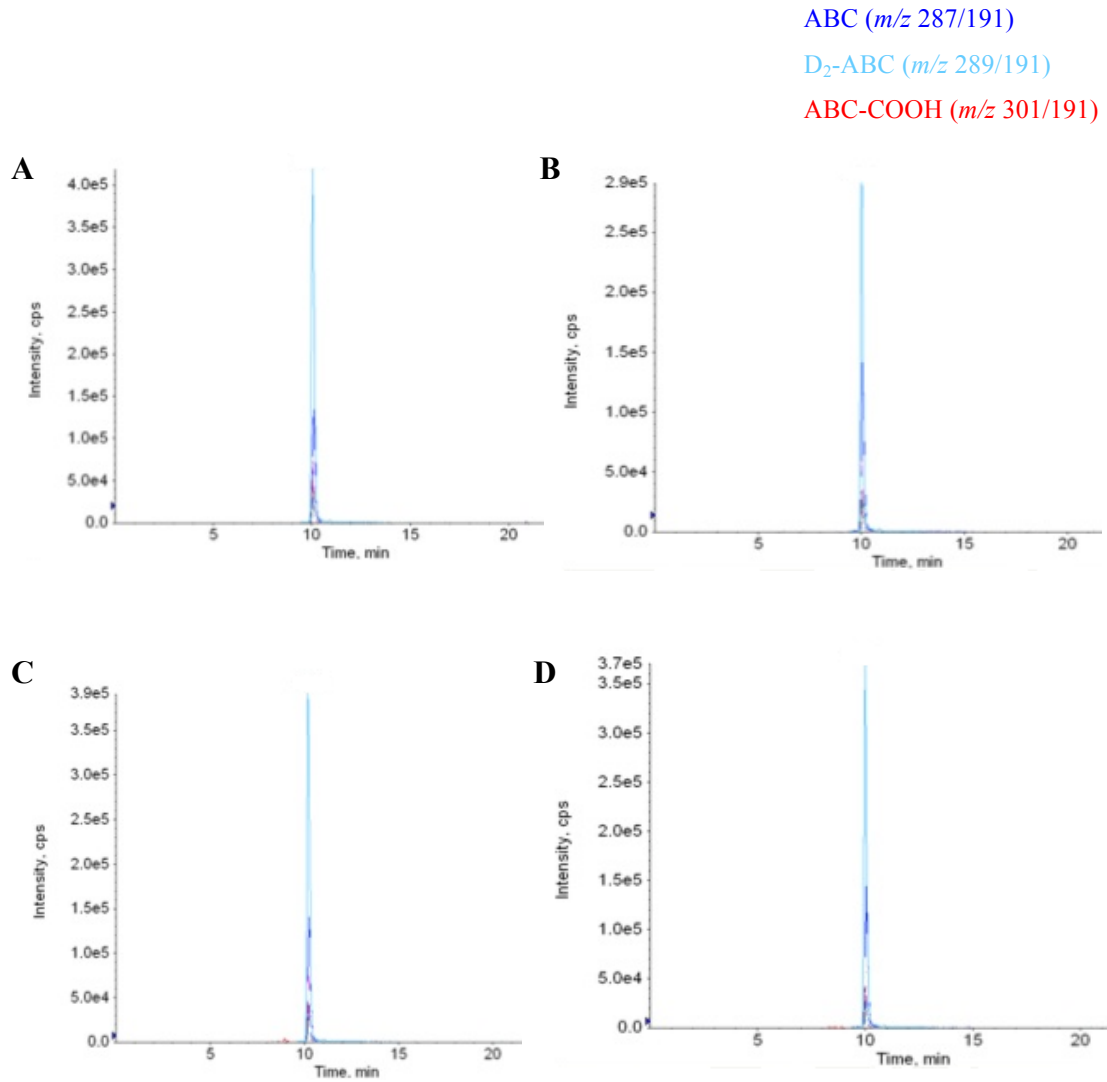
Figure S3B: MRM chromatograms obtained from the rate-substrate concentration experiments when D$_2$-ABC (10 μM) was incubated with human liver cytosol. Diagrams show representative chromatograms at the following concentrations and times: 500 μM at 0 min (**A**), 500 μM at 120 min (**B**), 20 mM at 0 min (**C**) and 20 mM at 120 min (**D**). Protein and NAD$^+$ concentrations were 0.75 mg/mL and 7.5 mM, respectively.

3.7 References

(1)   Masubuchi, N.; Makino, C.; Murayama, N. *Chem. Res. Toxicol.* **2007**, *20*, 455.

(2)   Srivastava, A.; Maggs, J. L.; Antoine, D. J.; Williams, D. P.; Smith, D. A.; Park, B. K. *Handb. Exp. Pharmacol.* **2010**, 165.

(3)   Sharma, A. M.; Uetrecht, J. *Drug Metab. Rev.* **2014**, *46*, 1.

(4)   Park, B. K.; Boobis, A.; Clarke, S.; Goldring, C. E. P.; Jones, D.; Kenna, J. G.; Lambert, C.; Laverty, H. G.; Naisbitt, D. J.; Nelson, S.; Nicoll-Griffith, D. A.; Obach, R. S.; Routledge, P.; Smith, D. A.; Tweedie, D. J.; Vermeulen, N.; Williams, D. P.; Wilson, I. D.; Baillie, T. A. *Nature Reviews Drug Discovery* **2011**, *10*, 292.

(5)   Walsh, J. S.; Reese, M. J.; Thurmond, L. M. *Chem. Biol. Interact.* **2002**, *142*, 135.

(6)   McDowell, J. A.; Chittick, G. E.; Ravitch, J. R.; Polk, R. E.; Kerkering, T. M.; Stein, D. S. *Antimicrob. Agents Chemother.* **1999**, *43*, 2855.

(7)   Mabic, S.; Castagnoli, N. *J. Med. Chem.* **1996**, *39*, 3694.

(8)   Ferraboschi, P.; Grisenti, P.; Santaniello, E. *Journal of Labelled Compounds & Radiopharmaceuticals* **1994**, *34*, 303.

(9)   Avery, M. A.; Bonk, J. D.; Mehrotra, S. *Journal of Labelled Compounds & Radiopharmaceuticals* **1996**, *38*, 249.

(10)   Charneira, C.; Godinho, A. L. A.; Conceicao Oliveira, M.; Pereira, S. A.; Monteiro, E. C.; Matilde Marques, M.; Antunes, A. M. M. *Chem. Res. Toxicol.* **2011**, *24*, 2129.

(11)   Bell, C. Thesis. Title: Characterisation of HLA-restricted T-cell responses to abacavir using lymphocytes from drug-naive volunteers, University of Liverpool, Liverpool, 2012.

(12)   Lee, S.-L.; Shih, H.-T.; Chi, Y.-C.; Li, Y.-P.; Yin, S.-J. *Chem. Biol. Interact.* **2011**, *191*, 26.

(13)   Brent, J. *N. Engl. J. Med.* **2009**, *360*, 2216.

(14)   Koppaka, V.; Thompson, D. C.; Chen, Y.; Ellermann, M.; Nicolaou, K. C.; Juvonen, R. O.; Petersen, D.; Deitrich, R. A.; Hurley, T. D.; Vasiliou, V. *Pharmacol. Rev.* **2012**, *64*, 520.

(15)   Tamai, H.; Yokoyama, A.; Okuyama, K.; Takahashi, H.; Maruyama, K.; Suzuki, Y.; Ishii, H. *Alcoholism-Clinical and Experimental Research* **2000**, *24*, 97S.

(16)   Shirota, F. N.; Demaster, E. G.; Nagasawa, H. T. *Toxicol. Lett.* **1987**, *37*, 7.

(17)   Nagasawa, H. T.; Demaster, E. G.; Redfern, B.; Shirota, F. N.; Goon, J. W. *J. Med. Chem.* **1990**, *33*, 3120.

(18)   DeMaster, E. G.; Redfern, B.; Nagasawa, H. T. *Biochem. Pharmacol.* **1998**, *55*, 2007.

(19)   Moore, S. A.; Baker, H. M.; Blythe, T. J.; Kitson, K. E.; Kitson, T. M.; Baker, E. N. *Structure with Folding & Design* **1998**, *6*, 1541.

(20)   Lipsky, J. J.; Shen, M. L.; Naylor, S. *Chem. Biol. Interact.* **2001**, *130*, 93.

(21)   Mays, D. C.; Nelson, A. N.; LamHolt, J.; Fauq, A. H.; Lipsky, J. J. *Alcoholism-Clinical and Experimental Research* **1996**, *20*, 595.

(22)   Mays, D. C.; Ortiz-Bermudez, P.; Lam, J. P.; Tong, I. H.; Fauq, A. H.; Lipsky, J. J. *Biochem. Pharmacol.* **1998**, *55*, 1099.

(23)   Pike, M. G.; Mays, D. C.; Macomber, D. W.; Lipsky, J. J. *Drug Metab. Disposition* **2001**, *29*, 127.

(24)   Bell, R. P. *Chem. Soc. Rev.* **1974**, *3*, 513.

(25)   Kushner, D. J.; Baker, A.; Dunstall, T. G. *Can. J. Physiol. Pharmacol.* **1999**, *77*, 79.

(26)   Cavalieri, E.; Garcia, H.; Mailander, P.; Patil, K. *Chem. Biol. Interact.* **1975**, *11*, 179.

(27)   Foster, A. B. *Trends Pharmacol. Sci.* **1984**, *5*, 524.

(28)   Nelson, S. D.; Trager, W. F. *Drug Metab. Disposition* **2003**, *31*, 1481.

(29)   Patanella, J. E.; Walsh, J. S. *Drug Metab. Disposition* **1992**, *20*, 912.

(30)   Bell, C. C.; Castelazo, A. S.; Yang, E. L.; Maggs, J. L.; Jeankins, R. E.; Tugwood, J.; O'Neill, P. M.; Naisbitt, D. J.; Park, B. K. *Chem. Res. Toxicol.* **2013**, *26*, 1064.

(31)   Lenz, D.; Juebner, M.; Bender, K.; Wintermeyer, A.; Beike, J.; Rothschild, M. A.; Kaeferstein, H. *Naunyn. Schmiedebergs Arch. Pharmacol.* **2011**, *383*, 647.

(32)   Jelski, W.; Zalewski, B.; Szmitkowski, M. *Dig. Dis. Sci.* **2008**, *53*, 2550.

(33)   Maeda, M.; Hasumura, Y.; Takeuchi, J. *Lab. Invest.* **1988**, *59*, 75.

(34)   Wang, M.-F.; Han, C.-L.; Yin, S.-J. *Chem. Biol. Interact.* **2009**, *178*, 36.

(35)   Xie, P. G. T.; Hurley, T. D. *Protein Sci.* **1999**, *8*, 2639.

(36)   Chessman, D.; Kostenko, L.; Lethborg, T.; Purcell, A. W.; Williamson, N. A.; Chen, Z.; Kjer-Nielsen, L.; Mifsud, N. A.; Tait, B. D.; Holdsworth, R.; Almeida, C. A.; Nolan, D.; Macdonald, W. A.; Archbold, J. K.; Kellerher, A. D.; Marriott, D.; Mallal, S.; Bharadwaj, M.; Rossjohn, J.; McCluskey, J. *Immunity* **2008**, *28*, 822.

(37)   Bell, C. C.; Faulkner, L.; Martinsson, K.; Farrell, J.; Alfirevic, A.; Tugwood, J.; Pirmohamed, M.; Naisbitt, D. J.; Park, B. K. *Chem. Res. Toxicol.* **2013**, *26*, 759.

(38)   Berridge, M. V.; Herst, P. M.; Tan, A. S. *Biotechnol. Ann. Rev.* **2005**, *11*, 127.

(39)   Riss TL, M. R., Niles AL, Benink HA, Worzella TJ and Minor L In *Assay Guidance Manual [Internet]. Bethesda (MD): Eli Lilly and Company and the National Center for Advancing Translational Sciences; 2004-2013.*; In: Sittampalam GS, G.-E. N., Arkin M, Auld D, Austin C, Bejcek B, Glicksman M, Inglese J, Lemmon V, Li Z, McGee J, McManus O, Minor L, Napper A, Riss T, Trask OJ and Weidner J, eds., Ed. 2001.

(40)   Gyuris, A.; Szlavik, L.; Minarovits, J.; Vasas, A.; Molnar, J.; Hohmann, J. *In Vivo* **2009**, *23*, 429.

(41)   Cihlar, T.; Birkus, G.; Greenwalt, D. E.; Hitchcock, M. J. M. *Antiviral Res.* **2002**, *54*, 37.

(42)   Melroy, J.; Nair, V. *Curr. Pharm. Des.* **2005**, *11*, 3847.

(43)   Gu, Z.; Allard, B.; de Muys, J. M.; Lippens, J.; Rando, R. F.; Nguyen-Ba, N.; Ren, C.; McKenna, P.; Taylor, D. L.; Bethell, R. C. *Antimicrob. Agents Chemother.* **2006**, *50*, 625.

(44)   Faletto, M. B.; Miller, W. H.; Garvey, E. P.; Clair, M. H. S.; Daluge, S. M.; Good, S. S. *Antimicrob. Agents Chemother.* **1997**, *41*, 1099.

(45)   Pizzocolo, C.; Castagna, A.; Lazzarin, A. *Future Virology* **2011**, *6*, 571.

(46)   Barratt, M. J.; Frail, D. *Drug repositioning [electronic book]: Bringing New Life to Shelved Assets and Existing Drugs / edited by Michael J. Barratt, Donald E. Frail*; Hoboken : John Wiley & Sons, c.2012, 2012.

(47)   Charneira, C.; Grilo, N. M.; Pereira, S. A.; Godinho, A. L. A.; Monteiro, E. C.; Marques, M. M.; Antunes, A. M. M. *Br. J. Pharmacol.* **2012**, *167*, 1353.

(48)   Giorgini, S.; Martinelli, C.; Tognetti, L.; Carocci, A.; Giuntini, R.; Mastronardi, V.; Torricellio, F.; Leoncini, F.; Lotti, T. *Dermatologic Therapy* **2011**, *24*, 591.

(49)   Stringer, R. A.; Williams, G.; Picard, F.; Sohal, B.; Kretz, O.; McKenna, J.; Krauser, J. *Drug Metab. Disposition* **2014**, *42*.

(50)   Alfirevic, A.; Gonzalez-Galarza, F.; Bell, C.; Martinsson, K.; Platt, V.; Bretland, G.; Evely, J.; Lichtenfels, M.; Cederbrant, K.; French, N.; Naisbitt, D.; Park, B. K.; Jones, A. R.; Pirmohamed, M. *Genome Medicine* **2012**, *4*, 51.

(51)   Wu, Y.; Farrell, J.; Pirmohmed, M.; Park, B. K.; Naisbitt, D. J. *J. Allergy Clin. Immunol.* **2007**, *119*, 973.

(52)   Selvam, P.; Murugesh, N.; Chandramohan, M.; Pannecouque, C.; De Clercq, E. *Indian Journal of Pharmaceutical Sciences* **2010**, *72*, 806.

CHAPTER 4

Using Asymmetric Synthetic Methods to Synthesise Analogues of Abacavir

CHAPTER 4

Using Asymmetric Synthetic Methods to Synthesise Analogues of Abacavir

4.1 Introduction

4.1.1 Synthesis of ABC.

The total and formal synthesis of ABC and its precursors has been well studied with all established routes using methods discussed in Chapter 1. The application of three of these syntheses is discussed herein.

4.1.1.1 Synthesis from Vince lactam and heterocycle construction.

Daluge *et al*. reported the first large-scale synthesis of ABC in 2000,[1] shortly after its initial release onto the market. The large-scale route was initiated with Vince lactam **28** (Scheme **4.1**).[1,2] This forms the basic structure of the stereoselective cyclopentenyl moiety of the final carbocyclic nucleoside. The bicyclic system underwent ring opening by water, reduction and work-up to provide the amino-alcohol cyclopentenyl **29**. Compound **29** was subsequently *N*-Boc protected to form compound **59**. 2,5-Diamino-4,6-dihydroxypyrimidine, compound **60**, underwent chlorination using Vilsmeier reagent to form compound **61**, which was subjected to acidic hydrolysis, neutralisation and precipitation to form **62**. Amide formation (compound **63**), was achieved through hydrolysis of **62** using phosphate buffer, ensuring the pH was below 4 to prevent the formation of unwanted *N,N*-dimethylamine pyrimidine by-products. The following steps: Addition of the chloro pyrimidine intermediate **63** to **59**, followed by ring closure of the pyrimidine formed the purine base and finally nucleophilic substitution of 6-Cl with cyclopropylamine yielded ABC. This route has also been shown to be effective on a research scale.[1]
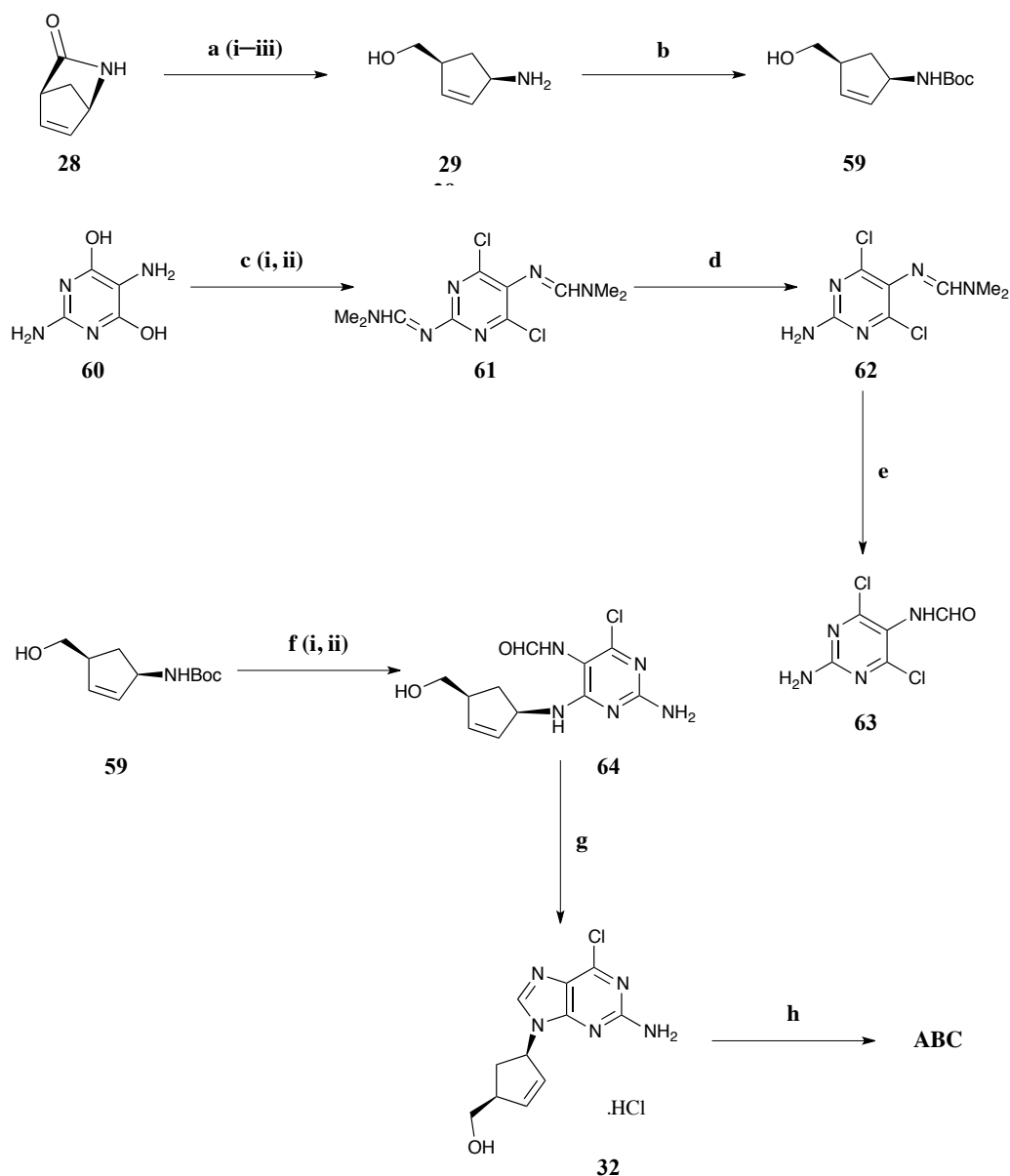
Scheme 4.1: Reagents and conditions: a) i) MsOH hydrated, H$_2$O, THF, 60 °C, 3 h, 97%; ii) LiAlH$_4$, THF; iii) NaF, 30 min, H$_2$O, 90%; b) Boc$_2$O, DMAP, THF, quant.; c) i) [Me$_2$NCHCl$^+$]Cl, CHCl$_3$, reflux, 2 days; ii) 5 N NaOH to pH 7, 81–92%; d) Conc. HCl, EtOH−H$_2$O, 55 °C, 30 min, 95%; e) Phosphate buffer, pH 3.2, reflux, 4 h, 72%; f) i) Conc. HCl, EtOH, reflux, 90 min; ii) **63**, 84–88%; g) TEOF, conc. HCl, 85–92%; h) Cyclopropylamine, EtOH, reflux, 3 h, 70–90%.

Vince & Hua have developed a slightly modified route, although still utilising the linear construction route of the purinic base after coupling with Vince lactam **28** (Scheme **4.2**).[3] Vince lactam, as demonstrated by Evans *et al.*,[4] can be prepared from

toluene-*p*-sulfonyl cyanide and cyclopentadiene to form racemic Vince lactam **27**. Resolution of this racemic compound was achieved using *Pseudomonas solanacearum* to give the unreacted chiral lactam and the ring opened product, an amino acid.[4] However, lactam **28** is also commercially available in its desired chiral form.

Vince lactam **28** underwent a series of reactions: Hydrolysis, amine protection, reduction and finally alcohol protection to yield di-protected intermediate **65**. Following this, **29** was coupled with 5-amino-4,6-dichloropyrimidine to yield **66**. As discussed in Chapter 1, Section **1.9.2.2**, an amine group is incorporated at the 2-position of **66** *via* diazonium cation formation, using *p*-chloroaniline, hydrochloric acid (HCl) and sodium nitrite (NaNO$_2$). This was followed by reduction using Zn/AcOH to form compound **31**. TEOF/catalytic (cat.) H$^+$ forms the imidazole ring (compound **32**) and substitution of 6-Cl with cyclopropylamine yields ABC in 14% yield over 10 steps.
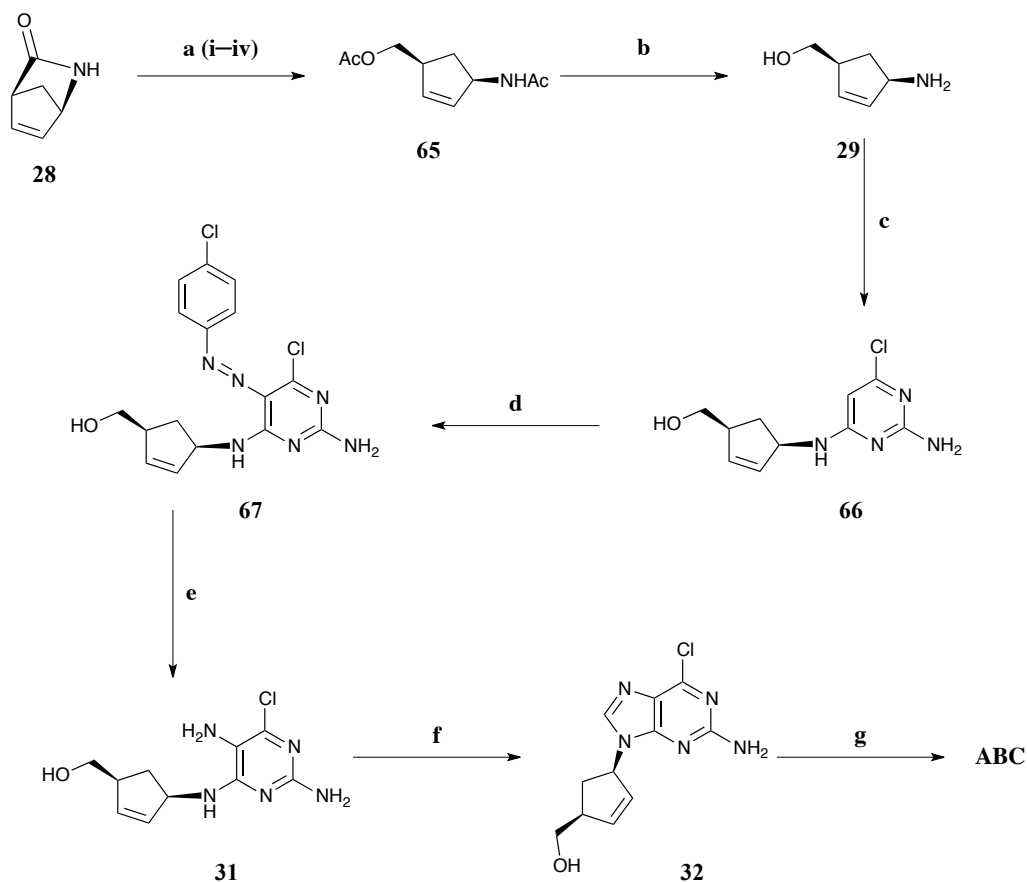
Scheme 4.2: Reagents and conditions: a) i) 1 N HCl, reflux, 1 h, 88%; ii) Ac$_2$O, pyridine, r.t., o/n, 83%; iii) NaBH$_4$, CaCl$_2$, THF, r.t., 18 h; iv) Ac$_2$O, pyridine, r.t., o/n, 73%; b) 0.5 N Ba(OH)$_2$, reflux, o/n; c) 2-Amino-4,6-dichloropyrimidine, NEt$_3$, *n*-BuOH, reflux, 48 h, 76%; d) *p*-Chloroaniline, 3 N HCl, NaNO$_2$, AcOH, NaOAc.3H$_2$O, r.t., o/n, 94%; e) Zn, AcOH, H$_2$O, EtOH, reflux, 3 h, 66%; f) TEOF, 12 N HCl, r.t., o/n, 80%; g) Cyclopropylamine, EtOH, 55 °C, 25 h, 68%.

4.1.1.2 Pd^0 mediated allylic substitution of purinic base and cyclopentyl carbocycle.

Crimmins and co-workers described an efficient asymmetric synthesis of both CBV and ABC (Scheme **4.3**):[5,6] A synthesis that has been utilised by other researchers in the formation of carbocyclic analogues.[7,8]
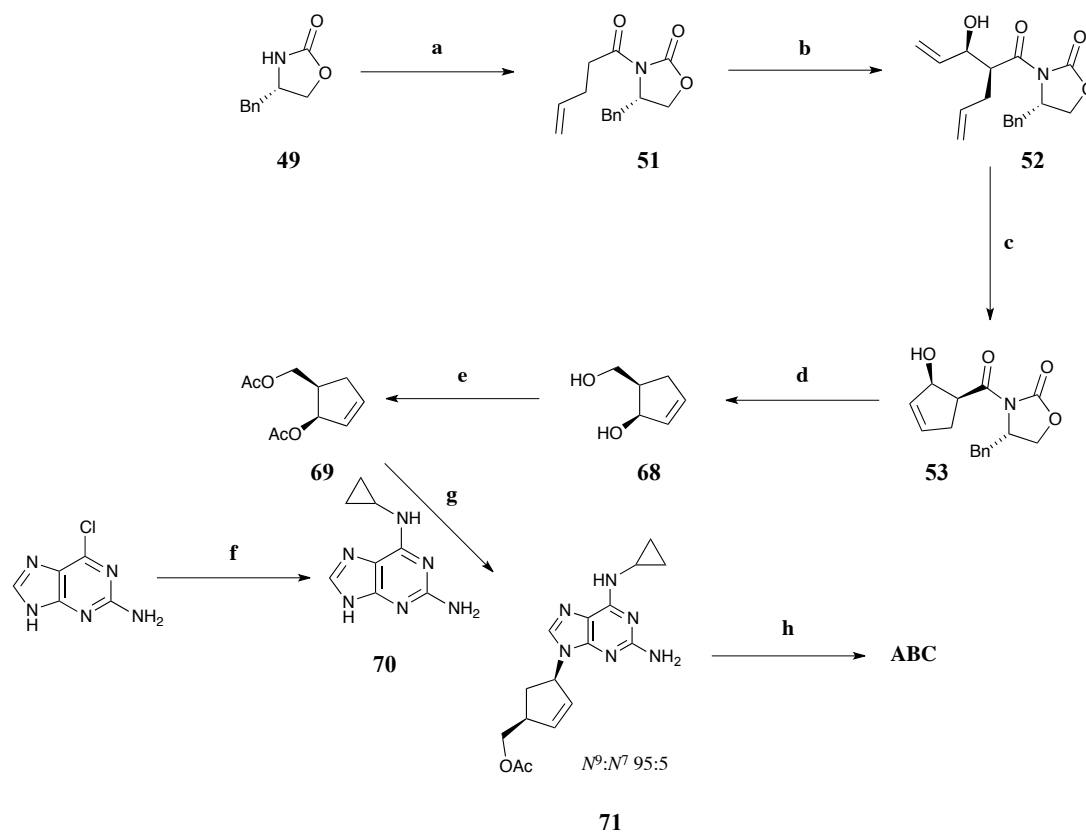
Scheme 4.3: Reagents and conditions: a) *n*-BuLi, 4-pentenoic acid, NEt$_3$, pivaloyl chloride, THF, −78 °C → 0 °C, 2 h, 99%; b) TiCl$_4$, (−)-sparteine, DCM, acrolein, −78 °C → 0 °C, 1 h, 82%; c) Benzylidine(bistricyclohexylphosphine)ruthenium(II) chloride, DCM, r.t., 30 min, 97%; d) LiBH$_4$, MeOH, THF, 0 °C, 1 h, 78%; e) Ac$_2$O, NEt$_3$, DMAP, DCM, 0 °C, 2 h, 90%; f) Cyclopropylamine, DMSO, 55 °C, 16 h; g) NaH, **70**, Pd(PPh$_3$)$_4$, 1:1 THF−DMSO, 45 °C, 65%; h) NaOH, H$_2$O, r.t., o/n, 81%.

As an alternative method to using cyclopentadiene as the initial material and introducing asymmetry *via* enzymatic or chiral ligand methods, a chiral oxazolidinone **49** was used with Grubbs mediated RCM to form the cyclopentyl carbocyclic moiety. Acylation of **49** with 4-pentenoic acid and pivaloyl chloride anhydride afforded intermediate **51**, which underwent an asymmetric syn aldol addition with acrolein along with titanium tetrachloride (TiCl$_4$) and (−)-spartenine determining the relative stereochemistry. RCM with 1st generation Grubbs catalyst

followed by reduction with LiBH$_4$ yielded diol **68**. Di-protection of this diol yields intermediate **69** and Crimmins and co-workers used established Trost Pd^0 allylic substitution methods to couple this carbocycle with 2-amino-6-(cyclopropylamino)purine **70** (Figure **4.1**). Removal of the acetyl group was achieved using NaOH to yield ABC. Compound **69** was coupled with **70**, rather than 2-amino-6-chloropurine, to maximise the N^9:N^7 ratio from 85:15 to 95:5. Synthesising ABC in this manner allows for carbocyclic modifications.
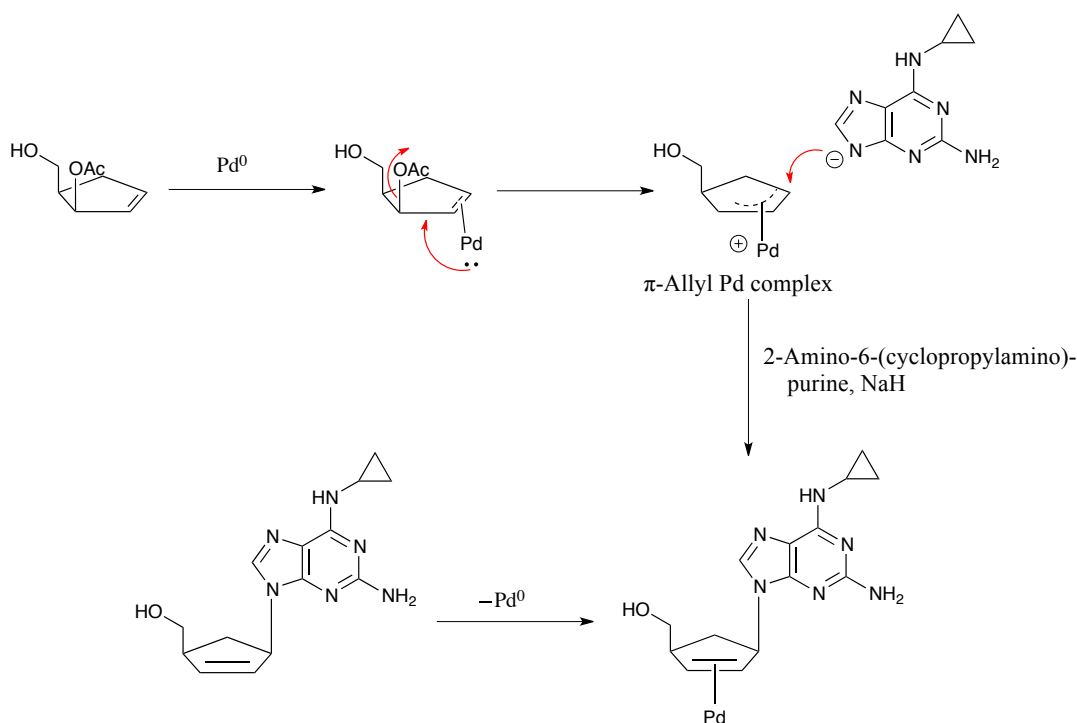
Figure 4.1: Mechanism depicting the coupling of di-protected diol **69** with 2-amino-6-(cyclopropylamino)purine **70** using Trost Pd^0 allylic substitution: Pd coordinates with the double bond of the allylic acetate and this occurs on the less hindered face. The acetate (leaving group) is lost and the π-allyl Pd complex is formed. The nucleophile (deprotonated 2-amino-6-(cyclopropylamino)purine will then attack from the less hindered face and Pd will become uncoordinated. The net result is retention of configuration.

Crimmins *et al*. have also reported a solid-phase synthesis of ABC, using a Pd-catalysed allylic coupling of a resin-bound carbocyclic sugar with a purine base.[9]

4.1.1.3 Enzymatic resolution and [2+2] cycloaddition.

The final route to be discussed is a recent enantioselective synthesis of ABC (Scheme **4.4**). Unlike the other methods previously mentioned, cyclopentadiene is used as the starting material. A hetero Diels–Alder [2+2] cycloaddition of cyclopentadiene with chlorosulfonyl isocyanate (CSI) followed by isomeric resolution using Lipase B[10] formed the correct bi-lactam intermediate **72**. Lipase B (also widely known as Lipolase from *Candida antarctica*) resolves racemic β-lactams through hydrolysis. The racemic mixture is hydrolysed in H_2O (1 equiv) and diisopropyl ether at 60 °C to form the β-amino acid product and the unreacted β-lactam.[11] These compounds are then easily separated.

Chiral **72** underwent amine protection using a highly electron withdrawing group: 4-methylbenzenesulfonic anhydride. Coupling of **73** with 2,6-dichloropurine was achieved using either $Pd_2(dba)_3$ or $Pd(OAc)_2$ with phosphorus-based ligand $P(i\text{-}OPr)_3$ and high $N^9:N^7$ regioselectivity was achieved. This mechanism is likely to occur *via* a π-allyl Pd coupling using the tosylate (Ts) group to stabilise the charge during ring opening. Following *N*-methylation of **74** and subsequent reduction and nucleophilic aromatic substitution with cyclopropylamine yielded **76**. Addition of the 2-amino group was achieved using 4-methoxybenzylamine and the *p*-methoxybenzyl ether group was removed using trifluoroacetic acid (TFA). All steps were high yielding (>70%). The synthesis was achieved in 24% yield over 9 steps. Bi-lactam **72** would serve as a key starting material for a wide range of ABC analogues.
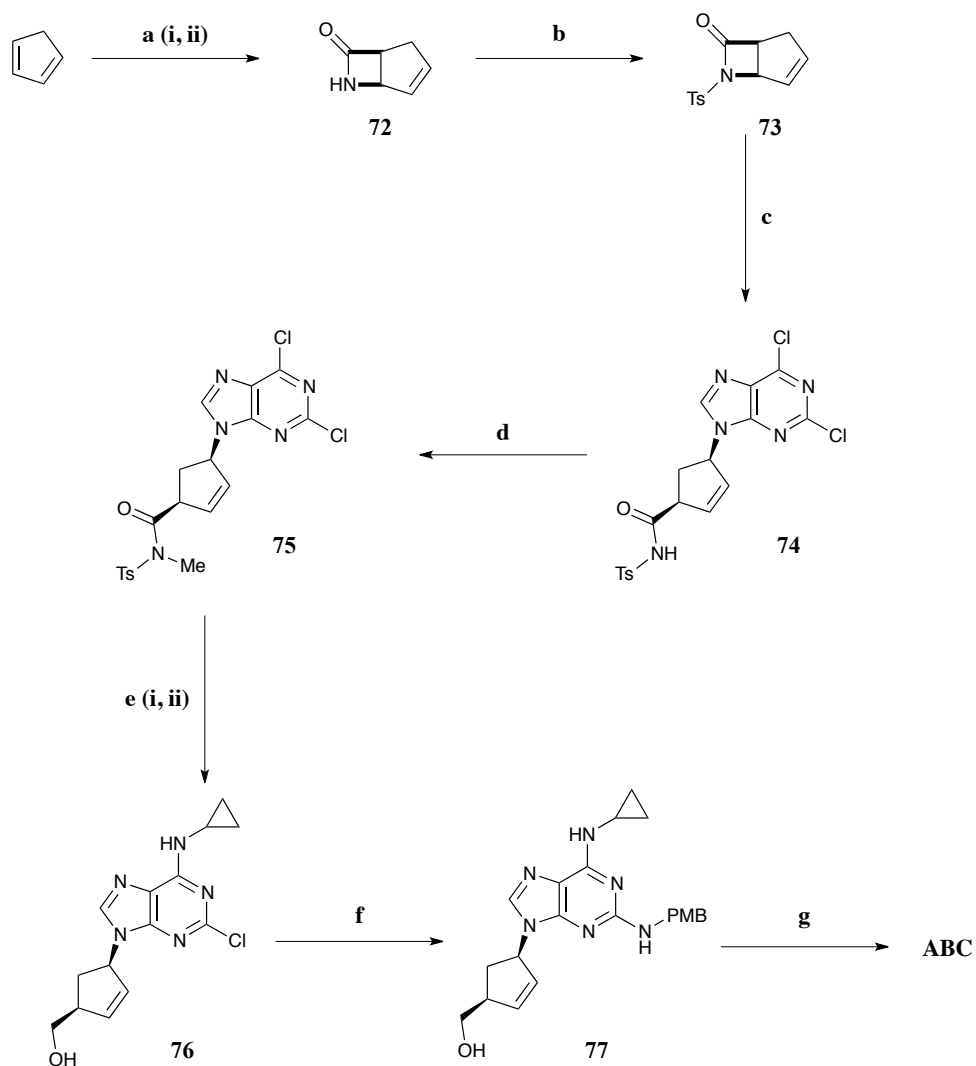
Scheme 4.4: a) i) CSI ii) Lipase B;[10] b) 4-Methylbenzenesulfonic anhydride, NEt₃, DMAP, DCM, r.t., 48 h, 75–81%; c) 2,6-Dichloropurine, tetrabutylammonium salt, Pd₂(dba)₃, P(*i*-OPr)₃, THF, r.t., 90 min, 75% d) PPh₃, DIAD, MeOH, 1:1 DCM–THF, r.t., 30 min, 94%; e) i) NaBH₄, *i*-PrOH, THF, 0 °C to r.t., 3 h, 86%; ii) Cyclopropylamine, EtOH, 50 °C, 5 h, 73%; f) 4-Methoxybenzylamine, DMSO, 150 °C, 16 h, 90%; g) TFA, reflux, 72 h, 73%. CSI, chlorosulfonyl isocyanate; DIAD, diisopropyl azodicarboxylate.

4.1.2 ABC analogue synthesis.

A range of ABC analogues have been synthesised from a variety of synthetic routes, often using the pathways discussed within this chapter and Chapter 1, Section **1.9**. Synthesis of analogues for ABC has been of interest to reduce associated toxicological issues, to modulate lipophilicity and anti-HIV activity. Modifications of the cyclopentyl moieties are often the most common structure alterations in the synthesis of such analogues; a selection of previously synthesised analogues is discussed below.

Crimmins and co-workers synthesised (–)-2'-methyl ABC using a slight variation of their established synthesis (see Scheme **4.3**).[5] The usual addition of acrolein at step 2 of this synthesis is altered with the addition of methylacrolein. The result of this is a methyl substituent at the 2'-position (Figure **4.2 A**), eventually yielding the required analogue.

Other modified total synthetic routes to produce analogues of ABC include the synthesis of; 5'-*homo*-ABC from a bicyclic α-hydroxy lactone intermediate (Figure **4.2 B**);[12] racemic nor-ABC from a cyclopentene epoxide starting material (Figure **4.2 C**);[13] 3'-methyl-ABC from [(1S,4S)-4-hydroxy-2-methylcyclopent-2-enyl]methyl acetate (Figure **4.2 D**)[14] and 5'-*homo*-dihydroxy-ABC from cyclopentadiene (Figure **4.2 E**).[15] Although there is little literature precedent for the synthesis of analogues from direct ABC modification, one example, using microwave-assisted reactions to produce N^2 analogues is reported (Figure **4.2 F**).[16]
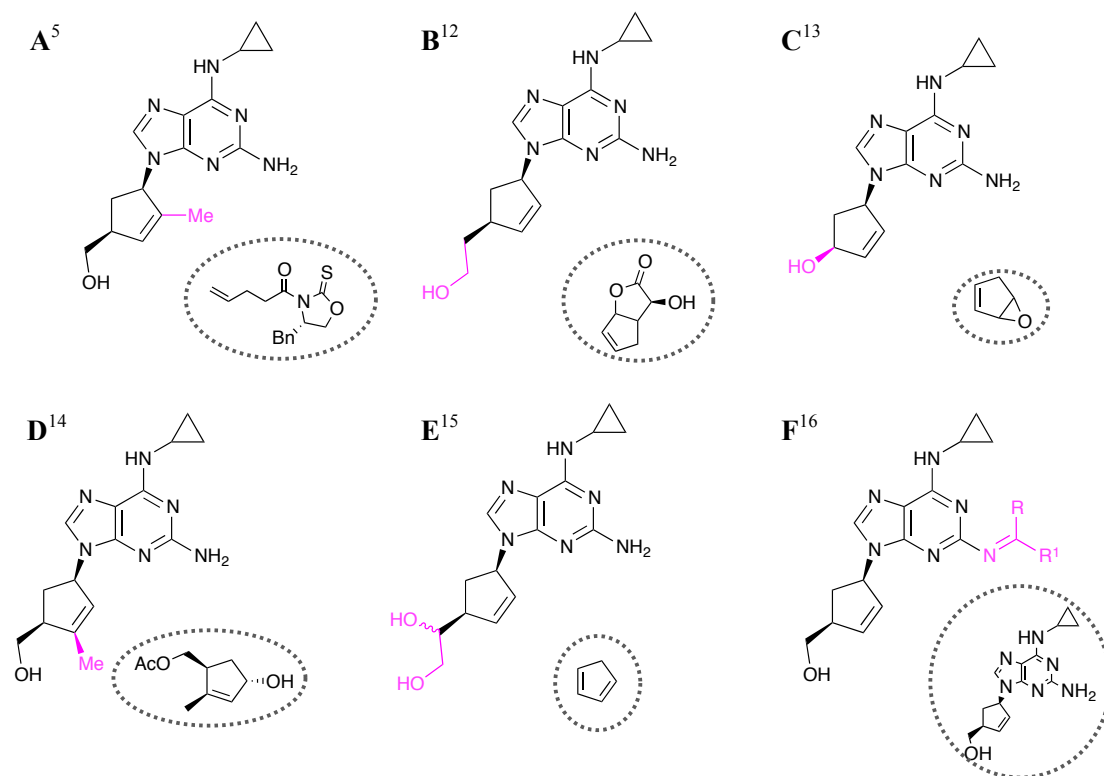
Figure 4.2: Series of ABC analogues synthesised *via* total synthetic routes (**A–E**) or through direct ABC modification (**F**). Their corresponding starting materials are shown within the dotted circles.

There are well-established routes to synthesise ABC and a number of its analogues. These routes will be utilised to synthesise analogues of ABC and such compounds will be used to probe mechanisms of ABC toxicity.

4.2 Aims

- To synthesise a range of 5'-OH and alkene analogues of ABC to block metabolism

- To synthesise N^2 analogues to block its metabolism and to disrupt binding within HLA-B*57:01

- To synthesise the enantiomer of ABC and to test this enantiomer in ABC-positive HLA-B*57:01 T-cells to probe its toxicity

- To develop a synthetic route to form intermediates for use within ABC analogue synthesis.

4.3 Results & Discussion

The following section describes the design and synthesis of a range of ABC analogues that can and have been used to probe its ABC-associated immune-mediated toxicity.

4.3.1 Design and synthesis of 5'-OH analogues to block *O*-oxidation.

As initially proposed by Walsh *et al.*,[17] the oxidation of the primary alcohol of ABC to its aldehyde (Figure **4.3 A**) could potentially contribute to its toxicity. Blocking this oxidation pathway would reduce ABC bioactivation through prevention of aldehyde formation (Figure **4.3 B**).
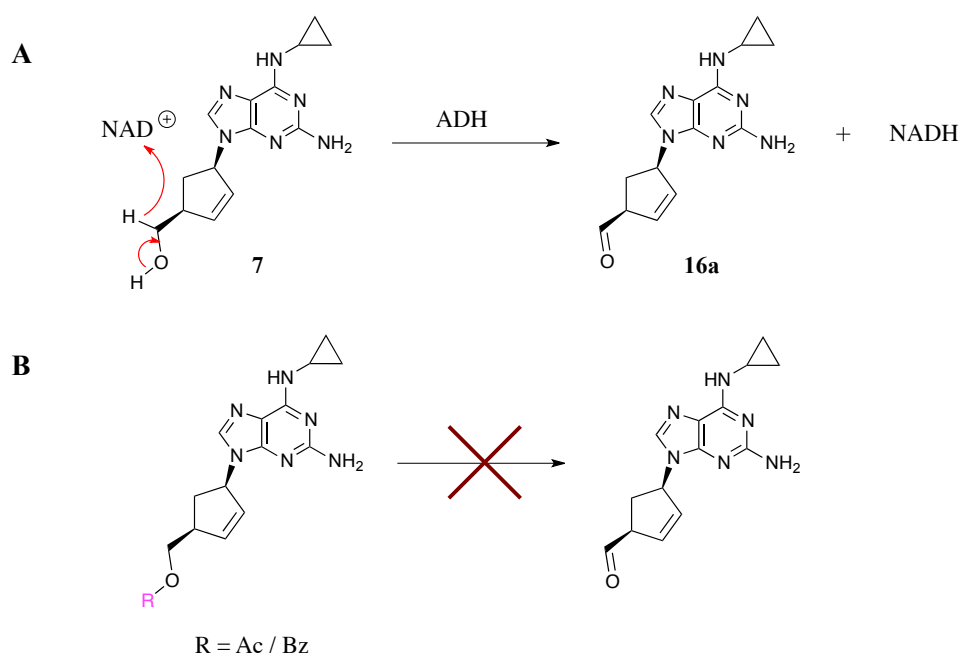
Figure 4.3: Oxidation of ABC **7** to its corresponding aldehyde **16a** by ADH and co-factor NAD$^+$ (**A**). Aldehyde formation can be prevented through blocking the 5'-OH group with an ester moiety (**B**).

Acetylation of the primary alcohol appeared to be the most logical route (Scheme **4.5**). This was attempted using a variety of reagents.
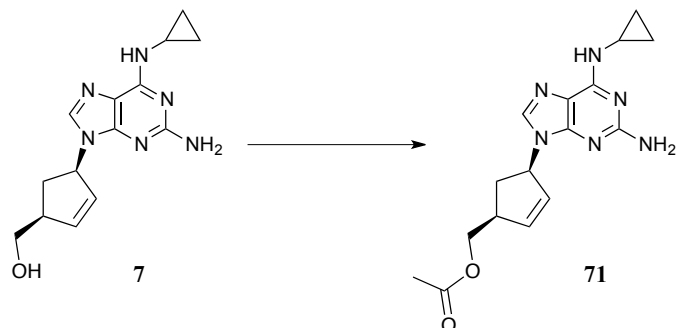
Scheme 4.5: Reagents and conditions: Ac$_2$O (1.3 equiv), NEt$_3$ (1.2 equiv), DCM, 0 °C, 4 h, 69%.

Initially, the method of acetylation using acetyl chloride (AcCl) and pyridine was employed, but this led to the formation of several side products and the desired product was difficult to obtain. The formation of side products was likely to stem from the nucleophilic amine groups at positions 2 and 6 on ABC. Following this, reaction of ABC with benzoyl chloride (BzCl) and pyridine was attempted but similar problems were encountered, with the formation of side products and little product formation. Finally, a successful method was found using Ac$_2$O and NEt$_3$. This yielded the desired product **71**, in a 69% yield.

The loss and/or replacement of the 5'-OH functional group would also prevent oxidation at this position. Without synthesising ABC itself, it would have been difficult to directly replace the hydroxyl group from the parent drug. Primary alcohols often undergo functional group interconversion to halides, carboxylic acids, esters and ethers but many of these groups would be unsuitable due to maintaining

oxidation ability and/or nucleophilicity. It was therefore decided to synthesise compound **78** using XtalFluor-E® (Scheme **4.6**). XtalFluor-E® is a deoxyfluorinating reagent that is relatively easy to handle and has improved air stability compared with other fluorinating reagents such as diethylaminosulfur trifluoride,[18] where toxic hydrogen fluoride is a side product.
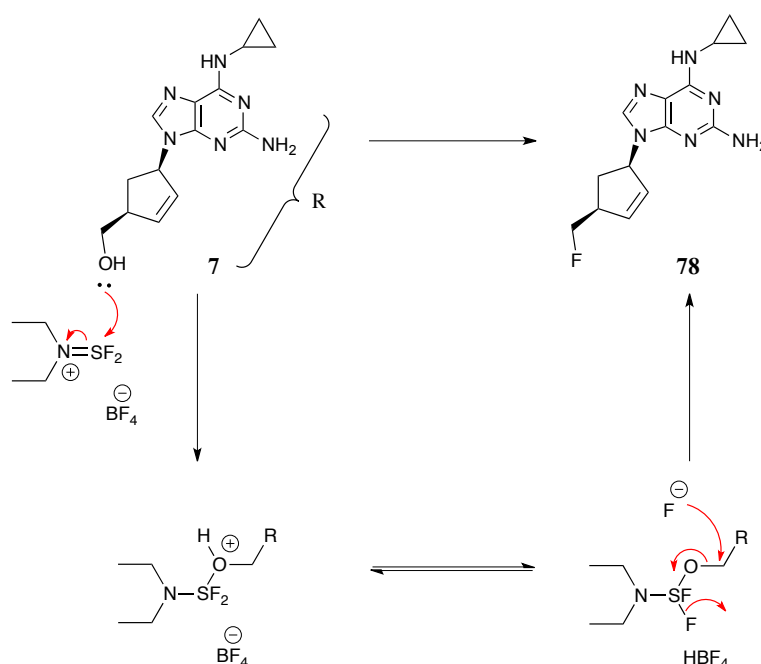
Scheme 4.6: The 5'-OH present within ABC can be substituted with fluorine using XtalFluor-E® reagent. The mechanism for this reaction is shown. Reagents and conditions: XtalFluor-E® (1.4 equiv), NEt$_3$.3HF (2.2 equiv), reflux, 3 h, 3%.

The reaction conditions, XtalFluor-E® (1.5 equiv) with DBU (1.5 equiv) were initially used. No desired product was obtained from this reaction, and after further research on the reagent, triethylamine trihydrofluoride (NEt$_3$.3HF) in replacement of DBU was used, as demonstrated by L'Heureux *et al*.[19] Overall, this improved the

reaction and although very low yields were achieved, enough of compound **78** was obtained for future immunological testing.

4.3.2 N^2 analogues to block *N*-oxidation.

Extending the focus beyond 5'-OH analogues, analogues preventing *N*-oxidation were also considered. These analogues mainly consisted of small functional groups so to limit any considerable disruption of binding with the HLA molecule. Acylation was chosen as the main method of formation of these analogues (Figure **4.4**).

R^1 = TBDMS/TMS

R^2 = Ac / Bz / Boc / Fmoc / CO*i*-Pr
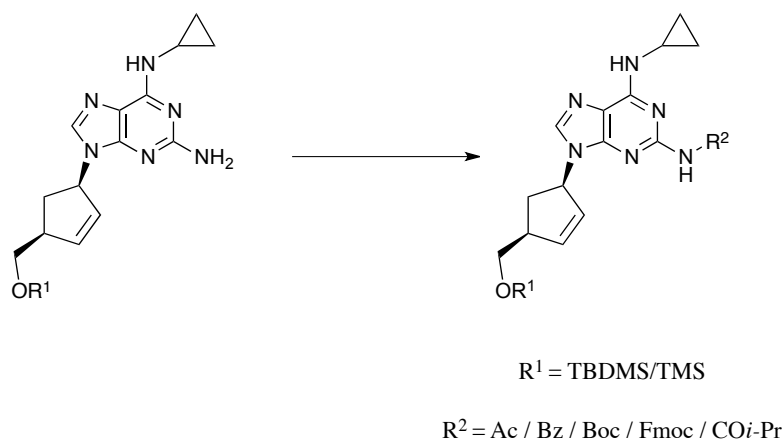
Figure 4.4: Attempted reactions of N^2 protection using several different reagents: AcCl, Ac$_2$O, BzCl, Boc, Fmoc, pivaloyl chloride (1.2–2.0 equiv). All attempted reactions required NEt$_3$ (1.5–2.0 equiv).

Although primary amine groups are known to exhibit stronger nucleophilic properties during acetylation compared to their alcohol equivalents, it was likely to be the reverse for ABC due to the purine aromatic system. This system would reduce the nucleophilic tendencies of the N^2 amine so protection of the 5'-OH was initially required. This was completed using *t*-butyldimethylsilyl chloride

(TBDMS−Cl) (Scheme **4.7**). This reaction was carried out with TBDMS−Cl (1.5 equiv) and imidazole (2 equiv) in DMF with achievement of good yields (65%).
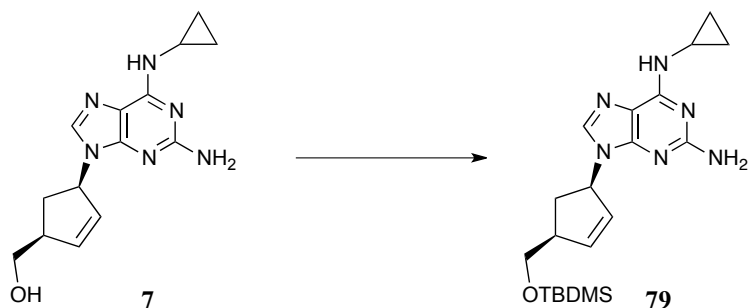
Scheme 4.7: Reagents and conditions: TBDMS−Cl (1.5 equiv), imidazole (2.1 equiv), DMF, r.t., 24 h, 65%. TBDMS, *t*-butyldimethylsilyl ether.

Following alcohol protection, acetylation, using acetyl chloride (AcCl, 1.5 equiv) was attempted.[20] Although, some product was formed, a very low yield was obtained (24%). The reaction was repeated with BzCl (1.5 equiv)[20] and the yield was again, extremely poor. Further reactions included acetylation with isobutyric anhydride using conditions applied by Challa *et al.* on nucleoside analogue, 2'-deoxyguanosine,[21] Boc and fluorenylmethyloxycarbonyl chloride (Fmoc−Cl) reactions with the latter demonstrated previously with guanosine nucleosides[22,23] (Figure **4.4**). When these reactions were applied to ABC, no product was obtained, with solvent solubility issues and significant side product formation occurring.

A slightly different approach was subsequently used: A peptide coupling reaction (Figure **4.4**) using benzoic acid (1.2 equiv), 1-hydroxybenzotriazole (HoBt) (0.001 equiv) and dicyclohexylcarbodiimide (DCC) (1 equiv) in DCM. Upon purification,

the required product was not formed. Again, this was likely to be the result of ABC insolubility within the solvent.

The final reactions attempted were acetylation reactions using Ac_2O and NEt_3 in a large excess of DCM (Scheme **4.4**). The conditions used to form *O*-acetylated ABC **71** were employed. Alcohol protection at the 5' position using TBDMS was first required. Following this, the acetylation reaction was attempted. It was found that a mixture of three products was formed: Mono-, di- and tri-acetylation had occurred and with the acidic conditions generated during the reaction, the TBDMS group was removed during the reaction (Figure **4.5**). All three products were separated *via* silica gel chromatography to yield compounds **71**, **80** and **81** – although compound **71** was the major product, which was isolated in a 53% yield.
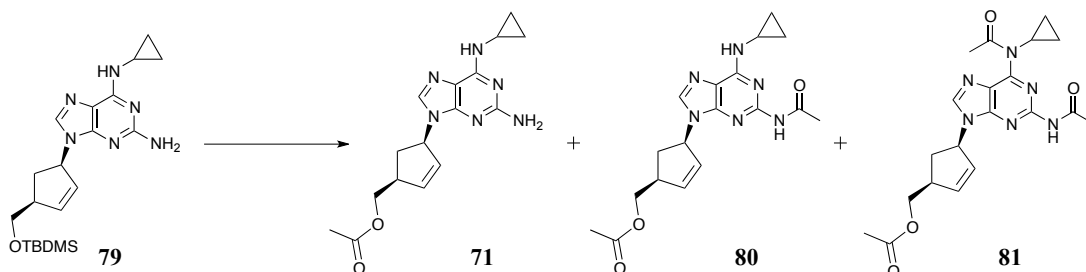
Figure 4.5: Formation of three acetylated products, **71**, **80** and **81**. These products were formed during the acetylation reaction of **79** with Ac_2O and NEt_3 in DCM.

During further repeats of this reaction where TBDMS was not removed (achieved through use of freshly distilled Ac_2O), intermediate **82** was formed (Scheme **4.8**). This compound was deprotected using tetra-*n*-butylammonium fluoride (TBAF) in THF to yield the desired compound **83** in a 71% yield.
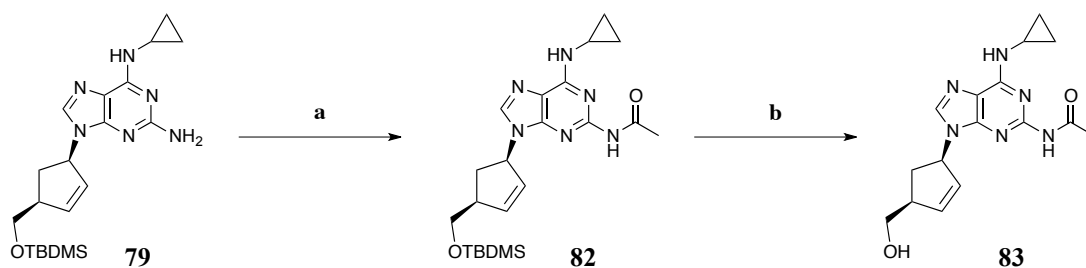
Scheme 4.8: Reagents and conditions: a) Ac_2O (1.2 equiv), NEt_3 (1.2 equiv), DCM, 0 °C, 4 h, 53%; b) TBAF (1 M in THF, 1 equiv), r.t., o/n, 71%. TBAF, tetra-*n*-butylammonium fluoride.

4.3.3 Cyclopentane analogues to block 1,4-Michael addition.

A set of analogues was designed to inhibit alkene migration: A potential contributing factor in ABC toxicity, through a 1,4-Michael addition, as discussed in Chapter 2. Elimination of the cyclopentyl alkene group would prevent this mechanism from occurring.

Using the most logical approach in designing these analogues, removal of the alkene to form DH-ABC **20** was the starting analogue (Scheme **4.9**). This compound was formed through reduction of ABC with H_2, using catalytic Pd/C and a good yield of 67% was achieved. It was clear from ^1H NMR that the desired product was formed, through disappearance of the alkene proton shifts at δ 6.11 and 5.76 ppm.
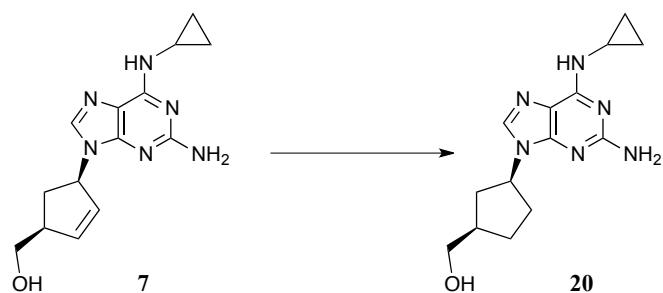
Scheme 4.9: Reagents and conditions: 10% Pd/C (cat.), H_2, MeOH, r.t., 4 h, 67%.

Following the success of synthesising **20**, analogues designed to replace the alkene group were attempted. These analogues included cyclopropanation, di-fluoro substituted cyclopropanation (Figure **4.6 A**) and di-hydroxylation (Figure **4.6 B**).
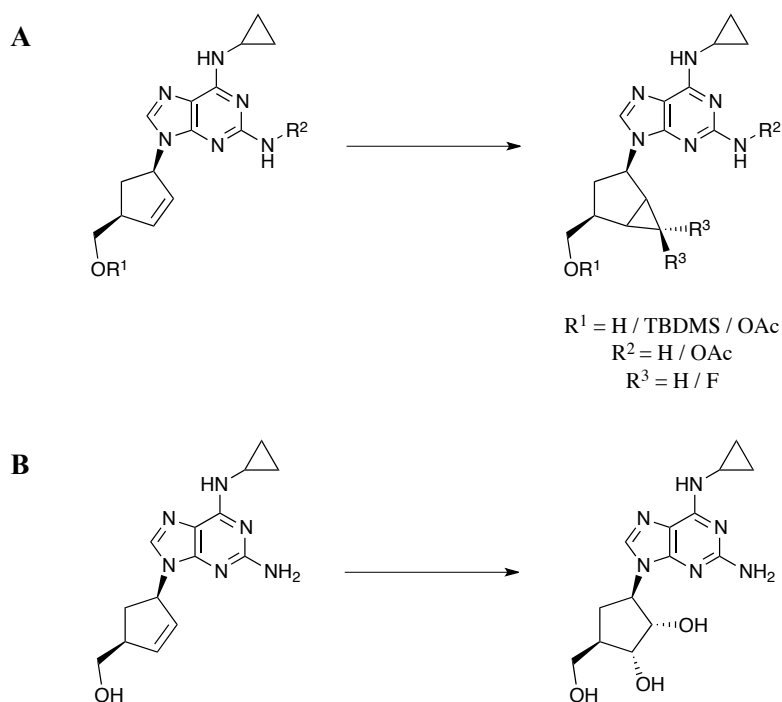
Figure 4.6: Carbocyclic alkene manipulations: Cyclopropanation using Simmons–Smith conditions on compounds **7**, **61** and **62**, or di-fluoro cyclopropanation using TFDA/NaH also on compounds **7**, **79** and **80** (**A**) and dihydroxylation of **7** using AD-mix-β (**B**). TFDA, trimethylsilyl fluorosulfonyldifluoroacetate.

The cyclopropanation reaction used Simmons–Smith conditions (diethyl zinc (2 equiv) and diiodomethane (4 equiv) in DCM) and such conditions have been applied to nucleosides.[24,25] Several polar side products were formed and significant starting material remained after 20 h. ABC, as discussed in Chapter 2, is only partially soluble in DCM at room temperature and less so at 0 °C: The temperature required for these reaction conditions. This insolubility may have been a contributing factor to lack of product formation. To overcome this insolubility issue, cycloproponation was attempted using O-TBDMS protected intermediate **79** (Figure **4.6 A**): A compound with high solubility in DCM compared to ABC. Under the same conditions, a considerable number of side reactions occurred with decomposition of starting material. The reasons for this unsuccessful reaction are not known although, the nucleophilic primary amine, N^2 may have been responsible for side product formation. To eliminate this factor, di-acetate compound **80** was used, and the reaction was repeated under the same conditions (Figure **4.6 A**). As before, similar results were obtained with no formation of desired product. No further reactions using these reaction conditions were attempted.

With no successful reactions using Simmons–Smith conditions, a new reagent, trimethylsilyl fluorosulfonyldifluoroacetate (TFDA) was used with catalytic sodium fluoride (NaF) in toluene (Figure **4.6 A**) as used by Wang *et al.*[26]

TFDA forms a difluorocarbene intermediate, which is able to undergo electrophilic reactions with alkenes. This reaction was attempted using both ABC and compound **79**: Both of which resulted in no desired product formation, and recovered starting material. The difluorocarbene intermediate is highly reactive and has shown to react

successfully with nucleoside analogues.[27] However, a number of side reactions with this reactive intermediate and the purine moiety were reported. To limit possible side reactions occurring, the reaction was repeated using di-protected compound **80** (Figure **4.6 A**). Unfortunately, significant side product formation remained and this is thought to occur from the highly reactive nature of the carbene intermediate, particularly at the high temperature used in this reaction. Further attempts with these reaction conditions were not pursued.

Substitution of the cyclopentyl alkene with hydroxyl groups was an analogue also attempted. Di-hydroxylation in this manner was attempted using Sharpless asymmetric hydroxylation conditions: AD-mix β (potassium carbonate (K_2CO_3), 0.5 mol; potassium ferricyanide, 0.5 mol; potassium osmate dihydrate, 0.0007 mol; $(DHQD)_2PHAL$, 0.002 mol) in 1:1 H_2O-t-BuOH (Figure **4.6 B**). This analogue was of particular interest due to the specific stereochemical nature of the reaction and the use of H_2O and t-BuOH was also encouraging as ABC is highly soluble in these solvents at room temperature. Although no side reactions occurred, the desired product was not formed. The reaction was left for a significant period of time (7 days) with gentle heating (40 °C) for 24 h and no product was formed. Starting material was recovered (95%). The lack of formation of product could be a result of steric hindrance exhibited by AD-mix β. For future work, and to either eliminate or confirm this hypothesis, AD-mix α could be used to form the enantiomer (Figure **4.7**) and directly using osmium tetraoxide (OsO_4). The reactions with AD-mix β were not explored further.
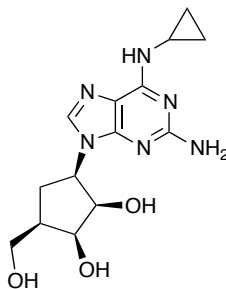
Figure 4.7: The possible formation of the alternative 2',3'-dihydroxylated analogue using AD-mix α.

4.3.3.1 Cross-reactivity and proliferation of ABC-specific human T-cell clones with DH-ABC 20.

Following success with compounds **20**, **71** and **83**, they were further utilised in immunological assays to measure the toxicity in T-cells. The chemical cross-reactivity experiments were conducted within the University of Liverpool, with full details of all methodological protocols available[28] and for details of these assays see Chapter 1, Section **1.10**. The cross-reactivity and proliferation results obtained from compound **20** are presented and discussed within. Over increasing concentrations of both ABC and DH-ABC **20** (0–100 μM), it was found that DH-ABC stimulated a select number of clones to proliferate at higher concentrations (50 and 100 μM) only, although this was still significantly less than ABC itself (Figure **4.8 A**). This was also found to be the case for cytokine release (ELISpot IFN-γ assay), where DH-ABC, at 50 and 100 μM, stimulated IFN-γ release (Figure **4.8 B**). In these two assays, it has been found that the removal of the cyclopentyl double bond has an effect on the stimulation of ABC-specific T-cell clones. There are two possible explanations for the lack of immunogenicity of DH-ABC. The cyclopentane ring is less rigid than its cyclopentenyl equivalent and this perturbation could result in altered binding within the HLA-B*57:01 protein. Alternatively, without a C=C, **20**

will not be able to be oxidised to an aldehyde by ADH and should ABC-**16** be responsible for T-cell stimulation, this would not be observed with **20**. ABC-**16** has been shown to undergo protein binding resulting in an immunogen, as discussed in Chapter 2. This would not be possible with **20**. However, should this be a valid rationale for reduced immunogenicity, it fails to explain why DH-ABC stimulates T-cell clones at higher concentrations.
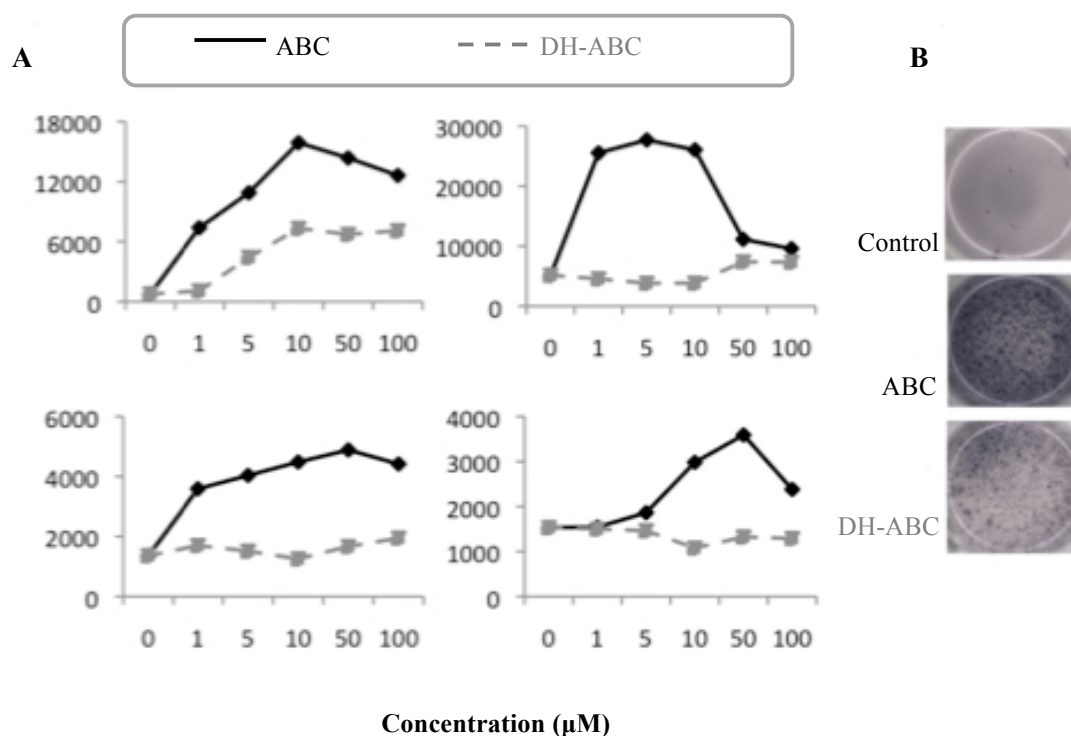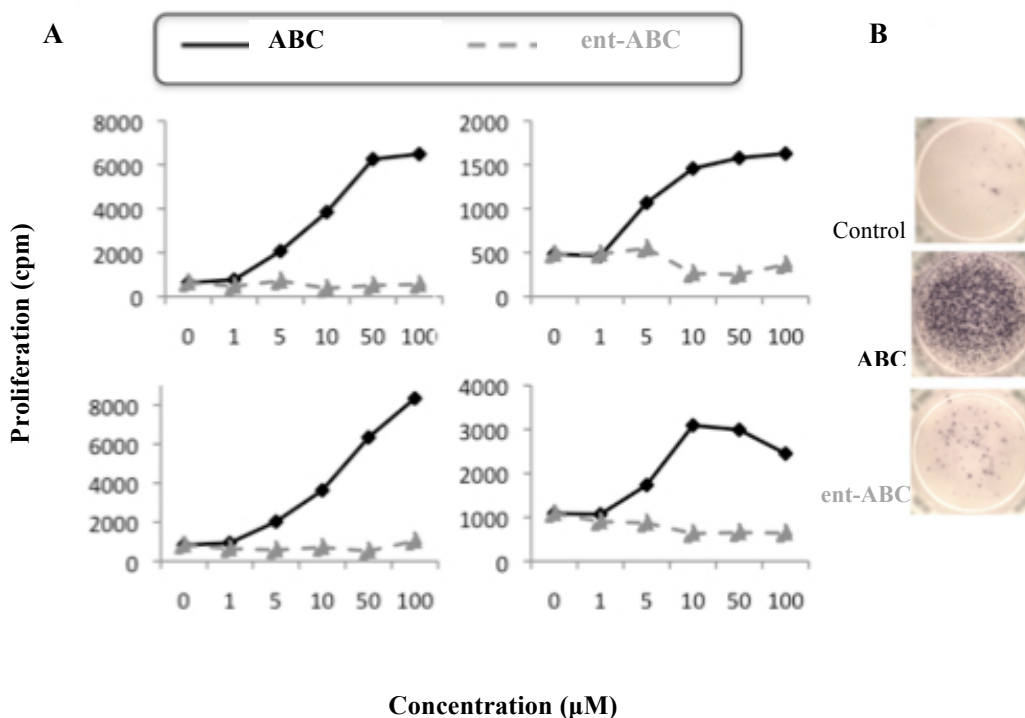

Figure 4.8: Cross-reactivity results obtained from ABC-specific T-cell clones in the presence of ABC **7** and DH-ABC **20**. Results obtained show proliferation of T-cell clones over increasing compound concentrations of 0–100 μM (**A**) and IFN-γ cytokine release, visualised using an ELISpot assay (**B**). The ELISpot wells were obtained after 48 h incubation of ABC-specific T-cell clones in the presence of ABC (50 μM) and DH-ABC (50 μM). Adapted from Bell, 2013.[28]

4.3.4 Synthesis of ABC enantiomers.

As reported in Section **3.1**, a synthesis of ABC was reported by MacKeith *et al.*,[29] where the absolute stereochemistry of ABC was achieved using an enzyme, *Pseudomonas fluorescens* lipase. Due to the problems associated with modifying ABC directly, this synthetic route was adapted to synthesise intermediates that could be used to form ABC analogues. During the synthesis, it became apparent that the enantiomer of ABC would be an interesting analogue. Although it is widely documented that a large proportion of enzymes are selective for one isomeric substrate only – the formation of ABC's enantiomer would allow an investigation of the selectivity of the enzymes involved in ABC metabolism. The synthesis was adapted as originally reported by MacKeith *et al.* (Scheme **4.9**).[29]
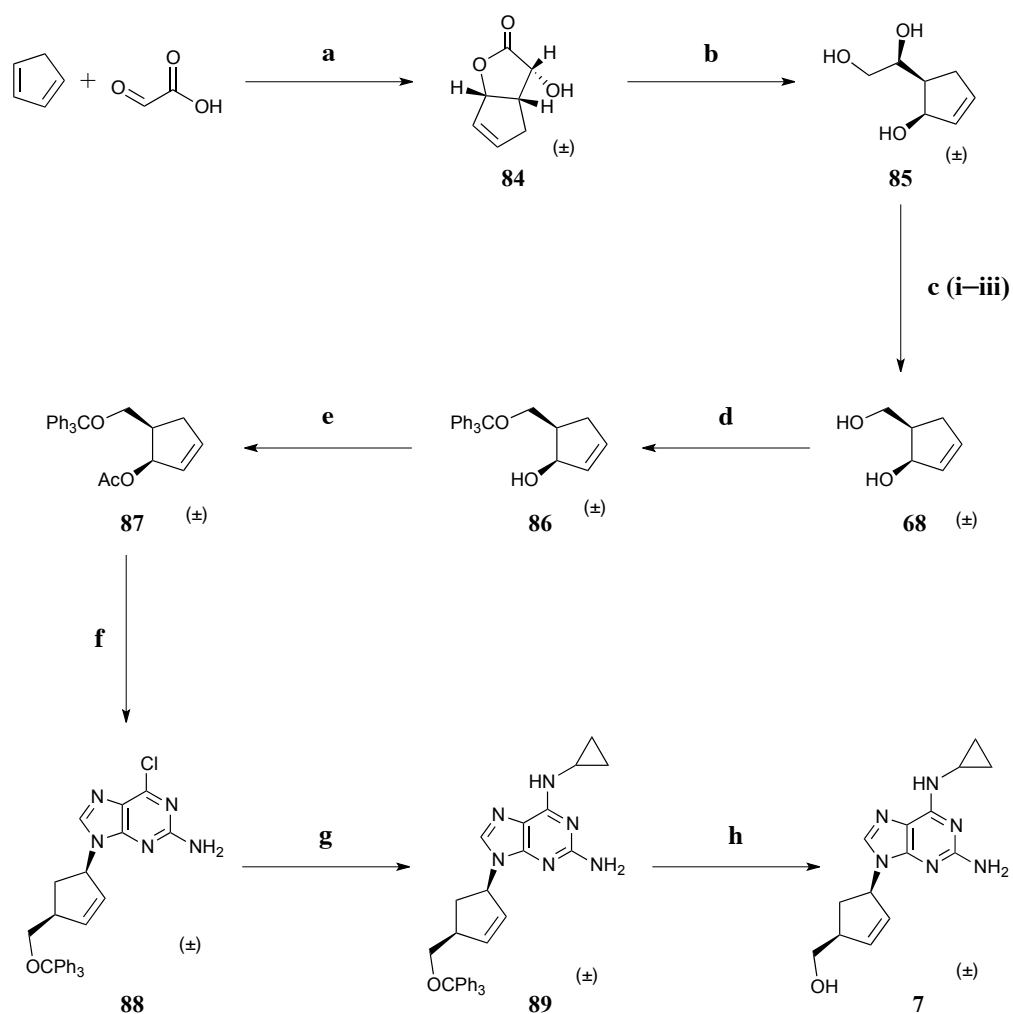
Scheme 4.10: Reagents and conditions: a) Cyclopentadiene (1 equiv), glyoxylic acid (1 equiv), H_2O, r.t., 4 days, 18%; b) LiAlH$_4$ (1 equiv), THF, r.t., o/n; c) i) Sodium metaperiodate (1 equiv), diethyl ether, H_2O, 0 °C, 2 h; ii) Ethylene glycol (0.4 equiv), 0 °C, 1 h; iii) NaBH$_4$ (1 equiv), NEt$_3$ (1 equiv), DCM, r.t., o/n, 59%; d) Trityl chloride (1 equiv), NEt$_3$ (1 equiv), DMAP (0.1 equiv), DCM, r.t., o/n, 72%; e) Ac$_2$O (excess), pyridine (excess), r.t. o/n, 39%; f) NaH (60% dispersed in mineral oil, 3.5 equiv), 2-amino-6-chloro purine (2 equiv), Pd(PPh$_3$)$_4$ (10 mol %), DMF, Ar, 50 °C, o/n, 17%; g) Cyclopropylamine (excess), MeOH, 50 °C, o/n, 72%; h) 80% Acetic acid (excess), 50 C, 48 h, 52%.

The initial step was the cycloaddition of glyoxylic acid and freshly prepared cyclopentadiene. This reaction yielded diastereoisomers **84a** and **84b** (Figure **4.10**), which were successfully separated by fractional crystallisation: The required

racemic isomer **84a** crystallised, whilst racemic isomer **84b** remained in the diethyl ether solution as an oil.
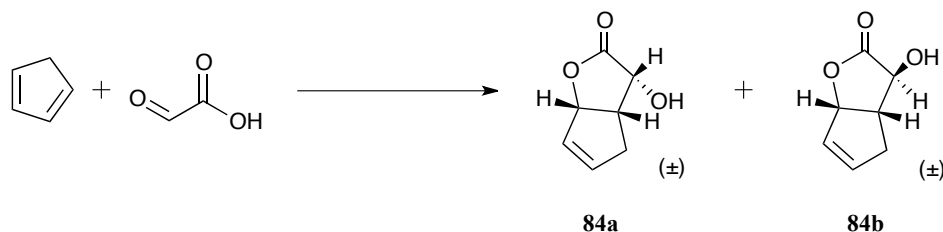
Figure 4.9: Formation of diastereoisomers **84a** and **84b** from cycloaddition of glyoxylic acid and cyclopentadiene in H_2O.

Ring opening of lactam product **84a** was achieved using lithium aluminium hydride (LiAlH$_4$) to yield **85**, which was used in the following step without further purification. Conversion of triol **85** to diol **68** was achieved using NaIO$_4$ (1 equiv) and ethylene glycol (0.4 equiv), followed by addition of NaBH$_4$ (1 equiv) to yield the required product **68**. The primary alcohol intermediate was selectively protected with trityl chloride (CPh$_3$Cl) to yield **86** (72%) and the secondary alcohol was further protected with Ac$_2$O to yield intermediate **87** with a 39% yield.

Step 6 consisted of coupling the di-protected intermediate **87** with 2-amino-6-chloropurine to yield **88**. Although reaction conditions were optimised, the best yield achieved was 17%. A common problem with this reaction is the formation of the N^7 isomer as well as the required N^9 isomer.[5,30] Although, use of 2-amino-6-chloropurine rather than other purine compounds can increase the N^9:N^7 ratio to 99:1.[31] It was also essential that this reaction was maintained under an inert atmosphere and fresh Pd(PPh$_3$)$_4$ catalyst (10 mol %) was used. The following step was nucleophilic aromatic substitution of 6-chloro with cyclopropylamine to form

compound **89** and excellent yields of 72% were achieved. The final step, removal of

O-protecting trityl group, was completed using 80% AcOH over 48 h to yield

racemic ABC **7** with a 52% yield (Figure **4.10**).
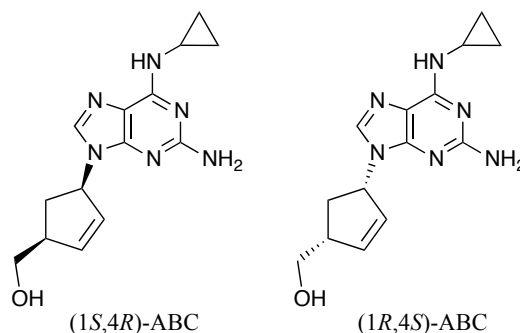
(1*S*,4*R*)-ABC   (1*R*,4*S*)-ABC

Figure 4.10: Synthetic formation of ABC enantiomers (1*S*,4*R*)-ABC (ABC **7**) and (1*R*,4*S*)-ABC (ent-ABC) using an 8-step synthetic route – a route adapted from MacKeith *et al.*[29]

The racemic mixture was separated using HPLC and a Chiracel® OD-H analytical

column. The conditions were used as published by Seshachalam *et al.*[32] ABC was

the first isomer to elute from the column (R_t = 27 min) followed closely by its

enantiomer, ent-ABC (R_t = 32 min). A representative chromatogram can be seen in

Supplementary Information Figure **S1**.

4.3.4.1 Cross-reactivity and proliferation of ABC-specific human T-cell clones with ent-ABC.

The chemical cross-reactivity experiments were conducted within the University of

Liverpool, with full details of all methodological protocols available[28] and for details

of these assays see Chapter 1, Section **1.10**. The cross-reactivity results for ent-ABC

were obtained and measured using both a proliferation and IFN-γ ELISpot assay

(Figure **4.11**).   At increasing concentrations of ent-ABC (0–100 μM), no

proliferation of ABC-specific T-cell clones was seen (Figure **4.11 A**). This was also reflected in the IFN-γ ELISpot assay, where little IFN-γ release was observed (Figure **4.11 B**). As discussed in Section **4.3.3.1**, there are again two possible explanations for the lack of immunogenicity of ent-ABC. The first possible reason is that ent-ABC will not bind within the HLA-B*57:01 protein due to its stereochemistry resulting in possible steric clashes with the protein, inhibiting binding. Alternatively, ent-ABC may not be a substrate for ADH, again due to its stereochemistry. Enzymes are highly substrate specific and this has been observed with CBV.[33] If ent-ABC is not a substrate for ADH, no 5'-OH oxidation will occur and therefore the suspected aldehyde immunogen will not be formed, resulting in reduced T-cell clone stimulation.

Figure 4.11: Cross-reactivity results obtained from ABC-specific T-cell clones in the presence of ABC and ent-ABC. Results obtained show proliferation of T-cell clones over increasing compound concentrations of 0–100 μM (**A**) and IFN-γ cytokine release, visualised using an ELISpot assay (**B**). The ELISpot wells were obtained after 48 h incubation of ABC-specific T-cell clones in the presence of ABC (50 μM) and ent-ABC (50 μM). Adapted from Bell, 2013.[28]

4.3.5 Synthesis of ABC intermediates for use in analogue synthesis.

4.3.5.1 Asymmetric synthesis I.

Although useful to yield ABC enantiomers, the inefficient and time-consuming synthesis discussed in Section **4.3.4** is not ideal to use for adaption to ABC analogues. The lack of stereochemical control and several low-yielding steps in this synthesis would prove problematic. A 12-step asymmetric synthesis was designed (Figure **4.12**). The third step establishes the absolute stereochemistry and from step 6, the scheme follows the non-selective synthesis.
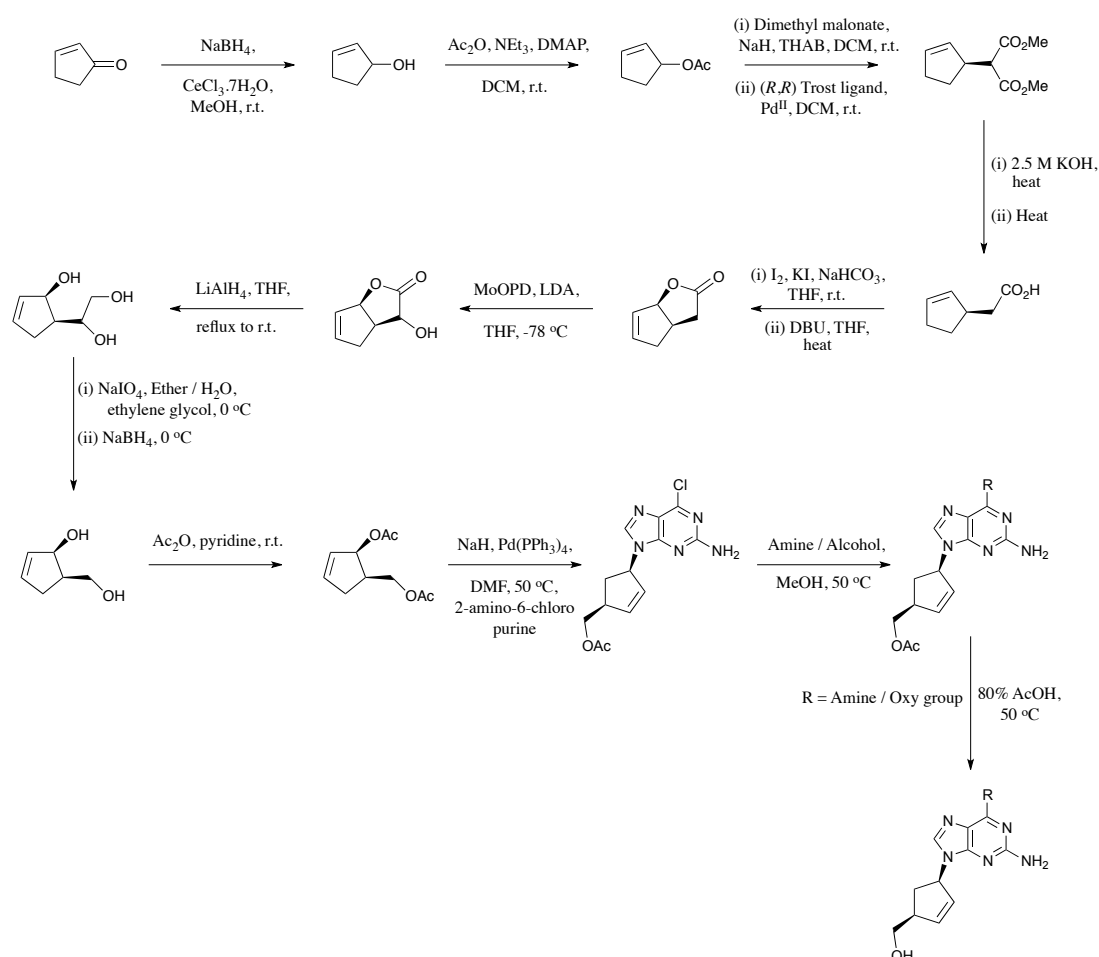
Figure 4.12: The designed 12-step synthesis of ABC and its intermediates using the conditions shown within the figure. Such intermediate compounds could assist in ABC analogue synthesis. THAB, tetrahexylammonium bromide; MoOPD, oxodiperoxymolybdenum (pyridine) (1,3-dimethyl-3,4,5,6-tetrahydro-2-pyrimidinone).

The first six steps of this synthesis can be seen in Scheme **4.11**. The first step is a Luche reduction; where cyclopentenone is reduced using NaBH$_4$ and cerium (III) chloride heptahydrate (CeCl$_3$.7H$_2$O) in MeOH. This reaction was successful, yielding compound **90**, which was used directly in the following step. CeCl$_3$.7H$_2$O was used to direct reduction of the ketone to alcohol, rather than reduction of the alkene group. The following step, alcohol protection, was completed using Ac$_2$O and NEt$_3$ in DCM to yield **91**. The volatility of products **90** and **91** was a key factor in the choice of reagents and conditions for both reactions. This was particularly the case in the formation of **91**, where low yields were initially a problem. Alternative conditions were attempted but without improvement. After significant optimisation of both the original reaction conditions and purification procedure, yields of 58% could be reliably obtained.
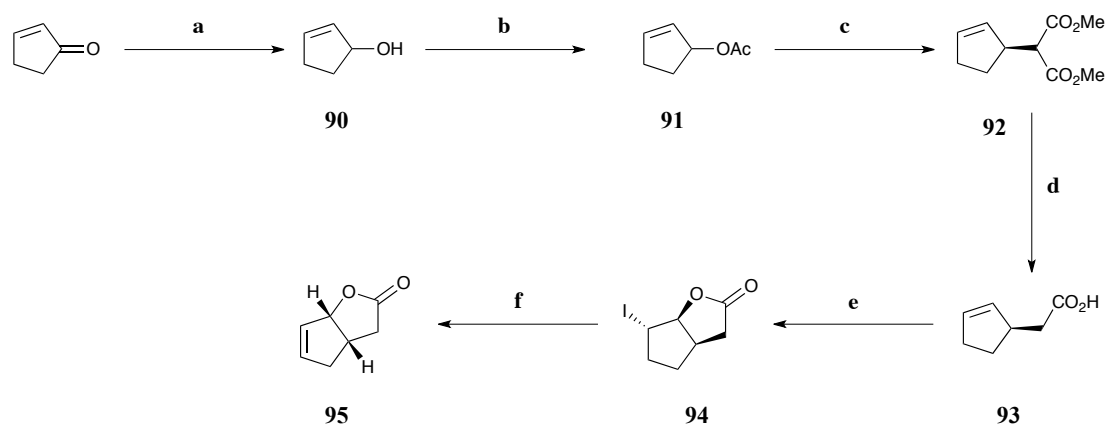
Scheme 4.11: Reagents and conditions: a) 2-Cyclopenten-1-one (1 equiv), CeCl$_3$.7H$_2$O (1.3 equiv), NaBH$_4$ (1.2 equiv), MeOH, 0 °C, 1 h; b) Ac$_2$O (1.5 equiv), NEt$_3$ (1.4 equiv), DMAP (0.1 equiv), DCM, 0 °C → r.t., o/n, 58%; c) Dimethyl malonate (3 equiv), CsCO$_3$ (4 equiv), THAB (2.5 equiv), allyl palladium (II) chloride dimer (0.0025 equiv), (*R*,*R*)-DACH-phenyl Trost ligand (0.065 equiv), DCM, r.t., 4 h; 88%; d) KOH (2.5 M, excess), reflux, 4 h, 72%; e) I$_2$ (2.2 equiv), KI (excess), sat. NaHCO$_3$, THF, r.t., 4 h, 94%; f) DBU (2.5 equiv), THF, reflux, o/n, 48%.

The absolute stereochemistry, in step 3, was achieved using allylpalladium(II)chloride dimer and (*R,R*)-DACH-phenyl Trost ligand:
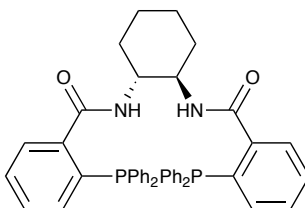
This step involved the palladium mediated coupling of dimethyl malonate and acetate **91** to form compound **92** with excellent yields (88%, $[\alpha]_D$ = –74.0°, *c* = 3.0).[34] This is a well-studied reaction with specific emphasis on gaining high enantiomeric excess (ee).[35] Based on this previous research, reaction conditions used by Trost and co-workers were utilised.[34,35] The base, NaH was replaced by caesium carbonate (Cs_2CO_3) to improve product ee.[35] Slow addition (over 1.5 h) of the deprotonated dimethyl malonate solution to the Pd^0 catalyst was also essential in achieving high ee values.

Di-ester **92** was hydrolysed to its di-carboxylate product using 2.5 M KOH and once acidified, the dicarboxylic acid was heated to 160 °C, promoting decarboxylation to form intermediate **93** in a 72% yield. Compound **93** underwent iodolactonisation with iodine/potassium iodide (I_2/KI) in H_2O–THF to form intermediate **94** with excellent yields of 94%.[36] The iodo-compound **94** was converted to unsaturated lactone **95** in a 48% yield using DBU in THF at reflux.[36]

The following step was α-oxidation of lactone **95** to yield hydroxylactone **84**. Although α-oxidation of lactones is not well reported, an oxidant and strong nucleophilic base are always required (Figure **4.13**).[37,38]
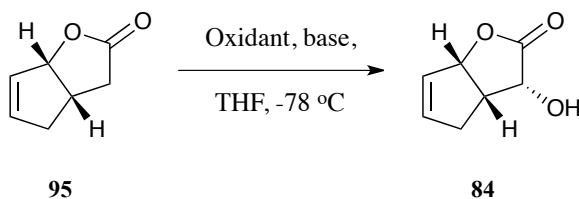
Figure 4.13: α-Hydroxylation of lactone **95** using an oxidant and a strongly nucleophilic base in THF to form compound **84**.

A common reagent used for such oxidations is Vedej's reagent (a MoO$_5$ complex).[39-42] The reagent was freshly prepared as shown in Scheme **4.11** and 1,3-dimethyl-3,4,5,6-tetrahydro-2(1H)-pyrimidinone (DMPU) was used in replacement of the highly toxic hexamethylphosphoramide (HMPA) reagent in accordance with a procedure developed by Anderson *et al.*[43]
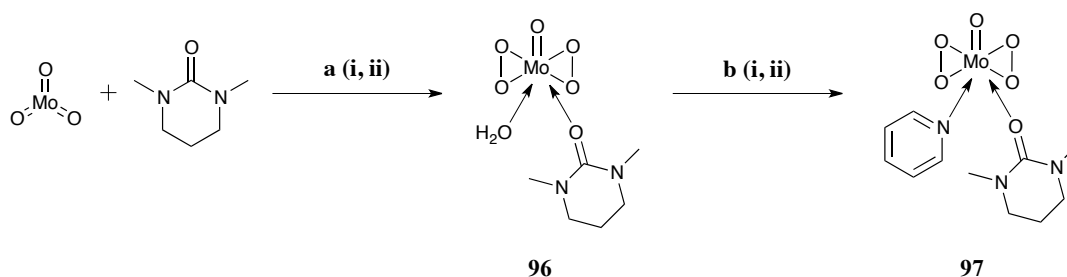
Scheme 4.12: Reagents and conditions: a) i) MoO$_3$ (1 equiv), 30% H$_2$O$_2$, 35–40 °C, 4 h; ii) DMPU (1 equiv), 10 °C, 20 min, 52%; b) i) P$_2$O$_5$ under vacuum, 24 h; ii) Pyridine (1 equiv), r.t., 10 min, 51%. DMPU, 1,3-dimethyl-3,4,5,6-tetrahydro-2-pyrimidinone.

The formation of the oxidising agent utilises a 2-step procedure, in which initially, molybdenum (VI) oxide (MoO$_3$) complexes with a molecule of water. This step required very careful heating, at 35 °C, with 30% H$_2$O$_2$ and following this, the resulting compound was further reacted with a molecule of DMPU to yield complex **96**. Following dehydration of this complex over phosphorus pentoxide (P$_2$O$_5$) in a

vacuum desiccator, the final reaction was completed with dropwise addition of pyridine to yield the active oxidant oxodiperoxymolybdenum (pyridine) (1,3-dimethyl-3,4,5,6-tetrahydro-2-pyrimidinone) (MoOPD), compound **97**. Care was taken when using and storing the reagent as stipulated by Anderson *et al*. due to the instability of complex **97** with light and heat.

To test the efficiency of the freshly prepared oxidant, two test reactions were performed on γ-butyrolactone (due to its similarity to the starting material **95**) (Scheme **4.13 A**) and camphor (an inexpensive substrate that gives excellent yields with this oxidant) (Scheme **4.13 B**).[43] Under optimised conditions, both substrates were converted to their corresponding α-hydroxylated products in excellent yields.
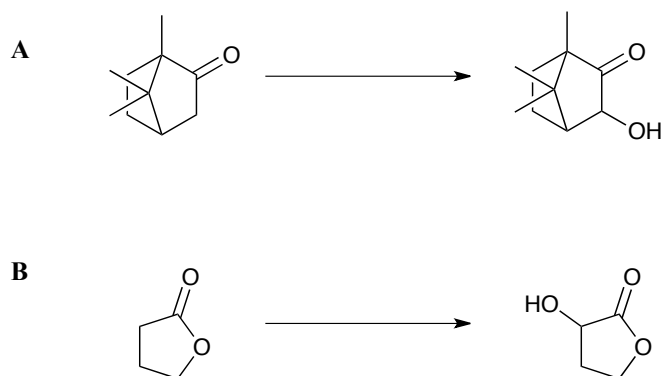
Scheme 4.13: Reagents and conditions for α-oxidation of camphor (**A**) and γ-butyrolactone (**B**): LDA (1.5 equiv), MoOPD (1.1 equiv), THF, −78 °C, 2 h, 72% (**A**) and 81% (**B**). LDA, lithium diisopropylamide.

Applying these optimised conditions to **95**, the reaction yielded very little product with a significant number of side reactions occurring. After purification *via* silica gel chromatography, it was clear from ^{1}H NMR that diastereoisomers were forming (Figure **4.14**). The formation of diastereoisomers should not interfere with future

analogue synthesis as the stereochemistry at this quaternary carbon would be lost during analogue synthesis at step 8, Figure **4.12**. However, the yields from this reaction were very poor.
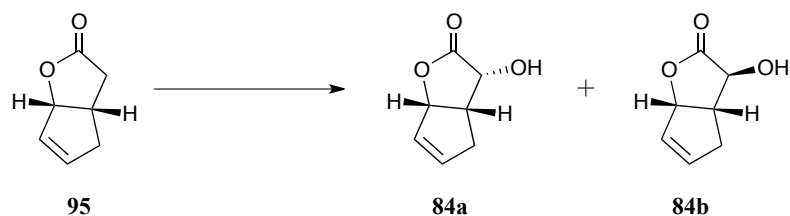
Figure 4.14: Formation of diastereoisomers from α-hydroxylation of **95** using LDA and MoOPD.

A series of test reactions were carried out in an attempt to optimise the yield of **84a** and **84b** (Table **4.1**).

Extended reaction times and increasing the number of equivalents of base proved detrimental, with increased side product formation (reactions B and C). Increasing the temperature, rigorous drying on MoOPD and increasing MoOPD equivalents, also had little effect on the reaction profile (reactions D and E). Finally, potassium bis(trimethylsilyl)amide (KHMDS), in replacement of lithium diisopropylamide (LDA), was used in reaction F and no reaction occurred, with starting material recoverable. For further work within this area, alternative oxidants, *N*-sulfonyloxaziridines could be used. These have found to be a higher yielding alternative to using metal based oxidants for lactone substrates.[44]

Table 4.1: Experiments A–F showing the optimisation of reactions conditions for α-hydroxylation of lactone **95**. KHMDS, potassium bis(trimethylsilyl)amide. SM, starting material.

Reaction	Reagent Conditions*			Yield (%)
	Base (equiv)	Temperature (°C)	Other Conditions	
A	LDA (1.5)	–78	MoOPD (1.1 equiv), 2 h	Diastereoisomers obtained – low yield (<20%)
B	LDA (1.5)	–78	MoOPD (1.1 equiv), 3 h	Increased number of side products – no yield obtained
C	LDA (2.0)	–78	MoOPD (1.1 equiv), 2 h	As reaction B
D	LDA (1.5)	–78 to –30	MoOPD (1.1 equiv), 2 h (with initial drying of SM over P_2O_5)	As reaction A
E	LDA (1.5)	–78 to –30	MoOPD (2 equiv), 2 h	As reaction A
F	KHMDS (1.5)	–78 to –30	MoOPD (1.1 equiv), 2 h	No reaction

* All reactions were completed on a 100–150 mg scale.

Following the problems with the aforementioned step 7, a slightly altered step 4 of the original synthesis was attempted (Figure **4.15**). This involved an oxidation of compound **92** in an open air flask with caesium fluoride (CsF) in DMF.[45] The addition of a hydroxyl group at this point would eliminate the need for lactone α-

hydroxylation. However, no reaction occurred and starting material was recovered. This same step was repeated using the LDA/MoOPD conditions and again, no product was formed and starting material recovered.
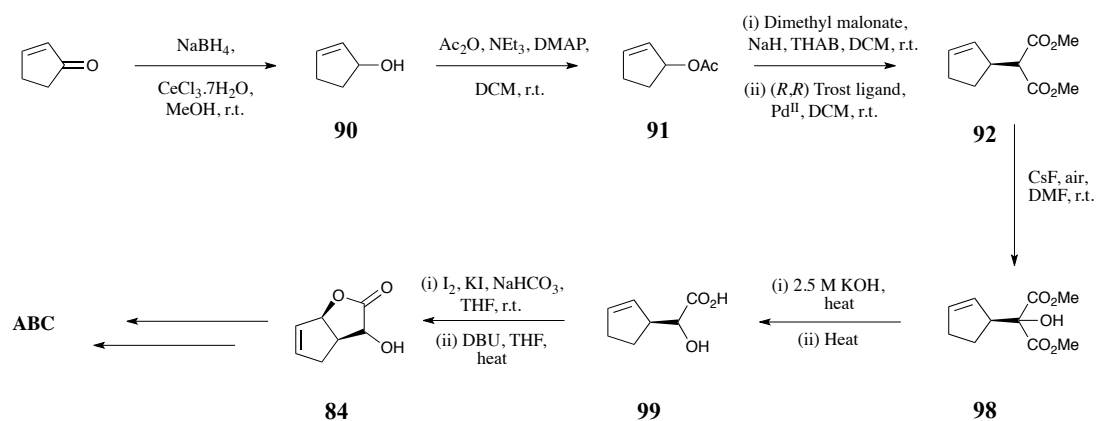
Figure 4.15: The design of an alternative pathway for the formation of intermediate **84**, where α-hydroxylation of an earlier intermediate **92** occurs rather than lactone **95** (Figure **4.14**).

Subsequently, the synthesis was redesigned slightly as shown in Figure **4.16**. The synthesis was initially tested using racemic intermediates, as not to use the expensive (R,R)-DACH-phenyl Trost ligand. Diethylbromomalonate was initially converted to compound **100** with excellent yields (93%) and this compound underwent further Pd^0 mediated coupling with intermediate **91**. This reaction originally used Cs_2CO_3 as the base, but no product was formed. Substitution of Cs_2CO_3 for NaH gave a 23% yield of **101** but significant starting material was recovered. Further optimisation revealed that the base, N,O-bis(trimethylsilyl)acetamide[46] improved the yield slightly to 37%.

NaOAc, DMF, heat

100

72, Pd^{II}, DPPE, base, DCM, r.t.

101

(i) 2.5 M KOH, heat

(ii) Heat

(i) I$_2$, KI, NaHCO$_3$, THF, r.t.

(ii) DBU, THF, heat

ABC

84

(±) **99**
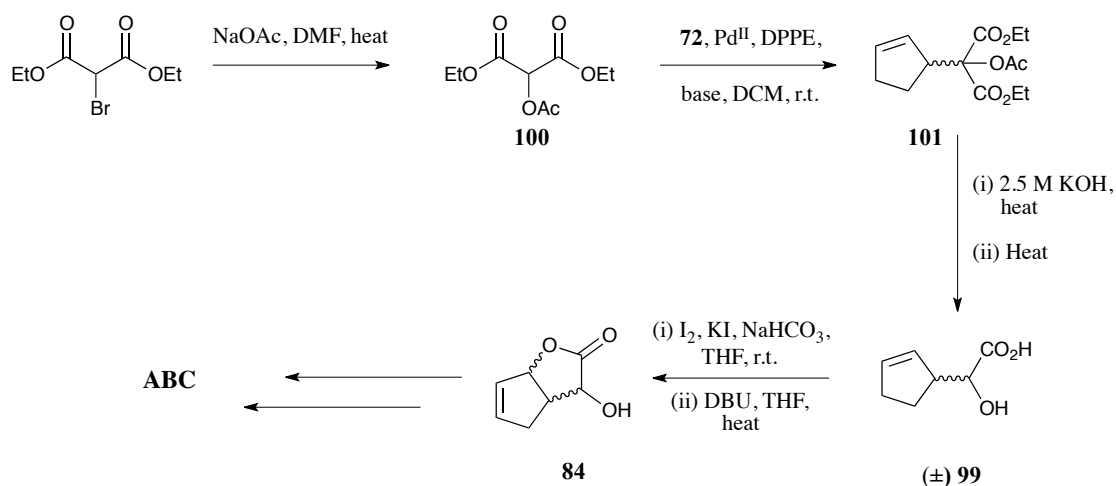
Figure 4.16: Design of an alternative synthetic pathway to yield ABC **7**. This pathway circumvents the need for α-hydroxylation of the bicyclic lactone intermediate **95**.

Along with the low yields, once step 3 was repeated using chiral (*R,R*)-DACH-phenyl Trost ligand, to form chiral **99**, diastereoisomers were formed. With all the problems experienced in the above syntheses, this asymmetric pathway was discarded and an alternative synthesis was found and developed.

4.3.5.2 Asymmetric synthesis II.

It was essential that intermediates for ABC analogues were found, and having experienced difficulties with previous syntheses, the synthetic route shown in Scheme **4.14** was researched and developed.[5,7] This synthesis was used to synthesise D$_2$-ABC and the initial 3 steps are the identical to those discussed in Chapter 2.
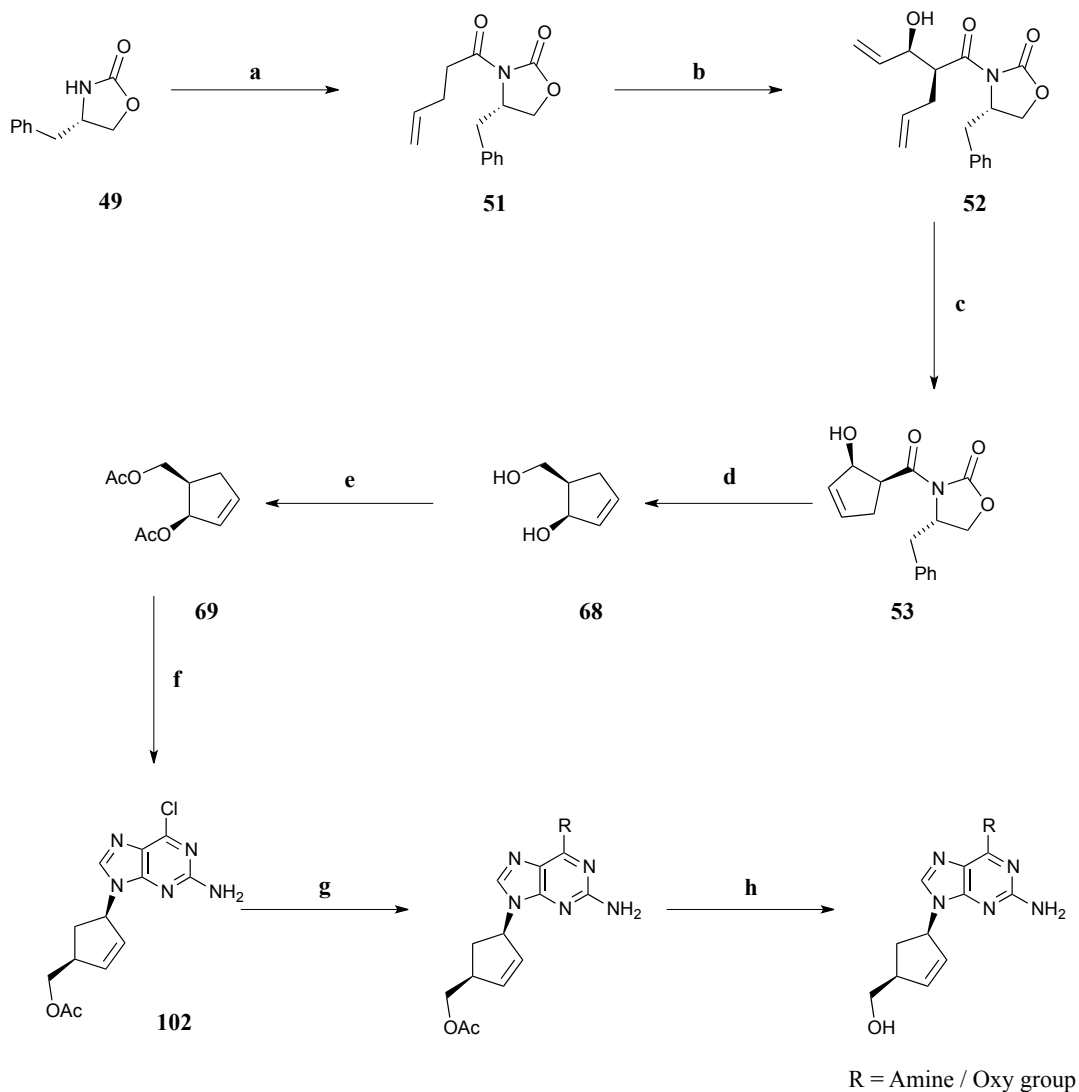
Scheme 4.14: Reagents and conditions: a) *n*-BuLi (1 equiv), pivaloyl chloride (1 equiv), NEt₃ (1 equiv), 4-pentenoic acid (1 equiv), *t*-BME, THF, –78 °C → r.t., N₂, 2 h, 85%; b) DIEA (2.2 equiv), DBBT (2.2 equiv), acrolein (2.1 equiv), DCM, –78 °C → r.t., N₂, 16 h, 87%; c) Grubbs catalyst 1ˢᵗ generation (5 mol %), DCM, r.t., Ar, 15 h, 70%; d) LiBH₄ (5 equiv), MeOH (excess), THF, 0 °C → r.t., 1 h; e) Ac₂O (1.6 equiv), NEt₃ (1.6 equiv), DMAP (0.1 equiv), DCM, 0 °C → r.t., o/n; f) NaH 60% dispersed in mineral oil, 1.2 equiv), 2-amino-6-chloro purine (1.1 equiv), Pd(PPh₃)₄ (10 mol %), DMF, THF, Ar, 65 °C, o/n, 34%. DMF, dimethylformamide.

Intermediate **68** was obtained by reduction of compound **53** with $LiBH_4$ and MeOH in THF. It was found to be preferential to use **68** without further purification due to compound loss associated with its volatility. The di-protection of **68** with Ac_2O and NEt_3 in DCM yielded di-acetate **69**, which underwent a further Pd^0 mediated reaction with 2-amino-6-chloropurine. This step is notoriously difficult, as previously discussed, with strict reaction conditions required for successful product formation.[5] Such reaction conditions included an inert atmosphere and absence of light. The reaction conditions were optimised as shown in Table **4.2**.

Table 4.2: Experiments A–D showing the optimisation of Pd^0 mediated coupling step of compound **69** with 2-amino-6-chloropurine.

Reaction	Reaction Conditions[*] (Reagents (equiv), Solvent, Temperature (°C), Time, Atmosphere)	Yield (%)
A	NaH (1.3), Purine (1.1), Pd(PPh$_3$)$_4$ (0.05), DMF, 50 °C, 3 h, N$_2$	No reaction (82% acetate SM (**69**) recovered
B	NaH (1.5), Purine (1.3), Pd(PPh$_3$)$_4$ (0.1), DMF/THF, 50 °C, 3 h, N$_2$	29 (slight triphenylphosphine impurity)
C	NaH (1.5), Purine (1.3), Pd(PPh$_3$)$_4$ (0.1), DMF/THF, 50 °C, o/n, Argon	30
D	NaH (1.5), Purine (1.3), Pd(PPh$_3$)$_4$ (0.1), DMF/THF, 60 °C, o/n, Argon	34

[*] All reactions were completed on a 150–200 mg scale.

With such low yields obtained in step 6 of the non-stereoselective synthesis (Section **4.3.4**), the palladium mediated coupling step was optimised further. The reaction conditions used in reaction A were not successful and no reaction occurred, with 82% of starting material recovered. In reaction B, the number of equivalents of NaH and 2-amino-6-chloropurine were increased to 1.5 and 1.3 equivalents respectively. The mole equivalent of Pd catalyst was also increased from 5 to 10 mol %. Alongside this, Pd(PPh$_3$)$_4$ and **69** were stirred for 20 min in THF rather than DMF. The NaH/purine solution remained in DMF and this was added dropwise to the palladium solution. The desired product was obtained in a 29% yield, but with slight triphenylphosphine oxide impurity: A by-product that proved difficult to remove by silica gel column chromatography. The conditions were optimised further as seen in reaction C. The reaction was stirred overnight, rather than for 3 h and under an argon atmosphere, rather than nitrogen. The yield increased to 30%. Finally, in reaction D, all previous conditions remained the same but the temperatures of the reactions were altered. Before addition to the palladium mixture, the NaH/purine solution was heated to 45 °C, shielded from light, for 30 min. Once both solutions were combined, the overnight temperature was increased from 50 to 65 °C. Again, the yield increased slightly to 34%.

With compound **102** in hand, the synthetic route was halted. The availability of this intermediate would allow for the synthesis of ABC analogues, particularly 6-position analogues. These analogues could be synthesised as depicted in Figure **4.17**, where **102** would undergo nucleophilic aromatic addition with amine, thiol or alcohol substrates, followed by 5'-OH deprotection in 1 M NaOH to yield a range of analogues. The synthesis and use of these analogues is discussed in Chapter 5.

Furthermore, compound **102** could be used to form other analogues of ABC, such as cyclopentyl and N^2 analogues.
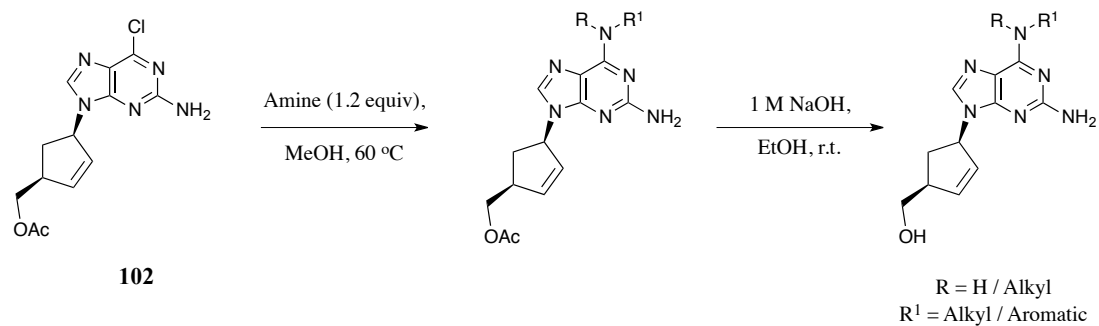
Figure 4.17: Using acetylated Cl-ABC **102**, a range of 6-position amine analogues can be synthesised, followed by 5'-OH deprotection using 1 M NaOH. The reactions conditions employed are shown within the figure.

4.4 Conclusions & Future Work

There has been significant research into the synthesis of carbocyclic nucleosides: The group of compounds to which ABC belongs. There are a range of synthetic protocols to synthesise ABC and its analogues. In order to probe the mechanism of ABC toxicity, it was essential that a synthetic route was utilised and/or modified to produce a suitable ABC intermediate that could be easily employed in the chemical synthesis of ABC analogues.

The initial research conducted did not use a total synthetic route but utilised a route from the parent drug itself. The lack of solubility of ABC in a wide range of solvents significantly hampered synthetic endeavours. However, compounds **20**, **71** and **83** were synthesised, with DH-ABC **20** of most interest. In immunological studies, it was found that only at high concentrations of DH-ABC (50 and 100 μM), did T-cell proliferation and cytokine release occur. The reason for this reduced immunological response is unknown, but it can be suggested that either DH-ABC binds in a different manner to ABC within the HLA-B*57:01 protein. Although still in a non-covalent manner or, due to the lack of the cyclopentyl ring, metabolism to an aldehyde intermediate cannot occur resulting in no further covalent protein/peptide binding. The latter does not explain why at higher concentrations of DH-ABC, T-cells are activated.

With only a small number of analogues synthesised from ABC itself, a *de novo* synthesis was evaluated. MacKeith *et al*. developed a synthetic route from cyclopentadiene, using an enzyme to produce enantiomerically pure material.[29] This

route was modified slightly to synthesise racemic ABC and the enantiomers were separated using chiral HPLC. As with DH-ABC, the enantiomer of ent-ABC was subjected to cross-reactivity assays. It was found that the enantiomer did not cause the ABC-specific T-cell clones to proliferate or release cytokine IFN-γ. Again, the reason for reduced immunogenicity could be due to either altered binding with the HLA-B*57:01 protein or the enantiomer ent-ABC may not be a substrate for ADH, and so metabolism to the reactive aldehyde intermediate would not occur.

Additional synthetic routes were probed – those that did not require enzymatic or chiral HPLC resolution. An asymmetric synthesis using (R,R)-DACH-phenyl Trost ligand was designed. The first 5 steps of this route worked well, but problems became apparent during α-oxidation of the lactone **95**. A variety of reaction conditions were attempted but isolation of the required product was not achieved, with consistently low yields. The synthetic route was also slightly modified, but again, the desired product was not obtained.

Crimmins and co-workers developed an efficient synthetic route to produce ABC, starting with a commercially available chiral oxazolidinone auxiliary. This synthetic route was ideal as several intermediates in this synthesis could be utilised to form ABC analogues, namely acetylated chloro-ABC **102**. Good to excellent yields were achieved for the majority of the synthesis but the Pd^0 mediated allyl coupling proved problematic. Optimisation of the conditions required for this step was conducted and compound **102**, a required intermediate for 6-position analogue synthesis (see Chapter 5) was obtained.

Further research into the successful synthesis of ABC analogues is required so a larger range of analogues (2-, 6-, 2'-, 3'- 4'- and 5'-position) can be synthesised (Figure **4.18 A**).
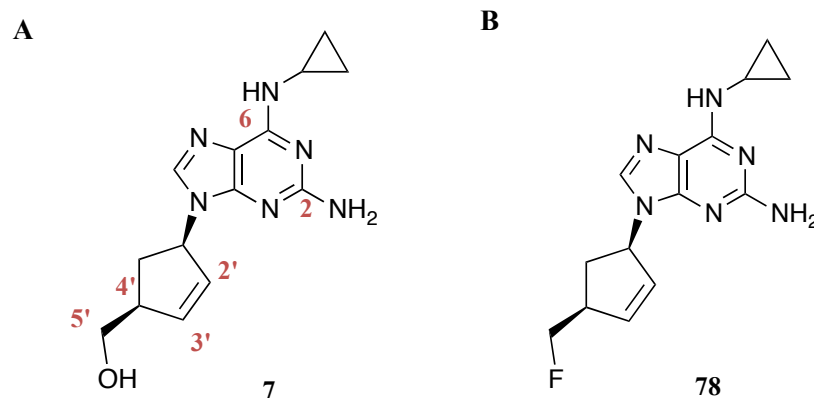
Figure 4.18: Possible positions on ABC **7** where modifications can be made for the synthesis of a wide range of analogues (**A**) and compound **78** which will require further immunological studies to establish any T-cell stimulatory effects in comparison to ABC.

This will allow for a thorough investigation into the mechanisms surrounding ABC toxicity and the moiety contributing to its toxicity can be deduced. Further to this, fluoro compound **78** (Figure **4.18 B**) will need to undergo immunological testing to further investigate the contribution of the primary alcohol to ABC toxicity.

4.5 Experimental

Immunology (cross-reactivity) experiments were conducted and obtained at the University of Liverpool by Catherine Bell and John Farrell (Dr. Dean Naisbitt's research group).

4.5.1 HPLC conditions for separation of ABC enantiomers.

4.5.1.1 Processing of samples for HPLC.

A stock solution (5 mg/mL) of ABC enantiomers was prepared and diluted to its working concentration of 1 mg/mL when required for analysis. These final solutions were injected onto the HPLC column without further processing.

4.5.1.2 Analysis of compounds.

The enantiomers were chromatographed at room temperature using a Chiracel® OD-H analytical column and a fixed eluent system of *n*-hex−EtOH−TFA, 92:8:0.1 (v/v) over 40 min, injecting 0.5 mL for each analysis. The eluent flow rate was 1 mL/min. The LC system consisted of a Gilson Gradient Manual Prep System with 2 × 306 pumps and 118 UV/Vis detector.

4.5.2 Synthesis.
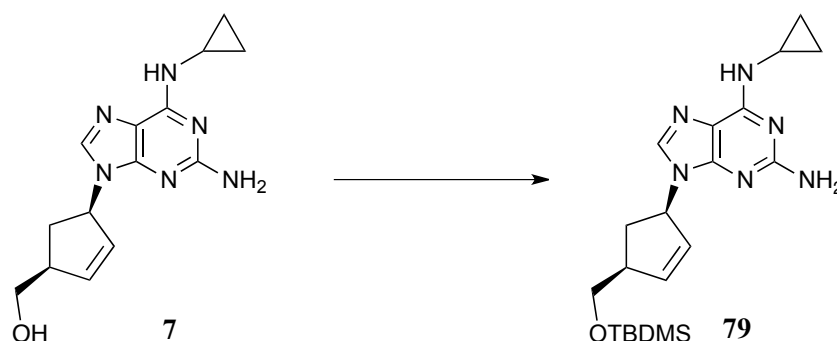
9-(((1*R*,4*S*)-4-((((*tert*-Butyldimethylsilyl)oxy)methyl)cyclopent-2-en-1-yl)-*N*[6]-cyclopropyl-9*H*-purine-2,6-diamine 79:[47] To a solution of ABC (0.60 g, 2.10 mmol) and imidazole (0.30 g, 4.40 mmol) in DMF (10 mL) was added TBDMS−Cl (0.48 g, 3.20 mmol) and the reaction was allowed to stir at room temperature under nitrogen for 24 h. Water was added (5 mL) and the resulting mixture was extracted into EtOAc (3 × 30 mL). The combined organic extracts were washed with H_2O (4 × 120 mL), brine (1 × 100 mL), dried over $MgSO_4$ and the solvent removed *in vacuo*. The crude product was purified by column chromatography (1:24 MeOH–DCM) to yield **79** (0.55 g, 65%) as a bright yellow solid.[47] mp: 91–93 °C. ^{1}H NMR ($CDCl_3$): δ 7.55 (s, 1H), 6.12 (ddd, *J* = 5.6, 2.1, 2.1 Hz, 1H), 5.82 (ddd, *J* = 5.6, 2.1, 2.1 Hz, 1H), 5.75 (br s, 1H), 5.57–5.51 (br m, 1H), 4.78 (br s, 2H), 3.69 (dd, *J* = 9.9, 5.4 Hz, 1H), 3.60 (dd, *J* = 9.9, 5.4 Hz, 1H), 3.03–2.95 (m, 2H), 2.74 (ddd, *J* = 13.8, 8.6, 8.5 Hz, 1H), 1.61 (ddd, *J* = 13.7, 6.3, 6.0 Hz, 1H), 0.89 (s, 9H), 0.87–0.83 (m, 2H), 0.64–0.59 (m, 2H), 0.05 (s, 6H). ^{13}C NMR ($CDCl_3$): δ 163.1, 160.4, 156.7, 151.3, 138.8, 136.0, 130.4, 115.1, 66.3, 59.0, 48.2, 36.9, 35.3, 31.8, 26.3 (3C), 24.0, 18.8, 7.8 (2C), −4.9 (2C), −6.2. *m/z* (ES+) 401.2481 calculated for $C_{20}H_{33}N_6OSi$: [M+H]$^+$

401.2485. IR (cm^{-1}): 3302 (N−H), 3197 (N−H), 1597, 1581 (C=C aromatic), 1238 (C−O), 837 (Si−O).

79 → **82**
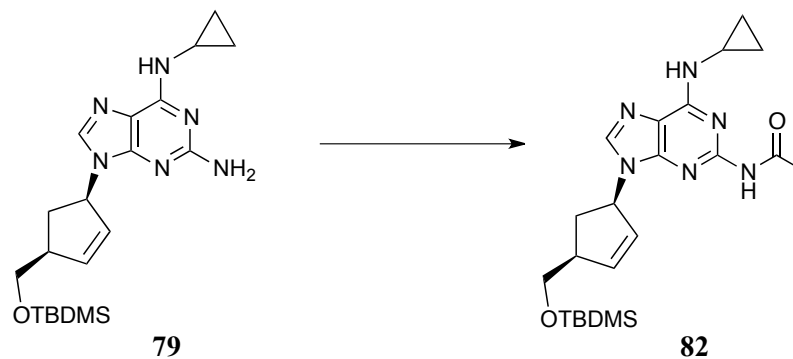
***N*-(9-((1*R*,4*S*)-4-((((*tert*-Butyldimethylsilyl)oxy)methyl)cyclopent-2-en-1-yl)-6-(cyclopropylamino)-9*H*-purin-2-yl)acetamide 82:** To a solution of **79** (0.36 g, 0.90 mmol) in DCM (20 mL) was added NEt$_3$ (0.2 mL, 1.10 mmol) followed by Ac$_2$O (0.1 mL, 1.10 mmol) dropwise at 0 °C. The reaction was allowed to stir at room temperature over 4 h whereupon excess DCM (50 mL) was added. The mixture was washed with H$_2$O (1 × 50 mL) and the organic layer dried over MgSO$_4$ and the solvent removed *in vacuo*. The crude product was purified by column chromatography (1:99 to 1:24 MeOH–DCM) to yield **82** (0.21 g, 53%) as an off-white solid. mp: 153–156 °C. ^{1}H NMR (CDCl$_3$): δ 8.22 (s, br, 1H), 7.74 (s, 1H), 6.15 (ddd, *J* = 5.6, 2.0, 2.0 Hz, 1H), 5.85 (ddd, *J* = 5.6, 2.1, 2.0 Hz, 1H), 5.63–5.59 (br m, 1H), 3.70 (dd, *J* = 10.0, 5.6 Hz, 1H), 3.60 (dd, *J* = 10.0, 5.5 Hz, 1H), 3.04–2.97 (m, 1H), 2.76 (ddd, *J* = 14.0, 7.0, 6.6 Hz, 1H), 2.65 (s, 3H), 2.05–1.99 (m, 1H), 1.65 (ddd, *J* = 14.0, 6.6, 6.6 Hz, 1H), 0.88 (s, 9H), 0.87–0.85 (m, 2H), 0.68–0.61 (m, 2H), 0.05 (s, 6H). ^{13}C NMR (CDCl$_3$): δ 170.1, 156.4, 153.3, 139.2, 138.0, 130.0, 117.0, 66.2, 59.6, 48.3, 35.3, 26.3 (3C), 25.6, 18.8, 7.7, –4.94 (2C). *m/z* (ES+)

443.2601 calculated for $C_{22}H_{35}N_6O_2Si$: $[M+H]^+$ 443.2591. IR (cm^{-1}): 2931 (C−H), 1620, 1466 (C=C aromatic), 1373 (C−N), 1249 (C−O), 833 (Si−O).
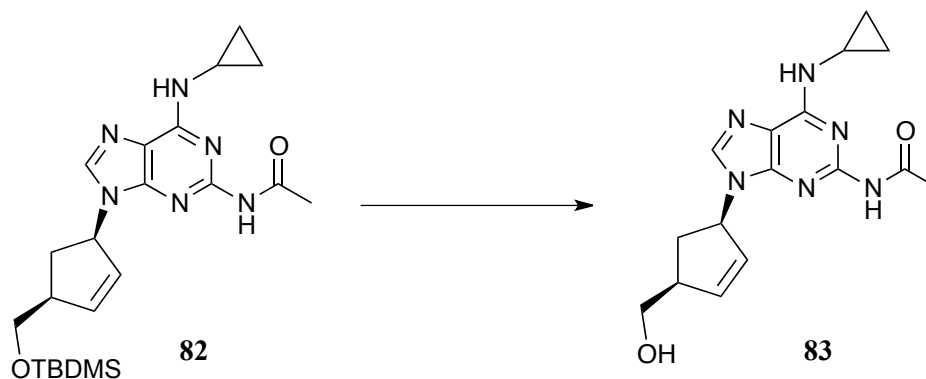
N-(6-(Cyclopropylamino)-9-((1R,4S)-4-(hydroxymethyl)cyclopent-2-en-1-yl)-9H-purin-2-yl)acetamide 83: To a solution of **82** (76 mg, 0.20 mmol) in anhydrous THF (5 mL) was added TBAF (0.2 mL, 1 M in THF) and the reaction was stirred overnight at room temperature. The solvent was removed *in vacuo* and the crude product purified by column chromatography (3:97 MeOH−DCM) to yield **83** (40 mg, 71%) as a colourless solid. mp: 130–133 °C. ^{1}H NMR (CDCl$_3$): δ 8.58 (br s, 1H), 7.76 (s, 1H), 6.75 (br s, 1H), 6.15 (ddd, J = 5.5, 2.1, 2.1 Hz, 1H), 5.86 (ddd, J = 5.5, 2.1, 2.1 Hz, 1H), 5.59–5.55 (br m, 1H), 3.76 (dd, J = 10.7, 4.9 Hz, 1H), 3.67 (dd, J = 10.7, 4.7 Hz, 1H), 3.07–3.06 (m, 1H), 3.02–2.99 (m, 1H), 2.95 (br s, 1H), 2.78 (ddd, J = 14.0, 5.7, 5.5 Hz, 1H), 2.60 (s, 3H), 1.84 (ddd, J = 14.0, 5.7, 5.5 Hz, 1H), 0.86–0.81 (m, 2H), 0.64–0.60 (m, 2H). ^{13}C NMR (CDCl$_3$): δ 170.6, 156.0, 152.9, 138.5, 138.1, 130.2, 116.8, 64.9, 60.2, 53.6, 47.8, 34.1, 25.3, 7.33 (2C). *m/z* (ES+) 328.3690 calculated for $C_{16}H_{20}N_6O_2$: $[M+H]^+$ 329.1726. IR (cm^{-1}): 3209 (N−H), 2978 (C−H), 1736 (C=N), 1608 (C=O), 1462 (C=C aromatic), 1369 (C−N), 1238 (C−O).
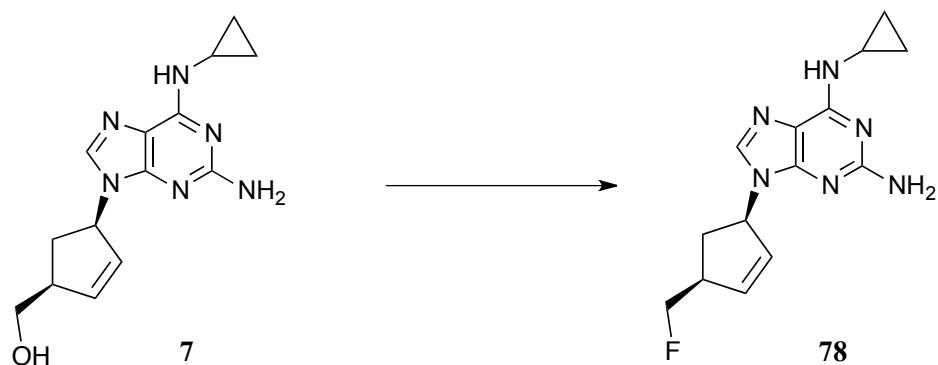
N^6-Cyclopropyl-9-((1R,4S)-4-(fluoromethyl)cyclopent-2-en-1-yl)-9H-purine-2,6-diamine 78: To a solution of NEt$_3$.3HF (3.2 mL, 2.0 mmol) in DCM (15 mL) was added XtalFluor-E® (0.30 g, 1.3 mmol) followed by ABC **7** (0.27 g, 0.9 mmol) at room temperature under nitrogen. The reaction mixture was heated to reflux for 3 h and after cooling, the reaction was quenched with 5% aqueous NaHCO$_3$. The mixture was extracted with DCM (3 × 30 mL) and the combined organic extracts were dried over MgSO$_4$ and the solvent removed *in vacuo*. The crude product was purified by column chromatography (1:99 to 1:19 MeOH–DCM) to yield **78** (8 mg, 3%) as a colourless solid. mp: 140–143 °C. ^{1}H NMR (CDCl$_3$): δ 7.61 (s, 1H), 6.14–6.12 (m, 1H), 5.94–5.92 (m, 1H), 5.52–5.48 (br m, 1H), 4.42 (dddd, J = 47.6, 29.2, 9.0, 4.9 Hz, 2H), 3.59–3.56 (m, 1H), 3.12–3.10 (m, 1H), 2.94–2.91 (m, 1H), 2.79 (ddd, J = 14.0, 8.9, 8.7 Hz, 1H), 1.65 (ddd, J = 12.0, 8.0, 8.0 Hz, 1H), 0.81–0.79 (m, 2H), 0.59–0.56 (m, 2H). *m/z* (ES+) 289.1586 calculated for C$_{14}$H$_{18}$N$_6$F: [M+H]$^+$ 289.1577. IR (cm^{-1}): 3309 (N−H), 3191 (N−H), 1691 (C=N), 1477 (C−H), 1029 (C−F).
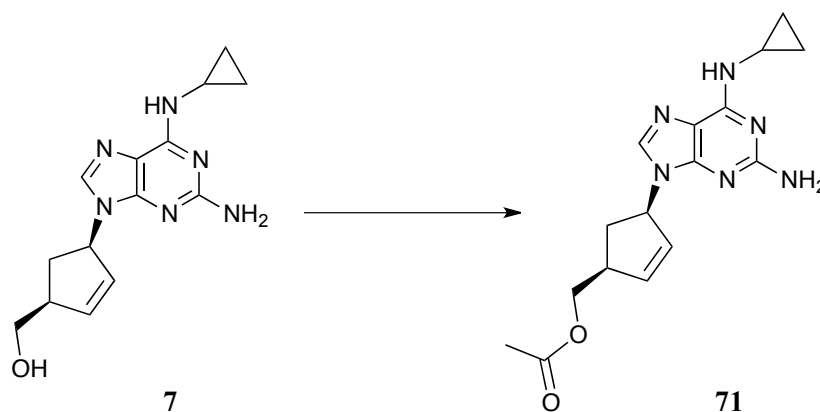
((1*S*,4*R*)-4-(2-Amino-6-(cyclopropylamino)-9*H*-purin-9-yl)cyclopent-2-en-1-yl)methyl acetate 71:[5] To a solution of ABC **7** (0.72 g, 2.5 mmol) in DCM (30 mL) was successively added NEt$_3$ (0.4 mL, 3.0 mmol) and Ac$_2$O (0.3 mL, 3.2 mmol) dropwise at 0 °C. The reaction was allowed to stir for 4 h and was quenched with saturated aqueous NH$_4$Cl. The mixture was extracted into DCM (3 × 20 mL) and the combined organic extracts were dried over MgSO$_4$. The solvent was removed *in vacuo*. The material was purified by column chromatography (1:99 to 3:97 MeOH–DCM) to yield **71** (0.57 g, 69%) as a colourless solid.[5] mp: 119–121 °C. ^{1}H NMR (CDCl$_3$): δ 7.52 (s, 1H), 6.11–6.09 (m, 2H), 5.90 (ddd, *J* = 5.6, 2.2, 2.1 Hz, 1H), 5.56–5.53 (br m, 1H), 4.20 (dd, *J* = 11.0, 5.8, 1H), 4.10 (dd, *J* = 10.9, 5.5 Hz, 1H), 3.16–3.12 (m, 1H), 2.99 (br s, 1H), 2.84 (ddd, *J* = 14.0, 8.8, 8.7 Hz, 1H), 2.07 (s, 3H), 1.64 (ddd, *J* = 14.0, 6.0, 5.9 Hz, 1H), 0.85–0.82 (m, 2H), 0.63–0.60 (m, 2H). ^{13}C NMR (CDCl$_3$): δ 171.4, 160.4, 156.6, 151.1, 137.4, 135.6, 131.1, 115.1, 66.9, 59.1, 44.8, 35.6, 24.1, 21.3, 7.8 (2C). *m/z* (ES+) 329.1724 calculated for C$_{16}$H$_{21}$N$_6$O$_2$: [M+H]$^+$ 329.1726. IR (cm^{-1}): 3320 (N−H), 3197 (N−H), 2943 (C−H), 1732 (C=O), 1585 (C=C aromatic), 1458 (CH$_2$), 1389 (C−N), 1234 (C−O).

237
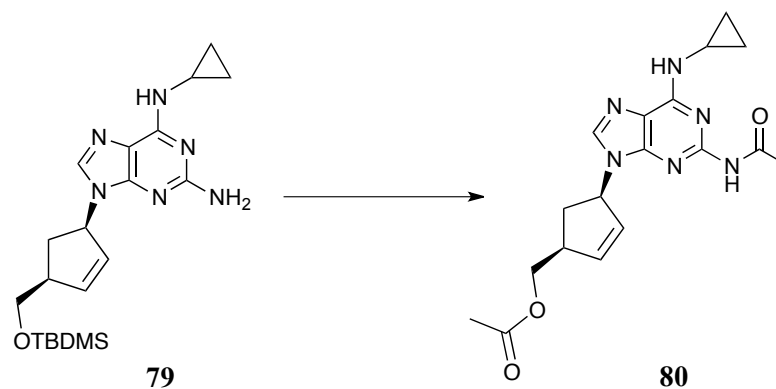
((1*S*,4*R*)-4-(2-Acetamido-6-(cyclopropylamino)-9*H*-purin-9-yl)cyclopent-2-en-1-yl)methyl acetate 80: A colourless solid (23%). mp: 135–137 °C. ^{1}H NMR (CDCl$_3$): δ 7.68 (s, 1H), 6.14 (ddd, *J* = 5.5, 2.1, 2.1 Hz, 1H), 5.94 (ddd, *J* = 5.6, 2.2, 2.1 Hz, 1H) 5.64–5.59 (br m, 1H), 4.19 (dd, *J* = 11.0, 5.8 Hz, 1H), 4.11 (dd, *J* = 11.0, 5.7 Hz, 1H), 3.21–3.14 (m, 1H), 3.09–3.01 (m, 1H), 2.98 (br s, 1H), 2.87 (ddd, *J* = 14.0, 8.8, 8.7 Hz, 1H), 2.06 (s, 3H), 1.77 (s, 3H), 1.66 (ddd, *J* = 14.0, 6.0, 5.9 Hz, 1H), 0.90–0.85 (m, 2H), 0.66–0.62 (m, 2H). ^{13}C NMR (CDCl$_3$): δ 171.3, 169.6, 156.7, 153.5, 138.4, 137.8, 137.6, 130.7, 117.2, 66.8, 59.5, 44.8, 35.7, 26.8, 25.7, 21.3, 7.7. *m/z* (ES+) 371.1830 calculated for C$_{18}$H$_{23}$N$_6$O$_3$: [M+H]$^+$ 371.1832. Anal. calc. for C$_{18}$H$_{22}$N$_6$O$_3$: C, 58.37; H, 5.99; N, 22.69. Found: C, 57.97; H, 6.00; N, 22.21. IR (cm^{-1}): 2974 (C−H), 1736 (C=N), 1608 (C=O), 1462 (C=C aromatic), 1230 (C−O).
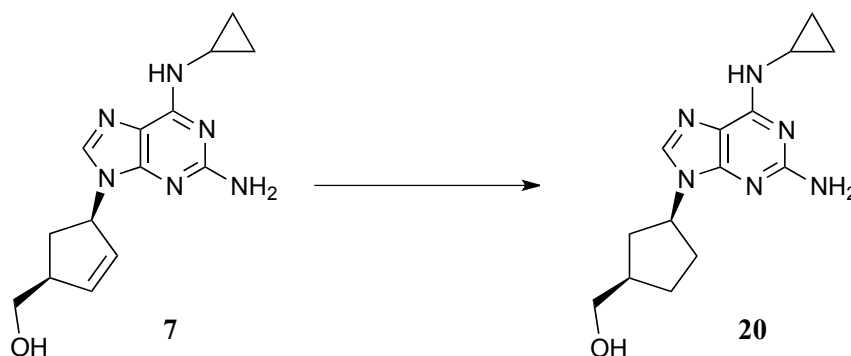
((1*R*,3*S*)-3-(2-Amino-6-(cyclopropylamino)-9*H*-purin-9-yl)cyclopentyl)methanol 20:[1] To a solution of ABC **7** (0.55 g, 2.0 mmol) in MeOH (10 mL) was added 10% Pd/C (cat.). A vacuum was applied to the flask and ensuring the solution was under a hydrogen atmosphere, it was allowed to stir for 4 h at room temperature. The mixture was filtered through celite and the solvent was removed *in vacuo* to obtain compound **20** (0.37 g, 67%) as a yellow solid. mp: 151–153 °C (lit.[1] mp as succinate salt: 170–175 °C). ^{1}H NMR (MeOD): δ 7.81 (s, 1H), 4.76–4.61 (m, 1H), 3.55 (dd, *J* = 6.2, 2.4 Hz, 1H), 3.31–3.21 (m, 1H), 2.86 (dd, *J* = 6.7, 3.3 Hz, 1H), 2.38–2.10 (m, 3H), 2.03–1.90 (m, 1H), 1.90–1.78 (m, 1H), 1.76–1.62 (m, 2H), 0.83–0.75 (m, 2H), 0.58–0.52 (m, 2H). ^{13}C NMR (MeOD): δ 161.7, 157.5, 152.0, 137.3, 114.9, 66.7, 56.5, 41.4, 36.7, 32.6, 27.6, 24.3, 7.6 (2C). *m/z* (ES+) 289.1781 calculated for $C_{14}H_{21}N_6O$: $[M+H]^+$ 289.1777. IR (cm^{-1}): 3330 (N−H), 3213 (N−H), 2955 (C−H), 1580 (C=C aromatic), 1390 (C−N), 1230 (C−O).

84a
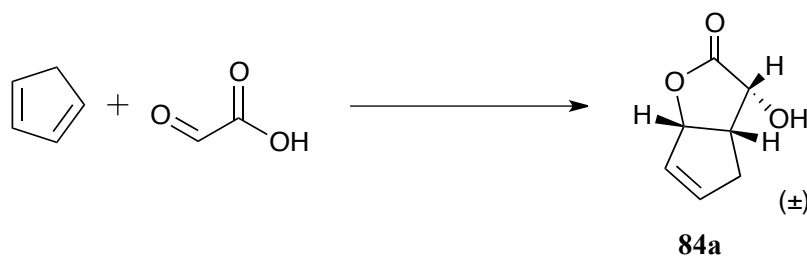
(±)-4-Hydroxy-2-oxabicyclo-[3.3.0]oct-7-en-3-one 84a:[48] Cyclopentadiene (22.0 mL, 0.26 mol) was added to a flask containing glyoxylic acid (20.30 g, 0.27 mol) in H_2O (70 mL) and allowed to stir for 4 days at room temperature. The solution was washed with *n*-hexane (4 × 100 mL). The aqueous layer was saturated with sodium chloride (NaCl) and extracted with EtOAc (12 × 150 mL). The organic layer was reduced to approximately 200 mL and washed with $NaHCO_3$ at 0 °C (2 × 150 mL). The aqueous layer was extracted with EtOAc (4 × 150 mL) and the organic layers were dried over $MgSO_4$ and the solvent removed *in vacuo*. The crude mixture was recrystallised from diethyl ether to yield diastereoisomer **84a** (5.49 g, 18%) as a colourless crystalline solid. Diastereoisomer **84b** remained in solution. mp: 82–87 °C (lit.[48] mp: 83–85 °C). ^{1}H NMR ($CDCl_3$): δ 6.29–6.26 (m, 1H), 5.96–5.93 (m, 1H), 5.35 (dd, J = 6.4, 2.2 Hz, 1H), 4.75 (d, J = 9.4 Hz, 1H), 3.64 (s, br, 1H), 3.27–3.19 (m, 1H), 2.81–2.73 (m, 1H), 2.51–2.43 (m, 1H). ^{13}C NMR ($CDCl_3$): δ 178.0, 142.6, 128.0, 87.9, 69.7, 41.0, 31.3. *m/z* (CI) 158.0820 calculated for $C_7H_{12}NO_3$: [M+NH$_4$]$^+$ 158.0816.   Anal. calc. for $C_7H_8O_3$: C, 59.99; H, 5.75; Found: C, 60.03; H, 5.71. IR (cm^{-1}): 3405 (br, O−H), 1735 (C=O), 1137 (C−O).
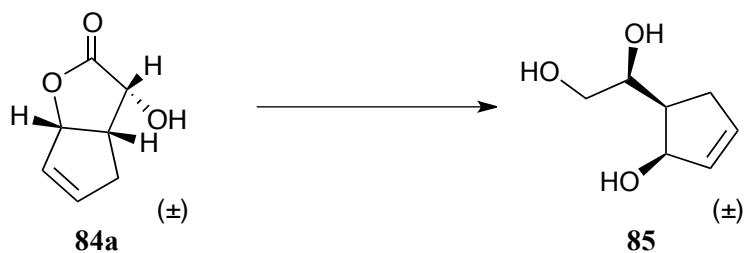
(±)-2-(1,2-Dihydroxyethyl)cyclopent-4-en-1-ol 85:[15] LiAlH$_4$ (1.60 g, 0.04 mol) in THF (40 mL) was cooled to 0 °C. Compound **84a** (5.40 g, 0.04 mol) in THF (20 mL) was added dropwise to the hydride solution and left to stir overnight under nitrogen. The mixture was stirred under reflux for 2 h and allowed to cool to room temperature. Diethyl ether (60 mL) was added dropwise to quench the reaction followed by water (10 mL). The aqueous solution was heated under reflux for a further hour, allowed to cool and filtered through celite. THF (70 mL) and H$_2$O (10 mL) were added to the remaining precipitate and stirred under reflux for another hour. The hot solution was filtered through celite and the combined extracts were concentrated *in vacuo* to yield crude **85** (5.10 g) as a brown oil.[15] ^{1}H NMR (CDCl$_3$): δ 6.06–6.05 (m, 1H), 5.92–5.90 (m, 1H), 4.90–4.88 (m, 1H), 3.93–3.89 (m, 1H), 3.79–3.75 (m, 1H), 3.64–3.60 (m, 1H), 2.34–2.24 (m, 3H). ^{13}C NMR (CDCl$_3$): δ 136.0, 132.7, 76.1, 73.2, 66.2, 44.6, 33.9. *m/z* (CI) 144.17 calculated for C$_7$H$_{12}$O$_3$: [M+NH$_4$]$^+$ 162 Da and [(M+NH$_4$)–H$_2$O]$^+$ 144 Da.
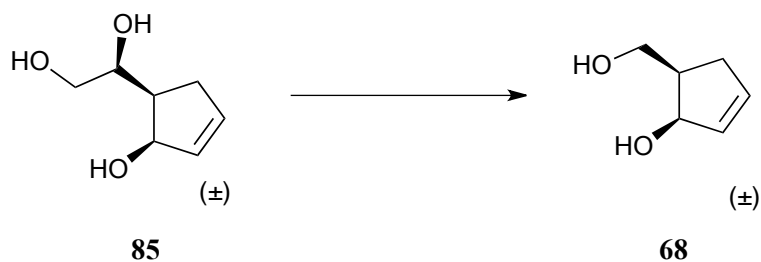
(±)-2-Hydroxymethylcyclopent-4-en-1-ol 68:[29] NaIO$_4$ (2.40 g, 11.0 mmol) was added to a vigorously stirred solution of the crude triol **85** (1.30 g) in a mixture of diethyl ether (50 mL) and H$_2$O (50 mL) at 0 °C. After stirring for 2 h, ethylene glycol (0.3 mL, 4.4 mmol) was added and the mixture was continued to be stirred at 0 °C for an hour. The yellow/orange solution was concentrated *in vacuo* to remove diethyl ether and EtOH (15 mL) was added. The mixture was cooled to 0 °C and NaBH$_4$ (0.40 g, 12.0 mmol) were added. The solution was allowed to stir for 1 h at 0 °C and the EtOH then removed. The orange solution was saturated with NaCl and extracted with EtOAc (6 × 60 mL). The organic extracts were washed with brine, dried over MgSO$_4$ and the solvent removed *in vacuo*. The crude product was purified by column chromatography (2:1 EtOAc–petroleum ether) to yield 0.56 g (59%) of **68** as a clear and colourless oil.[29] ^{1}H NMR (CDCl$_3$): δ 6.02–6.00 (m, 1H), 5.85–5.82 (m, 1H), 4.93–4.91 (m, 1H), 3.85–3.76 (m, 2H), 3.11 (s, br, 1H), 2.81 (s, br, 1H), 2.53–2.44 (m, 1H), 2.41–2.34 (m, 1H), 2.25–2.18 (m, 1H). ^{13}C NMR (CDCl$_3$): δ 135.7, 132.8, 78.3, 63.2, 42.9, 34.0. *m/z* (CI) 113.9962 calculated for C$_6$H$_{12}$NO: [(M+NH$_4$)–H$_2$O]$^+$ 114.0683. IR (cm^{-1}): 3305 (br, O−H), 2929 (C−H).
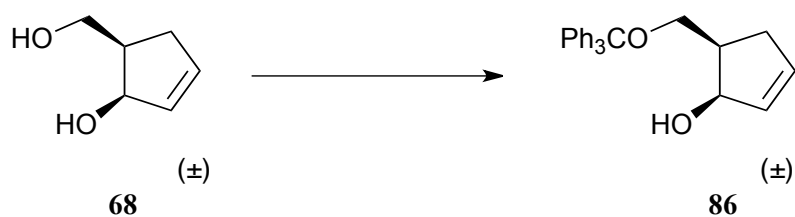
(±)-2-(Triphenylmethyloxymethyl)cyclopent-4-en-1-ol 86:[29] A solution of the diol **68** (0.50 g, 4.5 mmol), CPh$_3$Cl (1.30 g, 4.6 mmol), DMAP (0.06 g, 0.5 mmol), NEt$_3$ (0.6 mL, 4.6 mmol) in DCM (25 mL) was stirred under nitrogen at room temperature overnight. The mixture was washed with saturated aqueous NH$_4$Cl (1 × 30 mL), brine and dried over MgSO$_4$. The solvent was removed in vacuo. The crude product was purified by column chromatography (1:4 EtOAc–*n*-hex) to afford **86** (1.16 g, 72%) as a colourless solid.[29] mp: 97–100 °C. ^{1}H NMR (CDCl$_3$): δ 7.46–7.44 (m, 6H), 7.26–7.22 (m, 9H), 5.98–5.95 (m, 1H), 5.87–5.85 (m, 1H), 4.95–4.92 (m, 1H), 3.43–3.39 (m, 1H), 3.20 (t, *J* = 9.0 Hz, 1H), 2.61–2.53 (m, 1H), 2.38–2.30 (m, 1H), 2.17 (s, br, 1H), 2.13–2.05 (m, 1H). ^{13}C NMR (CDCl$_3$): δ 144.3, 135.2, 133.0, 128.9, 128.1, 127.5, 87.2, 78.1, 63.7, 42.2, 34.6. *m/z* (ES+) 379.1681 calculated for C$_{25}$H$_{24}$O$_2$Na: [M+Na]$^+$ 379.1674. IR (cm^{-1}): 3405 (br, O–H), 2931 (C–H), 1490 & 1446 (C=C aromatic).
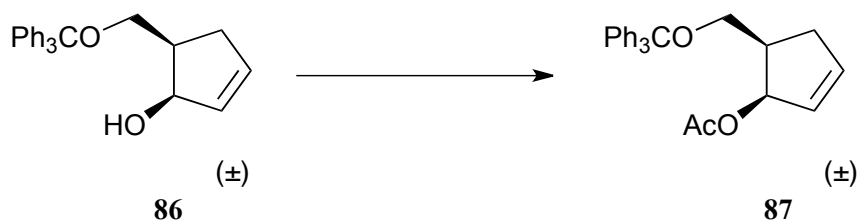
(±)-1-Acetoxy-2-(triphenylmethyloxymethyl)cyclopent-2-en-1-yl 87:[29] Mono-protected diol **86** (1.20 g, 3.2 mmol) was allowed to stir overnight at room temperature in a mixture of pyridine (2.0 mL, 25.0 mmol) and Ac$_2$O (2.4 mL, 25

mmol). Saturated aqueous NH_4Cl (10 mL) was added and the solution extracted with diethyl ether (2 × 15 mL). The combined organic layers were washed with sodium bicarbonate ($NaHCO_3$) and brine. The organic layer was dried over $MgSO_4$ and the solvent removed *in vacuo* to yield **87** (0.77 g, 39%) as a pale yellow solid.[29] mp: 121–124 °C. ^{1}H NMR ($CDCl_3$): δ 7.44–7.41 (m, 6H), 7.25–7.21 (m, 9H), 6.09–6.07 (m, 1H), 5.86–5.83 (m, 1H), 5.80–5.77 (m, 1H), 3.24–3.14 (m, 2H), 2.74–2.65 (m, 1H), 2.50–2.42 (m, 1H), 2.19–2.13 (m, 1H), 1.78 (s, 3H). ^{13}C NMR ($CDCl_3$): δ 171.0, 144.6, 137.8, 130.0, 129.1, 128.1, 127.3, 86.8, 78.8, 62.8, 41.8, 35.3, 21.5. *m/z* (ES+) 421.1779 calculated for $C_{27}H_{26}O_3Na$: $[M+Na]^+$ 421.1780. IR (cm^{-1}): 1724 (C=O), 1488 & 1444 (C=C aromatic), 1375 (C−O).

87   **88**
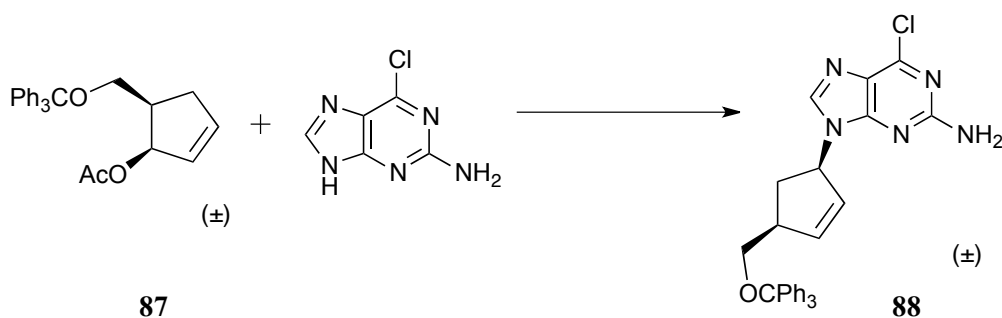
(±)-2-Amino-6-chloro-9-((4-(triphenylmethyloxymethyl)-cyclopent-2-en-1-yl)purine 88:[4] NaH (washed in anhydrous *n*-hex, 30 mg, 1.1 mmol) was dissolved in DMF (2 mL) and 2-amino-6-chloropurine (0.10 g, 0.6 mmol) in DMF (2 mL) was added to the NaH solution. The reaction was allowed to stir at room temperature in the dark, under argon, for 30 min. Acetate **87** (0.10 g, 0.3 mmol) was dissolved in DMF (5 mL) and $Pd(PPh_3)_4$ (0.30 g, 0.3 mmol) was added. The hydride mixture was added to this flask *via* a cannula and the mixture was allowed to stir overnight at 50 °C, in the dark, under argon. The reaction mixture was allowed to cool to room

temperature and extracted with EtOAc (6 × 15 mL), dried over MgSO$_4$ and the solvent removed *in vacuo*. The crude product was purified by column chromatography (1:1 EtOAc–*n*-hex) to yield **88** (0.17 g, 17%) as a colourless solid. mp: 85–89 °C ((–)-enantiomer lit.[4] mp: 82–90 °C). ^{1}H NMR (CDCl$_3$): δ 7.65 (s, 1H), 7.43–7.40 (m, 6H), 7.27–7.21 (m, 9H), 6.27–6.25 (m, 1H), 5.84–5.83 (m, 1H), 5.56–5.52 (br m, 1H), 5.20 (s, 2H), 3.18–3.13 (m, 3H), 2.80–2.72 (m, 1H), 1.62–1.56 (m, 1H). ^{13}C NMR (CDCl$_3$): δ 159.3, 153.9, 151.5, 144.3, 143.8, 141.9, 140.9, 129.3, 129.0, 128.9, 128.7, 87.0, 66.5, 60.8, 46.1, 35.7. *m/z* (ES+) 530.1729 calculated for C$_{30}$H$_{26}$ClN$_5$ONa: [M+Na]$^+$ 530.1724. IR (cm^{-1}): 3316 (N–H), 3239 (N–H), 2919 (C–H), 1608 (C=N), 1450 & 1403 (C=C aromatic), 1203 (C–O), 701 (C–Cl).
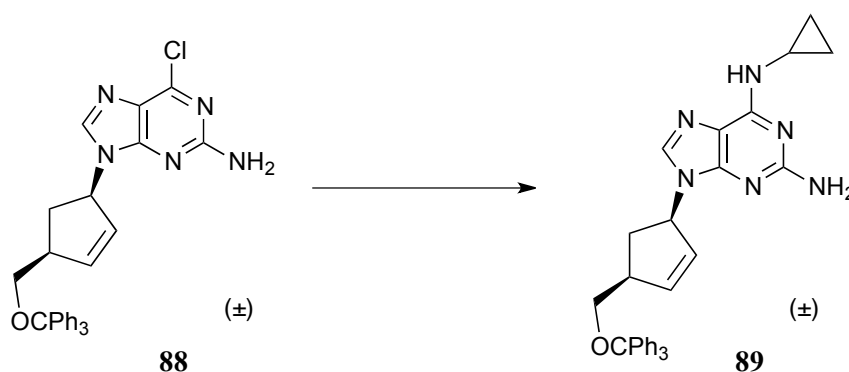
(±)-2-Amino-6-(cyclopropylamino)-9-(4-(triphenylmethyloxymethyl)-cyclopent-2-en-1-yl)purine 89: To an ice cold solution of the purine **89** (0.10 g, 0.2 mmol) in MeOH (5 mL) was added cyclopropylamine (0.1 mL, 1.4 mmol) and the resulting solution was stirred at 50 °C overnight. After removal of the solvent, the crude product was purified by column chromatography (7:3 EtOAc–*n*-hex) to afford **89** (60 mg, 72%) as an off-white solid. mp: 119–123 °C. ^{1}H NMR (CDCl$_3$): δ 7.43–7.41 (m, 6H), 7.36 (s, 1H), 7.31–7.23 (m, 9H), 6.22–6.19 (m, 1H), 5.84–5.82 (m, 1H),

5.54–5.50 (br m, 1H), 3.15–3.12 (m, 2H), 3.09–3.05 (m, 1H), 3.03–2.96 (m, 1H), 2.77 (ddd, J = 13.9, 8.3, 8.2 Hz, 1H), 1.59–1.52 (m, 1H), 0.88–0.82 (m, 2H), 0.62–0.58 (m, 2H). ^{13}C NMR (CDCl$_3$): δ 156.6, 144.4, 138.8, 130.2, 128.9, 128.2, 127.5, 115.2, 86.9, 66.8, 59.1, 46.1, 36.1, 30.1, 24.1, 7.8. *m/z* (ES+) 529.2720 calculated for C$_{33}$H$_{33}$N$_6$O: [M+H]$^+$ 529.2716.
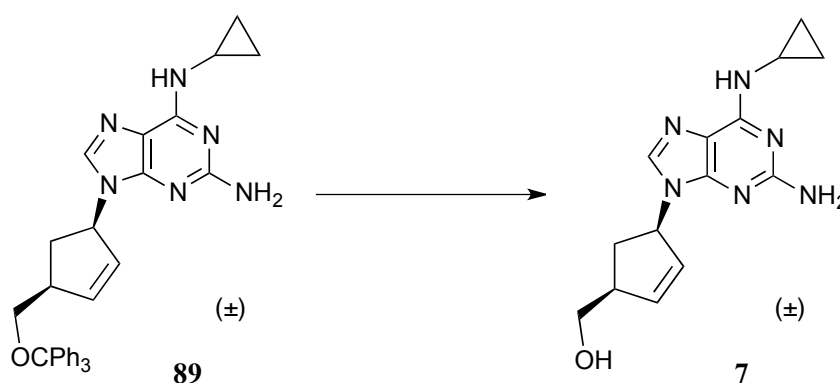
(±)-4-[2-Amino-6-(cyclopropylamino)-9*H*-purin-9-yl]cyclopent-2-en-1-yl methanol 7:[49] A solution of the purine **89** (0.10 g, 0.2 mmol) in 80% AcOH (2.0 mL, 35.0 mmol) was allowed to stir for 48 h at 50 °C. The solvent was removed *in vacuo* and the crude product purified by column chromatography (1:19 MeOH−DCM) to yield racemic **7** (28 mg, 52%) as an off-white powder. mp: 155–159 °C ((−)-enantiomer lit.[49] mp: 165 °C). ^{1}H NMR (DMSO-d$_6$): δ 7.48 (s, 1H), 6.12–6.10 (m, 1H), 5.77–5.74 (m, 1H), 5.44–5.39 (br m, 1H), 3.92 (dd, J = 11.0, 3.7 Hz, 1H), 3.81 (dd, J = 11.0, 2.9 Hz, 1H), 3.16–3.10 (m, 1H), 3.01–2.94 (m, br, 1H), 2.79 (ddd, J = 14.7, 9.8, 8.5 Hz, 1H), 2.22 (ddd, J = 14.6, 5.6, 5.0 Hz, 1H), 0.87–0.82 (m, 2H), 0.62–0.58 (m, 2H). ^{13}C NMR (DMSO-d$_6$): δ 160.4, 156.3, 138.3, 135.2, 130.4, 113.9, 64.5, 58.5, 55.3, 48.0, 34.7, 6.8 (2C). *m/z* (ES+) 287.1618 calculated for C$_{14}$H$_{18}$N$_6$O: [M+H]$^+$ 287.1620. IR (cm^{-1}): 3328 & 3250 (O−H & N−H), 2977 (C−H), 1592 (C=N), 1481 & 1427 (C=C aromatic).

90

Cyclopent-2-enol 90:[50] To an ice-cold solution of the 2-cyclopenten-1-one (5.1 mL, 0.06 mol) and CeCl$_3$.7H$_2$O (29.80 g, 0.08 mol) in MeOH (100 mL) was added NaBH$_4$ (2.50 g, 0.07 mol) slowly over 30 min with vigorous stirring. The mixture was allowed to stir at room temperature for 1 h followed by dropwise addition of water. The mixture was extracted with diethyl ether (3 × 100 mL) and the organic layer was dried over MgSO$_4$. The solvent was removed *in vacuo* to yield crude **90** (4.10 g) as an off-white volatile liquid.[50] ^{1}H NMR (CDCl$_3$): δ 6.00–5.97 (ddd, *J* = 5.5, 2.1, 2.1 Hz, 1H), 5.85–5.81 (ddd, *J* = 5.5, 2.2, 2.1 Hz, 1H), 4.87–4.86 (m, br, 1H), 2.55–2.46 (m, 1H), 2.32–2.22 (m, 2H), 1.73–1.65 (m, 1H). *m/z* (CI) 84.12 calculated for C$_5$H$_8$O: [(M+NH$_4$)–H$_2$O]$^+$ 84.

90   **91**

Cyclopent-2-en-1-yl acetate 91:[50] Cyclopent-2-enol **90** (2.20 g, 26.0 mmol) and DMAP (0.30 g, 2.8 mmol) were dissolved in DCM (60 mL) and cooled to 0 °C. NEt$_3$ (5.1 mL, 37.0 mmol) and Ac$_2$O (3.6 mL, 38.0 mmol) were added at 0 °C and the solution were allowed to stir overnight at room temperature. The mixture was diluted with diethyl ether (100 mL) and washed with 2 M HCl (2 × 60 mL) and NaHCO$_3$ (1 × 60 mL). The organic layer was dried over MgSO$_4$ and the solvent removed *in vacuo*. The crude product was purified by column chromatography (100% diethyl ether) to yield **91** (1.90 g, 58%) as a clear and colourless volatile

liquid.[50] ^{1}H NMR (CDCl$_3$): δ 6.12–6.09 (m, 1H), 5.84–5.81 (m, 1H), 5.72–5.67 (m, 1H), 2.57–2.47 (m, 1H), 2.37–2.24 (m, 2H), 2.03 (s, 3H), 1.87–1.78 (m, 1H). ^{13}C NMR (CDCl$_3$): δ 171.4, 137.9, 129.6, 80.8, 31.4, 30.1, 21.7. *m/z* (CI) 126.15 calculated for C$_7$H$_{14}$NO$_2$: [M+NH$_4$]$^+$ 144.0. IR (cm^{-1}): 2977 (C−H), 1731 (C=O), 1241 (C−O).

91   **92**
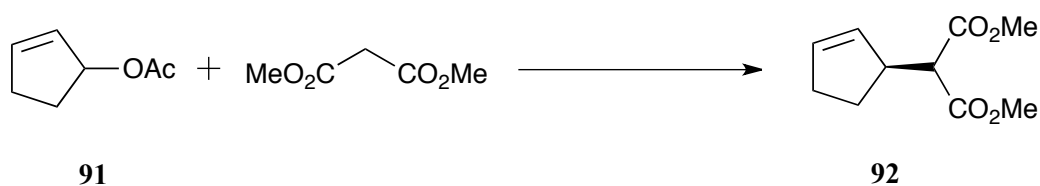
(*S*)-Dimethyl-2-(cyclopent-2-en-1-yl)malonate 92:[34] To a suspension of CsCO$_3$ (51.30 g, 0.16 mol) in anhydrous DCM (125 mL) was added dimethyl malonate (13.6 mL, 0.12 mol) and solution was allowed to stir at room temperature for 1 h under nitrogen. Tetrahexylammonium bromide (THAB, 42.90 g, 0.10 mol) was added and the solution was allowed to stir for a further 20 min. Anhydrous DCM (50 mL) was added to allylpalladium(II)chloride dimer (0.40 g, 0.1 mmol) and (*R,R*)-DACH-phenyl Trost ligand (1.80 g, 2.6 mmol) under nitrogen and stirred for 10 min. Compound **91** (5.00 g, 0.04 mol) in DCM (5 mL) was added and the solution was allowed to stir for a further 10 min. The dimethyl malonate solution was added to the palladium mixture over 1.5 h and the solution were allowed to stir under nitrogen at room temperature for a further hour. The reaction was quenched with water and extracted with diethyl ether (4 × 200 mL), dried over MgSO$_4$ and the solvent removed *in vacuo*. The crude product was purified by column chromatography (1:9 EtOAc−*n*-hex) to obtain **92** (6.83 g, 88%) as a clear volatile liquid. ^{1}H NMR (CDCl$_3$): δ 5.85–5.82 (m, 1H), 5.67–5.64 (m, 1H), 3.74 (s, 6H), 3.42–3.35 (m, 1H), 3.28 (d, *J* = 9.6 Hz, 1H), 2.42–2.27 (m, 2H), 2.18–2.09 (m, 1H), 1.64–1.55 (m, 1H).

^{13}C NMR (CDCl$_3$): δ 169.5, 133.5, 131.7, 57.0, 52.7, 45.8, 32.1, 28.2. *m/z* (CI) 199.22 calculated for C$_{10}$H$_{16}$O$_4$: [M+H]$^+$ 199.3. IR (cm^{-1}): 2954 (C−H), 1735 (C=O), 1149 (C−O). [α]$_D$ −74.0° (*c* = 3.0 in DCM), lit. [α]$_D$ −71.65° (*c* = 3.09 in DCM).[34]

92   **93**

(*R*)-2-(Cyclopent-2-en-1-yl)acetic acid 93:[51] The di-ester **92** (6.40 g, 30.0 mmol) in KOH (15 mL, 2.5 M) was heated under reflux for 4 h. The resulting solution was cooled to room temperature then to 0 °C and acidified to pH 1 with 3 M HCl. The acidified solution was extracted with diethyl ether (4 × 50 mL), dried over MgSO$_4$ and the solvent removed *in vacuo* to obtain the crude dicarboxylic acid as a colourless solid. This solid was heated (130–140 °C) until a liquid was obtained and this was further heated at 160 °C for 1 h. The crude product was purified *via* column chromatography (100% diethyl ether) to yield **93** (2.95 g, 72%) as a clear and colourless slightly volatile liquid. (For (*S*)-enantiomer).[51] ^{1}H NMR (CDCl$_3$): δ 5.80–5.77 (m, 1H), 5.70–5.68 (m, 1H), 3.14–3.06 (m, 1H), 2.46–2.41 (m, 2H), 2.40–2.27 (m, 2H), 2.20–2.11 (m, 1H), 1.53–1.45 (m, 1H). ^{13}C NMR (CDCl$_3$): δ 179.8, 133.8, 132.2, 42.2, 40.6, 32.2, 30.0. *m/z* (CI) 126.15 calculated for C$_7$H$_{10}$O$_2$: [M+NH$_4$]$^+$ 144.

93   **94**

(1R,5S,8S)-8-Iodo-2-oxabicyclo-[3.3.0]-oct-3-one 94:[52] To a mixture of **93** (0.60 g, 4.4 mmol) and saturated aqueous NaHCO$_3$ (9.0 mL) in THF (10 mL) was added a solution of I$_2$ (2.40 g, 9.6 mmol) and KI (4.80 g, 29.0 mmol) in H$_2$O (13 mL) and the solution was stirred for 4 h at room temperature. The resulting mixture was quenched dropwise with saturated aqueous sodium sulfite (Na$_2$SO$_3$) solution until the dark brown solution became clear and colourless. The solution was then extracted with diethyl ether (4 × 50 mL), dried over MgSO$_4$ and the solvent removed *in vacuo*. The resulting crude oil was recrystallised from 1:1 EtOAc–pentane to yield **94** (1.05 g, 94%) as an off-white solid. mp: 62–65 °C (lit.[52] mp for (1S,5R,8R)-enantiomer: 69–70 °C). ^{1}H NMR (CDCl$_3$): δ 5.21 (d, J = 6.0 Hz, 1H), 4.48 (d, J = 5.0 Hz, 1H), 3.21–3.13 (m, 1H), 2.90 (dd, J = 18.1, 9.7 Hz, 1H), 2.49–2.42 (m, 1H), 2.41 (d, J = 2.1 Hz, 1H), 2.36 (d, J = 2.1 Hz, 1H), 2.20–2.02 (m, 2H), 1.62–1.57 (m, 1H). ^{13}C NMR (CDCl$_3$): δ 177.0, 92.8, 36.5 (2C), 35.0, 32.6, 29.8. *m/z* (ES+) 274.9544 calculated for C$_7$H$_9$IO$_2$Na: [M+H]$^+$ 274.9545. Anal. calc. for C$_7$H$_9$IO$_2$: C, 33.36; H, 3.60. Found: C, 33.79; H, 3.59. IR (cm^{-1}): 2965 (C−H), 1770 (C=O), 1168 (C−O).

94   **95**

(1R,5S)-2-Oxabicyclo-[3.3.0]oct-7-en-3-one 95:[53] To a solution of iodo-lactone **94** (5.30 g, 20.0 mmol) in THF (60 mL) was added DBU (7.8 mL, 50.0 mmol) and the solution was refluxed under nitrogen overnight. The remaining solution was cooled to room temperature, diluted with diethyl ether (60 mL) and cooled to 0 °C whereupon saturated aqueous NH_4Cl solution (60 mL) was added slowly. The layers were separated and the aqueous layer was extracted with diethyl ether (3 × 60 mL). The combined organic extracts were dried over $MgSO_4$ and the solvent removed *in vacuo*. The crude product was purified by column chromatography (1:1 EtOAc–*n*-hex) to yield **95** (1.24 g, 48%) as a clear and colourless oil.[53] ^{1}H NMR (CDCl$_3$): δ 6.10–6.08 (m, 1H), 5.90–5.87 (m, 1H), 5.55–5.51 (m, 1H), 3.19–3.10 (m, 1H), 2.95–2.85 (m, 1H), 2.82–2.73 (m, 1H), 2.36–2.28 (m, 2H). ^{13}C NMR (CDCl$_3$): δ 177.6, 137.3, 129.5, 90.0, 60.8, 40.0, 36.5, 35.5. *m/z* (CI) 124.14 calculated for $C_7H_8O_2$: [M+NH$_4$]$^+$ 142. IR (cm^{-1}): 2962 (C–H), 1770 (C=O), 1164 (C–O), 1002 (=C–H).

96
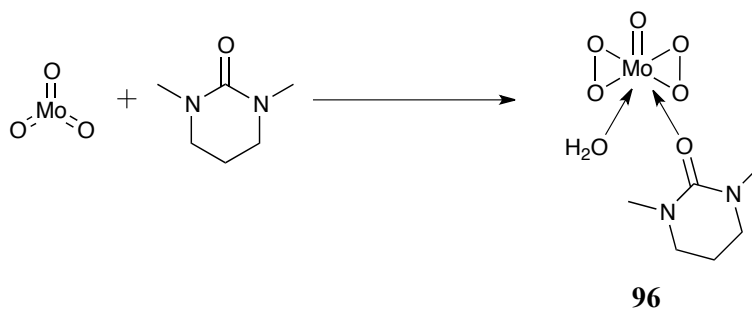
MoO₅.DMPU.H₂O 96: MoO_3 (10.05 g, 0.07 mol) was dissolved in 30% H_2O_2 (40 mL) and heated slowly, ensuring the internal temperature was consistently kept between 30–40 °C, for 4 h. The yellow solution was cooled to room temperature and filtered though celite, washing with H_2O. The filtrate was cooled to 10 °C and DMPU (8.4 mL, 0.07 mol) was added over 10 min. Stirring at 10 °C was continued for a further 10 min and the solid filtered under suction. The solid material was recrystallised with MeOH to yield the product **96** (11.60 g, 52%) as a partially suspended yellow solid.

96   **97**
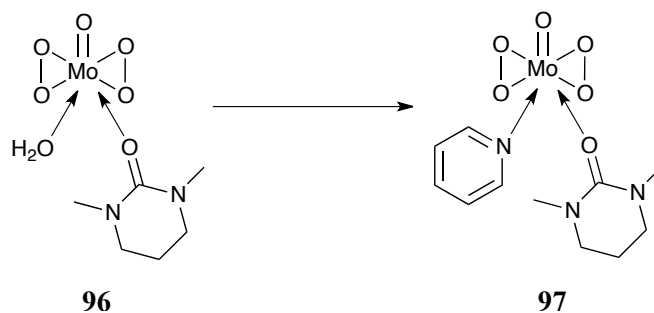
MoO₅.DMPU.Py 97:[43] Complex **96** was dried for 24 h over P_2O_5 in a vacuum dessicator, shielded from light. The remaining product (MoO_5.DMPU, 7.50 g, 0.02 mol) was dissolved in THF (50 mL) and under vigorous stirring, pyridine (1.6 mL, 0.02 mol) was added dropwise over 10 min at room temperature. The product was filtered and washed with anhydrous THF and dried in a vacuum desiccator shielded from light to yield the product **97** (4.80 g, 51%) as a fine yellow crystalline solid.

mp: 93–94 °C (lit.[43] mp: 93.5–94.5 °C). Anal. calc. for $C_{11}H_{17}MoN_3O_6$: C, 34.47; H, 4.47; N, 10.64. Found: C, 34.32; H, 4.44; N, 10.64. IR (cm^{-1}): 1595 (C=N), 1542 (C=C aromatic), 955 (Mo=O), 866 (O−O).

100
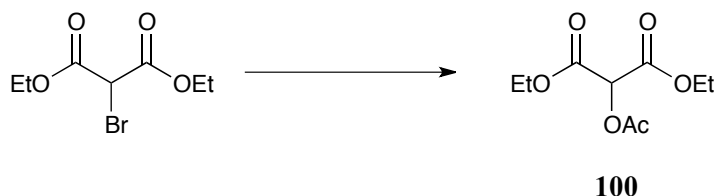
Diethyl-2-acetoxymalonate 100:[54] To a solution of diethylbromomalonate (0.7 mL, 4.0 mmol) in DMF (15 mL) was added to NaOAc (0.51 g, 6.0 mmol) and the solution was stirred at room temperature for 2 h whereupon water (2 mL) was added. The mixture was extracted with EtOAc (3 × 20 mL) and the combined organic extracts were washed with H_2O (3 × 40 mL), brine and dried over $MgSO_4$. The solvent was removed *in vacuo*. The crude product was purified by column chromatography (1:3 EtOAc–*n*-hex) to yield **100** (0.85 g, 93%) as a colourless liquid.[54] ^{1}H NMR (CDCl$_3$): δ 5.52 (s, 1H), 4.33–4.26 (m, 4H), 2.23 (s, 3H), 1.31 (t, *J* = 6.8 Hz, 6H). *m/z* (CI) 218.2 calculated for $C_9H_{14}O_6$: [M+[NH$_4$]$^+$ 236.3. IR (cm^{-1}): 2966 (C−H), 1766 (C=O), 1165 (C−O).

53   **68**
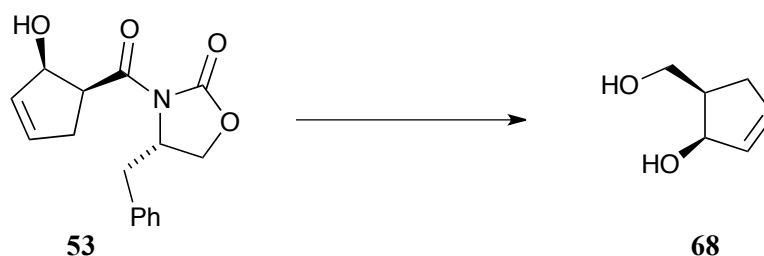
(1R,5R)-5-(Hydroxymethyl)cyclopent-2-enol 68:[5] To a suspension of LiBH$_4$ (6.3 mL, 0.19 mol) in THF (20 mL) cooled to 0 °C was added to a solution of **53** (1.20 g,

4.0 mmol) in THF (20 mL) and MeOH (0.5 mL, 0.01 mol) dropwise. The resulting solution was stirred at 0 °C for 1 h and allowed to warm to room temperature whereupon 10% NaOH (6.3 mL) was added and stirring was continued until the solution became clear. The mixture was extracted with diethyl ether (3 × 30 mL) and the aqueous layer was acidified with 1 M HCl and further washed with diethyl ether. The combined organic extracts were dried over MgSO$_4$. The solvent was removed *in vacuo* and the crude product **68** (yellow liquid) was used without purification.[5] ^{1}H NMR (CDCl$_3$): δ 5.94–5.92 (m, 1H), 5.87–5.84 (m, 1H), 5.10–5.06 (m, 1H), 4.03 (dd, J = 10.8, 7.1 Hz, 1H), 3.78 (dd, J = 10.8, 6.9 Hz, 1H), 2.66–2.58 (m, 1H), 2.51–2.42 (m, 1H), 2.27–2.20 (m, 1H). ^{13}C NMR (CDCl$_3$): δ 135.7, 132.8, 78.1, 63.9, 43.0, 34.0. *m/z* (CI) 114.07 calculated for C$_6$H$_{10}$O$_2$: [M+[NH$_4$]$^+$–H$_2$O] 114.1.

68   **69**

((1R,2R)-2-Acetoxycyclopent-3-en-1-yl)methyl acetate 69:[5] To a solution of **68** (0.50 g) in DCM (25 mL) was added DMAP (0.11 g, 0.8 mmol), NEt$_3$ (1.8 mL, 13.0 mmol) and Ac$_2$O (1.2 mL, 13.0 mmol) at 0 °C. The solution was allowed to stir overnight at room temperature whereupon saturated aqueous NH$_4$Cl was added. The quenched mixture was extracted into DCM (3 × 30 mL) and the combined organic extracts were dried over MgSO$_4$. The crude product was purified by column chromatography (1:9 EtOAc−*n*-hex) to yield compound **69** (0.34 g) as a yellow oil.[5] ^{1}H NMR (CDCl$_3$): δ 6.12–6.09 (m, 1H), 5.87–5.84 (m, 1H), 5.78–5.70 (m, 1H), 4.22 (dd, J = 10.9, 8.3 Hz, 1H), 4.14 (dd, J = 11.0, 7.1 Hz, 1H), 2.75–2.66 (m, 1H), 2.53–2.46 (m, 1H), 2.29–2.21 (m, 1H), 2.05 (s, 3H), 2.03 (s, 3H). ^{13}C NMR (CDCl$_3$): δ

171.5, 171.1, 137.2, 129.8, 78.5, 63.8, 39.9, 35.0, 21.5, 21.4. *m/z* (ES+) 221.08 calculated for $C_{10}H_{14}O_4Na$: $[M+Na]^+$ 221.1. IR (cm^{-1}): 1735 (C=O), 1373 (C−H), 1241 (C−O).

69

102
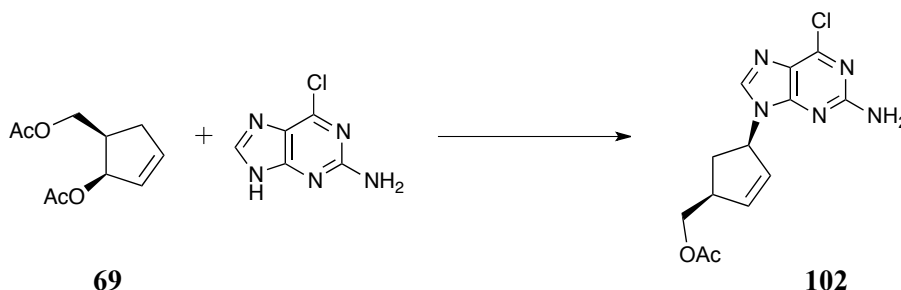
((1*S*,4*R*)-4-(2-Amino-6-chloro-9*H*-purin-9-yl)cyclopent-2-en-1-yl)methyl acetate 102:[5] To a stirred solution of NaH (60% dispersed in mineral oil, 0.07 g, 1.6 mmol) in DMF (3 mL) was added 2-amino-6-chloropurine (0.23 g, 1.4 mmol). The resulting mixture was allowed to stir at 45 °C under argon for 30 min and then cooled to room temperature. In a separate flask, compound **69** (0.25 g, 1.3 mmol) was added to a solution of Pd(PPh₃)₄ (0.14 g, 10 mol %) in THF (3 mL) and was allowed to stir at room temperature under argon for 20 min. This solution was added dropwise to the NaH solution and heated to 65 °C overnight under argon, shielded from light. The resulting solution was extracted into DCM and the combined organic extracts were washed with brine and dried over MgSO₄. The solvent was removed *in vacuo*. The crude product was purified by column chromatography (1:1 EtOAc−*n*-hex) to yield **102** (0.13 g, 34%) as a colourless solid.[5] mp: 119–121 °C. ¹H NMR (CDCl₃): δ 7.83 (s, 1H), 6.16 (ddd, *J* = 5.6, 2.2, 2.2 Hz, 1H), 5.91 (ddd, *J* = 5.6, 2.2, 2.1 Hz, 1H), 5.62–5.56 (br m, 1H), 4.23 (dd, *J* = 10.0, 5.6 Hz, 1H), 4.16 (dd, *J* = 10.0, 5.5 Hz, 1H), 3.22–3.16 (m, 1H), 2.87 (ddd, *J* = 14.0, 6.4, 6.4 Hz, 1H), 2.08 (s, 3H), 1.71 (ddd, *J* = 14.0, 6.4, 6.3 Hz, 1H). ¹³C NMR (CDCl₃): δ 170.3, 159.6, 153.5, 151.4, 141.9, 138.9, 130.1, 128.5, 65.1, 59.7, 45.0, 34.5, 21.3. *m/z* (ES+) 330.0729

calculated for $C_{13}H_{14}N_5O_2Na^{35}Cl$: $[M+Na]^+$ 330.0734. IR (cm^{-1}): 3340 $(N-H)$, 1720 $(C=O)$, 1615, 1560 & 1471 $(C=C$ aromatic$)$, 1261 $(C-O)$.

4.5.3 Immunology studies.

For generation of ABC-specific T-cell clones and assessment of cross-reactivity of ABC, ent-ABC and **20** using the IFN-γ ELISpot assay, the procedure in Chapter 3, Section **3.5.2** was followed.

4.5.3.1 Cross-reactivity of ABC-specific T-cell clones using LTT assay.

ABC-specific T-cell clones were generated according to Section **3.5.2**. ABC-specificity of T-cell clones $(5 \times 10^4$ cells/well$)$ was determined by addition of 50 μM abacavir and 1×10^4 irradiated autologous EBV-transformed B-cells to serve as APCs. $[^3H]$-Thymidine (0.5 μCi/well) was added after 48 h and proliferation determined via scintillation counting. Clones with a stimulation index (cpm in drug treated wells/cpm in control wells) of greater than 2 were expanded by repeated mitogen stimulation and were maintained in IL-2 containing medium for several weeks.

4.6 Supplementary Information
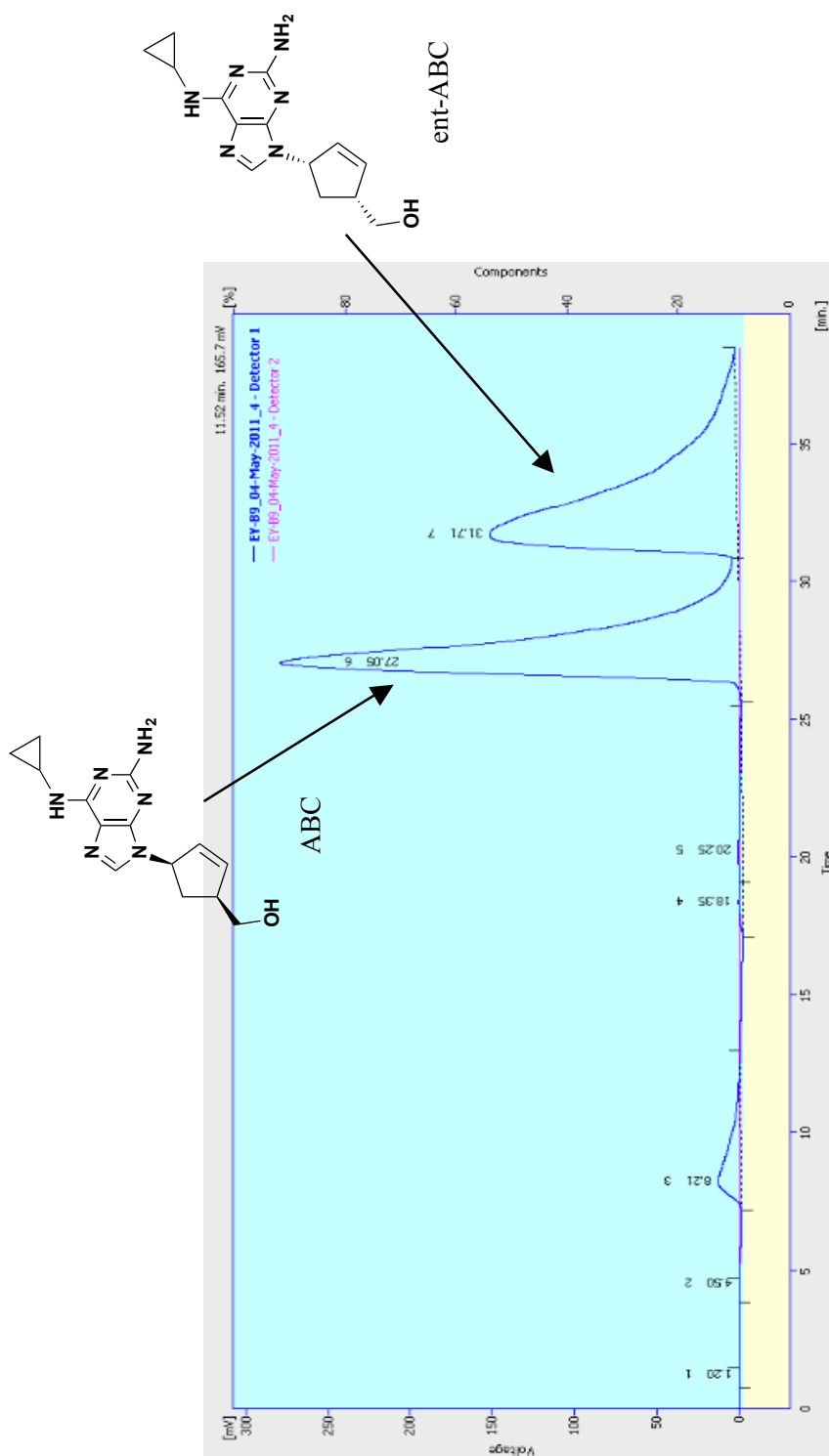
Figure S1: Representative HPLC chromatograms for the separation of ABC enantiomers: ABC (R_t = 27.1 min, 50.0 % area) and ent-ABC (R_t = 31.8 min, 47.6% area). The structures of these enantiomers can be seen on the chromatogram.

4.7 References

(1)   Daluge, S. M.; Martin, M. T.; Sickles, B. R.; Livingston, D. A. *Nucleosides Nucleotides & Nucleic Acids* **2000**, *19*, 297.

(2)   Vince, R.; Hua, M. *J. Med. Chem.* **1990**, *33*, 17.

(3)   Vince, R.; Hua, M. *Current Protocols in Nucleic Acid Chemistry / edited by Serge L. Beaucage et al.* **2006**, *Chapter 14*, Unit 14.4.

(4)   Evans, C. T.; Roberts, S. M.; Shoberu, K. A.; Sutherland, A. G. *Journal of the Chemical Society-Perkin Transactions 1* **1992**, 589.

(5)   Crimmins, M. T.; King, B. W.; Zuercher, W. J.; Choy, A. L. *J. Org. Chem.* **2000**, *65*, 8499.

(6)   Crimmins, M. T.; King, B. W. *J. Org. Chem.* **1996**, *61*, 4192.

(7)   Zhou, J.; Yang, M.; Akdag, A.; Wang, H.; Schneller, S. W. *Tetrahedron* **2008**, *64*, 433.

(8)   Brown, B.; Hegedus, L. S. *J. Org. Chem.* **2000**, *65*, 1865.

(9)   Crimmins, M. T.; Zuercher, W. J. *Org. Lett.* **2000**, *2*, 1065.

(10)   Forro, E.; Fulup, F. *Tetrahedron: Asymmetry* **2004**, *15*, 573.

(11)   Forro, E.; Fulop, F. *Org. Lett.* **2003**, *5*, 1209.

(12)   Olivo, H.; Yu, J. *Tetrahedron: Asymmetry* **1997**, *8*.

(13)   Huang, W.; Miller, M. J.; De Clercq, E.; Balzarini, J. *Organic & Biomolecular Chemistry* **2007**, *5*, 1164.

(14)   Bremond, P.; Audran, G.; Aubin, Y.; Monti, H. *Synlett* **2007**, 1124.

(15)   An, G.; Rhee, H. *Nucleosides Nucleotides & Nucleic Acids* **2000**, *19*, 1111.

(16)   Sriram, D.; Yogeeswari, P.; Myneedu, N. S.; Saraswat, V. *Bioorg. Med. Chem. Lett.* **2006**, *16*, 2127.

(17)   Walsh, J. S.; Reese, M. J.; Thurmond, L. M. *Chem. Biol. Interact.* **2002**, *142*, 135.

(18)   Beaulieu, F.; Beauregard, L.-P.; Courchesne, G.; Couturier, M.; LaFlamme, F.; L'Heureux, A. *Org. Lett.* **2009**, *11*, 5050.

(19)   L'Heureux, A.; Beaulieu, F.; Bennett, C.; Bill, D. R.; Clayton, S.; LaFlamme, F.; Mirmehrabi, M.; Tadayon, S.; Tovell, D.; Couturier, M. *J. Org. Chem.* **2010**, *75*, 3401.

(20)   Gupte, A.; Buolamwini, J. K. *Biorg. Med. Chem.* **2007**, *15*, 7726.

(21)   Challa, H.; Bruice, T. C. *Biorg. Med. Chem.* **2004**, *12*, 1475.

(22)   Hagen, M. D.; Scalfi-Happ, C.; Happ, E.; Chladek, S. *J. Org. Chem.* **1988**, *53*, 6.

(23)   Hagen, M. D.; Chladek, S. *J. Org. Chem.* **1989**, *54*, 3189.

(24)   Lee, J. A.; Moon, H. R.; Kim, H. O.; Kim, K. R.; Lee, K. M.; Kim, B. T.; Hwang, K. J.; Chun, M. W.; Jacobson, K. A.; Jeong, L. S. *J. Org. Chem.* **2005**, *70*, 5006.

(25)   Gagneron, J.; Gosselin, G.; Mathe, C. *J. Org. Chem.* **2005**, *70*, 6891.

(26)   Wang, Z. Y.; Silverman, R. B. *Biorg. Med. Chem.* **2006**, *14*, 2242.

(27)   Rapp, M.; Cai, X.; Xu, W.; Dolbier, W. R., Jr.; Wnuk, S. F. *J. Fluorine Chem.* **2009**, *130*, 321.

(28)   Bell, C. Thesis. Title: Characterisation of HLA-restricted T-cell responses to abacavir using lymphocytes from drug-naive volunteers, University of Liverpool, Liverpool, 2012.

(29)   MacKeith, R. A.; McCague, R.; Olivo, H. F.; Roberts, S. M.; Taylor, S. J.; Xiong, H. *Biorg. Med. Chem.* **1994**, *2*, 387.

(30)   Koshkin, A. A.; Fensholdt, J.; Pfundheller, H. M.; Lomholt, C. *J. Org. Chem.* **2001**, *66*, 8504.

(31)   Rosenbohm, C.; Pedersen, D. S.; Frieden, M.; Jensen, F. R.; Arent, S.; Larsen, S.; Koch, T. *Biorg. Med. Chem.* **2004**, *12*, 2385.

(32)   Seshachalam, U.; Rao, D. V. L. N.; Haribabu, B.; Chandrasekhar, K. B. *Chromatographia* **2006**, *64*, 745.

(33)   Patanella, J. E.; Walsh, J. S. *Drug Metab. Disposition* **1992**, *20*, 912.

(34)   Trost, B. M.; Bunt, R. C. *J. Am. Chem. Soc.* **1994**, *116*, 4089.

(35)   Trost, B. M.; Bunt, R. C. *Angewandte Chemie-International Edition in English* **1996**, *35*, 99.

(36)   Ainai, T.; Matsuumi, M.; Kobayashi, Y. *J. Org. Chem.* **2003**, *68*, 7825.

(37)   Taschner, M. J.; Aminbhavi, A. S. *Tetrahedron Lett.* **1989**, *30*, 1029.

(38)   Stork, G.; Rychnovsky, S. D. *J. Am. Chem. Soc.* **1987**, *109*, 1564.

(39)   Vedejs, E.; Engler, D. A.; Telschow, J. E. *J. Org. Chem.* **1978**, *43*, 188.

(40)   Hanessian, S.; Cooke, N. G.; Dehoff, B.; Sakito, Y. *J. Am. Chem. Soc.* **1990**, *112*, 5276.

(41)   Kabeya, M.; Hamada, Y.; Shioiri, T. *Tetrahedron* **1997**, *53*, 13969.

(42)   Vedejs, E., Larsen, S *Organic Syntheses* **1986**, *64*.

(43)   Anderson, J. C.; Smith, S. C. *Synlett* **1990**, 107.

(44)   Davis, F. A.; Chen, B. C. *Chem. Rev.* **1992**, *92*, 919.

(45)   Watanabe, T.; Ishikawa, T. *Tetrahedron Lett.* **1999**, *40*, 7795.

(46)   Thompson, W. J.; Tucker, T. J.; Schwering, J. E.; Barnes, J. L. *Tetrahedron Lett.* **1990**, *31*, 6819.

(47)   Menon, K.; Cellceutix Corp. Title: Carbocyclic nucleosides and their pharmaceutical use and compositions. Publication Number: WO2013103601 A1: 2013.

(48)   Kudis, S.; Helmchen, G. *Tetrahedron* **1998**, *54*, 10449.

(49)   Daluge, S. M.; Therapeutic nucleosides. Burroughs Wellcome Co. Patent Number: US5034394 A1: 1991.

(50)   Jacquet, O.; Bergholz, T.; Magnier-Bouvier, C.; Mellah, M.; Guillot, R.; Fiaud, J.-C. *Tetrahedron* **2010**, *66*, 222.

(51)   Hu, Q. Y.; Rege, P. D.; Corey, E. J. *J. Am. Chem. Soc.* **2004**, *126*, 5984.

(52)   Canham, S. M.; France, D. J.; Overman, L. E. *J. Am. Chem. Soc.* **2010**, *132*, 7876.

(53)   Dasgupta, T. K.; Felix, D.; Eschenmo.A; Kempe, U. M. *Helv. Chim. Acta* **1972**, *55*, 2198.

(54)   Rapi, Z.; Demuth, B.; Keglevich, G.; Grun, A.; Drahos, L.; Soti, P. L.; Bako, P. *Tetrahedron-Asymmetry* **2014**, *25*, 141.

CHAPTER 5

Using Structure–Activity Relationships to Investigate Abacavir Toxicity

CHAPTER 5

Using Structure–Activity Relationships to Investigate Abacavir Toxicity

5.1 Introduction

Recently published research proposed a new potential mechanism of ABC toxicity. This new concept is known as the 'altered repertoire mechanism.'[1-4] Although it has been suggested as a theory to specifically explain the toxicity associated with ABC, initial research has also shown it can be applied to CBZ hypersensitivity.[1]

5.1.1 Altered repertoire mechanism.

It was suggested that the altered repertoire mechanism can be applied to those molecules that stimulate the immune system *via* the antigen processing and MHC class I pathway.[4] The antigens bind within the MHC molecule and in doing so, it alters the self-peptides that bind (Figure **5.1**). The self-peptides that bind within the MHC are highly specific and by changing the range of peptides that bind, from those that would normally be presented, the CD8$^+$ T-cells will detect a *neo*-peptide and in turn will be activated.
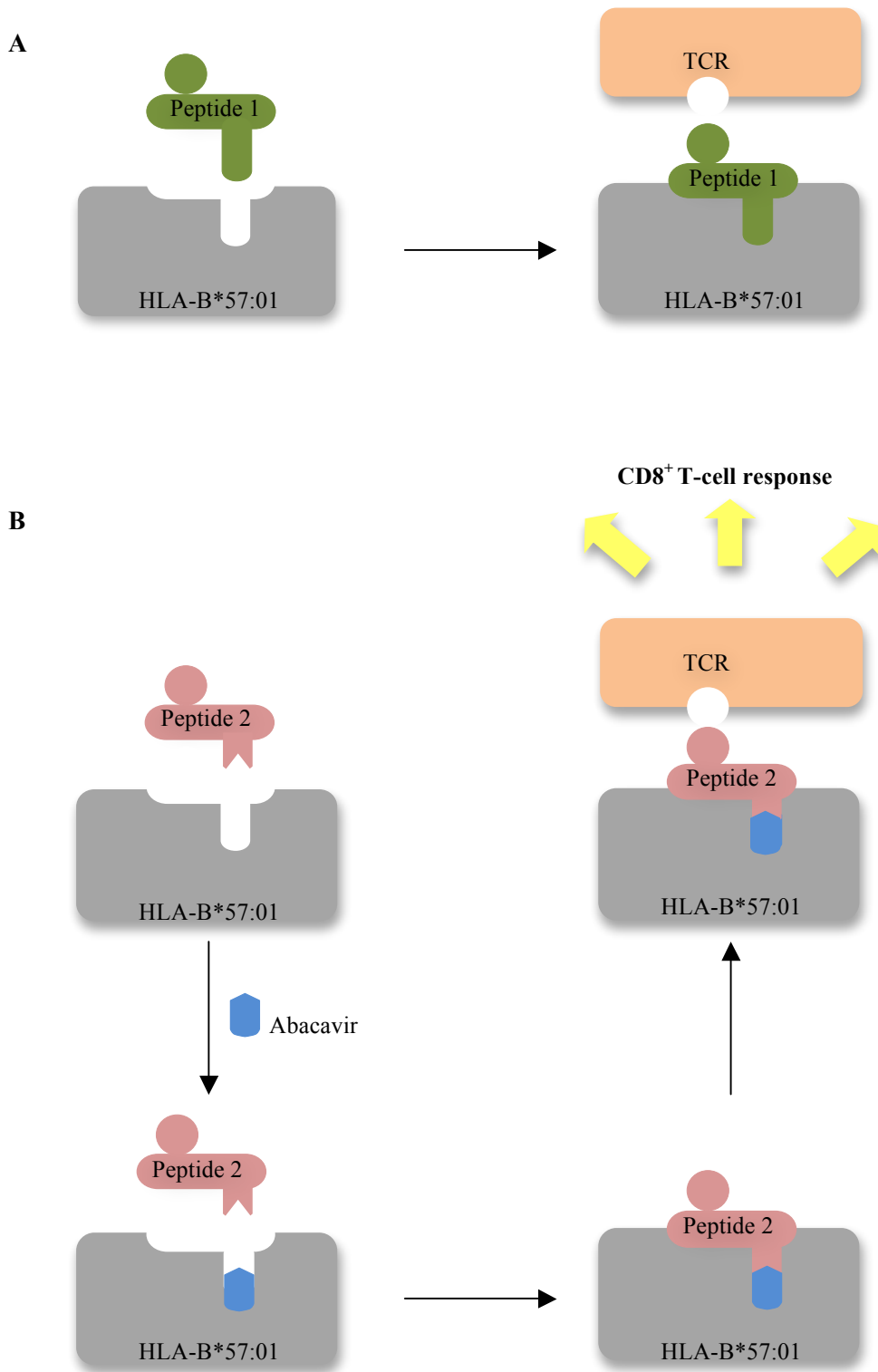
Figure 5.1: Mechanism for the altered repertoire concept. A normal self-peptide (Peptide 1) will bind within the HLA molecule and this will not induce an immune response (**A**). Peptide 2, a *neo* self-peptide cannot bind within the HLA molecule in the absence of ABC. Once ABC binds, it facilitates the binding of Peptide 2 within HLA-B*57:01 resulting in the stimulation of CD8$^+$ T-cells, causing an immune response (**B**).

5.1.2 Altered repertoire mechanism applied to ABC.

Three papers published recently, hypothesised that ABC-HSR arose from the altered repertoire mechanism.[1-3] The research presented showed that ABC bound within the F-pocket of the peptide-binding grove of the MHC and in doing so, altered the self-peptide repertoire, and subsequently stimulated a T-cell response (Figure **5.1**).

ABC does not induce an immune response in patients who bear the HLA-B*57:02, HLA-B*57:03, HLA-B*57:11 and HLA-B*58:01 alleles. The amino acid residues that differ in these alleles from HLA-B*57:01 are shown in Table **5.1** with differences ranging from two to four amino acids. Using this knowledge, Illing *et al*. had deduced that ABC specifically bound at the C-terminal end of the HLA-B*57:01 protein within the C, D, E and F-pockets.[1]

In experiments analysing the repertoire of peptides binding within cell lines expressing either HLA-B*57:01 or HLA-B*57:03 alleles, no ABC metabolites were detected, rather ABC itself; suggesting the parent drug, ABC, was responsible for T-cell stimulation. Within these experiments, Illing *et al*. detected a change of self-peptides eluting from cells bearing HLA-B*57:01. A large number of these peptides, in the presence of ABC, were found to contain Ile or Leu at the C-terminus (PΩ) of the peptide. This was a contrast compared to self-peptides that normally bind within this allele or HLA-B*57:03. These peptides were often found to terminate with the more bulky Trp or Phe amino acids.[5] This led the authors to postulate that, along with ABC undertaking the normal antigen processing pathway, a large proportion of normal self-peptides were unable to bind within HLA-B*57:01 during peptide loading in the presence of ABC. This was due to steric hindrance and as a

265

consequence, a new repertoire of peptides, bearing smaller C-terminal amino acids were found to bind.

Table 5.1: Amino acid differences in HLA allotypes: HLA-B*57:02, -B*57:03, -B*57:11 and -B*58:01 in comparison with HLA-B*57:01.

HLA Allotype	Amino Acid Difference with respect to HLA-B*57:01
HLA-B*57:02	Asp114Asn Ser116Tyr Leu156Arg
HLA-B*57:03	Asp114Asn Ser116Tyr
HLA-B*57:11	Ile94Thr Ile95Leu Val97Trp
HLA-B*58:01	Met45Thr Ala46Glu Val97Arg Val103Leu

X-ray structures of HLA-B*57:01 bearing *neo* self-peptides and ABC were obtained, and from this data, the interactions of ABC and the peptide were determined. The cyclopentyl, purinyl and cyclopropyl moieties of ABC were situated in the D, E and F-pockets respectively.   Several van der Waals interactions and H-bonds were discovered to form in this immunogenic complex and those with particular interest were Ser 116 and Val 97, which were involved in H-bonding and van der Waals interactions respectively.   These interactions explain why alleles such as HLA-

B*57:02 and HLA-B*57:03 do not initiate a T-cell response in the presence of ABC. In alleles HLA-B*57:02 and HLA-B*57:03, Tyr replaces Ser 116, an amino acid located in the F-pocket of the allele. Tyr is a large bulky amino acid and would disfavour ABC binding. This is similar for HLA-B*58:01, where Val 97 is replaced by charged Arg, again resulting in unfavoured binding of ABC. The position and interactions of the cyclopropyl group were found to be responsible for the altered PΩ amino acids, with smaller amino acids being favoured.

In support of the research by Illing *et al*., Ostrov *et al*. also postulated that ABC, as the parent drug, was present whilst peptide loading was occurring within the ER. Following vast combinatorial library research, they designed a synthetic peptide, pep-V (sequence HSITYLLPV), and this peptide exhibited a high affinity for HLA-B*57:01. This only occurred in the presence of ABC in a dose-dependent manner.[2] The researchers obtained an X-ray crystal structure of pep-V and ABC bound within HLA-B*57:01. From this, the H-bonding and van der Waals interactions of ABC within the complex were obtained (Figure **5.2**). Pep-V was shown to contribute to two of the van der Waals interactions.
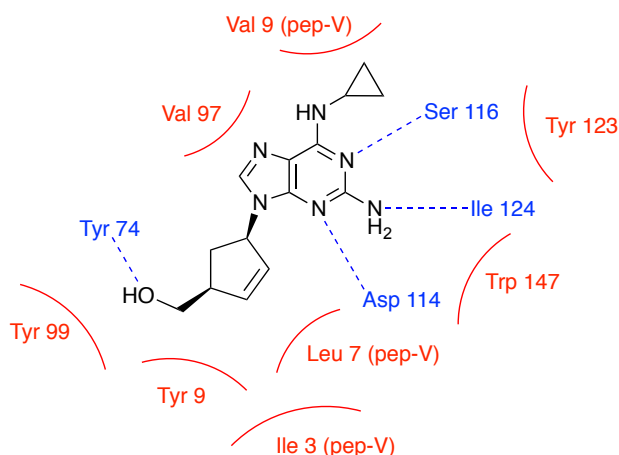
Figure 5.2: Interactions of ABC within the C, D, E and F-pockets of HLA-B*57:01. ABC undergoes H-bonding with four amino acids (Tyr 74, Asp 114, Ser 116 and Ile 124, as shown in blue) and in addition to this, several van der Waals interactions (Tyr 9, Val 97, Tyr 99, Tyr 123 and Trp 147, as shown in red) are present. Three of these van der Waals interactions appear from pep-V (amino acids Ile 3, Leu 7 and Val 9). Adapted from Ostrov *et al*.[2]

Ostrov *et al*. also demonstrated an altered repertoire of bound peptides within HLA-B*57:01 in ABC-treated cells compared to non-treated cells.[2] High levels of peptides eluted from ABC-treated cells were found to encompass a Val (and Ile) amino acid at PΩ, and conversely, in untreated cells, no recovered peptides possessed a Val at the this position. In ABC-treated cells, it was also found a lower number of peptides with Trp or Phe at this PΩ position: This was consistent with Illing *et al*.[1] Further to this and previous work conducted in 2008,[6] no eluted peptides possessed an Ala residue at the C-terminus, confirming that ABC becomes involved in intracellular antigen processing: A process which disfavours peptides bearing an Ala residue at the C-terminus. The presence of ABC during antigen processing results in the structure binding within the antigen-binding cleft of the HLA molecule. This complex would result in the binding of a new repertoire of peptides.

Further to this, Norcross *et al*. supported this hypothesis:[3] ABC induced the loading of peptides that favoured an Ile or Leu amino acid at the PΩ position, in a dose-dependent manner. In addition, it was found that the P2 anchor amino acids (Ala, Thr or Ser)[5] of the *neo* self-peptides remained the same as those peptides found in untreated cells. Interestingly, two drug-induced peptides, HSLPALIQI and STIRLLTSL had high affinity binding for HLA-B*57:01, not only in the presence of ABC, but also in its absence. These *neo* self-peptides *in vivo* would ordinarily have a low affinity for this HLA protein but upon ABC exposure, ABC may assist in the stabilisation of these peptides within the HLA complex.

The ABC-associated findings assisted the authors in postulating that ABC is able to alter the structure of the HLA complex directly, by either remaining within the HLA protein or modifying the peptide processing pathway and as a result, affect peptide loading and/or binding. Along with this, the role of tapasin is to stabilise MHC complexes and to promote binding of high affinity peptides,[7] thereby, modification of the tapasin/TAP pathway may also alter the repertoire of peptides, and ABC is known to undertake this pathway.[6]

In initial research, Illing *et al*. also demonstrated this mechanism with CBZ.[1] CBZ, an anti-epileptic drug, is strongly associated with an HLA-specific CBZ-induced SJS/TEN in patients whom possess the HLA-B*15:02 allele. Applying the same experimental techniques as used with ABC, Illing *et al*. found an altered set of peptides bound within the HLA-B*15:02 allele in the presence of CBZ. HLA-B*15:02, in the presence of CBZ, preferred peptides with increased hydrophobicity

and smaller residues at the P4 and P6 positions, but the response was 15% smaller than that generated by ABC. Further work is required to support these findings.

Whilst, collectively, the above data provides a solid understanding to ABC-HSR, it fails to explain why only 50% of HLA-B*57:01 positive patients develop the toxicity. In order to investigate and develop this research further, ABC analogues were designed to probe and further understand its interactions specifically within the F-pocket of HLA-B*57:01.

5.2 Aims

- To synthesise a range of amine and oxy analogues of ABC at the 6-position using an SAR approach

- To investigate whether synthesised 6-position analogues can reduce T-cell stimulation in HLA-B*57:01 ABC-stimulated T-cells

- To determine whether replacement of 6-cyclopropyl amine will eliminate ABC toxicity.

5.3 Results & Discussion

5.3.1 Synthesis of Cl-ABC 32.

To synthesise any 6-position analogues of ABC, Cl-ABC intermediate **32**, was required. The two-step method for this synthesis was taken from a large-scale patent, originally used to synthesise ABC (Scheme **5.1**).[8]
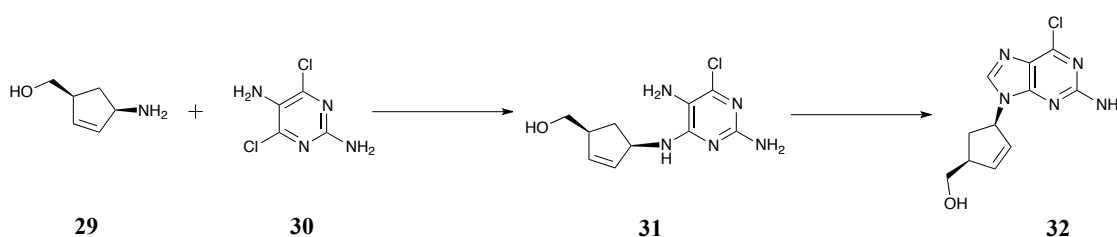
Scheme 5.1: Reagents and conditions: a) (1S,4R)-4-Amino-2-cyclopentene-1-methanol tartrate salt **29** (1 equiv), 2,5-diamino-4,6-dichloropyrimidine **30** (1 equiv), NaHCO$_3$ (3.5 equiv), *n*-BuOH, 95 °C, 16 h, 53%; b) TEOF (1.2 equiv) and conc. H$_2$SO$_4$ (0.05 equiv), *n*-BuOH, 70 °C, 20 h, 87%.

Both commercially available starting materials **29** and **30** were coupled together in *n*-butanol (*n*-BuOH), using the inorganic base, NaHCO$_3$ (3.5 equiv). The optimum temperature used was 95 °C and a 53% yield achieved. The ring closing reaction of **31** was completed using TEOF (1.2 equiv) and concentrated sulfuric acid (H$_2$SO$_4$, 0.05 equiv). The strict addition of reagent equivalents was vital for the formation of **32**. It was found that excess addition of either reagent, resulted in an unwanted side product. This side product was difficult to remove by silica gel column chromatography due to the comparable polarity to the desired product **32**. This reaction proceeded with 87% yield.

5.3.2 Synthesis of 6-position 1° and 2° amine analogues (compounds 103–118).

The synthesis for the majority of the 1° and 2° amine analogues was straightforward, providing there were no steric clashes or hindering groups. Most of the reactions were completed using standard nucleophilic aromatic substitution conditions (Scheme **5.2**) for this type of compound. These conditions comprised of heating the 1°/2° amine in MeOH to 60/70 °C overnight.[9] Compounds **115**–**118** were synthesised within the group at the University of Liverpool. The structures and yields of the compounds can be found in Table **5.2**.
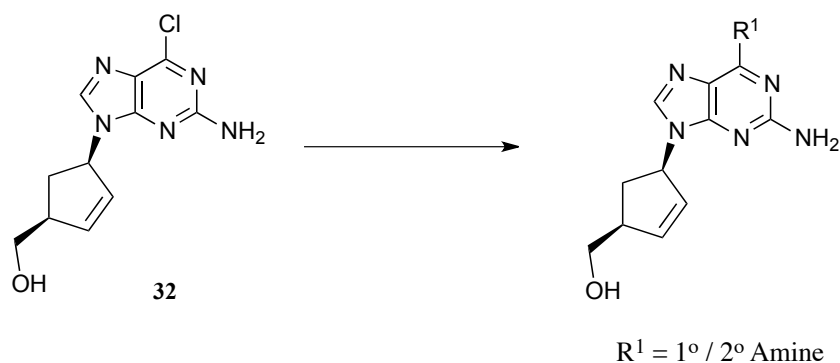
$R^1 = 1°/2°$ Amine

Scheme 5.2: General procedure for formation of 6-position 1° and 2° amine analogues. Reagents and conditions: 1°/2° Amine (1.5, 10 or 20 equiv), MeOH, 60–70 °C, o/n, 31–94%.

The reaction of **32** with *t*-butylamine to form compound **109** required excess amine (10 equiv) as the reaction proceeded extremely slowly at lower stoichiometrics. This was likely to be due to steric reasons as the *t*-Bu alkyl group is more hindered. A 57% yield was achieved from this reaction. Yields from all other reactions ranged from 31–94%. Excess amine reagent, *N*-methylcyclopropanamine (20 equiv), was also required for the synthesis of compound **114**. For the synthesis of compound

118, the reaction time was 3 days rather than overnight. All other conditions were as previously mentioned.

Table 5.2: The formation of 6-position 1° and 2° amine analogues using standard nucleophilic aromatic substitution conditions, forming compounds **103–118**. Compounds **117** and **118** were synthesised within the group at the University of Liverpool.
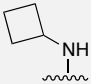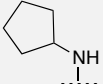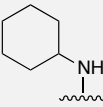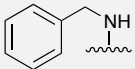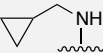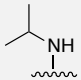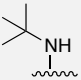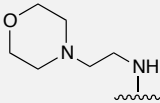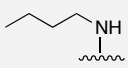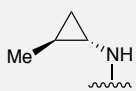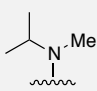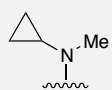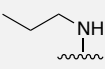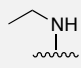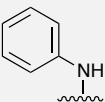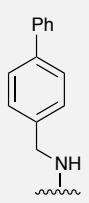
Compound Number	R^1 Group*	Yield (%)
103		62
104		85
105		71
106		81
107		73
108		71
109		57

Table 5.2 continued:

110		70
111		81
112		94
113		74
114		77
115		68
116		65
117		81
118		31

* All reactions were completed on a 50–250 mg scale.

The compounds synthesised were designed in a SAR manner, so as to disrupt binding and intermolecular bonding within the F-pocket of the HLA-B*57:01 allele.

By disrupting this binding, *neo* self-peptides would not be able to bind, resulting in reduced or no T-cell activation. Substituting the cyclopropyl substituent with larger alkyl rings: Cyclobutyl, cyclopentyl and cyclohexyl (compounds **103**–**105**) moieties should subtly disrupt the binding in the F-pocket itself, whereas those with larger, substitutions *e.g.* compounds **106**, **110**, **117** and **118**, would almost certainly cease the analogue from binding in a manner similar to ABC. The substitutions of the cyclopropyl ring with *n*-alkyl, isopropyl (*i*-Pr) or *t*-Bu groups (compounds **108**, **109**, **111**, **113**, **115** and **116**) produce very slight changes to the structure but these could significantly reduce binding. This would be expected with the *i*-Pr and *t*-Bu analogues due to the increased steric bulk of the methyl groups. The final cyclopropyl analogues, **107**, **112** and **114**, have only very slight variations in comparison to ABC but are capable of interrupting van der Waals bonding in and around the F-pocket.

5.3.2.1 Synthesis of compound 121.

With no commercially available amine reagent needed to synthesise compound **121**, *N*-methylcyclopropanamine was itself synthesised. This three-step synthesis was completed as seen in Scheme **5.3**. The starting material, cyclopropylamine, was protected with Boc in quantitative yields. Following this, the Boc protected amine **119** underwent deprotonation with NaH and subsequent addition of methyl iodide (MeI) to form intermediate **120** with a 73% yield. The final step posed more issues due to the volatility of the desired methylated amine compound **120**, but yields of 58% were achieved. The product, compound **121**, was stored at –20 °C until it was used as a reagent under nucleophilic aromatic substitution conditions with **32** to form compound **114**.
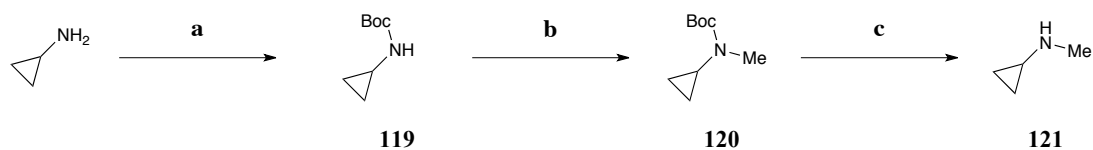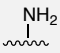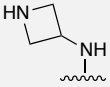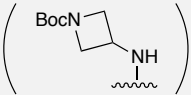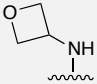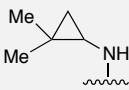
Scheme 5.3: Reagents and conditions: a) Cyclopropylamine (1 equiv), Boc$_2$O (1 equiv), DCM, 0 °C → r.t., o/n, 92%; b) NaH (1.5 equiv), MeI (1 equiv), DMF, 0 °C → r.t., o/n, 73%; c) AcCl (5 equiv), MeOH, r.t., o/n, 58%.

5.3.3 Synthesis of 6-position 1° amine analogues (compounds 122–126).

A select number of analogues could not be synthesised using the nucleophilic aromatic conditions as stated in Section **5.3.2**. This was due to volatility of the amine reagent or for electronic reasons. Rather than directly heating the reaction mixtures in a standard flask, a sealed tube was required (Table **5.3**).

Table 5.3: Synthesis of 1° amine analogues, compounds **122–126**. The compounds were synthesised using nucleophilic aromatic substitution of 6-Cl (compound **32**) with the respective amine reagent.

Compound Number	Analogue (R^1 Group)	Conditions[*]	Yield (%)
122	NH$_2$	7 N NH$_3$ (excess), MeOH	96
124	HN⟍ NH		53
	via		
(123)	BocN⟍ NH	(1-Boc-3-(amino)azetidine (1 equiv), MeOH)	(57)
125	O⟍ NH	3-amino-oxetane (5 equiv), EtOH	80
126	Me Me⟍ NH	2,2-dimethylcyclopropylamine (1 equiv), K$_2$CO$_3$ (1.5 equiv), *t*-BuOH	54

[*] All reactions were carried out in a sealed tube and were completed on a 50–300 mg scale.

During the synthesis of compound **122**, the volatility of ammonia (NH$_3$) proved to be problematic, but once the reaction was completed in a sealed tube and with a large excess of NH$_3$, the issue was corrected.[10] To synthesise compound **124**, 1-Boc-3-(amino)azetidine was used. The reaction was carried out in MeOH and once the intermediate product **124** was formed, the Boc group was removed using TFA in DCM to yield the azetidine product **124** with a 53% yield. The reaction to form compound **125** was conducted in EtOH. This improved the yield of the reaction, as

the temperature of the reaction in the sealed tube could be increased compared to using MeOH as the solvent. This increased temperature improved the reaction yield (from 42% to 80%). Compound **126** was synthesised using 2,2-dimethylcyclopropylamine hydrochloride. Under standard conditions (Scheme **5.2**), no product was observed. The difficulty in obtaining the product was likely due to steric reasons. Two methyl groups on the cyclopropyl ring would greatly hinder the amine to undergo nucleophilic attack. To overcome this problem, K_2CO_3 was used with *t*-BuOH and the reaction was carried out in a sealed tube. The inorganic base, K_2CO_3 was used as it would not interfere with the nucleophilic substitution: A common problem observed when using organic bases such as NEt_3. The solvent *t*-BuOH was also used, rather than EtOH or MeOH, as it again allowed for an increased temperature to be used but with no possibility of itself acting as a nucleophile. Under these conditions, the product **126** was obtained with a 54% yield.

Compound **122** was synthesised for comparative purposes against the *n*-alkyl amino chains (*i.e.* compounds **111**, **115** and **116**). Modifications of the cyclopropyl amino group were of great interest as they maintained the fundamental structure of ABC but slight changes on the cyclopropyl ring would produce analogues that have the potential of reducing or eliminating toxicity but maintaining a high level of antiviral activity and PK parameters. Examples of this include compounds **112** and **126**: These compounds bear either mono- or di-methyl groups on the cyclopropyl ring. These methyl groups could disrupt the binding sufficiently within the F-pocket so as to reduce a T-cell response.

Two further compounds **124** and **125** were designed to test the H-bonding effects within the HLA-B*57:01 molecule. Both compounds bear ring structures that are small enough to not deviate far from ABC's structure with both containing heteroatoms. The *O*-atom on the amino oxetane group (compound **125**) would act as an H-bond acceptor and therefore there would be potential interactions with amino acids present within the F-pocket region of the protein. Conversely, the *N*-atom in compound **124**, which bears an amino azetidine group, would act as an H-bond donor. But again, the amino acid interactions within the F-pocket would be interesting to investigate. This compound was synthesised *via* Boc-protected azetidine **123** and removal of the Boc-protecting group using TFA yielded **124** as the TFA salt.

5.3.4 Synthesis of fluoro-substituted cyclopropyl amine analogues (compounds 127–130).

Four substituted compounds **127**–**130** could not be synthesised. These are shown in Figure **5.3**. Ranges of conditions were attempted for these reactions as depicted in Table **5.4**. All substituted cyclopropyl amine reagents were used as salts and all reactions were completed on either 50 or 100 mg scales.

127	**128**	**129**	**130**
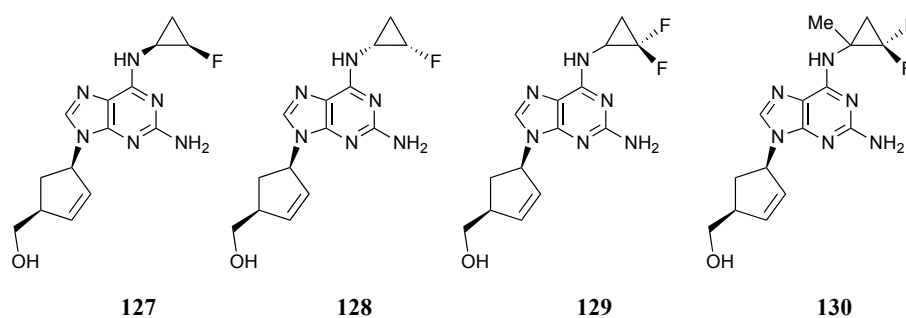
Figure 5.3: Substituted cyclopropylamine compounds **127**–**130** that could not be synthesised *via* nucleophilic aromatic substitution of 6-Cl.

Table 5.4: Varying conditions used in attempt to synthesise the fluorinated compounds **127–130**.
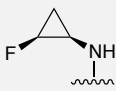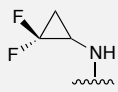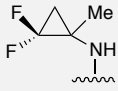
Compound/ R^1 Group		Conditions[*]	Yield (%)
127 (Ts) (1.1 equiv)	**A1**	K$_2$CO$_3$ (1.5 equiv), MeOH, 60 °C, 16 h	-
	A2	DIEA (1.2 equiv), DMF, 70 °C, 16 h	-
	A3	NEt$_3$ (1.1 equiv), DMF, 60 °C, 16 h	-
	A4	K$_2$CO$_3$ (1.5 equiv), Dioxane, 150 °C, 20 min, MW	-
	A5	NEt$_3$ (1.1 equiv), Dioxane, 170 °C, 30 min, MW	-
	A6	NEt$_3$ (2 equiv), DMSO, 180 °C, 60 min, MW	-
	A7	Pd(dba)$_2$ (0.1 equiv), K$_3$PO$_4$ (3.2 equiv), XPhos (0.5 equiv), DME, 20 min, 100 °C, MW	-
	A8	K$_2$CO$_3$ (2 equiv), *t*-BuOH, 100 °C, 1 h, MW	-
	A9	K$_2$CO$_3$ (2 equiv), *t*-BuOH, 100 °C, 3 days, Sealed Tube	1
128 (Ts) (1.1 equiv)	**B1**	K$_2$CO$_3$ (2 equiv), *t*-BuOH, 100 °C, 3 days, Sealed Tube	-

Table 5.4 continued:

129	C1	K$_2$CO$_3$ (3 equiv), t-BuOH, 100 °C, 2 days, Sealed Tube	-
	C2	K$_2$CO$_3$ (2.5 equiv), EtOH, 80 °C, 24 h, Sealed Tube	-
130	D1	K$_2$CO$_3$ (2.5 equiv), EtOH, 80 °C, 24 h, Sealed Tube	-

* All reactions were completed on a 50–100 mg scale.

Compound **127** was used as the test compound to determine optimum reaction conditions. Conditions A1 used for this compound proved unsuccessful, with no product formation and starting material was recovered. With the presumption that the inorganic base was contributing to no product formation, conditions A2 and A3 were attempted using DIEA and NEt$_3$ respectively in DMF. Using DMF would allow the temperature of the reaction to be increased, should it have required this. Unfortunately, no desired product was formed, with some side reactions evident. It was apparent that the fluorine atom was having a major influence on the substitution reaction: This is likely to be due to electronic reasons.

To force the reaction further, microwave conditions were used (conditions A4–A6, Table **5.4**). Reactions were completed in either DMSO or dioxane with varying base, temperature and reaction times. For all reactions, the formation of side products was vast and it was difficult to determine any product formation. For reaction A6, a major product was formed and once isolated, this was found to be compound **131** (Figure **5.4**). NEt$_3$ under these conditions had reacted with the starting material.

From this, no organic base was used for future aromatic substitution reactions. DMSO and *N*-methyl-2-pyrrolidone (NMP) were also unable to be used as solvents due to similar polarities with the starting material and required products.
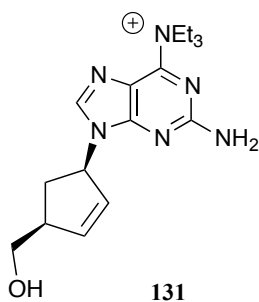
Figure 5.4: Major side product formed during reaction A6 Table **5.4**, forming compound **131**, with no desired product obtained.

A palladium-coupling reaction was attempted (reaction A7), using C−N cross-coupling reaction conditions. This has been seen to assist in the coupling of aryl halides with a range of amine substrates.[11-13] More notably, these cross-coupling reactions have been demonstrated with deoxynucleoside halides.[14,15] Although significantly less side reactions occurred, no product was obtained. Finally, using K_2CO_3 as the base and *t*-BuOH as the solvent (a hindered solvent with no possibility to act as a nucleophile itself) reactions A8 and A9 were attempted. A sealed tube has been shown to be advantageous with previous difficult aromatic substitution reactions (see Section **5.3.3**) and some product formation was apparent. Once isolated, mass spectrometry analysis showed a product with the desired accurate mass (*m/z* (ES+) 305.1526 calculated for $C_{14}H_{18}N_6OF$: [M+H]$^+$ 305.1527) but due to a low mass obtained, further analysis was not possible.

Using these reaction conditions (B1, Table **5.4**), the synthesis of the enantiomer was attempted (compound **128**). Some product was formed but no pure **128** were obtained. Compound **129** was also attempted with these conditions (C1, Table **5.4**), but again, no product was obtained. This was expected due to the difluoro substitution. The reaction was repeated using EtOH, a solvent found to previously assist with difficult substitution reactions, but this was also unsuccessful (C2, Table **5.4**). The same outcome was observed with compound **130**, with no product formation. The difluoro substitution would not only slow the reaction significantly, but the additional methyl group would also hinder nucleophilic addition. With a range of conditions attempted for these compounds and very little or no product obtained, they were not pursued further.

5.3.5 Synthesis of oxy 6-position analogues (compounds 132–139).
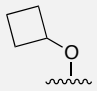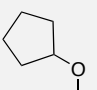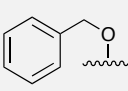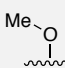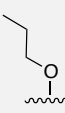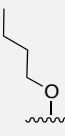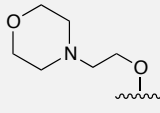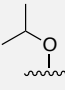
SAR design of the analogues was not limited solely to 6-position amines. Six oxy-analogues were synthesised as shown in Table **5.5**. The reaction conditions varied slightly to their amine equivalents (Scheme **5.4**).

$R^2 = $ Ether
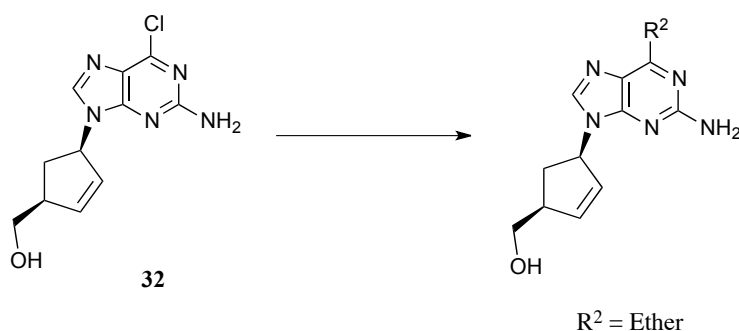
Scheme 5.4: General procedure used to synthesise 6-position oxy analogues. Reagents and conditions: Alcohol (excess, as solvent), NaH (3 equiv), 80 °C, 4 h, 51–85% yields.

Initially, DMF was used as the reaction solvent and reactions were extremely slow with very little or no product formation evident after 24 h. Along with this, the number of side products increased over time and purification of products posed many problems, often with no successful results. After further research into alternative methods Vince *et al.*[16] had successfully synthesised similar analogues using the alcohol itself as the reagent and solvent. The synthesis of 7 oxy analogues proceeded well using this method (using the alcohol reagent as the solvent), giving yields of 51–85%. NaH was used as the base and a temperature of 80 °C over 4 h was required. The reactions occurred more rapidly than their amine equivalents and with generally good yields.

Table 5.5: The formation of 6-position oxy analogues using nucleophilic aromatic substitution conditions (alcohol (excess), NaH (3 equiv), 80 °C, 4 h) to form compounds **132–139**.

Compound	R^2 Group*	Yield (%)
132		70
133		73
134		57
135		75
136		85
137		51
138		0
139		80

* All reactions were completed on a 50–500 mg scale.

Problems were only encountered with one analogue, compound **138**. The reaction conditions used were those as previously described (Scheme **5.4**). It was clear from early analysis that reaction yields for this reaction were poor due to significant formation of side products and remaining starting material. Difficulties arose during purification (*via* silica gel chromatography); excess morpholine reagent was difficult to remove using this method and polarities of starting material, desired product and side products were very similar and so contributed to difficult purification. With no successful results *via* this method, short-path vacuum distillation using Kugelrohr apparatus was attempted. Although this method was successful at removing excess morpholine reagent, the issues with removing starting material and side products remained. The synthesis of this analogue was not pursued further due to time constraints.

5.3.6 Cross-reactivity of ABC-specific human T-cell clones with 6-position analogues.

The cross-reactivity studies were carried out within the University of Liverpool and for details of these assays see Chapter 1, Section **1.10.2**. The cross-reactivity results for a select number of *N-* and *O-* 6-position analogues, as depicted in Figure **5.5**, were determined by both proliferation and ELISpot IFN-γ assays. The ELISpot assay results are discussed within.
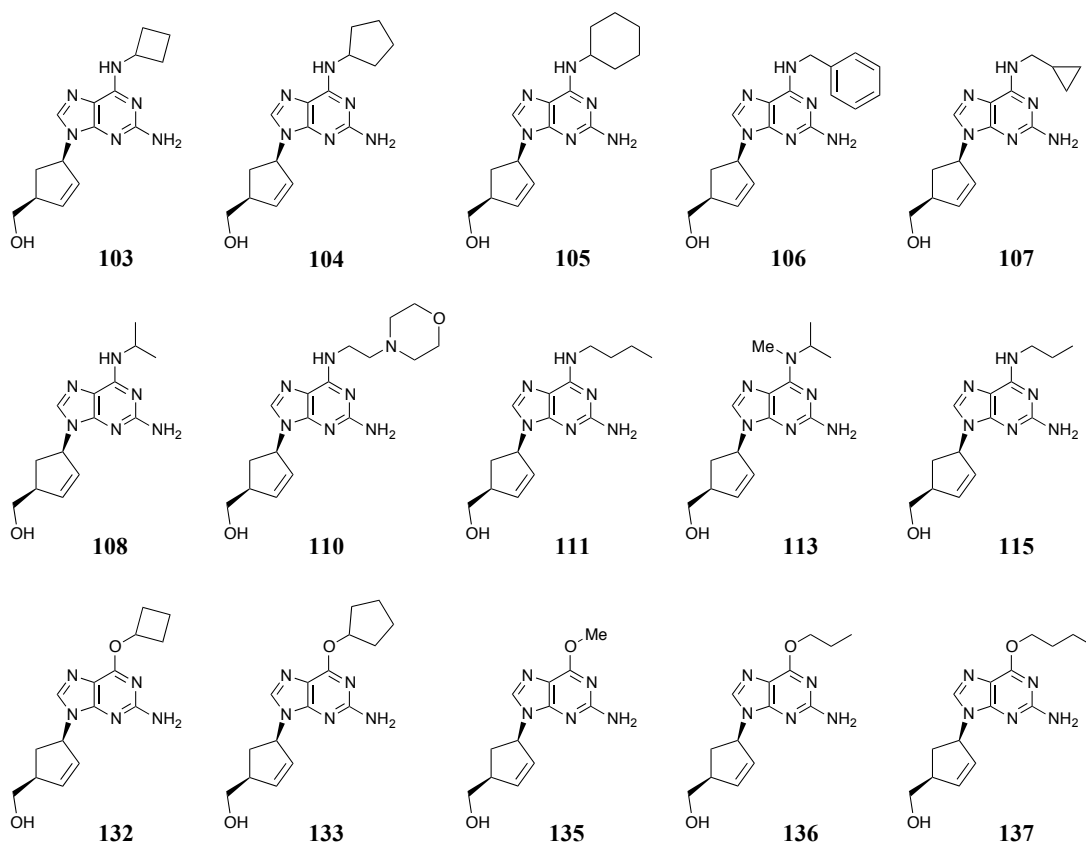
Figure 5.5: The select number of 6-position amine and oxy analogues that were investigated in the ELISpot assay (results shown in Figures **5.6** and **5.7**).

Over increasing compound concentrations (10–250 μM), it can be seen that analogues **107**, **111**, **115**, **136** and **137** stimulated IFN-γ release to the same extent as ABC, where all other analogues did not (Figure **5.6 A–D**). The analogues that resulted in T-cell stimulation have 6-position alkyl moieties. Interestingly, these analogues have less bulky, non-heteroatom, longer chained 6-position substituents compared to those analogues that did not stimulate T-cell clones (Figure **5.5**). These analogues are likely to stimulate T-cells as a result of binding within the HLA-B*57:01 protein – in a similar manner to ABC. This is visualised within Figure **5.8**, where ABC, or one of the aforementioned analogues, can bind within HLA-B*57:01 and alter the set of peptides that are normally displayed by this allele. It is probable

that these analogues will undergo comparable amino acid, namely van der Waals, interactions within the protein as seen with ABC, mainly within the F-pocket region.
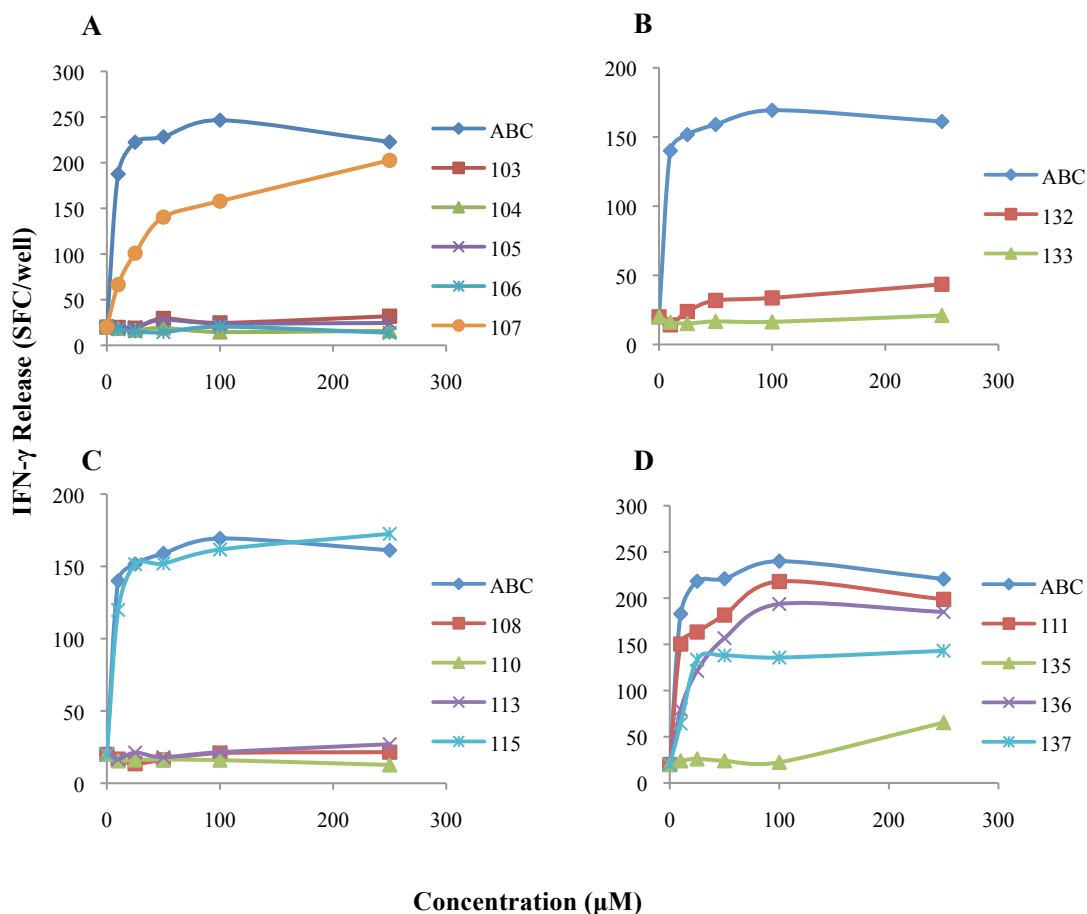
Figure 5.6: Cross-reactivity results for compounds **103–107** (**A**); **132** and **133** (**B**); **108**, **110**, **113** and **115** (**C**); **111**, **135–137** (**D**) showing IFN-γ release, over increasing compound concentrations of 10–250 μM after a 48 h incubation with ABC-specific T-cell clones. Data was visualised using an ELISpot assay and is represented as SFC/well.

The two most notable analogues were compounds **108** and **113**. These analogues bear remarkable similarity to ABC and yet do not result in cytokine release (Figures **5.6 C** and **5.7**). Both compounds **108** and **113** are likely to experience increased steric interactions whilst binding within the protein, resulting in unfavourable binding and no stimulation of T-cells.
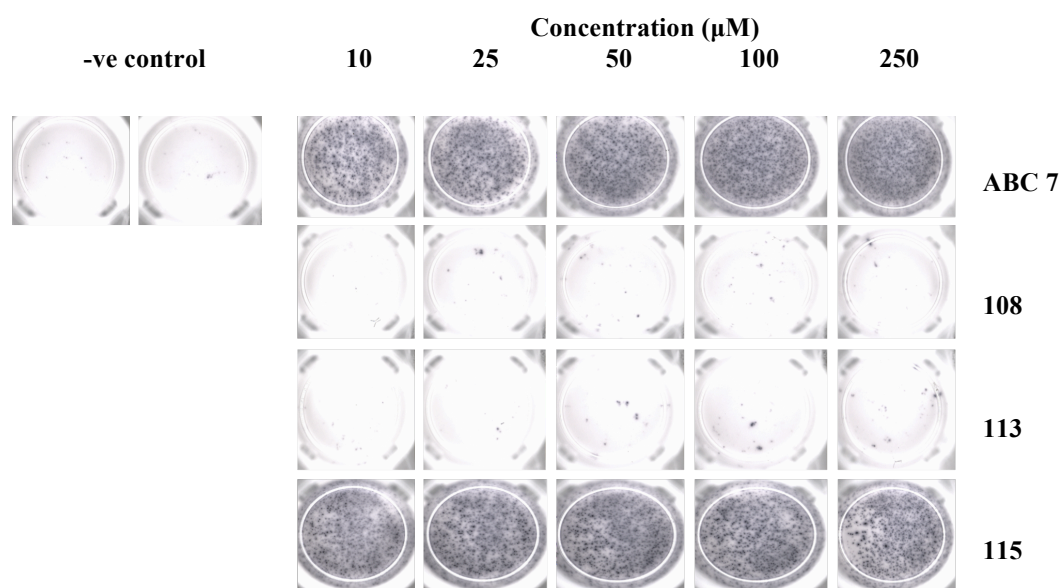
Figure 5.7: ELISpot assay data showing cytokine IFN-γ release for compounds **108**, **113** and **115**, against the positive control ABC, over concentrations of 10–250 μM. Compound **115** stimulates cytokine release, whereas compounds **108** and **113** do not.
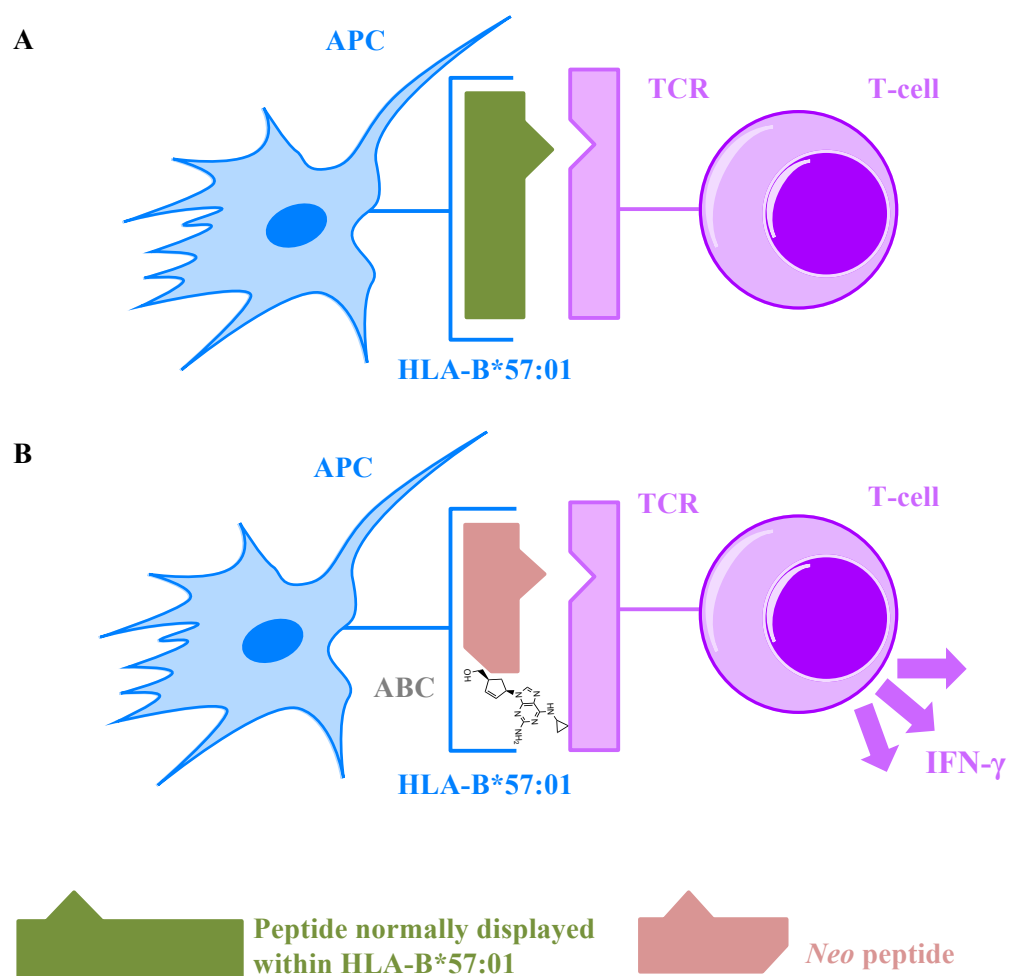
Figure 5.8: In the absence of ABC, self-peptides are displayed within the HLA-B*57:01 allele to T-cells (**A**). In the presence of ABC, and other selected analogues **107**, **111**, **115**, **136** and **137**, the T-cells are stimulated, in *in vitro* experiments. Adapting the altered repertoire mechanism, ABC and these analogues are able to form stable interactions within HLA-B*57:01, most notably within the F-pocket, resulting in an altered set of peptides binding, stimulating T-cells. The stimulation of T-cells will result in cytokine IFN-γ release, which is detected and visualised *via* the ELISpot assay (**B**).

5.3.7 *In silico* molecular docking studies with 6-position analogues.

In silico studies were conducted within the University of Liverpool. Molecular docking can be used to predict the binding orientation of a ligand within a proteins binding site, and establish its potential binding interactions in this preferred

conformation.[17,18] It is a key tool for use in structure-based drug design. The computer program GOLD[19] can be used to generate docking solutions, as well as evaluate the results. By assigning a quantitative measure of binding affinity to each generated pose, this can be completed. One such measure, which can be applied, is the GOLDScore fitness function. Values obtained from GOLDScore consider the key interactions between the ligand and protein: H-bonding, van der Waals interactions, lipophilic interactions and internal strain energy.[20,21]

The HLA-B*57:01 protein crystal structure was obtained from the Protein Data Bank (accession code 3UPR). Firstly, removing ABC from the protein and then docking it back in developed a suitable docking protocol. This was to ensure the docking protocol was capable of reproducing the native binding pose. Using rigid docking the native binding pose of ABC was found to be highly reproducible. This rigid protocol was then applied to the 6-position analogues to observe their potential binding interactions in the HLA-B*57:01 protein, specifically the F-pocket, in comparison to ABC. The resulting GOLDScore values are shown in Table **5.6**. These results, together with data obtained from T-cell assays (Section **5.3.6**), would be used to develop a correlation between GOLDScore values and T-cell stimulation.

Table 5.6: Qualitative T-cell response results and quantitative GOLDScore values, for a select number of 6-position amino and oxy analogues, obtained using the rigid docking protocol. GOLDScore values were obtained using GOLD 5.1. A general trend was observed, where analogues generating GOLDScore values of >50 showed a positive T-cell response.
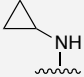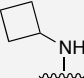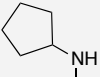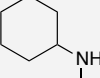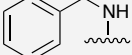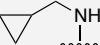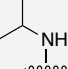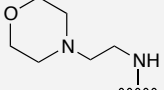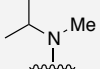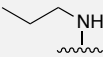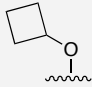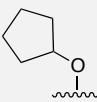
Compound	R^1/R^2 Group	T-Cell Response	GOLDScore
ABC 7		Yes	64.1
103		No	34.4
104		No	46.0
105		No	31.4
106		No	28.1
107		Yes	55.7
108		No	48.4
110		No	−175.1
113		No	24.1

Table 5.6 continued:

115		Yes	64.3
132		No	29.0
133		No	45.2

Using the developed rigid docking protocol, there was found to be a positive relationship between T-cell stimulation and GOLDScore values (Table **5.6**). Those analogues with higher GOLDScore values, particularly above 50, were shown to be more likely to exhibit T-cell activation. After further examination of analogues within the protein it can be seen that those with lower GOLDScore values interact unfavourably with certain amino acids. These steric clashes would inhibit the altered repertoire of peptides binding within HLA-B*57:01 and so preventing T-cell stimulation. It was therefore decided that the arbitrary value 50, would be used a cut-off point to predict whether analogues, in *in silico* studies, could cause a T-cell response.

The key protein–substrate interactions can be seen in Figure **5.9 A–F**. The cyclopropyl moiety of ABC (Figure **5.9 A**) undergoes van der Waals interactions with Ser 116, Tyr 123 and Ile 124, and N^2 interacts with Asp 114. Intermolecular bonding occurs with a range of protein amino acid residues beyond these 4 amino acids. After docking compound **108** into the protein (Figure **5.9 B**), it was observed that almost identical amino acid interactions, as seen with ABC, occurred, although

one distinct steric clash occurred between an *i*-Pr methyl group and Tyr 123. This one interaction was significant enough to disrupt a stable protein–substrate complex from forming and the consequence was seen not only in the lower GOLDScore value (48.4, Table **5.6**), but also with a negative T-cell response. These observations were not only limited to compound **108** but were also seen for compound **113** (Figure **5.9 C**). As before, steric interactions also occurred with an *i*-Pr methyl moiety and Tyr 123, resulting in unfavourable substrate binding. Compound **110** gave a very low GOLDScore result (–175.1, Table **5.6**) and no *in vitro* T-cell activation occurred. Studying this compound further (Figure **5.9 D**), a large proportion of interactions exhibited by ABC binding are disrupted by the large 6-aminoethyl morpholine group. Most notable is the considerable steric interaction of the morpholine moiety with Tyr 123. With the steric clashes evident in the binding of these 3 compounds, the lower GOLDScore values and eliminated T-cell activation can be explained.

Conversely, when compounds **107** and **115** (Figure **5.9 E** and **F**) were docked into the protein, a large proportion of favourable protein interactions were maintained. The 6-amino propyl or the 6-amino methylene cyclopropyl moiety were able to additionally improve binding due to further stable interactions within the F-pocket of the HLA-B*57:01. No detrimental steric interactions occurred with either compound. These compounds docked with GOLDScore values of 55.7 and 64.3 respectively, and T-cell activation was evident from the cross-reactivity T-cell assays (Figure **5.6 A** and **C**).
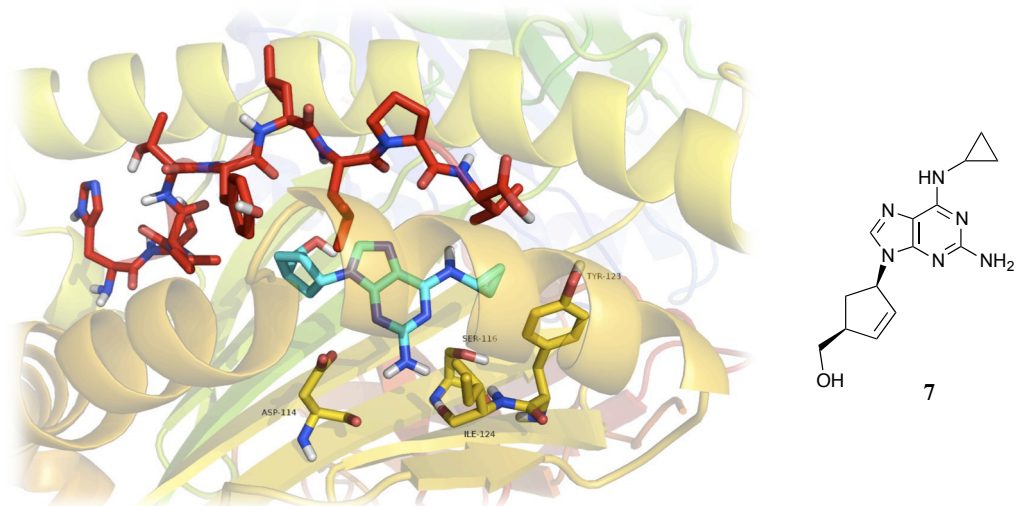
A

Figure 5.9 A: Protein represented as a cartoon. Pep-V is shown in red, ABC (2D structure also shown) is shown in blue and key amino acid residues (Asp 114, Ser 116, Tyr 123 and Ile 124) in yellow. Amino acid residues Ser 116, Tyr 123 and Ile 124, present within the F-pocket, interact with the cyclopropyl moiety of ABC and N^2 interacts with Asp 114. These interactions stabilise the binding of ABC within HLA-B*57:01.
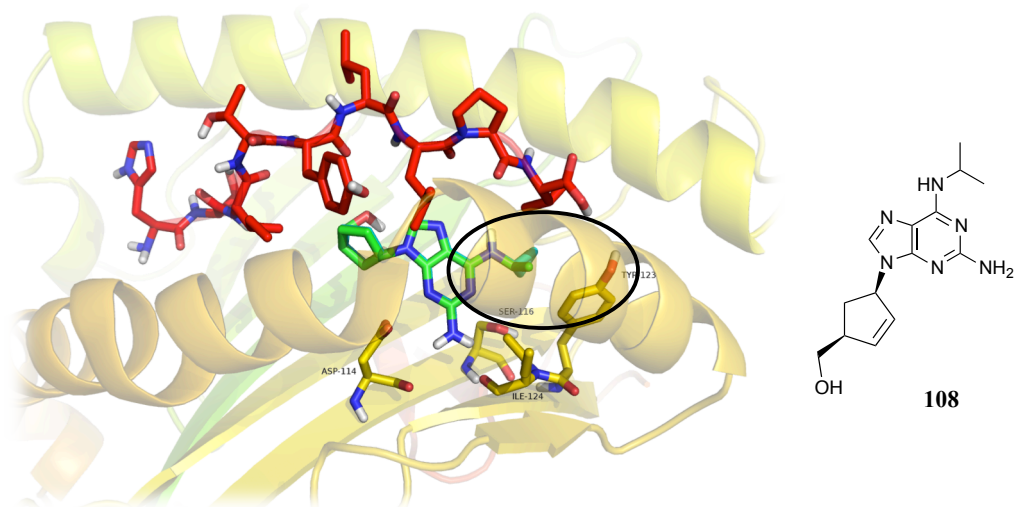
B

Figure 5.9 B: Protein represented as a cartoon. Pep-V is shown in red, ABC is shown in blue, and compound **108** (2D structure also shown) has been overlaid in green and key amino acid residues (Asp 114, Ser 116, Tyr 123 and Ile 124) in yellow. The steric interaction of a methyl group from the *i*-Pr moiety with Tyr 123 is highlighted within the figure and this is responsible for an altered binding within the F-pocket of the protein, disrupting its binding within the protein, giving a lower GOLDScore value (48.4) compared to ABC.
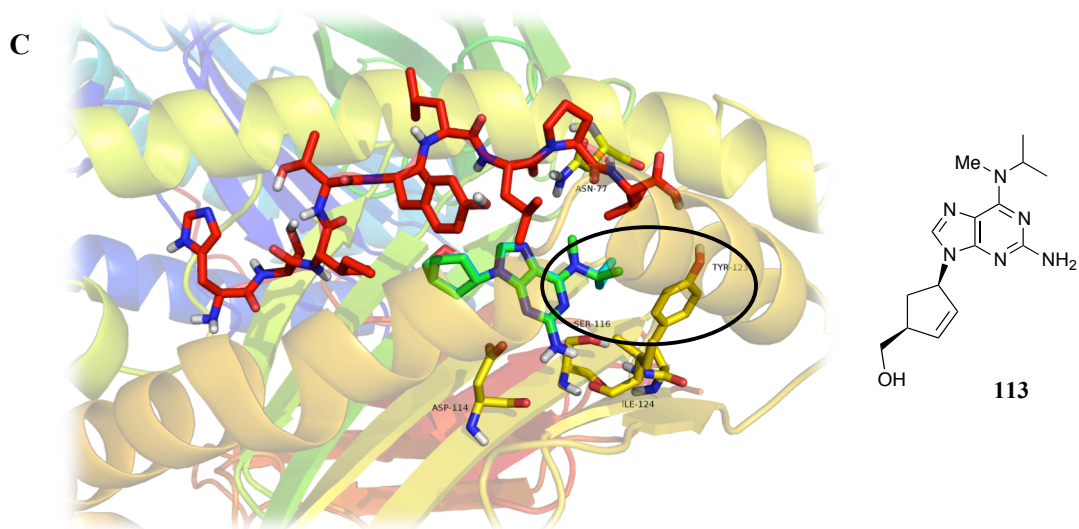
Figure 5.9 C: Protein represented as a cartoon. Pep-V is shown in red, ABC is shown in blue, and compound **113** (2D structure also shown) has been overlaid in green and key amino acid residues (Asn 77, Asp 114, Ser 116, Tyr 123 and Ile 124) in yellow. There is a visible interaction of a methyl group with Tyr 123 from N^6, leading to altered binding within the F-pocket and resulting in a lower GOLDScore value (24.1).
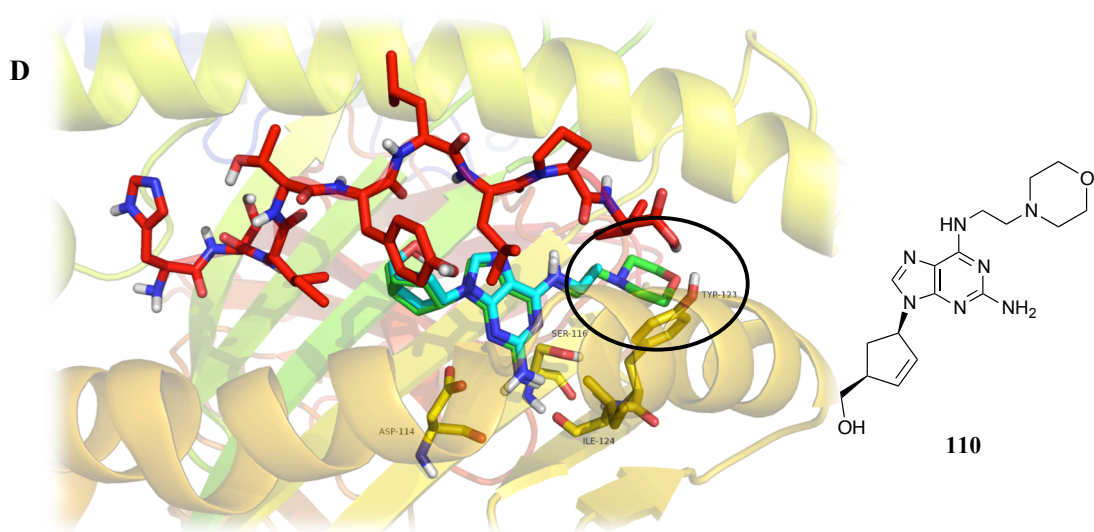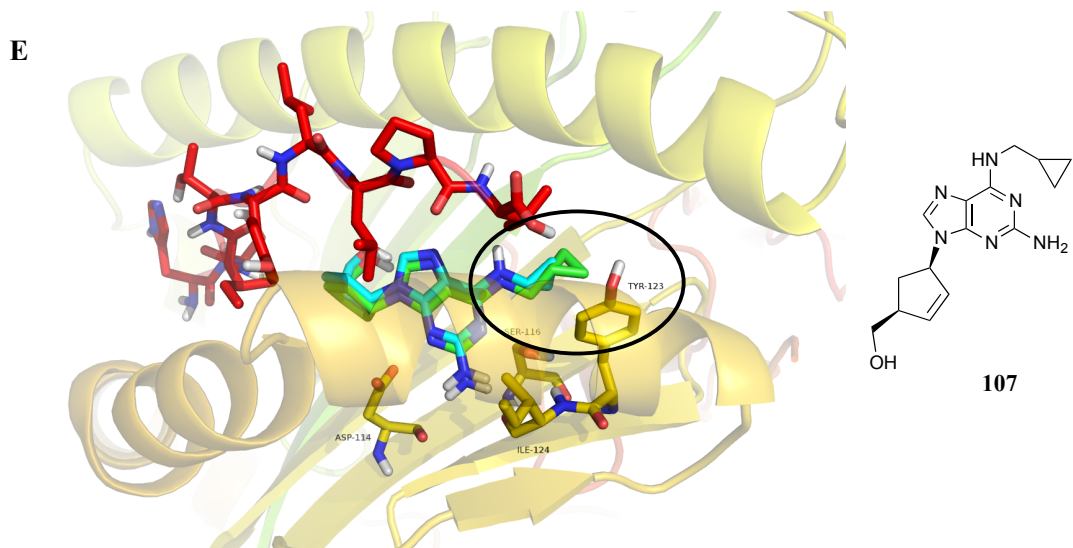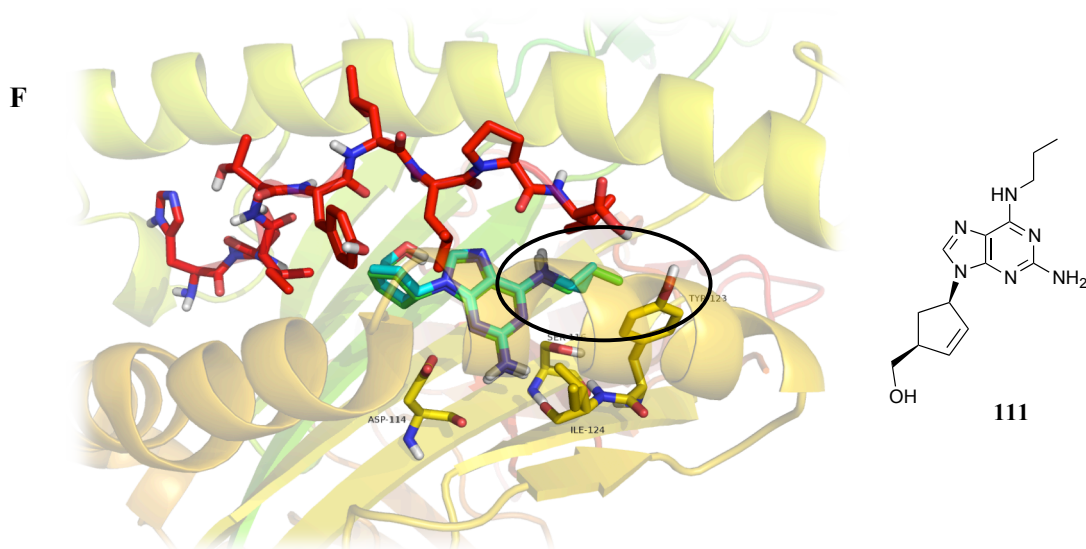

Figure 5.9 D: Protein represented as a cartoon. Pep-V is shown in red, ABC is shown in blue, and compound **110** (2D structure also shown) has been overlaid in green and key amino acid residues (Asp 114, Ser 116, Tyr 123 and Ile 124) in yellow. As depicted within the figure, there is a large steric clash between the morpholine moiety and Tyr 123. The large morpholine group is unable to securely bind within the F-pocket due to these steric interactions, resulting in a large negative GOLDScore value (−175.1).

Figure 5.9 E: Protein represented as a cartoon. Pep-V is shown in red, ABC is shown in blue, and compound **107** (2D structure also shown) has been overlaid in green and key amino acid residues (Asp 114, Ser 116, Tyr 123 and Ile 124) in yellow. Although **107** bound with a slightly different conformation to ABC, the CH_2–cyclopropyl group is able to interact favourably with Tyr 123, leading to a high GOLDScore value (55.7).

Figure 5.9 F: Protein represented as a cartoon. Pep-V is shown in red, ABC is shown in blue, and compound **115** (2D structure also shown) has been overlaid in green and key amino acid residues (Asp 114, Ser 116, Tyr 123 and Ile 124) in yellow. Compound **115** bound with a very similar conformation to ABC within the F-pocket and in particular, it maintains the van der Waals interactions with Tyr 123, assisting with its binding within HLA-B*57:01, giving a higher GOLDScore value (64.3).

As presented in Section **5.3.6**, cross-reactivity data (presented as ELISpot (IFN-γ) data) were obtained from a select number of 6-position analogues (following incubation of each compound with ABC-specific T-cell clones), generated within the University of Liverpool. Not all analogues underwent these cross-reactivity experiments, but GOLDScore values have been generated for these outstanding compounds (Table **5.7**).

Without reactivity data for the compounds as depicted in Table **5.7**, it is difficult to confirm whether these compounds would elicit a T-cell response. However, the rigid docking protocol could be used in a predictive manner, with careful consideration of the GOLDScore values allowing us to predict if a response will occur. Should the T-cell data for these compounds reflect the GOLDScore values, docking can therefore be used to direct the synthesis of future compounds.

Table 5.7: Table representing quantitative GOLDScore values for outstanding 6-position amine and oxy analogues. The data were obtained using a rigid docking protocol. GOLDScore values were obtained using GOLD 5.1. The GOLDScore values will be compared to the T-cell cross-reactivity results and docking can eventually be used to direct future analogue synthesis.
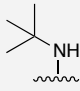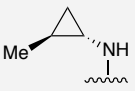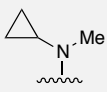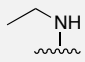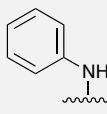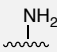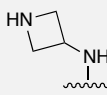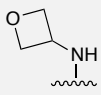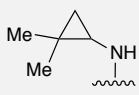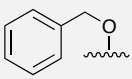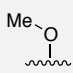
Compound	R^1/R^2 Group	GOLDScore
109		18.9
112		22.3

Table 5.7 continued:

114		34.4
116		57.2
117		−59.8
122		51.9
124		42.0
125		47.6
126		−5.6
134		−52.6
135		55.1

As shown in Table **5.7**, it can be seen that those compounds that are likely to stimulate T-cell clones possess smaller 6-position moieties (compounds **116**, **122** and **135**). These compounds bear groups at this position small enough to maintain the relevant van der Waals interactions (as with ABC) and bind easily within the F-pocket of HLA-B*57:01. Conversely, three compounds have generated negative

GOLDScore values: Compounds **117** (–59.8), **126** (–5.6) and **134** (–52.6). The values for compounds **117** and **134** are not surprising due to the large aromatic substituents at the 6-position and such large groups at this position have shown to generate low GOLDScore values (Table **5.7**). Compound **126** has two additional methyl groups at the β-position on the cyclopropylamine ring. These methyl groups are likely to have a significant impact in the binding of **126** within the F-pocket due to large steric interactions with the neighbouring amino acids.

The remaining five analogues, compounds **109**, **112**, **114**, **124** and **125** have also generated lower GOLDScore values than the threshold used to analyse these data. The steric bulk of the *t*-Bu group within compound **109**, as with compound **126**, is likely to exhibit steric interactions when binding within the protein. This is also likely to be a similar reason for lower GOLDScore values for compounds **112** (22.3) and **114** (34.4). The additional methyl group on both these compounds, either on the cyclopropyl ring (**112**) or on *N*-methyl, will add to the steric hindrance of the group at this position. Finally, the amino azetidine and oxetane moieties, compounds **124** and **125** respectively, have also generated lower GOLDScore values, although, these values are close to the threshold, 50. However, they are predicted to not elicit a T-cell response. Further molecular docking analysis of these analogues would be interesting due to the small nature of the group and the presence of a heteroatom within the ring structures. The possible H-bonding of these heteroatoms to neighbouring amino acids within the HLA-B*57:01, in particular within and surrounding the F-pocket would be interesting to investigate. Also, the threshold at which the docking defines a compound as having the potential to generate a T-cell response or not may require modification, depending upon the new results, with 50

currently being used as the most obvious cut-off. This value can be subject to change: The molecular docking studies are in their infantry, and as our understanding of analogue binding within HLA-B*57:01 develops it will help define a more accurate and permanent value.

5.3.8 Cytotoxicological and pharmacological studies with 6-position analogues

The antiviral and cytotoxicity studies were carried out at the University of Liverpool. The theory and discussion of these assays is discussed in Chapter 1, Section **1.11**. To probe the pharmacological activity of a select number of the synthesised 6-position analogues, cytotoxicity and efficacy of these analogues was tested. The results of these assays can be seen in Table **5.8**. Assays measuring cytotoxicity (IC_{50}) in MT4 cells was measured over 24 h and 5 days and antiviral (EC_{50}) values were obtained after 5-day incubations. All comparisons are made with the control, ABC.

After 24 h and 5 days, the cytotoxicity for ABC was found to be 301.8 μM and 199.2 μM respectively. The IC_{50} values for compounds **103**–**106**, **110**, **132** and **133** ranged from 10.2–44.5 μM over 24 h and 2.4–12.2 μM over 5 days. These compounds exhibited significant toxicity compared to ABC over both time points. The most notable analogues **107**, **108**, **113** and **115** gave comparable cytotoxicity values to ABC at 24 h and 5 days. Interestingly, compounds **108** and **113** did not stimulate T-cells in cross-reactivity experiments. The disparity in toxicity is likely to be due to variation of cell types used, within the cytotoxicity (mitochondrial toxicity) and T-cell experiments. Compound **115** showed the most promise with IC_{50} values of 295.4 μM and 197.9 μM at 24 h and 5 days respectively but this was shown to exhibit significant stimulation of T-cells (Figure **5.5**).

For all analogues, the cytotoxicity values increased in samples taken after 5 days, compared to those obtained after 24 h. A possible reason being the generation of a toxic intermediate metabolite and the nature of this metabolite would lead to decreased MT4 cell viability. Due to the lower number of MT4 cells there would be less conversion of MTT to MTT formazan, resulting in increased IC_{50} values. This toxic compound could possibly be the aldehyde intermediate, generated from oxidation of 5'-OH to its corresponding carboxylic acid.

The antiviral EC_{50} value generated for ABC was 3.8 µM. Most analogues proved to be much less potent than ABC EC_{50} values >5 µM, with **108**, **113** and **115** presenting comparable efficacy values: 2.7, 2.4 and 5.3 µM respectively (Table **5.8**). Comparing the selectivity index (IC_{50}/EC_{50}) of these analogues (Table **5.8**), it can be seen that the most significant compounds are **107**, **108**, **113** and **115** − analogues presenting high IC_{50} and low EC_{50} values as with ABC. The structures of these compounds are very subtly different to ABC but as discussed in Section **5.3.2**, they exhibit slight steric interactions with the HLA-B*57:01 protein resulting in subtly different levels of T-cell activation.

Table 5.8: Cell viability was assessed using the spectrophotometric MTT assay. Cytotoxicity (IC_{50}) values generated in MT4 cells over 24 h and 5 days and efficacy (EC_{50}) values generated against $HIVIII_B$ in MT4, using the spectrophotometric MTT assay; which visualises the viral cytotoxicity. These data were completed for select 6-position amine and oxy analogues. The selectivity index is shown within the table (IC_{50}/EC_{50}). All data are given as the mean ± standard deviation of four independent experiments, performed on different days. IC_{50} values were generated using GraphPad Prism 3.0 software.
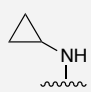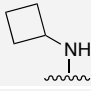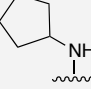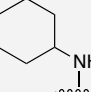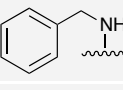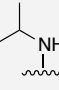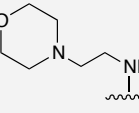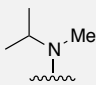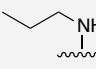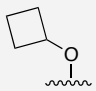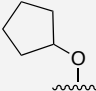
Compound	R^1/R^2 Group	Cytotoxicity IC_{50} (µM) ± SD	Cytotoxicity IC_{50} (µM) ± SD	Efficacy EC_{50} (µM) ± SD	Selectivity Index (IC_{50}/EC_{50})
		24 h	5 days	5 days	5 days
7		301.8 ± 17.00	199.2 ± 11.80	3.8 ± 0.19	52.56
103		30.2 ± 1.21	11.5 ± 0.75	12.6 ± 0.17	0.91
104		44.5 ± 3.71	12.2 ± 0.74	11.6 ± 0.51	0.10
105		12.0 ± 2.36	9.9 ± 0.66	15.0 ± 0.33	0.66
106		34.6 ± 3.26	11.7 ± 0.39	17.9 ± 3.31	0.65
107		233.3 ± 9.00	171.2 ± 5.20	6.8 ± 0.89	25.18
108		126.4 ± 12.20	77.7 ± 3.63	2.7 ± 0.03	28.70
110		11.7 ± 0.45	2.8 ± 0.14	8.5 ± 0.86	0.33

Table 5.8 continued:

113		95.8 ± 8.88	65.3 ± 5.18	2.4 ± 0.02	27.20
115		295.4 ± 28.30	197.9 ± 7.46	5.3 ± 0.77	37.34
132		12.7 ± 0.43	3.0 ± 0.09	6.4 ± 0.48	0.47
133		10.2 ± 0.34	2.4 ± 0.07	5.9 ± 0.42	0.41

5.3.9 Initial PK screening for ABC and compound 108.

With compound **108** showing promise in pharmacological and immunological studies showing low cytotoxicity, comparable efficacy to ABC and no T-cell activation, initial PK experiments were conducted.

5.3.9.1 Plasma concentration–time relationship for ABC and compound 108.

Mean plasma concentration–time graphs (Figure **5.10 A** and **B**) were obtained using male SD rats (n = 3) *via* intravenous (IV, 1 mg/kg) and oral (PO, 10 mg/kg) administration over selected times points.

A
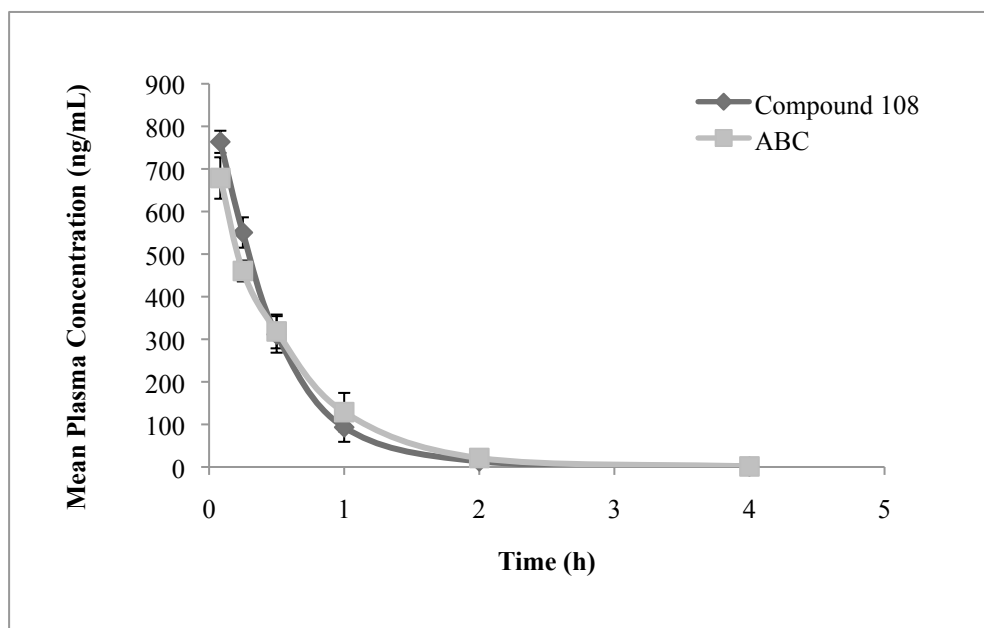
B
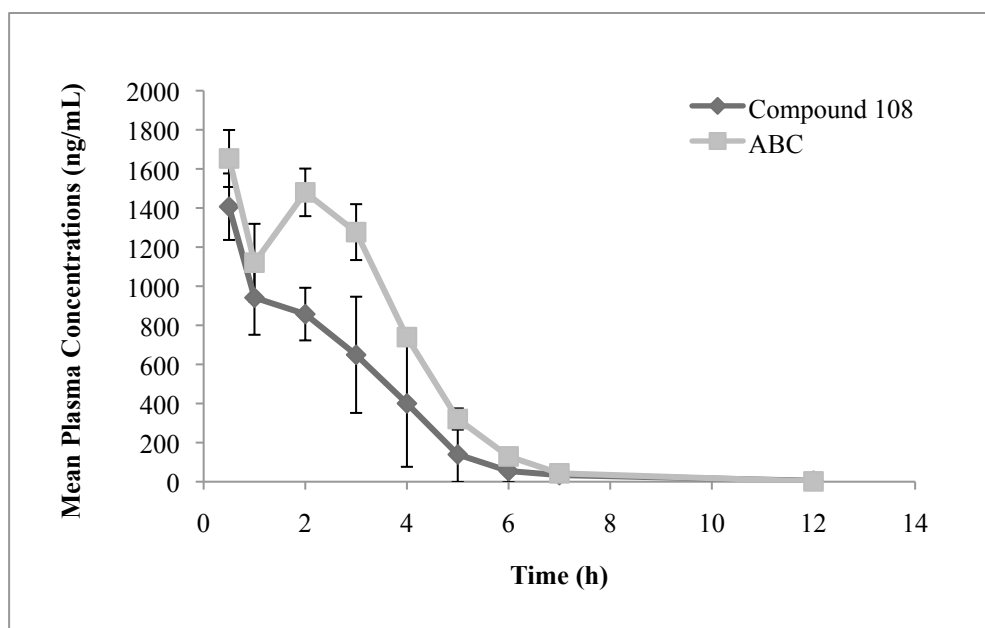
Figure 5.10: Graph showing the plasma concentration–time curves for ABC and compound **108** following IV administration with dosage of 1 mg/kg (**A**) and PO administration with dosage of 10 mg/kg (**B**) in male SD rats. Samples were taken over 24 h and unquantifiable data (<1 ng/mL) was excluded (samples obtained between 12–24 h). Data represents the mean value ± SD (n = 3). IV, intravenous; PO, *per os* (oral).

From Figure **5.10**, it can be seen that the relationship of compound plasma concentrations over time (5 min to 4 h) *via* IV and PO administration for ABC and compound **108** are similar for both means of administration. Data obtained from >4 h was below the quantifiable limit (BQL).

5.3.9.2 PK parameter relationships for ABC and compound 108.

PK parameters (Table **5.9**) were obtained using male SD rats (n = 3) *via* an IV (1 mg/kg) and PO (10 mg/kg) dose administration. Four PK parameters (clearance, CL; T_{max}; C_{max}; bioavailability, F) for both ABC and **108** are shown in Table **5.9**. CL and C_{max} values for **108** are very similar to ABC, and although F for **108** is lower than for ABC, it still shows excellent bioavailability ($\sim$ 80%).

Table 5.9: PK parameters for ABC and compound **108**. IV and PO doses were administered to 6 male SD rats (3 rats for each route of administration) at a dose of 1 mg/kg and 10 mg/kg respectively. Data is represented as the mean ± SD (n = 3).

PK Parameter (ABC)	Mean ± SD (n = 3)
IV dose at 1 mg/kg in male SD rats	
CL (L/h/kg)	2.20 ± 0.33
PO dose at 10 mg/kg in male SD rats	
T_{max} (h)	0.50 ± 0.00
C_{max} (ng/mL)	1653 ± 146
F (%)	124 ± 6.82

PK Parameter (108)	Mean ± SD (n = 3)
IV dose at 1 mg/kg in male SD rats	
CL (L/h/kg)	2.23 ± 0.28
PO dose at 10 mg/kg in male SD rats	
T_{max} (h)	0.50 ± 0.00
C_{max} (ng/mL)	1407 ± 170
F (%)	79.90 ± 19.70

Comparing the initial PK data, it shows that compound **108** over a 24 h time-course has a comparable rat PK profile following IV and PO administration compared to ABC. These initial experiments show that the replacement of 6-cyclopropylamine with 6-isopropylamine does not appear to have a significant impact on overall disposition.

5.4 Conclusions & Future Work

It was proposed by two independent research groups that ABC toxicity arose from the non-covalent binding of ABC within the HLA-B*57:01 protein. Upon binding, ABC was exposed to several van der Waals interactions with a number of amino acids, resulting in assisted stabilised binding within the protein. Such binding resulted in an altered repertoire of peptides displayed by the protein, the consequence being an immunological response. Notably, the binding of ABC was assisted by the 6-position cyclopropyl moiety within the F-pocket of the protein. It was therefore the aim of this research to synthesise a range of 6-position analogues of ABC in an attempt to inhibit binding within HLA-B*57:01 and probe this suggested mechanism of toxicity further.

A series of *N*- and *O*- 6-position analogues were synthesised from Cl-ABC **32** using standard aromatic nucleophilic substitution. Such analogues bore *n*-, *i*-alkyl chains, alkyl ring structures with or without the incorporation of heteroatoms, and aromatic groups. Most desired analogues were achieved with excellent yields. Those analogues that bore cyclic heteroatom or sterically hindered alkyl moieties proved the most difficult to synthesise, but most difficulties were overcome with slightly modified reaction conditions. Fluoro-cyclopropyl starting compounds were problematic, and although a range of reaction conditions was attempted, these analogues could not be synthesised.

A select number of both *N*- and *O*- analogues were chosen to undergo immunological testing, where proliferation and IFN-γ release of ABC-specific T-

cells was monitored. The majority of analogues did not stimulate the T-cell clones, with compounds **107**, **111**, **115**, **136** and **137** resulting in a positive response. Further molecular modelling studies of these analogues illustrated that they too underwent similar binding to ABC, with all van der Waals interactions with key amino acids maintained. Conversely, two notable compounds **108** and **113** did not stimulate the T-cell clones, although they both bear a remarkable similarity to the structure of ABC. Further docking studies of these compounds revealed that although both compounds bound in a similar manner to ABC, steric interactions of the *i*-Pr methyl group with the bulky Tyr 123 amino acid within the F-pocket of the HLA-B*57:01 protein made this binding unfavourable. *In silico* studies revealed that the larger the 6-position substituent, the more unfavourable the binding was within the protein – likely to be due to steric interactions. Analogues that bore *n*-alkyl 6-position moieties were more likely to stimulate a T-cell response through favourable binding of these groups within the F-pocket of the protein.

Along with the immunological and molecular modelling studies, pharmacological testing was also conducted on these same analogues. The antiviral testing was conducted using the HIVIII$_B$ virus. Most analogues were shown to be less active than ABC, although compounds **108** and **113** had comparable efficacy results to ABC. It was further noted that as well as these compounds having similar antiviral activity to ABC, they did not stimulate cytokine release or proliferation of T-cell clones in the immunological assays. Compound **108** was selected for initial PK profiling and plasma concentration–time data and PK parameters were obtained. All values for **108** were similar to ABC (namely plasma concentration–time data, C_{max} and bioavailability).

For future studies, there are many potential avenues available for the development of a safer alternative to ABC. Although **108** shows much promise *in vitro* and in initial *in vivo* studies, further PD studies will be required. The remaining 6-position analogues require immunological, *in silico*, and pharmacological testing. This will not only allow for further probing and understanding of ABC toxicity, and to determine whether a compound with equivalent pharmacological and PK parameters to ABC can be discovered, but most importantly, with no immunogenic properties. Further to these biological studies, additional chemical synthesis of 6-position analogues can be conducted. Further studies into the synthesis of 6-fluorocyclopropyl compounds, the 6-oxycyclopropyl analogue, and 6-position thiol compounds should be investigated.

5.5 Experimental

Compounds **115**, **117**, **118**, **135**–**137** and **139** were synthesised at the University of Liverpool by Matthew Pye. Dr. Alex Lawrenson performed molecular docking studies and generated GOLDScore values at the University of Liverpool. Immunology (cross-reactivity) experiments and pharmacological (cytotoxicity/efficacy) experiments were also conducted and obtained at the University of Liverpool by Mohammad Alhaidari and John Farrell (Dr. Dean Naisbitt's research group) and Dr Philip Martin (Prof. Andrew Owen's research group) respectively.

5.5.1 Synthesis.
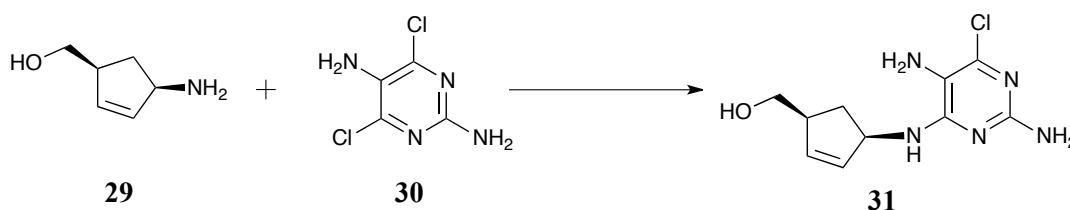
((1*S*,4*R*)-4-((2,5-Diamino-6-chloropyrimidin-4-yl)amino)cyclopent-2-en-1-yl)methanol 31:[22] To (1*S*,4*R*)-4-amino-2-cyclopentene-1-methanol tartrate salt **29** (1.00 g, 4.0 mmol) in *n*-BuOH (10 mL) was added DADCP **30** (0.69 g, 4.0 mmol) and NaHCO$_3$ (1.12 g, 13.0 mmol) and the mixture was allowed to stir for 16 h at 95 °C. The mixture was cooled and filtered under vacuum. The resulting solvent from the filtrate was removed *in vacuo*. The crude product was purified by column chromatography (1:49 to 1:24 MeOH–DCM) to yield **31** (0.52 g, 53%) as a pale brown solid. mp: 157–159 °C (lit.[22] mp: 158.5–160.5 °C). ^{1}H NMR (MeOD): δ 5.87 (ddd, *J* = 5.5, 2.0, 1.9 Hz, 1H), 5.80 (ddd, *J* = 5.6, 2.0, 2.0 Hz, 1H), 5.15–5.07

(m, 1H), 3.56–3.47 (m, 1H), 3.28 (m, 1H), 2.83–2.79 (m, 1H), 2.53 (ddd, J = 13.4, 6.4, 6.4 Hz, 1H), 1.36 (ddd, J = 13.4, 6.3, 5.9 Hz, 1H). ^{13}C NMR (MeOD): δ 158.2, 157.3, 143.2, 135.8, 133.9, 114.4, 66.4, 57.8, 57.7, 35.8. *m/z* (ES+) 256.0955 calculated for $C_{10}H_{15}N_5O^{35}Cl$: $[M+H]^+$ 256.0965 and 258.0928 calculated for $C_{10}H_{15}N_5O^{37}Cl$: $[M+H]^+$ 258.0936. IR (cm^{-1}): 3451 (N−H), 3324 (N−H), 3125 (br, O−H), 2931 (C−H), 1570 (C=C aromatic), 1430 (CH$_2$), 690 (C−Cl).

31   **32**
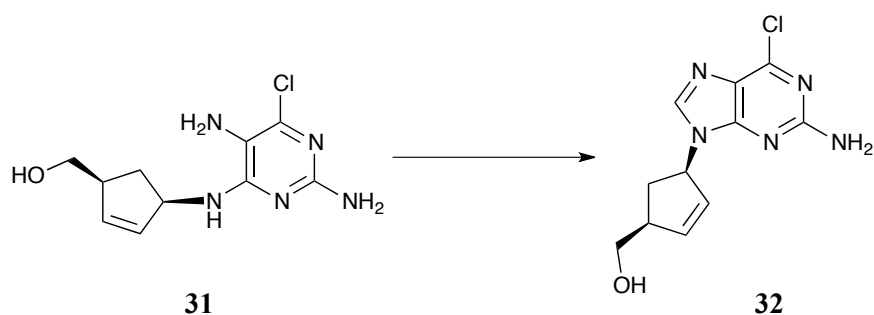
((1*S*,4*R*)-4-(2-Amino-6-chloro-9*H*-purin-9-yl)cyclopent-2-en-1-yl)methanol 32:[23]

To a solution of **31** (0.50 g, 2.0 mmol) in *n*-BuOH (15 mL) was added TEOF (0.4 mL, 2.4 mmol) and H$_2$SO$_4$ (0.05 µL, 0.1 mmol). The brown solution was allowed to stir for 20 h at 70 °C. The solution was allowed to cool whereupon the solvent was removed *in vacuo* and the crude mixture was purified by column chromatography (1:99 to 5:95 MeOH−DCM) to yield **32** (0.45 g, 87%) as a brown solid. mp: 158–161 °C (lit.[23] mp: 160–162 °C). ^{1}H NMR (CDCl$_3$): δ 7.95 (s, 1H), 6.18 (ddd, J = 5.5, 2.2, 2.1 Hz, 1H), 5.82 (ddd, J = 5.5, 2.2, 2.0 Hz, 1H), 5.56–5.52 (br m, 1H), 3.85 (dd, J = 10.7, 4.2 Hz, 1H), 3.76 (dd, J = 10.7, 3.9 Hz, 1H), 3.48 (MeOH), 3.13–3.09 (m, 1H), 2.81 (ddd, J = 14.4, 6.4, 6.2 Hz, 1H), 1.98 (ddd, J = 14.4, 6.2, 5.3 Hz, 1H). ^{13}C NMR (CDCl$_3$): δ 159.1, 153.5, 151.6, 142.2, 139.5, 130.0, 115.9, 65.0, 61.1, 50.4 (MeOH), 48.1, 33.6. *m/z* (ES+) 288.0626 calculated for $C_{11}H_{12}N_5O^{23}Na^{35}Cl$: $[M+Na]^+$ 288.0628 and 290.0603 calculated for $C_{11}H_{12}N_5O^{23}Na^{37}Cl$: $[M+Na]^+$

290.0599. IR (cm^{-1}): 3325 (N−H), 3205 (N−H), 1581 (C=C aromatic), 1246 (C−O), 640 (C−Cl).

119
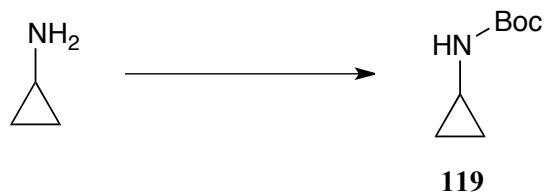
***tert*-Butyl cyclopropylcarbamate 119:**[24] To a solution of cyclopropylamine (1.00 g, 0.02 mol) in DCM (35 mL) was added Boc₂O (3.68 g, 0.02 mol) at 0 °C. The reaction mixture was allowed to stir overnight at room temperature. Following this, the solvent was removed *in vacuo* to yield **119** (2.76 g, 92%) as a pale yellow crystalline solid. mp: 63–65 °C (lit.[24] mp: 62.5–64 °C). ^{1}H NMR (CDCl₃): δ 4.75 (br s, 1H), 2.54–2.52 (m, 1H), 1.44 (s, 9H), 0.69–0.66 (m, 2H), 0.48–0.46 (m, 2H). ^{13}C NMR (CDCl₃): δ 157.1, 79.7, 28.8 (3C), 23.3, 7.1 (2C). *m/z* (CI) 157.11 calculated for C₈H₁₅NO₂: [M+H]$^+$ 158.1. Anal. calc. for C₈H₁₅NO₂: C, 61.12; H, 9.62; N, 8.91. Found: C, 61.00; H, 9.66; N, 8.95. IR (cm^{-1}): 3359 (N−H), 2970 (C−H), 1693 (C=O), 1207 (C−O).

119   **120**
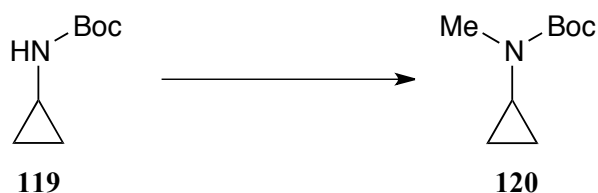
***tert*-Butyl cyclopropyl(methyl)carbamate 120:**[24] To a solution of **119** (2.52 g, 0.02 mol) in DMF (50 mL) was added NaH (60% dispersed in mineral oil, 0.77 g, 0.03 mol) at 0 °C. The solution was allowed to stir for 30 min and MeI (1.2 mL, 0.02 mol) was added dropwise at 0 °C. The solution was allowed to stir for a further 5 h

at room temperature and was quenched with saturated aqueous NH$_4$Cl. The mixture was extracted with EtOAc (3 × 50 mL) and the combined organic extracts were washed with water (4 × 200 mL), brine and dried over MgSO$_4$. The solvent was removed *in vacuo*. The crude product was purified by column chromatography (3:17 EtOAc–*n*-hex) to yield **120** (2.00 g, 73%) as a pale yellow viscous oil.[24] ^{1}H NMR (CDCl$_3$): δ 2.83 (s, 3H), 2.53–2.48 (m, 1H), 1.46 (s, 9H), 0.72–0.69 (m, 2H), 0.61–0.57 (m, 2H). ^{13}C NMR (CDCl$_3$): δ 157.1, 79.2, 34.7, 30.5, 28.6 (3C), 7.9 (2C). *m/z* (CI) 171.13 calculated for C$_9$H$_{17}$NO$_2$: [M+H]$^+$ 172.2. IR (cm^{-1}): 2978 (C−H), 1700 (C=O), 1153 (C−O).

120   **121**

N-Methylcyclopropanamine 121:[24] To an ice-cold solution of **120** (1.45 g, 8.0 mmol) in MeOH (30 mL) was added AcCl (3 mL, 42.0 mmol) dropwise. The solution was allowed to stir at room temperature overnight. The reaction was basified with 1 M NaOH until the solution became pH 9–10. The solution was extracted into DCM (4 × 50 mL) and dried over MgSO$_4$. The solvent was removed *in vacuo* to yield **121** (0.35 g, 58%) as a clear, colourless liquid.[24] ^{1}H NMR (CDCl$_3$): δ 2.74 (s, 3H), 2.60–2.54 (m, 1H), 1.20–1.18 (m, 2H), 0.88–0.83 (m, 2H). ^{13}C NMR (CDCl$_3$): δ 33.9, 32.2, 4.2 (2C).
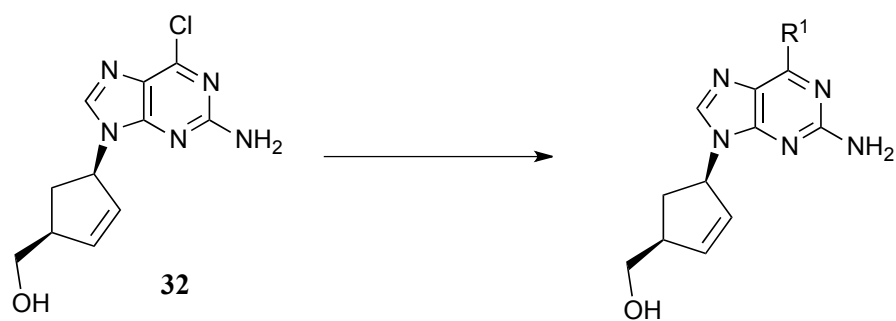
General Procedure A: To a solution of **32** (1 equiv) in MeOH (10 mL) was added the primary or secondary amine (2 equiv) and the solution was allowed to stir overnight at 60–70 °C. The mixture was allowed to cool and the MeOH was removed *in vacuo*. The crude solid was purified by column chromatography (1:49 to 1:19 MeOH–DCM) to yield the appropriate product.
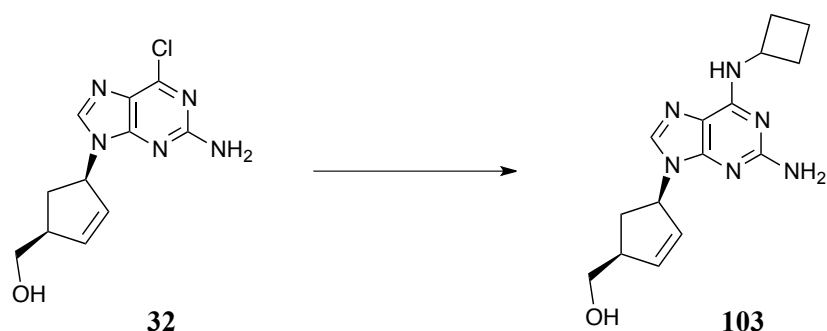
((1*S*,4*R*)-4-(2-Amino-6-(cyclobutylamino)-9*H*-purin-9-yl)cyclopent-2-en-1-yl)methanol 103:[25] General Procedure A was followed to yield **103** (71 mg, 62%) as a cream coloured solid. mp: 180–183 °C (for racemic lit.[25] mp: 181–183 °C). ¹H NMR (CDCl₃): δ 7.46 (s, 1H), 6.08 (ddd, *J* = 5.2, 2.1, 2.0 Hz, 1H), 6.01 (br s, 1H), 5.73 (ddd, *J* = 5.2, 2.0, 1.9 Hz, 1H), 5.41–5.37 (br m, 1H), 4.66 (br m, 1H), 3.85 (dd, *J* = 10.3, 4.0 Hz, 1H), 3.75 (dd, *J* = 10.8, 3.2 Hz, 1H), 3.48 (MeOH), 3.08–3.07 (m, 1H), 2.75 (ddd, *J* = 14.5, 6.1, 6.0 Hz, 1H), 2.39–2.38 (m, 2H), 2.09 (ddd, *J* = 14.5,

6.0, 5.6 Hz, 1H), 1.94–1.89 (m, 2H), 1.73–1.70 (m, 2H). ^{13}C NMR (CDCl$_3$): δ 159.6, 154.7, 138.5, 137.1, 130.8, 115.4, 65.5, 61.8, 50.4 (MeOH), 48.2, 32.9, 32.1, 15.4. *m/z* (ES+) 301.1783 calculated for C$_{15}$H$_{21}$N$_6$O: [M+H]$^+$ 301.1777. IR (cm^{-1}): 3313 (N−H), 3213 (N−H), 2938 (C−H), 1589 (C=C aromatic), 1477 (CH$_2$), 1392 (CH$_3$), 1257 (C−N), 1033 (C−O).
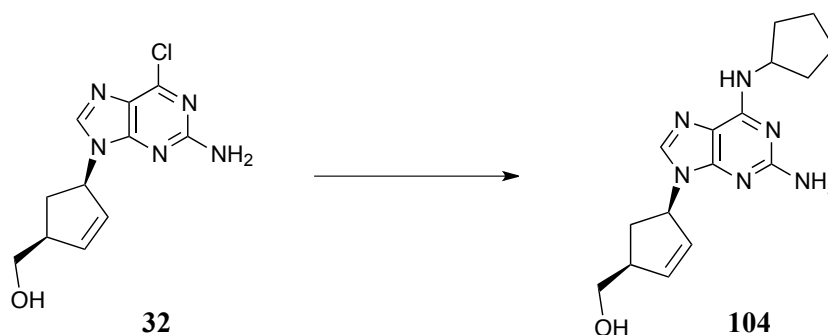
((1*S*,4*R*)-4-(2-Amino-6-(cyclopentylamino)-9*H*-purin-9-yl)cyclopent-2-en-1-yl)methanol 104:[25] General Procedure A was followed to yield **104** (0.10 g, 85%) as a pale brown solid. mp: 142–145 °C (for racemic lit.[25] mp: 143–146 °C). ^{1}H NMR (CDCl$_3$): δ 7.47 (s, 1H), 6.10 (ddd, *J* = 5.5, 2.1, 2.1 Hz, 1H), 6.02 (br s, 1H), 5.76 (ddd, *J* = 5.4, 2.2, 2.1 Hz, 1H), 5.42–5.41 (br m, 1H), 4.86–4.84 (m, 1H), 4.48 (br s, 1H), 3.86 (dd, *J* = 10.8, 4.1 Hz, 1H), 3.76 (dd, *J* = 10.8, 3.4 Hz, 1H), 3.48 (MeOH), 3.11–3.09 (m, 1H), 2.77 (ddd, *J* = 14.5, 6.0, 5.9 Hz, 1H), 2.12–2.05 (m, 2H), 1.75–1.72 (m, 1H), 1.65–1.62 (m, 4H), 1.54–1.49 (m, 2H). ^{13}C NMR (CDCl$_3$): δ 159.4, 155.0, 138.2, 136.5, 130.5, 115.1, 65.2, 61.4, 50.4 (MeOH), 47.8, 33.4, 32.6, 23.8 (2C). *m/z* (ES+) [M+H]$^+$ 315.1492 calculated for C$_{16}$H$_{23}$N$_6$O found [M+H]$^+$ 315.1933. IR (cm^{-1}): 3324 (N−H), 3205 (br, O−H), 2931 (C−H), 1581 (C=C aromatic), 1477 (CH$_2$), 1392 (CH$_3$), 1249 (C−O).
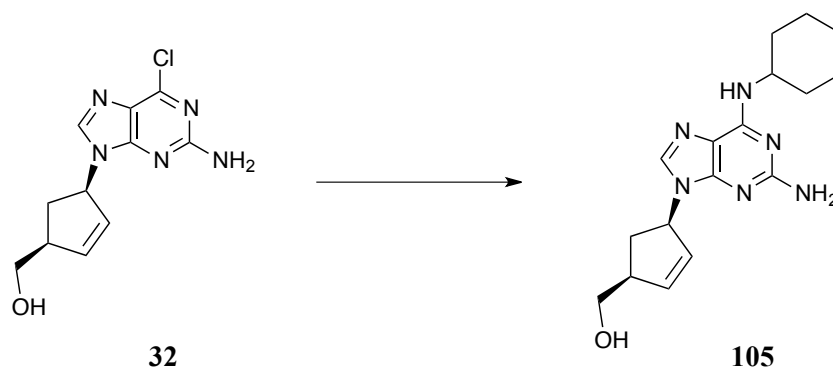
((1S,4R)-4-(2-Amino-6-(cyclohexylamino)-9H-purin-9-yl)cyclopent-2-en-1-

yl)methanol 105: General Procedure A was followed to yield **105** (87 mg, 71%) as

a cream coloured solid. mp: 191–194 °C. ^{1}H NMR (CDCl$_3$): δ 7.53 (s, 1H), 6.13

(ddd, J = 5.5, 2.2, 2.1 Hz, 1H), 5.79 (ddd, J = 5.5, 2.2, 2.1 Hz, 1H), 5.44–5.43 (br m,

1H), 4.03 (br s, 1H), 3.81 (dd, J = 10.8, 4.4 Hz, 1H), 3.71 (dd, J = 10.8, 3.9 Hz, 1H),

3.48 (MeOH), 3.42–3.38 (m, 1H), 3.11–3.05 (m, 1H), 2.79 (ddd, J = 14.4, 6.2, 6.0

Hz, 1H), 2.04–1.94 (m, 3H), 1.80–1.75 (m, 2H), 1.66–1.62 (m, 1H), 1.48–1.37 (m,

2H), 1.33–1.18 (m, 3H). ^{13}C NMR (CDCl$_3$): δ 159.6, 154.1, 138.2, 135.8, 129.7,

113.8, 64.7, 59.9, 50.4 (MeOH), 47.5, 33.8, 32.9, 29.5 (2C), 25.4 (2C), 24.6. m/z

(ES+) 329.2095 calculated for C$_{17}$H$_{25}$N$_6$O: [M+H]$^+$ 329.2090. IR (cm^{-1}): 3317

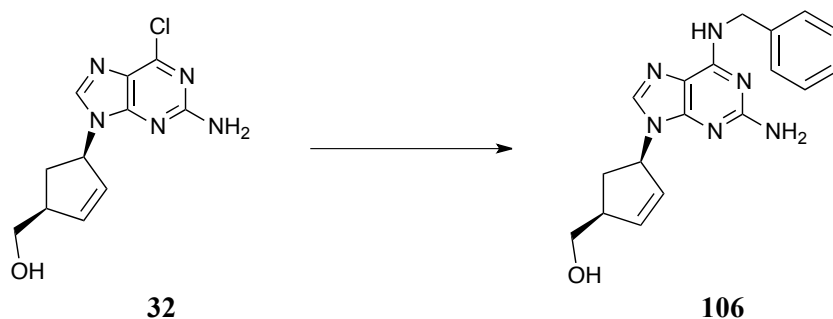(N−H), 3209 (br, O−H), 1597 (C=C aromatic), 1481 (CH$_2$).

((1S,4R)-4-(2-Amino-6-(benzylamino)-9H-purin-9-yl)cyclopent-2-en-1-

yl)methanol 106:[26] General Procedure A was followed to yield **106** (90 mg, 81%) as

an orange solid. mp: 174–176 °C (for racemic lit.[26] mp: 174–176 °C). ^{1}H NMR (MeOD): δ 7.74 (s, 1H), 7.47–7.30 (m, 5H), 6.24 (ddd, J = 5.3, 2.1, 2.0 Hz, 1H), 5.93 (ddd, J = 5.3, 2.1, 2.1 Hz, 1H), 5.59–5.55 (br m, 1H), 4.80 (s, 2H), 3.73 (dd, J = 10.8, 5.2 Hz, 1H), 3.66 (dd, J = 10.8, 5.2 Hz, 1H), 3.40–3.39 (m, 1H), 2.85 (ddd, J = 14.0, 6.4, 6.2 Hz, 1H), 1.79 (ddd, J = 13.9, 6.3, 5.8 Hz, 1H). ^{13}C NMR (MeOD): δ 159.9, 154.6, 138.3, 137.9, 129.2, 128.2, 127.8, 127.8, 127.3, 127.2, 126.8, 126.5, 113.2, 64.0, 59.0, 50.4 (MeOH), 44.2, 43.5, 33.8. *m/z* (ES+) 337.1781 calculated for $C_{18}H_{21}N_6O$: $[M+H]^+$ 337.1777. IR (cm^{-1}): 3298 (br, O−H), 3248 (=C−H), 2935 (C−H), 1585 (C=C), 752 (C−H aromatic).
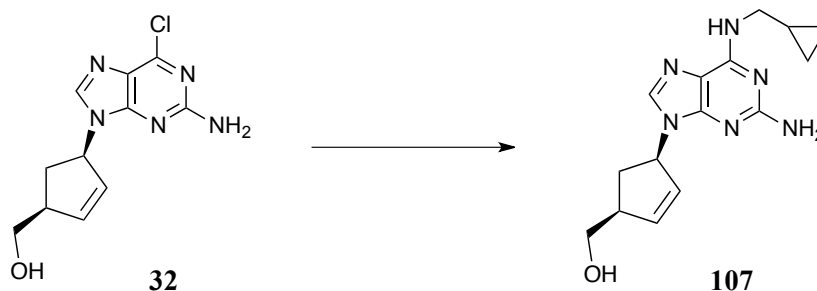
((1*S*,4*R*)-4-(2-Amino-6-((cyclopropylmethyl)amino)-9*H*-purin-9-yl)cyclopent-2-en-1-yl)methanol 107:[26] General Procedure A was followed to yield **107** (57 mg, 73%) as an off-white solid. mp: 180–182 °C (for racemic lit.[26] mp: 182–183 °C). ^{1}H NMR (CDCl₃): δ 7.49 (s, 1H), 6.05 (ddd, J = 5.5, 2.1, 2.0 Hz, 1H), 5.72 (ddd, J = 5.5, 2.1, 2.1 Hz, 1H), 5.45–5.32 (br m, 1H), 3.71 (dd, J = 10.8, 4.5 Hz, 1H), 3.61 (dd, J = 10.8, 4.1 Hz, 3H), 3.48 (MeOH), 3.37–3.19 (m, 2H), 3.00 (m, 1H), 2.71 (ddd, J = 14.3, 6.3, 6.2 Hz, 1H), 1.85 (ddd, J = 14.3, 6.4, 5.7 Hz, 1H), 1.11–0.97 (m, 1H), 0.53–0.44 (m, 2H), 0.26–0.17 (m, 2H). ^{13}C NMR (CDCl₃): δ 159.6, 155.0, 138.3, 136.2, 130.1, 114.3, 64.9, 60.6, 50.4 (MeOH), 47.6, 33.2, 10.6, 3.3 (2C). *m/z* (ES+)

301.1780 calculated for $C_{15}H_{21}N_6O$: $[M+H]^+$ 301.1777. IR (cm^{-1}): 3340 (N−H), 3.89 (N−H), 1593 (C=C aromatic), 1377 (CH$_2$), 1261 (C−O).
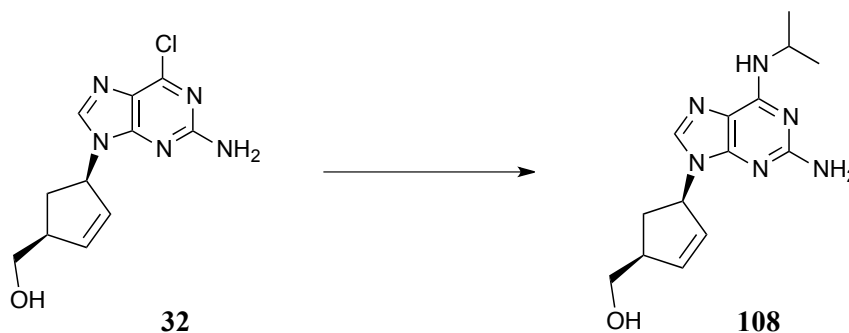
((1*S*,4*R*)-4-(2-Amino-6-(isopropylamino)-9*H*-purin-9-yl)cyclopent-2-en-1-yl)methanol 108:[26] General Procedure A was followed to yield **108** (40 mg, 71%) as a colourless crystalline solid. mp: 152–153 °C (for racemic lit.[26] mp: 153–155 °C). ^{1}H NMR (CDCl$_3$): δ 7.68 (s, 1H), 6.14–6.12 (m, 1H), 5.87–5.86 (m, 1H), 5.48–5.45 (br m, 1H), 3.61 (dd, *J* = 10.9, 5.3 Hz, 1H), 3.55 (dd, *J* = 10.9, 5.2 Hz, 1H), 3.48 (MeOH), 3.32–3.30 (m, 1H), 2.97–2.96 (m, 1H), 2.73 (ddd, *J* = 13.9, 6.4, 6.1 Hz, 1H), 1.65 (ddd, *J* = 13.8, 6.5, 5.8 Hz, 1H), 1.23 (d, *J* = 6.5 Hz, 6H). ^{13}C NMR (CDCl$_3$): δ 161.8, 155.7, 151.3, 139.4, 136.8, 130.8, 114.5, 65.4, 60.5, 50.4 (MeOH), 49.0, 47.2, 35.3, 22.9 (2C). *m/z* (ES+) 289.1778 calculated for $C_{14}H_{21}N_6O$: $[M+H]^+$ 289.1777. IR (cm^{-1}): 3313 (N−H), 3012 (=C−H), 2927 (C−H), 1592 (C=C aromatic), 1481 (CH$_2$), 1388 (CH$_3$).
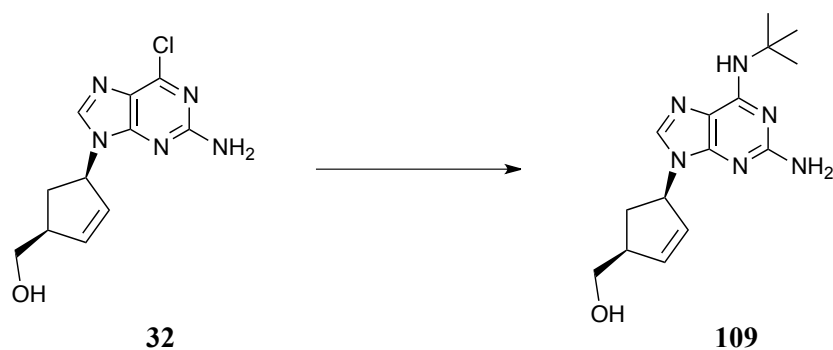
((1*S*,4*R*)-4-(2-Amino-6-(*tert*-butylamino)-9*H*-purin-9-yl)cyclopent-2-en-1-yl)methanol 109: General Procedure A was followed using *t*-butylamine (10 equiv) to yield **109** (0.23 g, 57%) as a cream coloured solid. mp: 159–161 °C (for racemic lit.[26] mp: 161–163 °C). ¹H NMR (CDCl₃): δ 7.43 (s, 1H), 6.11–6.10 (m, 1H), 5.75–5.73 (m, 1H), 5.65 (br s, 1H), 5.40–5.37 (br m, 1H), 4.72 (br s, 2H), 3.92 (dd, J = 10.9, 3.5 Hz, 1H), 3.80 (dd, J = 10.8, 2.2 Hz, 1H), 3.48 (MeOH), 2.78 (ddd, J = 14.7, 6.5, 6.3 Hz, 1H), 2.53–2.31 (m, 1H), 2.22 (ddd, J = 14.5, 6.3, 5.5 Hz, 1H), 1.64 (ddd, J = 14.4, 6.3, 6.2 Hz, 1H), 1.50 (s, 9H). ¹³C NMR (CDCl₃): δ 159.0, 155.0, 154.9, 149.0, 138.1, 135.7, 130.1, 115.0, 64.9, 60.7, 51.8, 50.4 (MeOH), 47.6, 35.0, 28.9 (3C). *m/z* (ES+) 303.1928 calculated for C₁₅H₂₂N₆O: [M+H]⁺ 303.1926. IR (cm⁻¹): 3336 (N−H), 3313 (N−H), 2962 (C−H), 1593 (C=C), 1458 (CH₂), 1203 (C−O).

**((1S,4R)-4-(2-Amino-6-((2-morpholinoethyl)amino)-9H-purin-9-yl)cyclopent-2-en-1-yl)methanol 110:** General Procedure A was followed to yield **110** (61 mg, 70%) as a colourless crystalline solid. mp: 148–151 °C. ^{1}H NMR (CDCl$_3$): δ 7.53 (s, 1H), 6.45 (br s, 1H), 6.11 (ddd, J = 5.4, 2.1, 2.1 Hz, 1H), 5.77 (ddd, J = 5.4, 2.2, 2.1 Hz, 1H), 5.45–5.41 (br m, 1H), 3.81 (dd, J = 10.8, 4.1 Hz, 1H), 3.77–3.72 (m, 5H), 3.64 (br s, 1H), 3.48 (MeOH), 3.10–3.09 (m, 2H), 2.78 (ddd, J = 14.5, 6.2, 5.6 Hz, 2H), 2.80–2.64 (m, 2H), 2.52–2.48 (m, 4H), 2.07 (ddd, J = 14.5, 6.3, 5.6 Hz, 1H). ^{13}C NMR (CDCl$_3$): δ 159.4, 155.2, 138.1, 136.7, 130.3, 115.0, 66.8 (2C), 65.0, 61.2, 57.4, 53.4 (2C), 50.4 (MeOH), 47.6, 36.8, 32.6. m/z (ES+) 360.2150 calculated for C$_{17}$H$_{26}$N$_7$O$_2$: [M+H]$^+$ 360.2148. IR (cm^{-1}): 3340 (N−H), 3201 (br, O−H), 2947 (C−H), 1643 (C=N), 1597 (C=C), 1462 (CH$_2$), 1257 (C−N), 1107 (C−O).
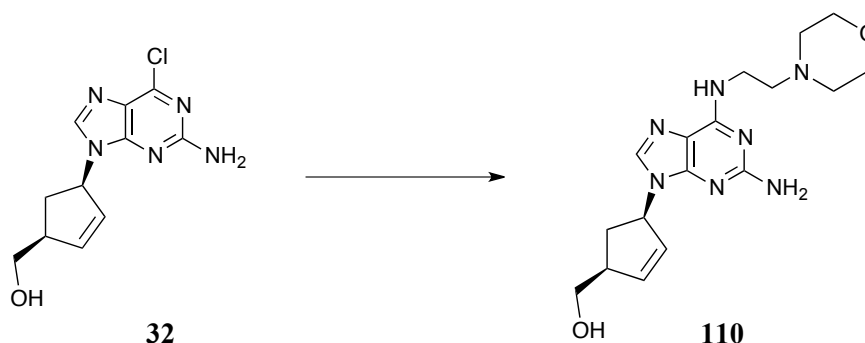

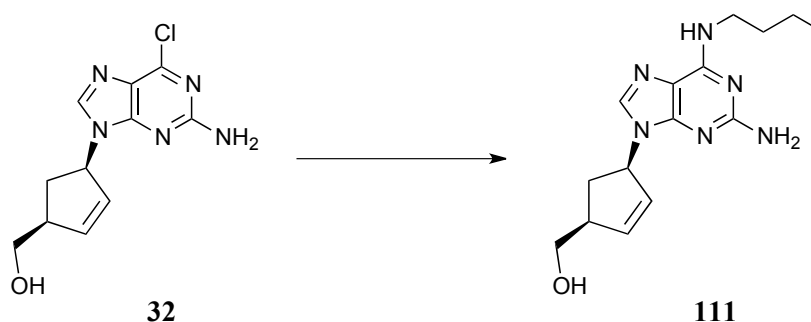**((1S,4R)-4-(2-Amino-6-(butylamino)-9H-purin-9-yl)cyclopent-2-en-1-yl)methanol 111:**[26] General Procedure A was followed to yield **111** (0.14 g, 81%) as

a cream coloured solid. mp: 113–115 °C (for racemic lit.[26] mp: 116–118 °C). ^{1}H

NMR (CDCl$_3$): δ 7.66 (s, 1H), 6.12 (ddd, J = 5.0, 2.0, 2.0 Hz, 1H), 5.84 (ddd, J =

5.1, 2.1, 2.0 Hz, 1H), 5.47–5.43 (br m, 1H), 3.59 (dd, J = 12.0, 4.0 Hz, 1H), 3.53 (dd,

J = 12.0, 4.0 Hz, 1H), 3.48 (MeOH), 3.45 (br s, 1H), 3.27–3.25 (m, 1H), 2.97–2.92

(m, 1H), 2.81–2.77 (m, 1H), 2.72 (ddd, J = 12.0, 6.4, 5.8 Hz, 1H), 1.66–1.54 (m,

3H), 1.43–1.34 (m, 2H), 0.91 (t, J = 8.0 Hz, 3H). ^{13}C NMR (CDCl$_3$): δ 161.3, 156.1,

150.7, 139.1, 136.5, 130.4, 114.2, 65.1, 60.2, 50.4 (MeOH), 40.7, 35.1, 20.6, 18.1,

13.8. m/z (ES+) 303.1930 calculated for C$_{15}$H$_{23}$N$_6$O: [M+H]$^{+}$ 303.1933. IR (cm^{-1}):

3329 (N−H), 3194 (br, O−H), 3163 (=C−H), 2927 (C−H), 1647 (C=C), 1503 (C=C

aromatic), 1466 (CH$_2$), 1385 (CH$_3$), 1246 (C−N), 1199 (C−O).

((1S,4R)-4-(2-Amino-6-((((1S,2S)-2-methylcyclopropyl)amino)-9H-purin-9-

yl)cyclopent-2-en-1-yl)methanol 112: General Procedure A was followed to yield

112 (0.14 g, 94%) as an off-white solid. mp: 109–111 °C. ^{1}H NMR (CDCl$_3$): δ

7.52 (s, 1H), 6.12 (ddd, J = 5.4, 2.1, 2.1 Hz, 1H), 5.79–5.77 (m, 1H), 5.46–5.41 (br

m, 1H), 3.82 (dd, J = 10.8, 4.3 Hz, 1H), 3.72 (dd, J = 10.8, 3.7 Hz, 1H), 3.48

(MeOH), 3.11–3.08 (br m, 2H), 2.79 (ddd, J = 14.4, 6.4, 6.3 Hz, 1H), 2.60 (br s, 1H),

2.00 (ddd, J = 14.4, 6.3, 5.7 Hz, 1H), 1.15 (d, J = 6.1 Hz, 3H), 1.00–0.94 (m, 1H),

0.76–0.72 (m, 1H), 0.66–0.61 (m, 1H). ^{13}C NMR (CDCl$_3$): δ 159.4, 155.9, 149.7,

138.2, 136.4, 130.2, 114.6, 64.9, 60.9, 50.4 (MeOH), 47.6, 32.9, 31.0, 17.2, 15.5, 15.0. *m/z* (ES+) 301.1776 calculated for $C_{15}H_{21}N_6O$: $[M+H]^+$ 301.1777. IR (cm^{-1}): 3316 (N−H), 3201 (br, O−H), 2950 (C−H), 1589 (C=C aromatic), 1465 (CH$_2$), 1389 (CH$_3$), 1088 (C−O).
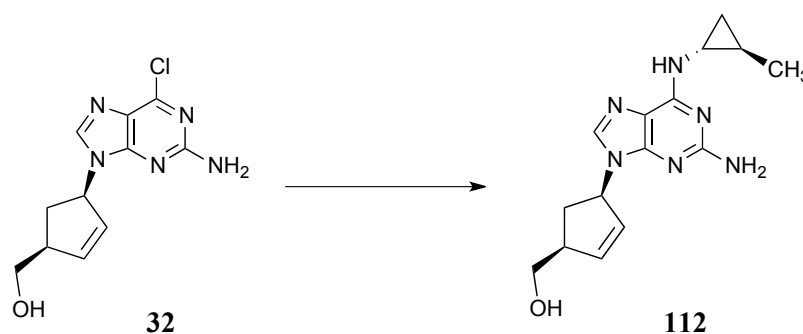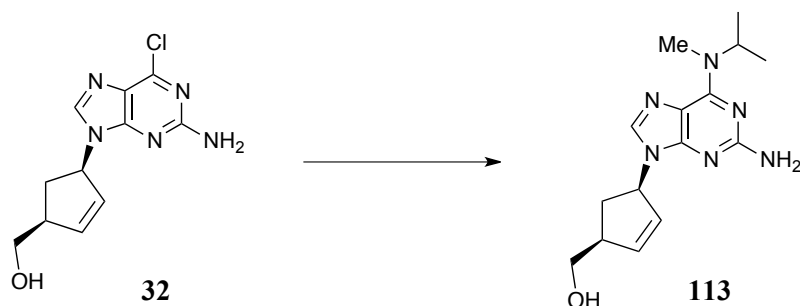

((1*S*,4*R*)-4-(2-Amino-6-(isopropyl(methyl)amino)-9*H*-purin-9-yl)cyclopent-2-en-1-yl)methanol 113:[23] General Procedure A was followed to yield **113** (79 mg, 74%) as an off-white solid.[23] mp: 135–139 °C. ^{1}H NMR (CDCl$_3$): δ 7.49 (s, 1H), 6.10 (ddd, *J* = 5.5, 2.2, 2.0 Hz, 1H), 5.75 (ddd, *J* = 5.5, 2.2, 2.1 Hz, 1H), 5.43–5.40 (br m, 1H), 3.91 (dd, *J* = 10.8, 3.8 Hz, 1H), 3.79 (dd, *J* = 10.8, 3.0 Hz, 1H), 3.48 (MeOH), 3.24 (s, 3H), 3.13–3.11 (m, 2H), 2.77 (ddd, *J* = 14.6, 6.4, 6.3 Hz, 1H), 2.20 (ddd, *J* = 14.6, 6.4, 5.6 Hz, 1H), 1.23 (d, *J* = 6.7 Hz, 6H). ^{13}C NMR (CDCl$_3$): δ 158.7, 155.3, 151.8, 138.3, 135.9, 131.0, 116.3, 65.7, 62.1, 53.8, 50.4 (MeOH), 48.1, 32.3, 20.2. *m/z* (ES+) 303.1932 calculated for $C_{15}H_{23}N_6O$: $[M+H]^+$ 303.1933. IR (cm^{-1}): 3320 (N−H), 2966 (C−H), 1562 (C=C aromatic), 1454 (CH$_2$).
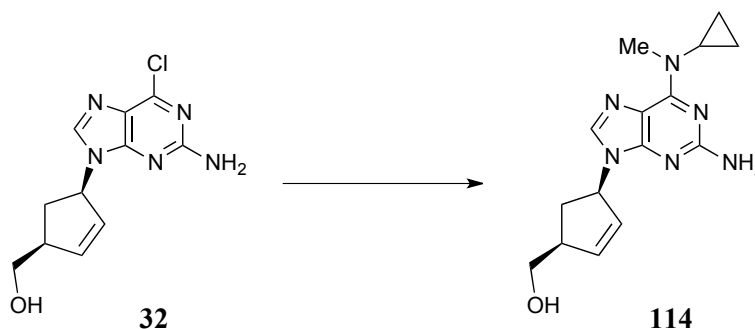
((1S,4R)-4-(2-Amino-6-(cyclobutylamino)-9H-purin-9-yl)cyclopent-2-en-1-yl)methanol 114:[23] General Procedure A was followed using *N*-methylcyclopropanamine (20 equiv) to yield **114** (0.16 g, 77%) as a colourless crystalline solid.[23] mp: 138–140 °C. ^{1}H NMR (CDCl$_3$): δ 7.69 (s, 1H), 6.13–6.12 (m, 1H), 5.86–5.85 (m, 1H), 5.49–5.44 (br m, 1H), 3.60 (dd, *J* = 10.7, 5.2 Hz, 1H), 3.53 (dd, *J* = 10.8, 5.1 Hz, 1H), 3.48 (MeOH), 3.27 (s, 3H), 3.11–3.07 (m, 1H), 2.96–2.94 (m, 1H), 2.72 (ddd, *J* = 14.4, 6.8, 6.2 Hz, 1H), 1.67–1.60 (m, 1H), 0.89–0.85 (m, 2H), 0.68–0.64 (m, 2H). ^{13}C NMR (CDCl$_3$): δ 158.3, 155.7, 150.7, 136.8, 134.2, 128.3, 113.4, 62.9, 57.9, 50.4 (MeOH), 46.5, 34.5, 32.8, 31.4, 7.2, 7.1. *m/z* (ES+) 301.1779 calculated for C$_{15}$H$_{21}$N$_6$O: [M+H]$^{+}$ 301.1777. IR (cm^{-1}): 3302 (N−H), 3202 (N−H), 1679 (C=C), 1567 (N−H), 1205 (C−N), 1033 (O−H).
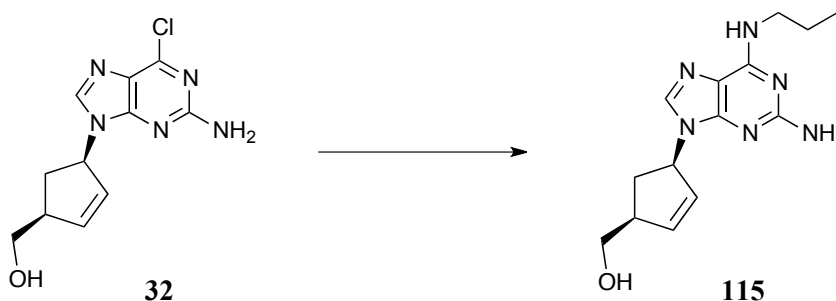
((1S,4R)-4-(2-Amino-6-(propylamino)-9H-purin-9-yl)cyclopent-2-en-1-yl)methanol 115:[27] General Procedure A was followed to yield **115** as a colourless

solid (70 mg, 68%). mp: 140–141 °C (lit.[27] mp: 144–146 °C). ^{1}H NMR (CDCl$_3$): δ 7.46 (s, 1H), 6.12 (ddd, J = 5.5, 2.1, 2.1 Hz, 1H), 5.85 (ddd, J = 5.5, 2.1, 2.1 Hz, 1H), 5.34–5.30 (br m, 1H), 4.06 (s, 2H), 3.60 (dd, J = 10.8, 4.7 Hz, 1H), 3.50 (dd, J = 10.8, 3.9 Hz, 1H), 3.48 (MeOH), 2.93–2.89 (m, 1H), 2.65 (ddd, J = 14.2, 6.4, 6.0 Hz, 1H), 1.69 (ddd, J = 14.2, 6.4, 5.7 Hz, 1H), 1.60–1.46 (m, 2H), 0.87 (t, J = 7.4 Hz, 3H). ^{13}C NMR (CDCl$_2$): δ 159.8, 155.0, 149.5, 138.2, 135.5, 129.5, 113.6, 64.4, 59.4, 50.4 (MeOH), 47.5, 41.9, 33.9, 22.4, 10.8. *m/z* (ES+) 289.1777 calculated for C$_{14}$H$_{21}$N$_6$O: [M+H]$^+$ 289.1773. IR (cm^{-1}): 3340 (N−H), 3259 (br, O−H), 2854 (C−H), 1597 (C=N), 1470 (C=C), 1396 (C=C aromatic), 1389 (C−O), 1254 (C−N).
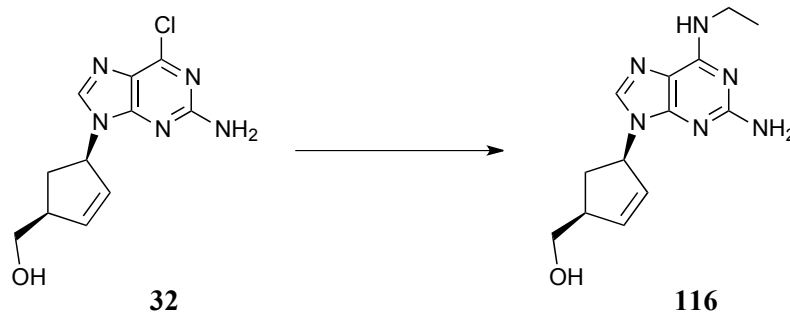
((1*S*,4*R*)-4-(2-Amino-6-(ethylamino)-9*H*-purin-9-yl)cyclopent-2-en-1-yl)methanol 116:[16] General Procedure A was followed to yield **116** (0.10 g, 65%) as an off-white solid. mp: 161–163 °C (lit.[16] mp: 162–164 °C). ^{1}H NMR (MeOD): δ 7.65 (s, 1H), 6.10 (ddd, J = 5.6, 2.1, 2.1 Hz, 1H), 5.85 (ddd J = 5.6, 2.2, 2.1 Hz, 1H), 5.45–5.41 (br m, 1H), 3.59–3.47 (m, 4H), 3.26 (m, 1H), 2.96–2.91 (m, 1H), 2.70 (ddd, J = 13.9, 6.5, 6.3 Hz, 1H), 1.60 (ddd, J = 13.9, 6.4, 5.9 Hz, 1H), 1.20 (t, J = 7.2 Hz, 3H). ^{13}C NMR (MeOD): δ 161.8, 156.3, 151.3, 139.3, 136.9, 130.8, 115.1, 65.5, 60.5, 54.7, 36.2, 35.4, 15.01. *m/z* (ES+) 275.1619 calculated for C$_{13}$H$_{19}$N$_6$O: [M+H]$^+$ 275.1620. IR (cm^{-1}): 3321 (N−H), 3197 (N−H), 3163 (br, O−H), 2927 (C−H), 1689 (C=N), 1589 (C=C), 1466 (CH$_2$), 1250 (C−N), 1120 (C−O).
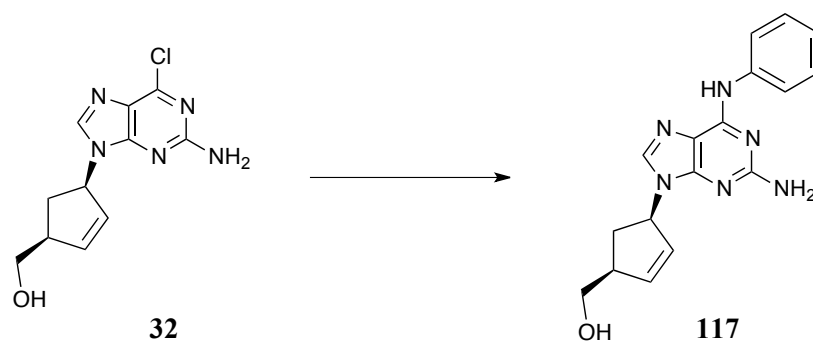
((1S,4R)-4-(2-Amino-6-(phenylamino)-9H-purin-9-yl)cyclopent-2-en-1-

yl)methanol 117:[26] General Procedure A was followed to yield **117** (90 mg, 81%) as

a brown solid. mp: 173–176 °C (lit.[26] mp: 177–179 °C). ^{1}H NMR (CDCl$_3$): δ

7.80–6.83 (m, 5H), 6.07 (ddd, J = 5.4, 2.1, 2.0 Hz, 1H), 5.90–5.65 (m, 1H), 5.44–

5.39 (br m, 1H), 3.70 (dd, J = 10.8, 4.4 Hz, 1H) 3.60 (dd, J = 10.8, 4.0 Hz, 1H), 3.48

(MeOH), 3.02–2.97 (m, 1H), 2.73 (ddd, J = 14.3, 6.5, 6.2 Hz, 1H), 1.83 (ddd, J =

14.3, 6.4, 5.6 Hz, 1H). ^{13}C NMR (CDCl$_3$): δ 159.3, 152.8, 150.1, 139.0, 138.8,

137.1, 130.0, 129.4, 129.0, 123.6, 120.7, 115.8, 114.8, 64.9, 60.8, 50.4 (MeOH),

47.8, 33.6. m/z (ES+) 323.1620 calculated for C$_{17}$H$_{19}$N$_6$O: [M+H]$^+$ 323.1612. IR

(cm^{-1}): 3329 (N−H), 3217 (br, O−H), 2945 (C−H), 1578 (C=N) 1454 (C=C), 1379

(C=C aromatic), 1254 (C−O), 1032 (C−N).
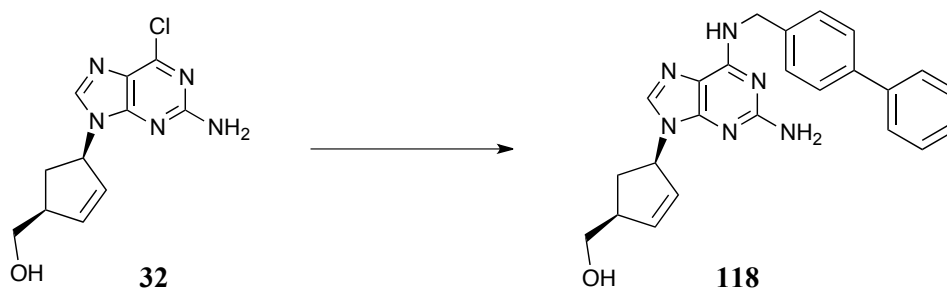
((1S,4R)-4-(6-(([1,1'-Biphenyl]-4-ylmethyl)amino)-2-amino-9H-purin-9-

yl)cyclopent-2-en-1-yl)methanol 118: To a solution of **32** (90 mg, 0.4 mmol) in

MeOH (10 mL) was added 4-phenylbenzylamine (90 mg, 0.5 mmol) and the resulting solution was allowed to stir for 3 days at 80 °C. The solvent was removed *in vacuo* and the crude product was purified by column chromatography (0.5:95.5 to 7:93 MeOH–DCM) to yield the **118** as a yellow solid (40 mg, 31%). mp: 198–200 °C. ^{1}H NMR (MeOD): δ 7.88–7.01 (m, 9H), 6.02–5.90 (m, 2H), 5.45–5.32 (br m, 1H), 4.50 (s, 2H), 3.59 (dd, J = 10.8, 4.2 Hz, 1H), 3.53 (dd, J = 10.8, 3.9 Hz, 1H), 3.01–2.88 (m, 1H), 2.70 (ddd, J = 14.0, 6.5, 6.2 Hz, 1H), 1.65 (ddd, J = 14.0, 6.3, 5.8 Hz, 1H). ^{13}C NMR (MeOD): δ 161.3, 154.9, 140.5, 140.0, 138.4, 137.0, 135.7, 129.2, 128.0 (2C), 127.8 (2C), 126.6 (2C), 126.1 (2C), 114.3, 64.4, 59.5, 49.0, 43.5, 34.0. m/z (ES+) 413.2090 calculated for $C_{24}H_{25}N_6O$: $[M+H]^+$ 413.2091.   IR (cm^{-1}): 3483 (N−H), 3267 (N−H), 3147 (br, O−H), 3066 (C−H), 1639 (C=N) 1593 (C=C), 1485 (C=C aromatic), 1261 (C−O), 1230 (C−N).
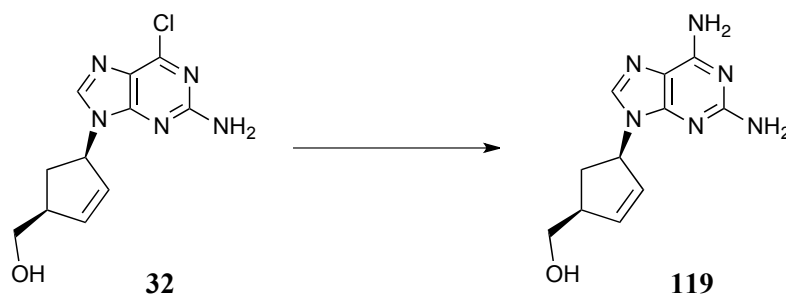
((1*S*,4*R*)-4-(2,6-Diamino-9*H*-purin-9-yl)cyclopent-2-en-1-yl)methanol 119:[28] To a solution of **32** (0.10 g, 0.4 mmol) in MeOH (3 mL) in a sealed tube was added NH$_3$ solution (1 mL, 7 N in MeOH) and the resulting solution was allowed to stir for 24 h at 90 °C. The solvent was removed *in vacuo* and the crude product was purified by column chromatography (3:97 to 7:93 MeOH–DCM) to yield **119** (89 mg, 96%) as a pale orange solid. mp: 176–179 °C (lit.[28] mp: 178–180 °C). ^{1}H NMR (CDCl$_3$): δ 7.73 (s, 1H), 6.12 (ddd, J = 5.5, 2.2, 2.1 Hz, 1H), 5.86 (ddd, J = 5.5, 2.1, 2.1 Hz, 1H),

5.49–5.45 (br m, 1H), 3.57 (ddd, J = 24.4, 10.9, 5.3 Hz, 2H), 3.48 (MeOH), 2.98–

2.92 (m, 1H), 2.72 (ddd, J = 13.9, 6.6, 6.4 Hz, 1H), 1.65 (ddd, J = 13.9, 6.4, 5.8 Hz,

1H). ^{13}C NMR (CDCl$_3$): δ 161.7, 157.6, 152.4, 139.6, 137.8, 130.9, 114.4, 65.6,

60.7, 50.4 (MeOH), 35.5. m/z (ES+) 247.1308 calculated for C$_{11}$H$_{15}$N$_6$O: [M+H]$^+$

247.1307.   IR (cm^{-1}): 3425 (N−H), 3313 (N−H), 2873 (C−H), 1631 (C=N), 1581

(C=C), 1049 (C−O).

32   **123**
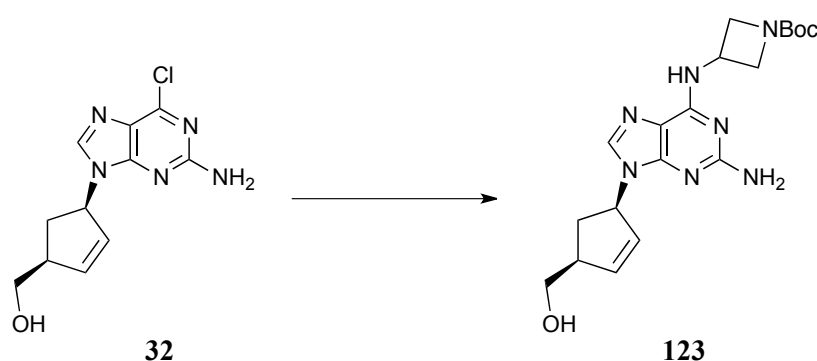
***tert*-Butyl-3-((2-amino-9-((1*R*,4*S*)-4-(hydroxymethyl)cyclopent-2-en-1-yl)-9*H*-**

purin-6-yl)amino)azetidine-1-carboxylate 123: To a solution of **32** (0.15 g, 0.6

mmol) in MeOH (5 mL) in a sealed tube, was added 1-Boc-3-(amino)azetidine (0.1

mL, 0.6 mmol) and the solution was allowed to stir at 90 °C for 48 h. The solvent

was removed *in vacuo* and the crude mixture was purified by column

chromatography (1:49 to 1:19 MeOH−DCM) to yield **123** (0.13 g, 57%) as an off-

white solid. ^{1}H NMR (CDCl$_3$): δ 7.72 (s, 1H), 6.14 (ddd, J = 5.1, 2.2, 2.2 Hz, 1H),

5.86 (ddd, J = 5.0, 2.2, 2.2 Hz, 1H), 5.50–5.46 (br m, 1H), 4.28–4.24 (m, 2H), 4.08–

4.04 (m, 1H), 3.87–3.84 (m, 2H), 3.61 (dd, J = 8.1, 4.0 Hz, 1H), 3.55 (dd, J = 12.0,

8.0 Hz, 1H), 3.02–2.94 (m, 1H), 2.73 (ddd, J = 13.9, 6.6, 6.3 Hz, 1H), 1.66 (ddd, J =

13.8, 6.4, 5.8 Hz, 1H), 1.42 (s, 9H). ^{13}C NMR (CDCl$_3$): δ 161.7, 158.2, 155.7, 139.5,

137.6, 130.9, 114.8, 81.1, 80.9, 65.6, 60.7, 43.0, 41.8, 35.5, 30.7, 28.6 (3C). *m/z* (ES+) 402.2258 calculated for $C_{19}H_{28}N_7O_3$: $[M+H]^+$ 402.2254.
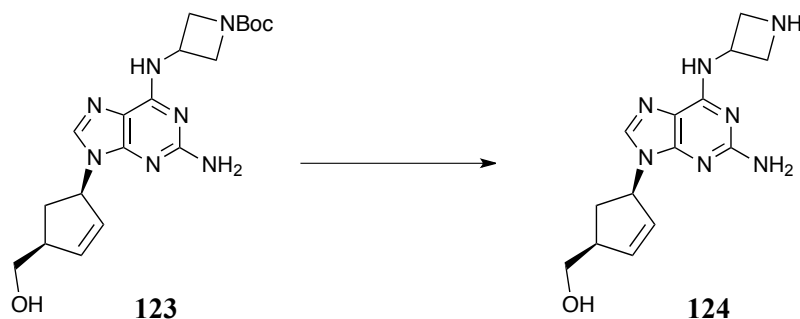
((1*S*,4*R*)-4-(2-Amino-6-(azetidin-3-ylamino)-9*H*-purin-9-yl)cyclopent-2-en-1-yl)methanol 124: TFA (0.2 mL, 2.0 mmol) was added to a solution of **123** (0.13 g, 0.3 mmol) in DCM (10 mL) at 0 °C and the solution was allowed to stir under nitrogen for 12 h after which time, the solvents were removed *in vacuo* and the crude product was purified by column chromatography (3:7 MeOH–DCM) to yield **124** (52 mg, 53%, as TFA salt) as a yellow solid. mp: >250 °C. ^{1}H NMR (MeOD): δ 7.97 (s, 1H), 6.18–6.16 (m, 1H), 5.84–5.83 (m, 1H), 5.55–5.52 (br m, 1H), 4.36–4.31 (m, 3H), 3.66 (dd, *J* = 10.5, 4.1 Hz, 1H), 3.54 (dd, *J* = 10.8, 4.5 Hz, 1H), 2.97–2.94 (m, 2H), 2.79–2.73 (m, 1H), 1.71–1.67 (m, 1H), 1.37–1.21 (m, 1H). ^{13}C NMR (MeOD): δ 163.4 (TFA), 155.5, 151.8, 143.0, 140.3, 130.1, 116.7 (TFA), 113.8, 110.8, 65.2, 61.3, 55.6, 50.8 (2C), 43.3, 35.3. *m/z* (ES+) 302.1729 calculated for $C_{14}H_{20}N_7O$: $[M+H]^+$ 302.1729. IR (cm^{-1}): 3340 (N−H), 2978 (C−H), 1666 (C=C), 1404 (C=C aromatic), 1184 (C−O).

32   **125**
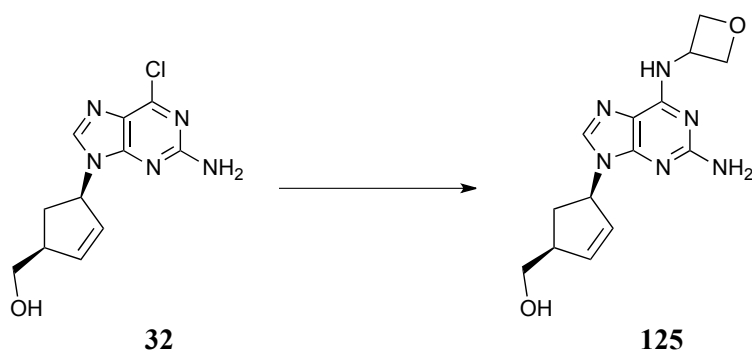
((1*S*,4*R*)-4-(2-Amino-6-(oxetan-3-ylamino)-9*H*-purin-9-yl)cyclopent-2-en-1-yl)methanol 125: To a solution of **32** (0.11 g, 0.4 mmol) was added 3-amino oxetane (0.2 mL, 2.0 mmol) in EtOH (3 mL) and the resulting mixture was allowed to stir in a sealed tube at 85 °C for 48 h. The mixture was allowed to cool and the solvent removed *in vacuo*. The crude product was purified by column chromatography (1:19 to 1:4 MeOH–DCM) to yield **125** (90 mg, 80%) as an orange solid. mp: Decomposed at 215 °C. ^{1}H NMR (MeOD): δ 7.97 (s, 1H), 6.18–6.16 (m, 1H), 5.88–5.86 (m, 1H), 5.55–5.50 (br m, 1H), 4.57–4.51 (m, 2H), 4.26–4.20 (m, 1H), 3.78 (dd, *J* = 11.9, 3.2 Hz, 1H), 3.70 (dd, *J* = 11.8, 3.8 Hz, 1H), 3.64–3.60 (m, 1H), 3.57–3.53 (m, 1H), 3.02–2.99 (m, 1H), 2.70 (ddd, *J* = 14.0, 6.4, 6.3 Hz, 1H), 1.71–1.64 (m, 1H), 1.36–1.24 (m, 1H). ^{13}C NMR (MeOD): δ 154.9, 152.3, 142.2, 140.3, 130.3, 110.4, 78.2 (2C), 65.2, 63.6, 59.7, 48.6, 35.3. *m/z* (ES+) 303.1573 calculated for $C_{14}H_{19}N_6O_2$: [M+H]$^+$ 303.1569. IR (cm^{-1}): 3317 (N–H), 3155 (=C–H), 1689 (C=C), 1295 (C–N), 1092 (C–O).

32   **126**
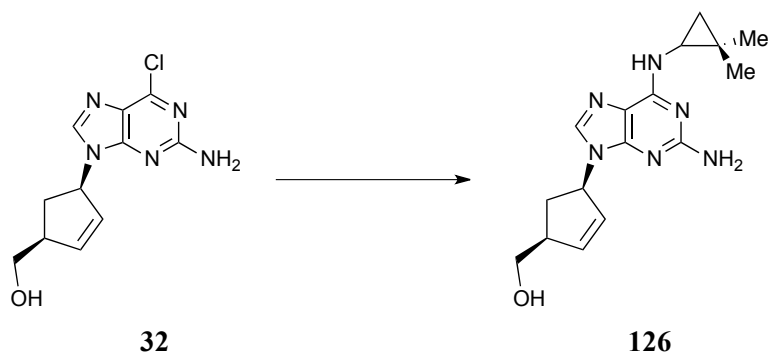
((1*S*,4*R*)-4-(2-Amino-6-((2,2-dimethylcyclopropyl)amino)-9*H*-purin-9-yl)cyclopent-2-en-1-yl)methanol 126: To a solution of **32** (0.11 g, 0.4 mmol) in *t*-BuOH (3 mL) in a sealed tube was added 2,2-dimethylcyclopropylamine hydrochloride (0.05 g, 0.4 mmol) and K_2CO_3 (0.10 g, 0.7 mmol) and the pale yellow mixture was allowed to stir for 72 h at 90 °C. The solvent was removed *in vacuo* and the crude mixture was purified by column chromatography (5:95 MeOH–DCM) to yield **126** (70 mg, 54%) as an off-white solid. mp: 176–180 °C. ^{1}H NMR (CDCl$_3$): δ 7.70 (s, 1H), 6.14 (ddd, *J* = 5.5, 2.1, 2.0 Hz, 1H), 5.87 (ddd, *J* = 5.5, 2.1, 2.0 Hz, 1H), 5.50–5.46 (br m, 1H), 3.61 (dd, *J* = 10.9, 5.4 Hz, 1H), 3.55 (dd, *J* = 10.8, 5.2 Hz, 1H), 3.48 (MeOH), 3.10–3.06 (m, 1H), 2.98–2.96 (m, 1H), 2.74 (ddd, *J* = 14.0, 6.5, 6.3 Hz, 1H), 2.70 (br s, 1H), 1.66 (ddd, *J* = 13.8, 6.3, 5.8 Hz, 1H), 1.14 (s, 3H), 1.03 (s, 3H), 0.76 (dd, *J* = 7.6, 5.4 Hz, 1H), 0.41 (t, *J* = 4.7 Hz, 1H). ^{13}C NMR (CDCl$_3$): δ 161.8, 157.6, 139.3, 137.1, 130.8, 114.6, 65.5, 60.5, 50.4 (MeOH), 36.2, 35.4, 25.1, 20.9, 19.5, 19.0. *m/z* (ES+) 315.1931 calculated for $C_{16}H_{23}N_6O$: [M+H]$^+$ 315.1933. IR (cm^{-1}): 3325 (N−H), 3205 (br, O−H), 2939 (C−H), 1585 (C=C aromatic), 1469 (CH$_2$), 1392 (CH$_3$).

32
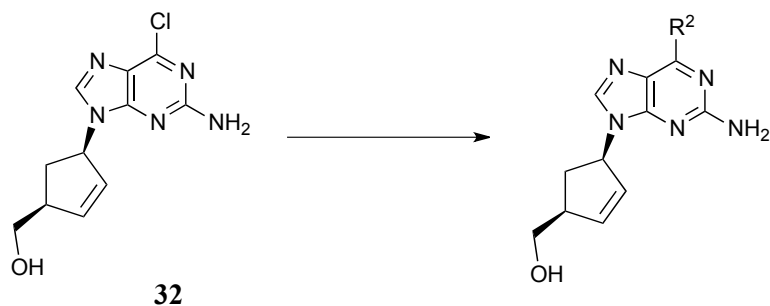
General Procedure B: To a solution of **32** (1 equiv) in the appropriate alcohol reagent (1 mL) was added NaH (60% dispersed in mineral oil, 3 equiv) and the solution was heated to 80 °C and allowed to stir for 4 h. The mixture was allowed to cool, diluted with 1:99 MeOH–DCM and purified by column chromatography (3:97 to 6:94 MeOH–DCM) to yield the appropriate product.

32   **132**
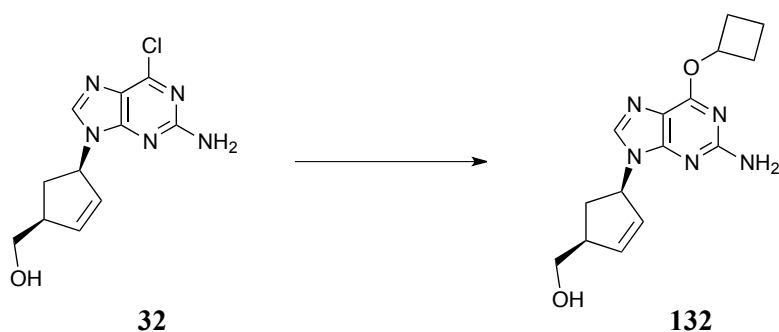
((1*S*,4*R*)-4-(2-Amino-6-cyclobutoxy-9*H*-purin-9-yl)cyclopent-2-en-1-yl)methanol 132: General Procedure B was followed to yield **132** (80 mg, 70%) as an off-white solid. mp: 150–152 °C. ^{1}H NMR (CDCl$_3$): δ 7.65 (s, 1H), 6.12 (ddd, *J* = 5.5, 2.1, 2.0 Hz, 1H), 5.77 (ddd, *J* = 5.5, 2.2, 2.0 Hz, 1H), 5.49–5.44 (br m, 1H), 5.42–5.34 (m, 1H), 3.90 (dd, *J* = 10.8, 3.9 Hz, 1H), 3.80 (dd, *J* = 10.8, 3.2 Hz, 1H), 3.48 (MeOH), 2.98–2.94 (m, 1H), 2.79 (ddd, *J* = 14.6, 9.6, 6.4 Hz, 1H), 2.50–2.42 (m, 2H), 2.33–2.23 (m, 2H), 2.13 (ddd, *J* = 14.6, 6.3, 5.8 Hz, 1H), 1.89–1.81 (m, 1H), 1.72–1.60 (m, 1H). ^{13}C NMR (CDCl$_3$): δ 161.1, 159.1, 153.2, 139.2, 138.7, 130.7,

333

116.7, 77.6, 71.4, 65.5, 61.9, 50.4 (MeOH), 48.1, 32.8, 31.0, 13.9.   *m/z* (ES+) 316.1775 calculated for $C_{16}H_{22}N_5O_2$: [M+H]$^+$ 316.1774. IR (cm^{-1}): 3303 (N−H), 3184 (=C−H), 2942 (C−H), 1627 (C=N), 1581 (C=C aromatic), 1461 (CH$_2$), 1250 (C−N), 1076 (C−O).
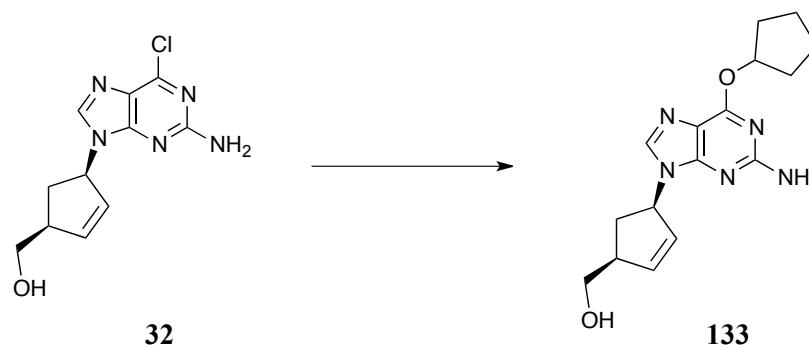
((1*S*,4*R*)-4-(2-Amino-6-(cyclopentyloxy)-9*H*-purin-9-yl)cyclopent-2-en-1-yl)methanol 133:[26] General Procedure B was followed to yield **133** (43 mg, 73%) as an off-white solid. mp: 187–189 °C (for racemic lit.[26] mp: 188–190 °C). ^{1}H NMR (CDCl$_3$): δ 7.63 (s, 1H), 6.12 (ddd, *J* = 5.5, 2.1, 2.1 Hz, 1H), 5.77 (ddd, *J* = 5.5, 2.1, 2.1 Hz, 1H), 5.66–5.62 (m, 1H), 5.49–5.44 (br m, 1H), 3.90 (dd, *J* = 10.8, 3.9 Hz, 1H), 3.80 (dd, *J* = 10.8, 3.2 Hz, 1H), 3.48 (MeOH), 3.15–3.10 (m, 1H), 2.79 (ddd, *J* = 14.6, 6.3, 6.0 Hz, 1H), 2.14 (ddd, *J* = 14.6, 6.4, 5.6 Hz, 1H), 2.01–1.81 (m, 5H), 1.63–1.60 (m, 2H), 1.35–1.28 (m, 1H). ^{13}C NMR (CDCl$_3$): δ 161.7, 159.1, 153.2, 139.1, 138.6, 130.7, 117.0, 79.8, 77.6, 65.5, 61.9, 50.4 (MeOH), 48.1, 33.3, 32.7, 30.1, 24.3. *m/z* (ES+) 302.1614 calculated for $C_{15}H_{20}N_5O_2$: [M+H]$^+$ 302.1617. IR (cm^{-1}): 3325 (N−H), 3197 (=C−H), 2954 (C−H), 1581 (C=C aromatic), 1446 (CH$_2$), 1246 (C−O).
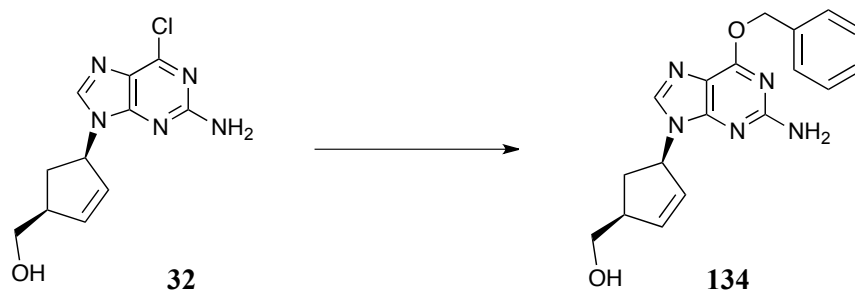
((1S,4R)-4-(2-Amino-6-(benzyloxy)-9H-purin-9-yl)cyclopent-2-en-1-yl)methanol

134: General Procedure B was followed to yield **134** (36 mg, 57%) as a colourless crystalline solid. mp: 171–175 °C. ^{1}H NMR (MeOD): δ 7.81 (s, 1H), 7.47 (d, J = 7.1 Hz, 2H), 7.39–7.22 (m, 3H), 6.15 (ddd, J = 5.5, 2.2, 2.0 Hz, 1H), 5.91–5.82 (m, 1H), 5.58–5.53 (br m, 1H), 5.52 (s, 2H), 3.70 (dd, J = 10.8, 3.8 Hz, 1H), 3.65 (dd, J = 10.8, 3.7 Hz, 1H), 2.98 (m, 1H), 2.75 (ddd, J = 13.9, 6.4, 6.3 Hz, 1H), 1.69 (ddd, J = 13.9, 6.3, 5.8 Hz, 1H). ^{13}C NMR (MeOD): δ 161.9, 161.4, 154.6, 139.6, 139.2, 137.8, 130.7, 129.4, 129.3, 129.2, 129.0, 115.4, 68.9, 65.4, 60.8, 35.3. *m/z* (ES+) 360.1440 calculated for $C_{18}H_{19}N_5O_2$: [M+H]$^+$ 360.1436. IR (cm^{-1}): 3302 (N−H), 3301 (N−H), 1601, 1574 & 1523 (C=C aromatic), 1234 (C−O).

((1S,4R)-4-(2-Amino-6-methoxy-9H-purin-9-yl)cyclopent-2-en-1-yl)methanol

135:[16] General Procedure B was followed to yield **135** as a colourless solid (0.66 g, 75%). mp: 134–136 °C (lit.[16] mp: 135–137 °C). ^{1}H NMR (CDCl₃): δ 7.61 (s, 1H),

6.17–5.59 (m, 2H), 5.42–5.38 (br m, 1H), 3.96 (s, 3H), 3.75 (dd, J = 10.8, 3.2 Hz, 1H), 3.69 (dd, J = 10.8, 3.7 Hz, 1H), 3.48 (MeOH), 3.01–2.99 (m, 1H), 2.80–1.84 (m, 2H). ^{13}C NMR (CDCl$_3$): δ 161.9, 159.3, 153.2, 139.1, 138.9, 130.4, 116.3, 65.2, 61.2, 54.2, 50.4 (MeOH), 48.16, 33.3. *m/z* (ES+) 262.1304 calculated for C$_{12}$H$_{15}$N$_5$O$_2$: [M+H]$^+$ 262.1303. IR (cm^{-1}): 3321 (N−H), 3201 (br, O−H), 2935 (C−H), 1581 (C=N), 1477 (C=C), 1392 (C=C aromatic), 1246 (C−O), 1038 (C−N).

32 **136**
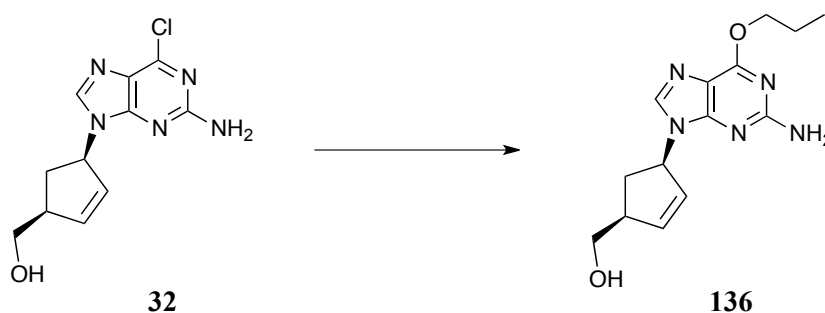
((1*S*,4*R*)-4-(2-Amino-6-propoxy-9*H*-purin-9-yl)cyclopent-2-en-1-yl)methanol

136: General Procedure B was followed to yield **136** as a yellow solid (40 mg, 85%). mp: 128–130 ºC. ^{1}H NMR (CDCl$_3$): δ 7.60 (s, 1H), 6.21–5.55 (m, 2H), 5.40 (ddd, J = 9.4, 5.2, 1.9 Hz, 1H), 4.34 (t, J = 6.8 Hz, 2H), 3.79 (dd, J = 10.8, 3.7 Hz, 1H), 3.69 (dd, J = 10.8, 3.1 Hz, 1H), 3.48 (MeOH), 3.15–2.94 (m, 1H), 2.82–1.90 (m, 2H), 1.84–1.62 (m, 2H), 0.95 (t, J = 7.4 Hz, 3H). ^{13}C NMR (CDCl$_3$): δ 162.0, 159.2, 153.2, 139.2, 138.8, 130.6, 116.6, 68.8, 65.3, 61.6, 50.4 (MeOH), 48.2, 33.0, 22.6, 10.8. *m/z* (ES+) 312.1436 calculated for C$_{14}$H$_{20}$N$_5$O$_2$: [M+H]$^+$ 312.1436. IR (cm^{-1}): 3321 (N−H), 3201 (br, O−H), 2967 (C−H), 1578 (C=N), 1450 (C=C), 1404 (C=C aromatic), 1238 (C−O), 1061 (C−N).
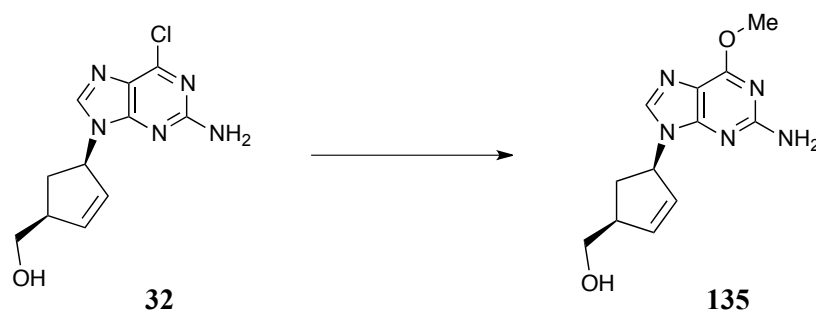
((1*S*,4*R*)-4-(2-Amino-6-butoxy-9*H*-purin-9-yl)cyclopent-2-en-1-yl)methanol

137:[26] General Procedure B was followed to yield **137** as a pale yellow solid (50 mg, 63%). mp: 121–122 ºC (for racemic lit.[26] mp: 122–123 °C). ¹H NMR (CDCl₃): δ 7.61 (s, 1H), 6.12 (ddd, *J* = 5.5, 2.1, 2.1 Hz, 1H), 5.70 (ddd, *J* = 5.5, 2.1, 2.0 Hz, 1H), 5.42–5.39 (br m, 1H), 4.37 (t, *J* = 6.6 Hz, 1H), 3.84 (dd, *J* = 10.8, 3.8 Hz, 1H), 3.68 (dd, *J* = 10.8, 3.1 Hz, 1H), 3.48 (MeOH), 3.02–2.98 (m, 1H), 2.70 (ddd, *J* = 14.3, 6.4, 6.1 Hz, 1H), 2.07–1.81 (m, 1H), 1.80–1.54 (m, 2H), 1.52–1.47 (m, 2H), 0.88 (t, *J* = 7.4 Hz, 3H). ¹³C NMR (CDCl₃): δ 161.9, 159.2, 153.2, 139.0, 138.8, 130.5, 116.4, 67.0, 65.2, 61.4, 50.4 (MeOH), 48.1, 33.2, 31.3, 19.5, 14.2. *m/z* (ES+) 304.1774 calculated for C₁₅H₂₂N₅O₂: [M+H]⁺ 304.1778. IR (cm⁻¹): 3313 (N−H), 3201 (br, O−H), 2951 (C−H), 1581 (C=N), 1508 (C=C), 1462 (C=C aromatic), 1400 (C−O), 1245 (C−N).

32   **139**

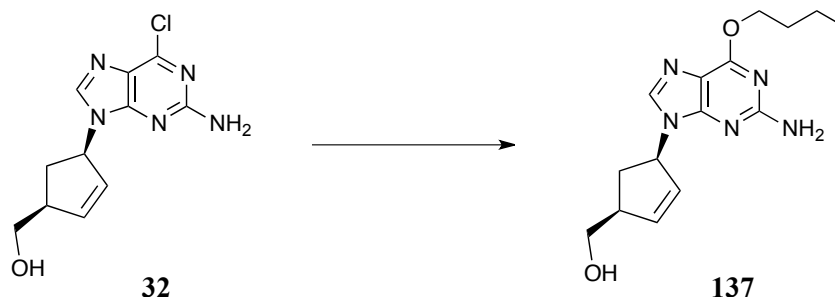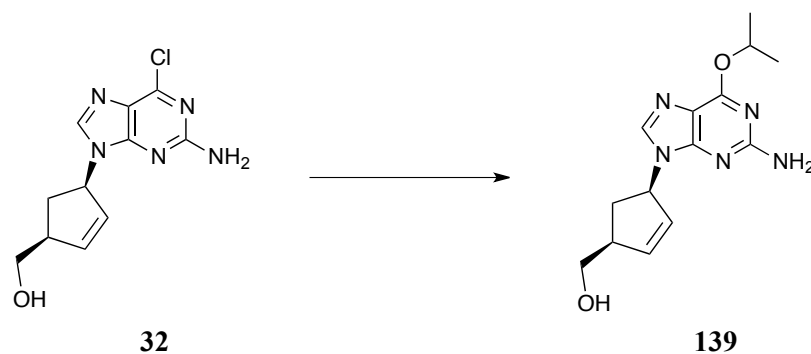**((1*S*,4*R*)-4-(2-Amino-6-isopropoxy-9*H*-purin-9-yl)cyclopent-2-en-1-yl)methanol 139:[26]** General Procedure B was followed to yield **139** as a colourless solid (70 mg, 80%). mp: 180–182 °C (lit.[26] mp: 188–191 °C). ^{1}H NMR (CDCl$_3$): δ 7.71 (s, 1H), 6.14–6.11 (m, 1H), 5.79–5.74 (m, 1H), 5.49–5.38 (m, 2H), 3.78 (dd, *J* = 10.8, 3.6 Hz, 1H), 3.68 (dd, *J* = 10.8, 3.4 Hz, 1H), 3.48 (MeOH), 3.16–2.98 (m, 1H), 2.76 (ddd, *J* = 14.3, 6.4, 6.3 Hz, 1H), 2.09–1.89 (m, 1H), 1.40 (d, *J* = 6.2 Hz, 1H). ^{13}C NMR (CDCl$_3$): δ 161.3, 159.4, 153.4, 138.9, 130.4, 116.4, 70.0, 65.1, 61.0, 50.4 (MeOH), 48.2, 33.5, 22.4. *m/z* (ES+) 290.1617 calculated for C$_{14}$H$_{20}$N$_5$O$_2$: [M+H]$^+$ 290.1616. IR (cm^{-1}): 3325 (N−H), 3192 (br, O−H), 2980 (C−H), 1579 (C=N) 1454 (C=C), 1404 (C=C aromatic), 1246 (C−O), 1059 (C−N).

5.5.2 Docking study protocols.

5.5.2.1 Ligand preparation.

Ligands prepared for docking in Spartan '08 (Wavefunction INC., Irvine 1991–2009). Native SMA ligand exported from PDB, 3UPR[2] crystal structure and opened in Spartan. For each required analogue the cyclopropyl ring was replaced. Molecular mechanics, MMFF energy minimisation calculation performed with all atoms frozen except the newly added substitution. Structures were saved using SD file format ready for docking.

5.5.2.2 Docking study.

GOLD 5.1 (CCDC Software Limited, Cambridge, UK) was used to find potential binding poses of ABC **7** and 6-position amine and oxy analogues in the F-pocket of HLA-B*57:01 (PDB code 3UPR).[2] Hydrogen molecules were added to the protein and the native ligand ABC was removed and used to define the binding site as 6 Å around the ligand. Rigid docking was performed such that the option to 'Fix Ligand Rotatable Bonds' was checked. Ligands were loaded and docked using the rescore option and the GOLDScore fitness function, with the 'Perform Local Optimisation' option unchecked. All other settings were left at default.

5.5.3 Immunological studies.

5.5.3.1 T-cell culture and cloning.

Cells from three HLA-B*57:01 positive individuals were selected from our cell bank containing peripheral blood mononuclear cells ($70–150 \times 10^6$; stored in vials of 10×10^6 cells) from 1000 HLA-typed donors. The demographics of the first 400 study subjects and HLA allele frequencies have been reported previously.[29] Ethical approval for the study was obtained from the local research ethics committee and all volunteers were consented prior to blood donation. Confidentiality was maintained throughout the study.

5.5.3.2 Drug-specific T-cell responses.

ABC-specific proliferative responses were assessed by culturing T-cell clones (5×10^4/well; 200 μL) with autologous irradiated EBV-transformed B-cells (used as antigen presenting cells; 1×10^4/well) and ABC (50 μM). IFN-γ secretion after abacavir stimulation was measured using ELISpot in accordance with the

manufacturer's instructions (Mabtech AB, Sweden). The effect of chemical modification of the 6-amino cyclopropyl group of ABC on the T-cell response was measured by incubating clones and irradiated EBV-transformed B-cells with the compounds (10, 25, 50, 100 and 250 μM) and measuring IFN-γ secretion. Cytokine secretion was selected as a T-cell readout as it provided the greatest discrimination between ABC-treated and control cells. HLA-B*57:01-restricted T-cell activity of the ABC analogues was tested using 6 clones selected from all 3 donors. ABC was used as a positive control.

5.5.4 Pharmacological studies.

For the determination of compounds **103**–**108**, **110**, **113**, **115**, **132** and **133**, cytotoxicity and inhibition of HIVIII$_B$ replication in MT4 cells, the procedure in Chapter 3, Section **3.5.3** was followed.

5.5.5 PK profiling.

PK experiments were carried out by Shanghai ChemPartner Co. Ltd., China. Brief experimental conditions and parameters can be found overleaf.

Test system	6 male SD rats (210–240 g) (for each compound) were purchased from SLAC Laboratory Animal Co. Ltd.
Food status	Fasted overnight, free access to water and fed 4 h post dose
Administration	IV: 1 mg/kg *via* foot dorsal vein injection (n = 3 per compound) PO: 10 mg/kg *via* oral gavage (n = 3 per compound)
Blood collection	The animal was restrained manually at the required time points and approximately 150 µL of blood sample was collected *via* the tail vein or *via* pre-cannulated jugular vein into EDTA-2K tubes. The blood samples were kept on ice then centrifuged (2000 × g, 4 °C, 10 min) to obtain plasma within 20 min post sampling
Sampling intervals	0.083, 0.25, 0.5, 1, 2, 4, 6, 8, 12 and 24 h

IV and PO solutions were prepared in 10% DMSO, 10% solutol HS15 and 80% saline to achieve the correct concentration. The bioavailability was determined using:

When:

$$\frac{AUC_{last}}{AUC_{inf}} > 80\%$$

$$F = \frac{(AUC_{inf-ex} * Dose_{IV})}{(AUC_{inf-IV} * Dose_{ex})} * 100$$

5.5.5.1 LC-MS/MS sample preparation and conditions for PK profiling.

Plasma samples were prepared for LC-MS/MS analysis as follows: To an aliquot of plasma sample (30 µL) was added ACN (150 µL) containing the IS (diclofenac, 80 ng for ABC **7** and dexanethasone, 40 ng for compound **108**). The mixture was vortexed for 2 min and centrifuged (6000 rpm, 10 min). The supernatant (1 µL) was injected into the LC-MS/MS for analysis. All samples were analysed on an LC-

MS/MS API 5500 triple quadrupole system. An Acquity UPLC BEH C18 column (2.1 × 50 mm, 1.7 μm) was used for chromatographic separation at 60 °C. The mobile phases were as follows: Mobile phase A – NH$_4$OAc (1 mM) in H$_2$O, 0.1% formic acid (FA); mobile phase B – NH$_4$OAc (1 mM) in MeOH, 0.1% FA. The compounds, including all metabolites, were eluted from the chromatographic column using a linear gradient as depicted below, using a flow rate of 0.6 mL/min. The mass spectrometer was operated in positive ion ESI mode and analyses were performed in MRM scanning mode.

5.6 References

(1)   Illing, P. T.; Vivian, J. P.; Dudek, N. L.; Kostenko, L.; Chen, Z.; Bharadwaj, M.; Miles, J. J.; Kjer-Nielsen, L.; Gras, S.; Williamson, N. A.; Burrows, S. R.; Purcell, A. W.; Rossjohn, J.; McCluskey, J. *Nature* **2012**, *486*, 554.

(2)   Ostrov, D. A.; Grant, B. J.; Pompeu, Y. A.; Sidney, J.; Harndahl, M.; Southwood, S.; Oseroff, C.; Lu, S.; Jakoncic, J.; de Oliveira, C. A. F.; Yang, L.; Mei, H.; Shi, L.; Shabanowitz, J.; English, A. M.; Wriston, A.; Lucas, A.; Phillips, E.; Mallal, S.; Grey, H. M.; Sette, A.; Hunt, D. F.; Buus, S.; Peters, B. *Proc. Natl. Acad. Sci. U. S. A.* **2012**, *109*, 9959.

(3)   Norcross, M. A.; Luo, S.; Lu, L.; Boyne, M. T.; Gomarteli, M.; Rennels, A. D.; Woodcock, J.; Margulies, D. H.; McMurtrey, C.; Vernon, S.; Hildebrand, W. H.; Buchli, R. *AIDS* **2012**, *26*, F21.

(4)   Bharadwaj, M.; Illing, P.; Theodossis, A.; Purcell, A. W.; Rossjohn, J.; McCluskey, J. In *Annual Review of Pharmacology and Toxicology, Vol 52*; Insel, P. A., Amara, S. G., Blaschke, T. F., Eds. 2012; Vol. 52, p 401.

(5)   Barber, L. D.; Percival, L.; Arnett, K. L.; Gumperz, J. E.; Chen, L.; Parham, P. *J. Immunol.* **1997**, *158*, 1660.

(6)   Chessman, D.; Kostenko, L.; Lethborg, T.; Purcell, A. W.; Williamson, N. A.; Chen, Z.; Kjer-Nielsen, L.; Mifsud, N. A.; Tait, B. D.; Holdsworth, R.; Almeida, C. A.; Nolan, D.; Macdonald, W. A.; Archbold, J. K.; Kellerher, A. D.; Marriott, D.; Mallal, S.; Bharadwaj, M.; Rossjohn, J.; McCluskey, J. *Immunity* **2008**, *28*, 822.

(7)   Wearsch, P. A.; Cresswell, P. *Curr. Opin. Cell Biol.* **2008**, *20*, 624.

(8)   Lawrence, R. M.; Process for the preparation of (1S,4R)-cis-4-[2-amino-6-chloro-9H-purin-9-yl]-2-cyclopentene-1-methanol. Glaxo Group Limited. Patent Number: EP1660498 B1: 2009.

(9)   Daluge, S. M.; Martin, M. T.; Sickles, B. R.; Livingston, D. A. *Nucleosides Nucleotides & Nucleic Acids* **2000**, *19*, 297.

(10)   Kasibhatla, S. R.; Hong, K.; Biamonte, M. A.; Busch, D. J.; Karjian, P. L.; Sensintaffar, J. L.; Kamal, A.; Lough, R. E.; Brekken, J.; Lundgren, K.; Grecko, R.; Timony, G. A.; Ran, Y.; Mansfield, R.; Fritz, L. C.; Ulm, E.; Burrows, F. J.; Boehm, M. F. *J. Med. Chem.* **2007**, *50*, 2767.

(11)   Maiti, D.; Fors, B. P.; Henderson, J. L.; Nakamura, Y.; Buchwald, S. L. *Chemical Science* **2011**, *2*, 57.

(12)   Surry, D. S.; Buchwald, S. L. *Angewandte Chemie-International Edition In English* **2008**, *47*, 6338.

(13)   Wolfe, J. P.; Wagaw, S.; Buchwald, S. L. *J. Am. Chem. Soc.* **1996**, *118*, 7215.

(14)   Lakshman, M. K.; Hilmer, J. H.; Martin, J. Q.; Keeler, J. C.; Dinh, Y. Q. V.; Ngassa, F. N.; Russon, L. M. *J. Am. Chem. Soc.* **2001**, *123*, 7779.

(15)   Lakshman, M. K. *J. Organomet. Chem.* **2002**, *653*, 234.

(16)   Vince, R.; Kilama, J.; Pham, P. T.; Beers, S. A.; Bowdon, B. J.; Keith, K. A.; Parker, W. B. *Nucleosides Nucleotides* **1995**, *14*, 1703.

(17)   Kitchen, D. B.; Decornez, H.; Furr, J. R.; Bajorath, J. *Nature Reviews Drug Discovery* **2004**, *3*, 935.

(18)   Kalyaanamoorthy, S.; Chen, Y.-P. P. *Drug Discovery Today* **2011**, *16*, 831.

(19)   http://www.ccdc.cam.ac.uk/Solutions/GoldSuite/Pages/GOLD.aspx.

(20)   *Virtual Screening in Drug Discovery*; Juan Alvarez, B. S., Ed.; CRC Press, 2006.

(21)   Verdonk, M. L.; Cole, J. C.; Hartshorn, M. J.; Murray, C. W.; Taylor, R. D. *Proteins-Structure Function and Genetics* **2003**, *52*, 609.

(22)   Evans, C. T.; Roberts, S. M.; Shoberu, K. A.; Sutherland, A. G. *Journal of the Chemical Society-Perkin Transactions 1* **1992**, 589.

(23)   Daluge, S. M.; Livingston, D. A.; Therapeutic nucleosides. SmithKline Beecham Corporation. Patent Number: US6392085 B1: 2002.

(24)   Tars, K.; Leitans, J.; Kazaks, A.; Zelencova, D.; Liepinsh, E.; Kuka, J.; Makrecka, M.; Lola, D.; Andrianovs, V.; Gustina, D.; Grinberga, S.; Liepinsh, E.; Kalvinsh, I.; Dambrova, M.; Loza, E.; Pugovics, O. *J. Med. Chem.* **2014**, *57*, 2213.

(25)   Daluge, S. M.; Therapeutic nucleosides. Burroughs Wellcome Co. Patent Number: US5034394 A1: 1991.

(26)   Daluge, S. M.; 6-substituted purine carbocyclic nucleosides. Burroughs Wellcome Co. Patent Number: US5049671 A1: 1991.

(27)   Parker, W. B.; Shaddix, S. C.; Rose, L. M.; Pham, P. T.; Hua, M.; Vince, R. *Nucleosides Nucleotides Nucl. Acids* **2000**, *19*, 795.

(28)   Lackey, J. W.; Mook, J. R. A.; Partridge, J. J.; Synthesis of cyclopentene derivatives. Glaxo Inc. Patent Number: US5057630 A1: 1991.

(29)   Alfirevic, A.; Gonzalez-Galarza, F.; Bell, C.; Martinsson, K.; Platt, V.; Bretland, G.; Evely, J.; Lichtenfels, M.; Cederbrant, K.; French, N.; Naisbitt, D.; Park, B. K.; Jones, A. R.; Pirmohamed, M. *Genome Medicine* **2012**, *4*, 51.

CHAPTER 6

Final Discussion

6.1 Final Conclusions & Future Work

ADRs remain a major issue within health care and imperatively, the mechanisms of these ADRs must be resolved. Type A and type B reactions are the most common ADRs but in particular, type B are most frequently researched due to their idiosyncratic and unpredictable nature. Drug-induced HSRs fall within the type B category and the fundamental mechanisms surrounding DHS toxicity is largely influenced by genetic variability.[1] ABC-HSR, as with many drug-induced HSRs, is genetically influenced, with only those patients bearing the HLA-B*57:01 allele susceptible to this toxicity.[2,3] The principal mechanism of ABC toxicity is largely unknown although hypotheses have been proposed. Two major mechanisms of immune-mediated toxicity are the hapten mechanism and the p-i concept, and in particular, the hapten mechanism has been implemented in explaining ABC-HSR.[4] During the latter stages of this research, an alternative mechanism was proposed: The 'altered repertoire' mechanism.[1,5-7] The main aim of this thesis was to establish the major route of ABC toxicity.

In 2002, Walsh and co-workers proposed the first mechanism of ABC-HSR: Metabolism of ABC **7** by ADH to a highly reactive aldehyde species.[4] Such species have been known to cause toxicity *in vivo*.[8] The short-lived aldehyde metabolite proved difficult to isolate, as shown by Charneira *et al.*[9] and in this thesis (Chapter 2). With no specific evidence of this species, it was difficult for Walsh *et al.* to prove their theory, although the isolation of haptenated proteins resulting from reactions with an aldehyde intermediate was discovered. Charneira *et al.*,[9,10] Grilo *et al.*,[11] and Meng *et al.*[12] have further researched this: Protein adducts, both *in vitro*

346

and *in vivo*, have been isolated. More importantly, these adducts were formed from one aldehyde metabolite, ABC-CHO **16c** (Figure **6.1**).[10] The formation of this aldehyde further adds to the complicated nature of ABC metabolism and the specific ADH and/or ALDH isozymes involved in this process.

Walsh *et al*.[4] were first to uncover the ADH isozymes involved in the metabolic process, but the involvement of ALDH was not suggested. It has been shown in this work that there is some contribution of ALDH to ABC metabolism (Chapter 3), although ADH is itself capable of metabolising ABC-**16** to ABC-**17** (Figure **6.1**).[4] It has been shown, through methoxylamine trapping experiments, that aldehyde formation does occur, although the half-life of the aldehyde has not been determined, due to its highly reactive nature.   The aldehyde would react with proteins spontaneously; the effects of which would be seen close to the site of metabolism. The location of this would be predicted to be in the liver, although these metabolites are able to travel in the circulatory system. However, certain classes of ADH and ALDH enzymes are also found within the skin.[13] Grilo *et al*.[11] have experienced difficulty in obtaining haptenated adducts from patients *in vivo* and as such would show that although adduct formation is occurring the contribution to ABC toxicity could be relatively small.
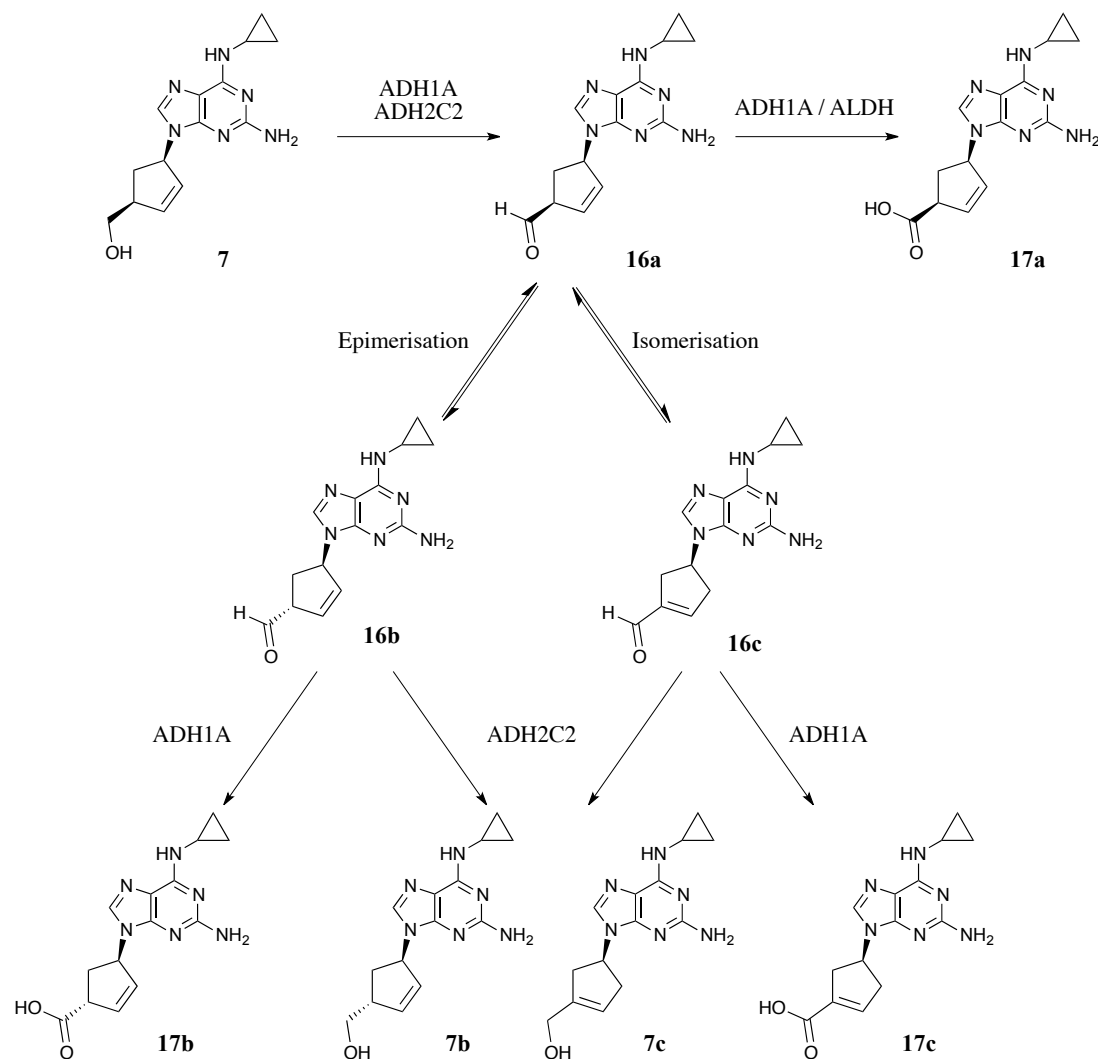
Figure 6.1: Biochemical oxidation of ABC **7** to its stereo-equivalent aldehyde intermediate **16a** by ADH and further metabolism of **16a** to the major carboxylic acid isomer **17a** *in vitro* by ADH1A (αα)/ALDH. At the beginning of this work, the involvement of ALDH in this oxidation pathway was unknown and ADH1A was shown to oxidise ABC to **17a**.[4] Aldehyde **16a** can undergo epimerisation to **16b**, which in turn is oxidised by ADH1A to carboxylic acid **17b** or reduced to an isomer of ABC, **7b**. Alternatively, **16a** can undergo isomerisation to aldehyde **16c**, which has shown to undergo *in vitro* and *in vivo* protein adduct formation. Isomer **16c** can also undergo further oxidation to carboxylic acid **17c** or reduction to an isomeric parent compound **7c**. Adapted from Walsh *et al.*[4] and Charneira *et al.*[9]

The use of deuterium in drug therapy and to research drug mechanisms is widely recognised[14-16] and this idea was adopted in this work (Chapters 2 and 3). The 8-step total synthesis of D_2-ABC **42** (Figure **6.2**) was successfully completed (Chapter 2) and this was further used in *in vitro* experiments with crude liver cytosol, where the metabolism of D_2-ABC mimicked that of ABC (Figure **6.2**) (Chapter 3). The rate of metabolism of the deuterated form was retarded and a primary KDIE of 1.88 was calculated between ABC and D_2-ABC. Interestingly, as shown by Stringer *et al.*,[17] metabolic switching can occur, in which an alternative metabolic pathway becomes more dominant over the usually preferred pathway. This may occur if the normal dominant pathway is slowed. In the case of D_2-ABC, this may result in the glucuronidation pathway becoming more preferable, resulting in a pharmacologically inactive metabolite. However, the *in vitro* antiviral results for D_2-ABC shows that it has comparable efficacy to ABC, at least in MT4 cells, but this would need to be confirmed *in vivo*. The *in vitro* T-cell assays showed that D_2-ABC stimulated ABC-specific T-cell clones to the same extent as ABC. It can be concluded from this, that although we have shown that the oxidative metabolism can be slowed, the toxicity is likely to be maintained. Metabolism of D-ABC aldehyde **58** to ABC-COOH **17** (Figure **6.2**) by ADH/ALDH would be slowed and this may result in higher accumulations of **58**, allowing for adduct formation. Alternatively, the oxidative metabolism at 5'-C may not contribute to ABC-HSR, thus another part of the molecule must be involved (Chapter 5). It would be interesting to perform the T-cell assays over a shorter time period (the assays are normally conducted over 48 h). This would show at which time point and/or concentration, is the stimulation of T-cells by D_2-ABC to that of ABC should there be any variation at all.
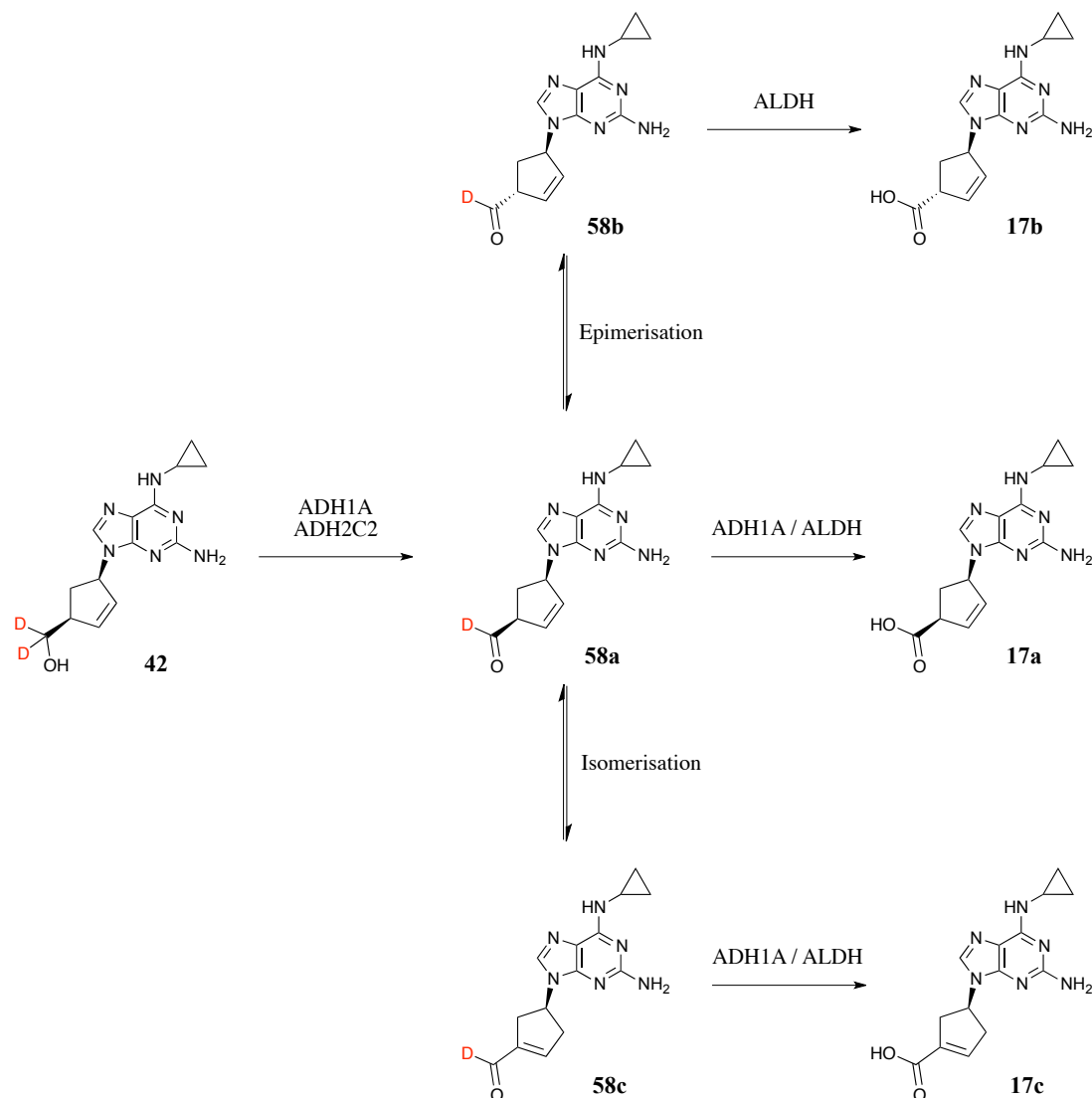
Figure 6.2: D$_2$-ABC **42** has been shown to mimic the oxidative metabolism exhibited by ABC: D$_2$-ABC is metabolised by ADH to an aldehyde intermediate **58a**. This intermediate can be further oxidised by ADH/ALDH to ABC-**17a**. Alternatively, **58a** can undergo epimerisation or isomerisation to form aldehydes **58b** and **58c** respectively, which in turn can be oxidised to their carboxylic acid equivalents, **17b** and **17c** respectively.

There is much further work required in this metabolism area: The calculation of the relative rate constants k is much needed in order to fully define any KDIE. Due to the two-step metabolism of ABC/D$_2$-ABC, 1st step being oxidation to their aldehyde equivalents (compounds **16** and **58**) and the 2nd step, further oxidation to ABC-**17**, it

is difficult to define the RDS of this oxidative metabolism. Therefore the KDIE calculated is an overall value and this must be calculated for the individual steps. Although widely researched, oxidation of alcohols to carboxylic acids by ADH is a complex process, with a number of transition states and hydrogen tunnelling.[18] There is comparatively less literature for the oxidation and direct involvement of ALDH and together with the complex metabolism by ADH it further shows how intricate this metabolic process is. The further *in silico*, chemical and mathematical research required for this work is far beyond the scope of this thesis. Further chemical research would involve the synthesis of 4'-C and 5'-C methylated analogues (see Chapter 2, Section **2.4**, Figure **2.11**). Methylation of molecules has been shown to increase the biological and pharmacological properties of a drug.[19] The 4'-C methyl analogue would allow for oxidative metabolism to occur to a carboxylic acid, as with ABC, but double bond migration to ABC-**16c**, would not be allowed to occur. This would prevent a 1,4-Michael addition mechanism from occurring; a mechanism known to contribute significantly *in vitro* and *in vivo* to ABC-HSR. A 1,2-Schiff mechanism however may still be possible. Although, using the 4'-C methyl compound, the contribution of other ABC-aldehyde isomers, **16a** and **16b** may become predominant perhaps resulting in similar haptenated adducts. The 5'-C methyl analogue would prevent oxidative metabolism completely, and running this analogue in the relevant T-cell assays, could show greatly reduced stimulation of T-cells. Although metabolic switching (as previously discussed) is highly likely to occur with this analogue, potentially making this analogue antivirally inactive. Along with these two analogues, the synthesis of D-ABC (deuteration of 4'-C) would allow investigational work of a possible secondary KDIE. Further metabolism experiments should be designed to measure substrate disappearance, rather than

product formation. The method utilised within this work was adapted from Patenella *et al.*,[20] it assumes that the substrates (ABC/D_2-ABC) are fully converted to their respective products. However, the metabolism experiments can be monitored more accurately by measuring substrate disappearance; this will provide more precise results as it allows the concentration of substrate used to be determined without assuming that it is fully converted to its product, which may not be the case.

Although many total syntheses of ABC have been published, there is little available literature for the direct chemical reactivity of ABC. The lack of solubility of ABC in a wide range of commonly used solvents for reactions was a major issue for the direct modification of ABC, particularly when trying to modify N^2 (Chapter 4). Although, reactions conducted in polar solvents *e.g.* MeOH and DMF, yielded desired products, such as DH-ABC **20** (Figure **6.3 B**). Previous work published by Walsh *et al.* showed that DH-ABC reduced the number of non-extractable residues, implying less protein adduct formation compared to ABC.[4] This was further supported in this work, in which DH-ABC greatly reduced IFN-γ release in ABC-specific T-cell clones and reduced proliferation (LTT test) of T-cell clones (Chapter 4). There are two possible explanations of this: i.) DH-ABC, in its parent form, has an altered conformation to ABC; ii.) It has a saturated cyclic 'sugar' moiety. The saturation of the cyclopentane ring will remove the C=C restrictions experienced by ABC and will therefore alter its conformation, not only within the cyclopentane ring, but also the nucleoside base. This may affect the binding within HLA-B*57:01 and as seen with the *in silico* binding of 6-position analogues, any slight alterations at the nucleoside base will affect its binding within the protein. Further *in silico* analysis will assist in explaining this further. Conversely, the absence of the alkene will

prevent covalent adduction in a 1,4-Michael addition manner, although a 1,2-Schiff base mechanism may still occur. This is therefore interesting, such that protein adduct formation is still able to occur, but is restricted to a particular mechanism. This may explain the reduction, but not elimination, in T-cell stimulation. DH-ABC could undergo a similar set of metabolism experiments, as applied to D_2-ABC, to monitor the oxidative metabolism pathway, and this may highlight any formation of haptenated products.

Although the total syntheses for ABC were challenging (Chapter 4), a synthesis was developed and this can be further adapted during the synthesis of a wider range of ABC analogues, particularly those containing 'sugar' moiety modifications. The synthesis of the ABC enantiomer (ent-ABC) (Figure **6.3 C**) was successful and the further immunological experiments of this compound were of interest (Chapter 4). The lack of a T-cell response, measured through the LTT test and ELISpot assay, from ent-ABC showed that ABC-HSR is stereospecific. It is known that a wide range of biological systems and processes *e.g.* enzymes, are highly stereoselective and therefore it is difficult to determine at this stage which biological process is responsible: ADH/ALDH (enzymatic) or HLA-B*57:01. It may be that ent-ABC is unable to be metabolised by the stereospecific ADH/ALDH enzymes with no aldehyde formation and subsequently no immune-mediated response. Conversely, ent-ABC may not bind in the same manner as ABC within the HLA-B*57:01 protein and therefore the intermolecular forces, as experienced with ABC, would not occur, failing to initiate an immune response *via* either the p-i concept or the altered repertoire mechanism. *In silico* and additional immunological experiments are required to explain this finding further.
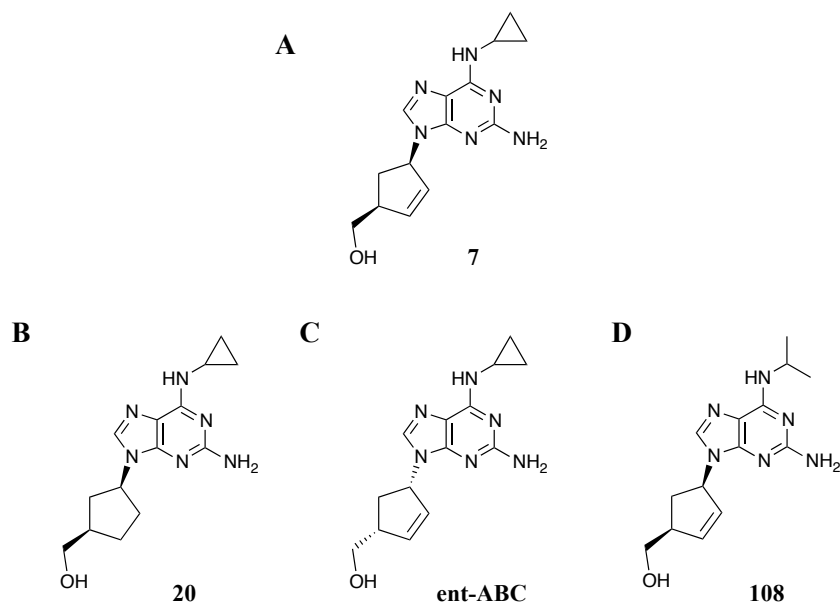
Figure 6.3: ABC **7** (**A**), DH-ABC **20** (**B**), ent-ABC (**C**) and compound **108** (**D**).

A wide range of 6-position analogues were synthesised and these analogues were used to probe the altered repertoire mechanism (Chapter 5). The analogues, consisting of 1° and 2° amine and oxy analogues, were subjected to further experimental studies. *In silico* studies allowed us to model these analogues within the HLA-B*57:01 protein to determine the interactions with specific amino acids. In particular those within the F-pocket; these intermolecular forces have been suggested to assist with ABC's binding within the protein. The acquired GOLDScore values were used in a complimentary manner to explain the results obtained from the ELISpot assay, in which the majority of analogues did not stimulate ABC-specific T-cell clones. However, not all these analogues retained efficacy with comparison to ABC. It was found that the *i*-Pr analogue **108** (Figure **6.3 D**) had the most significant results, with negative stimulation of *in vitro* T-cell clones and efficacy maintained. In initial PK testing, positive results were obtained, as compound **108**'s PK parameters were almost comparable to ABC's. Those analogues, which failed to

stimulate T-cell clones and sustained similar efficacy values to ABC, must be subjected to similar PK testing, as with compound **108**. Further to this, there are several analogues in which T-cell and antiviral experiments have not been completed. Once these results are obtained, all collated results will assist in directing future 6-position analogue synthesis.

It would be interesting to subject these analogues to the metabolism experiments (as shown with D_2-ABC, Chapter 3) to monitor the oxidative metabolism, compared to ABC. These analogues, should they be substrates for ADH/ALDH, form their respective aldehyde intermediates. It is interesting that most of these analogues did not stimulate an immune response *in vitro*, even though the aldehyde metabolites are theoretically formed. The metabolism experiments would confirm presence of these metabolites and would therefore help to determine the mechanism of ABC-HSR: The presence of aldehyde metabolites would suggest that the altered repertoire mechanism is the prevailing pathway to explaining ABC-HSR. However, it could also be possible that an alternative metabolism of these analogues exists, although, the same pathway as ABC would be expected. The metabolism of alcohols to aldehydes could also occur *via* an alternative enzymatic pathway.[8]

Although several mechanisms of ABC toxicity have been proposed, a definite mechanism has yet to be determined. Our findings have confirmed the oxidative pathway of ABC metabolism and the involvement of ALDH in this metabolism has also been determined (Chapter 3). The altered repertoire mechanism appears to be the most plausible explanation for ABC-HSR, and our initial experiments have supported this (Chapter 5). It was stated by Illing *et al.*,[5] that the 6-position

cyclopropyl amino moiety of ABC assists with its binding within the HLA complex. *In silico* studies have allowed us to model our rationally designed analogues and data supports the altered repertoire hypothesis since compounds with larger or more bulky 6-position substituents exhibited higher GOLDScore values with positive *in vitro* T-cell responses. The p-i mechanism has been discarded, as it was shown by McCluskey *et al.*,[21] that ABC must undergo intracellular processing. However, this should be confirmed with the synthesised 6-position analogues. The application of the hapten mechanism with the 6-position analogues is still under investigation. With respect to the hapten mechanism not all of these analogues are likely to be substrates of ADH/ALDH, so aldehyde formation may not be possible for all compounds, limiting the T-cell response to certain analogues. Alternatively, the hapten mechanism may not be applicable at all if we can show that the entire set of analogues are substrates for ADH/ALDH enzymes but the relative aldehyde intermediates formed do not stimulate ABC-like toxicity. It has been shown *in vitro* that in ABC-specific T-cell clones, stimulation of T-cells can be eliminated with antiviral activity maintained, solely through subtle modification at the 6-position. It would be beneficial to analyse the repertoire of peptides that are displayed by HLA-B*57:01, using experimental techniques as applied by Illing *et al.*[5] and Ostrov *et al.*,[6] in the presence of all synthesised analogues, regardless of whether an immune response is stimulated or not. These results would assist in confirming or rejecting the altered repertoire hypothesis. Furthermore, *in vivo* experiments are required for all synthesised analogues: Detection should be directed to haptenated products or parent/metabolite compounds. Haptenated products would assist with further developing the hapten theory, as suggested by Walsh *et al.*,[4] Charneira *et al.*,[9,10] Grilo *et al.*[11,22] and Meng *et al.*[12]

In initial studies, Illing *et al.*[5] have demonstrated that CBZ-induced HSR can also be explained by the altered repertoire mechanism; the genetic association with this drug is HLA-B*15:02. Although these studies are extremely preliminary, this demonstrates that this mechanism is not limited to ABC, nor to HLA-B*57:01. It is unclear as to what the relationship is between these immune-stimulating molecules and their associated HLA alleles. The strong association of these drugs with HLA molecules, *e.g.* ABC (HLA-B*57:01),[2,3] CBZ (HLA-B*15:02)[23,24] and allopurinol (HLA-B*58:01),[25,26] are open to questions: Is there a key link between the structures of these drugs that are associated with this form of toxicity? Alternatively, is there a link with these HLA molecules, in which they share a common structural component, which is strongly associated with immune-related ADRs? It would be beneficial to discover whether there is a unified link so to apply predictive measures in future drug design efforts.

There are many drugs that require genetic screening pre-prescription or before market release, and in particular, all prospective ABC patients must undertake genetic screening for the HLA-B*57:01 allele before administration of therapy. This leads to the question, would it be beneficial to conduct HLA screening for all pre-released drugs? If so, the genetic variations of HLA molecules may prove a hindrance for its application. There are over 8500 alleles for HLA class I molecules alone,[27] and with such genetic variation, which are usually ethnicity linked, would it make genetic screening of every drug unaffordable? Screening of patients' HLA alleles before commencing drug therapy may certainly benefit the patient and reduce HLA-associated ADRs, but it should also be noted that other external factors, such as chemical toxins, might induce these adverse reactions, and these issues should be

considered. Evidently, it would be paramount to firstly identify the HLA association, should it occur, with future drugs. The cost-to-benefit ratio, along with potentially denying a patient a breakthrough drug treatment where ADRs may outweigh the benefits, should be carefully calculated and considered.

What is still undetermined, is the reason why only 50% of patients bearing the HLA-B*57:01 allele experience ABC-HSR.[28] Other genetic or environmental factors must contribute to ABC's toxicity. Additionally, the mechanism of cardiac toxicity resulting from ABC administration has been less widely studied and it is unknown whether either any of the proposed mechanisms for ABC-HSR also contribute to this alternative toxicity.

The research discussed in this thesis shows that the mechanisms underlying ABC-HSR is complex and one defining mechanism to explain this toxicity is still under investigation. The new hypothesis, the altered repertoire mechanism, is in its infancy and there is clearly much further research that should be conducted, to fully define whether this mechanism could be applied to ABC toxicity. In particular, future research should be applied further afield with the use of other drugs that induce HSRs, to explaining their HLA-associated toxicity. This additional research will lead to safe drug design and ultimately, this specific toxicity could be prevented in future drugs.

6.2 References

(1)   Bharadwaj, M.; Illing, P.; Theodossis, A.; Purcell, A. W.; Rossjohn, J.; McCluskey, J. In *Annual Review of Pharmacology and Toxicology, Vol 52*; Insel, P. A., Amara, S. G., Blaschke, T. F., Eds. 2012; Vol. 52, p 401.

(2)   Mallal, S., Nolan, D., Witt, C., Masel, G., Martin, A.M., Moore, C., Sayer, D., Castley, A., Mamotte, C., Maxwell, D., James, I. *The Lancet* **2002**, *359*.

(3)   Hetherington, S.; Hughes, A. R.; Mosteller, M.; Shortino, D.; Baker, K. L.; Spreen, W.; Lai, E.; Davies, K.; Handley, A.; Dow, D. J.; Fling, M. E.; Stocum, M.; Bowman, C.; Thurmond, L. M.; Roses, A. D. *Lancet* **2002**, *359*, 1121.

(4)   Walsh, J. S.; Reese, M. J.; Thurmond, L. M. *Chem. Biol. Interact.* **2002**, *142*, 135.

(5)   Illing, P. T.; Vivian, J. P.; Dudek, N. L.; Kostenko, L.; Chen, Z.; Bharadwaj, M.; Miles, J. J.; Kjer-Nielsen, L.; Gras, S.; Williamson, N. A.; Burrows, S. R.; Purcell, A. W.; Rossjohn, J.; McCluskey, J. *Nature* **2012**, *486*, 554.

(6)   Ostrov, D. A.; Grant, B. J.; Pompeu, Y. A.; Sidney, J.; Harndahl, M.; Southwood, S.; Oseroff, C.; Lu, S.; Jakoncic, J.; de Oliveira, C. A. F.; Yang, L.; Mei, H.; Shi, L.; Shabanowitz, J.; English, A. M.; Wriston, A.; Lucas, A.; Phillips, E.; Mallal, S.; Grey, H. M.; Sette, A.; Hunt, D. F.; Buus, S.; Peters, B. *Proc. Natl. Acad. Sci. U. S. A.* **2012**, *109*, 9959.

(7)   Norcross, M. A.; Luo, S.; Lu, L.; Boyne, M. T.; Gomarteli, M.; Rennels, A. D.; Woodcock, J.; Margulies, D. H.; McMurtrey, C.; Vernon, S.; Hildebrand, W. H.; Buchli, R. *AIDS* **2012**, *26*, F21.

(8)   O'Brien, P. J.; Siraki, A. G.; Shangari, N. *Crit. Rev. Toxicol.* **2005**, *35*, 609.

(9)   Charneira, C.; Godinho, A. L. A.; Conceicao Oliveira, M.; Pereira, S. A.; Monteiro, E. C.; Matilde Marques, M.; Antunes, A. M. M. *Chem. Res. Toxicol.* **2011**, *24*, 2129.

(10)   Charneira, C.; Grilo, N. M.; Pereira, S. A.; Godinho, A. L. A.; Monteiro, E. C.; Marques, M. M.; Antunes, A. M. M. *Br. J. Pharmacol.* **2012**, *167*, 1353.

(11)   Grilo, N. M.; Antunes, A. M. M.; Caixas, U.; Marinho, A. T.; Charneira, C.; Conceicao Oliveira, M.; Monteiro, E. C.; Matilde Marques, M.; Pereira, S. A. *Toxicol. Lett.* **2013**, *219*, 59.

(12)   Meng, X.; Lawrenson, A. S.; Berry, N. G.; Maggs, J. L.; French, N. S.; Back, D. J.; Khoo, S. H.; Naisbitt, D. J.; Park, B. K. *Chem. Res. Toxicol.* **2014**.

(13)   Cheung, C.; Smith, C. K.; Hoog, J. O.; Hotchkiss, S. A. M. *Biochem. Biophys. Res. Commun.* **1999**, *261*, 100.

(14)   Mabic, S.; Castagnoli, N. *J. Med. Chem.* **1996**, *39*, 3694.

(15)   Ferraboschi, P.; Grisenti, P.; Santaniello, E. *Journal of Labelled Compounds & Radiopharmaceuticals* **1994**, *34*, 303.

(16)   Avery, M. A.; Bonk, J. D.; Mehrotra, S. *Journal of Labelled Compounds & Radiopharmaceuticals* **1996**, *38*, 249.

(17)   Stringer, R. A.; Williams, G.; Picard, F.; Sohal, B.; Kretz, O.; McKenna, J.; Krauser, J. *Drug Metab. Disposition* **2014**, *42*.

(18)   Kohen, A.; Klinman, J. P. *Acc. Chem. Res.* **1998**, *31*, 397.

(19)   Schoenherr, H.; Cernak, T. *Angewandte Chemie-International Edition in English* **2013**, *52*, 12256.

(20) Patanella, J. E.; Walsh, J. S. *Drug Metab. Disposition* **1992**, *20*, 912.

(21) McCluskey, J.; Peh, C. A. *Reviews in Immunogenetics* **1999**, *1*, 3.

(22) Grilo, N. M.; Charneira, C.; Pereira, S. A.; Monteiro, E. C.; Matilde Marques, M.; Antunes, A. M. M. *Toxicol. Lett.* **2014**, *224*, 416.

(23) Locharernkul, C.; Loplumlert, J.; Limotai, C.; Korkij, W.; Desudchit, T.; Tongkobpetch, S.; Kangwanshiratada, O.; Hirankarn, N.; Suphapeetiporn, K.; Shotelersuk, V. *Epilepsia* **2008**, *49*, 2087.

(24) Hung, S. L.; Chung, W. H.; Jee, S. H.; Chen, W. C.; Chang, Y. T.; Lee, W. R.; Hu, S. L.; Wu, M. T.; Chen, G. S.; Wong, T. W.; Hsiao, P. F.; Chen, W. H.; Shih, H. Y.; Fang, W. H.; Wei, C. Y.; Lou, Y. H.; Huang, Y. L.; Lin, J. J.; Chen, Y. T. *Pharmacogenetics and Genomics* **2006**, *16*, 297.

(25) Hung, S. L.; Chung, W. H.; Liou, L. B.; Chu, C. C.; Lin, M.; Huang, H. P.; Lin, Y. L.; Lan, J. L.; Yang, L. C.; Hong, H. S.; Chen, M. J.; Lai, P. C.; Wu, M. S.; Chu, C. Y.; Wang, K. H.; Chen, C. H.; Fann, C. S. J.; Wu, J. Y.; Chen, Y. T. *Proc. Natl. Acad. Sci. U. S. A.* **2005**, *102*, 4134.

(26) Tassaneeyakul, W.; Jantararoungtong, T.; Chen, P.; Lin, P.-Y.; Tiamkao, S.; Khunarkornsiri, U.; Chucherd, P.; Konyoung, P.; Vannaprasaht, S.; Choonhakarn, C.; Pisuttimarn, P.; Sangviroon, A.; Tassaneeyakul, W. *Pharmacogenetics and Genomics* **2009**, *19*, 704.

(27) http://www.ebi.ac.uk/ipd/imgt/hla/stats.html.

(28) Nolan, D. *Crit. Rev. Clin. Lab. Sci.* **2009**, *46*, 153.